Polymerisation in Flow and Solid State.

Acrylic acid to pure poly(acrylic acid) in one hour, and the synthesis of defined tacticity polymers *via* topochemical polymerisation.

Laurens Brocken

Supervised by
Prof. I. R. Baxendale

A thesis presented for the degree of
Doctor of Philosophy

Durham University
University College
21-04-2016

Declaration

This is an Industrial CASE Doctoral Scholarship funded project supported by Unilever and any material shown is confidential.

Dedication

Dedicated to my mum.

Thank you for your support and always being there when I needed you.

Een gouden hart!

Acknowledgements

I would like to thank Prof. Ian Baxendale for the opportunity he gave me doing this PhD. It all came together at Prebends' Bridge (Durham) during a walk on the 14-05-2012. I am very honoured you asked me to work on the Unilever project. Over the years many stories have been made together and I will think about them with a smile!

Secondly I would like to thank Unilever for co-funding my PhD and in particular Dr Jean Whittaker and Dr Paul Price helping me with plenty "polymer issues". From now on no more complaints about aqueous GPC from my side. Thank you very much again for having me for three months during my placement. I had a great time!

I would also like to thank Dr Marcus Baumann for his help with the plenty of questions I had over the last years, Dr Christian Stanetty for giving me heads up the time you were here and Dr Paolo Filipponi for the practical help in the lab.

Carl, we have started our PhD together and have helped each other a lot while we had our ups and downs during our PhD. Some bonds are made for life and I will always remember our bond.

James thank you for being my squash buddy. I have not come across many people who can hit a ball that hard... Laura, thank you for your language knowledge. You have saved me a couple of times from making very awkward errors. Te, you have added the Chinese flavour to the group and made it an intercontinental group. I wish you all the best with finishing your PhD!

All the group members who have been part or are still part of the Baxendale

group, you all made it to an amazing experience. Of the technical staff, who have been always very helpful, I would like to thank Dr Juan Aguilar in particular for all the NMR help.

Some people have supported me no matter what I did. I could always ask them for help or they were there to listen. My best friend Joram deserves a huge thanks! Without your help my thesis would not have been as what it is. Ook al spelen we dit spel niet meer, ik heb heel hard op B gedrukt. Onhoudbaar in de kruising! Dank voor de voorzet... Nogmaals dank voor de vele opbeurende woorden en de keren dat jij er was als ik er doorheen zat. Niet alleen voor wat betreft mijn PhD...

Lieve Marijn, ook van jou heb ik onvoorwaardelijke steun gekregen. Telkens was jij er als dat nodig was, of dit nu 's avond laat was of een bezoek aan Liverpool. Ik kan altijd een beroep op jou en Michel doen, slapen in Nijmegen geen probleem, beschimmelde schoenen in de kelder, geen probleem en zo kan ik nog wel even doorgaan. Ik ben dan ook heel erg dankbaar dat jij mijn zus bent!

Lieve Francesca, you have been helping me a lot lately. You have corrected my English if I asked for it and were there when I needed you. You have seen me during the hardest part of my PhD. I love the fact that we are dancing together and I am convinced we will make it to the top one day...

Lieve mam, jij bent een van de drijvende krachten achter het feit dat ik in Durham zit. Met jou kan ik alles bespreken wat ik maar wil en ik kan altijd voor advies bij jou terecht. Wij gaan het eind van deze periode zeker vieren en ik kijk er al naar uit. Lieve mam, wij weten dat ook de mensen van boven meekijken en dat zij hier ook aan hebben bijgedragen. Jij hebt een gouden hart!

Abbreviations

Abbreviation	Meaning
δ	chemical shift (NMR spectroscopy)
ν	wavenumber (IR spectroscopy)
λ_{max}	wavelength of maximum absorbance
A	frequency factor
Å	Ångström (unit of length)
AIBN	Azobisisobutyronitrile
ARGET	activator regenerated by electron transfer
ASAP	Atmospheric Solids Analysis Probe
ATRP	atom transfer radical polymerisation
BPR	back pressure regulator
br	broad (NMR spectroscopy)
°C	degree Celsius
$CDCl_3$	deuterated chloroform
CFC	convective flow coil
CRP	Controlled Radical Polymerisation
cm^{-1}	inverse centimetre
cm^2	centimetre squared
Conv.	conversion
d	doublet (NMR spectroscopy)
$Đ$	dispersity
Da	Dalton

Continued on next page

Continued from previous page

Abbreviation	**Meaning**
D_2O	deuterated water
DEPT	distortionless enhancement through polarisation transfer
DMA	*N*,*N*-dimethyl acrylamide
DoE	Design of Experiment
DP	degree of polymerization
E_a	activation energy
equiv.	equivalent
FEP	fluorinated ethylene propylene
FT-IR	fourier-transform infrared
g	gram
GPC-SEC	gel permeation chromatography - size exclusion chromatography
HPLC	high performance liquid chromatography
HRMS	high resolution mass spectroscopy
Hz	hertz
I	initiator
ICAR	initiators for continuous activator regeneration
IR	infrared
J	coupling constant (NMR spectroscopy)
K	Kelvin
L	litre
LALS	low angle light scattering
LCMS	liquid chromatography mass spectroscopy
m	multiplet (NMR spectroscopy)
M	molar
min	minute
mL	millilitre

Continued on next page

Continued from previous page

Abbreviation	**Meaning**
M_n	number average molecular weight
M_w	molecular weight
MWCO	molecular weight cut off
NMP	nitroxide mediated polymerisation
NMR	nuclear magnetic resonance
o.n.	over night
pAA	poly(acrylic acid)
PEEK	poly(ether ether ketone)
ppm	part per million
PTFE	polytetrafluoroethylene
q	quartet (NMR spectroscopy)
R	gas constant
rad	radical
RAFT	Reversible addition-fragmentation chain transfer approach
R_e	Reynolds number
res.	residual
rpm	rotations per minute
Rt	residence time
rt	room temperature
SARA	supplemental activator and reducing agent
SET-LRP	single electron transfer living radical polymerisation
t	triplet (NMR spectroscopy)
t	time
$t_{1/2}$	half-life time
T	temperature
T_a	Taylor number

Continued on next page

Continued from previous page

Abbreviation	**Meaning**
T_{abs}	absolute temperature
TLC	thin layer chromatography
UV	ultraviolet
vs.	versus

Abstract

The aim of this thesis was to develop and facilitate new approaches to polymer synthesis. The chosen tools for this task were flow chemistry and topochemical polymerisation. Flow chemistry has proven its strength in the past and is a technique suitable for performing synthesis at scale.

Three areas were explored in this thesis. In the first results chapter the free radical polymerisation of aqueous solution of acrylic acid (**7**) has been studied using a continuous flow reactor to quickly screen reaction parameters such as temperature, residence time, monomer- and initiator concentration. The experimental data sets produced established a theoretical basis for conducting scale up processes to efficiently produce larger quantities of poly(acrylic acid) (**8**) delivered with good control over the molecular weight and dispersity. The data sets were used to study the ability to synthesise polymers on demand.

The developed methodology to synthesise aqueous soluble polymers in flow, possessing a variety of molecular weights and dispersities have been achieved. However, full conversion was hard to achieve without increasing the dispersity and purification was therefore necessary. The second results chapter studied the direct purification to obtain purified polymer under one hour. This opened up a new way to synthesise and isolate polymers.

Performing a free radical polymerisation in flow does not result in the control over tacticity of the polymerisation. The third results chapter studied the synthesis of polymers *via* topochemical polymerisation and the advantages it can add to general polymer synthesis.

Contents

List of Figures

List of Tables

List of Schemes

Chapter 1

Introduction

1.1 Precis

Flow polymerisation has been shown to facilitate access to new polymers which cannot be synthesised under conventional batch conditions through improved control over the various reaction parameters. In this chapter, a brief overview is given of the various syntheses of polymers and polymeric particles that have been performed in flow to date. As part of this overview it is endeavoured to describe both the polymerisation process as well as commenting upon its scope.

1.2 Flow chemistry processing

Over the last 25 years there has been a major growth in interest regarding the synthesis of chemical compounds using continuous processing. In a flow chemistry procedure, a chemical reaction is run as a continuous dynamic sequence where each aspect of the reaction can be altered in real time and the effect in terms of flow stream composition can be monitored downstream; either *via* passive (i.e. ReactIR, [1] UV, [2] NMR, [3, 4]) or invasive sampling (i.e. LC-MS, [5] MS, [6] HPLC, [7] gravimetric analysis [8]). This facilitates the investigation of many reaction parameters in a fast serial processing regime using a single reactor set-up that delivers reliable and reproducible data. This contrasts with classical batch processing where each reaction

is run as an independent transformation leading to a single optimisation data output. Consequently, more comprehensive and full optimisation is often performed in flow than may be undertaken in batch. This is especially true where automation of the reaction sequence in flow including the subsequent analysis has been conducted. In its ultimate format self-optimising reactors that are able to run independently and use statistical design software to determine the best set of reaction conditions for a given chemical process have been reported. [9–11]

1.2.1 Flow chemistry advantages and disadvantages

The last two and a half decades have seen renewed interest in the use of flow chemistry as a technique for the synthesis of mainly small molecules ($M_w < 600$) but also increasingly for macromolecular compounds. The major growth of flow chemistry can be ascribed to the numerous advantages that it offers over batch based processing techniques. For instance, the reaction temperature can be easily elevated above the atmospheric boiling point of the reaction solvent without recourse to specialist pressure containment (super heating). A similar effect can be attained by the use of microwave reactors. For flow reactors the design and small internal volumes of most reactors enable simple pressurisation of the fluidic flow by restriction of the outlet. Consequently reaction temperatures exceeding 100 °C above the standard solvent boiling point and 20 - 100 bar pressures are typically encountered using standard off the shelf-commercial reactors. Heat transfer is also much more effective (including the introduction of multiple stage temperature zones) as are the mixing efficiencies that can be achieved. The improvement in mixing efficiency is especially beneficial for multi-phase reactions and has seen a dramatic increase in the number of gas-liquid and liquid-liquid reactions which are being performed in flow. A further aspect which has contributed to the wider adoption of flow processing is the ability to formulate telescoped multi-step syntheses which deliver in linked processing trains, more complex chemical architectures. The ability to add in-line work-up and purification steps as part of an integrated sequence rapidly expands the scope and

range of chemical steps which can be coupled. Beyond these general advantages, industrial manufacturing can gain from adopting continuous flow. The scalability of flow processes is possible, using time rather than reactor size as the key scaling parameter. All these advantages have been extensively discussed in a number of seminal papers and review articles. [12–14]

Flow chemistry also has some drawbacks and shortfalls; otherwise it would have already superseded batch procedures for the synthesis of new molecules. An immediate consideration is often the *initial investment* costs both with respect to the equipment (including on-going servicing costs) and also the need for additional training in order to educate the users in the workings of the equipment and best practice. Flow chemistry certainly requires a *different skill and mind set* compared to classical batch based chemistry. Flow processing is much more fully thought through in its approach considering upfront many more aspects of the reaction as part of the full process. Consequently flow chemists tend to adopt a more chemical engineering approach thinking in terms of unit operations and how each of these will fit together, this includes the up- and down-stream impact of making a change to each stage. By comparison batch processing by nature of its compartmentalisation means aspects can be considered more independently and sequentially. For example, quenching and work-up of a batch reaction can often be considered and changed once a reaction is underway. This is not possible in a flow process where such aspects need to be meticulously planned for and as far as possible integrated into the design of the sequence from the start. Therefore, flow chemistry has a higher degree of complexity.

Another area where difficulties can arise is in compensating for the potentially *different reaction kinetics* of sequenced steps when performing multi-step flow syntheses. This invariably requires a much better understanding of the overall reaction including the stability and lifetimes of all reactive intermediates. In practice it is often necessary to introduce residence hold vessels (volume buffer vessels) between key stages which allow the batching of material acting as stock solutions for the next stage. Such approaches help to balance disperse kinetics and residence times thus

enabling a continuous processing scenario, albeit with batch vessels interconnecting the reactors.

Solvent selection is certainly a more critical consideration in a flow processes. Not only must thought be given to ensuring the compatibility of a solvent for each stage of the potential multi-stage sequence thus maintaining reactivity but also issues of salting out and precipitation must generally be avoided. Solvent exchange and managing dilution effects when multi-stage reagent addition is used can also introduce complications which may increase complexity.

There are several other aspects which contrast batch and flow thinking. For example, the reaction stoichiometry is considered differently. In batch, stoichiometry and concentration are derived by the relative amounts of the reagents and the volume of solvent at $t = 0$. Over time, there will be a decrease in the concentration of a reagent and a proportional increase in the amount of a product/ by-product. In flow concentrations change as reagent flow streams combine through mixing of the relative streams establishing a new concentration profile, here $t = 0$ is defined as the mixing point and homogeneity is often achieved faster. Consequently the reaction and therefore concentration change of species occurs in terms of their progression downstream of this point. Essentially a reaction profile can be created over time by sampling at specific coordinates along the reactor's length (Figure 1.1). This

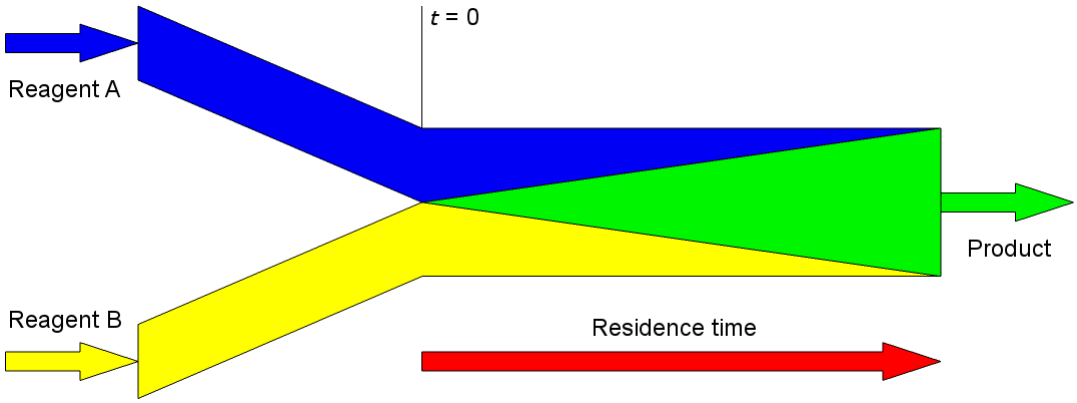

Figure 1.1: Change of concentration of starting material in flow.

is further exemplified by the concept of reaction time; in batch this is determined by the period a reaction vessel is held at a specific temperature. This is somewhat

different in flow, where these parameters are given by the volumetric capacity of the reactor and the flow rate at which material is injected into the reactor. This then corresponds to a residence time for a perceived theoretical fluid plug traversing through the system.

In summary, to successfully adopt flow chemistry, several fundamental changes in synthesis planning and execution are required. As a result, the benefits gained from adopting flow chemistry must be worth the change in working practice. After all, chemists have had over a quarter of a millennium since Antoine-Laurent de Lavoisier established 'modern chemistry' and so questions should be asked as to why change is required? This is a difficult question and is best answered by exemplification and highlighting the benefits which have been derived from existing case studies.

1.2.2 Polymers in flow

One of the areas flow chemistry has been productively applied is in polymer synthesis. Over the past twenty years various polymerisation techniques have been translated and evaluated in flow resulting in a comprehensive body of scientific literature. However, only a few review papers summarising the area have been produced. [15–17] Two of the most recent reviews were published by Frey *et al.* [18] and Hutchinson *et al.* [19] and are recommended reading. This introduction aims to give an alternative overview by highlighting the variation in polymerisation techniques used as well as more information on the reactor designs. It also incorporates some additional areas not covered in the previous reviews including the coverage of purification of polymers in flow.

It should be stressed that not all polymerisation techniques or polymer preparations are suited for running in flow. Polymerisation reactions that result in very viscous solutions (gel) or generate extensive solids should in most cases be avoided, as this will cause major issues in flow. [20] However, it should be noted that polymers which form precipitate or suspended particles can be produced when special processing equipment is used. [21] Indeed, several reactor designs have been utilised

including reactors that incorporate a secondary dilution stream, [20] systems with added ultrasonic mini agitation cell devices to create mini emulsions [22] and also two phase plug flow systems. [23] Consequently, reactor design and configuration are critically important factors, contributing to the success of the preparation.

A wide variety of flow set-ups have been used to conduct polymerisation reactions in flow, each possessing its own charactoristics. [15–17, 19, 20] Often fluidic flow regimes within the reactor are used to categorise the reactors, however it should be acknowledged that reactors can have multiple zones with different flow regimes through the incorporation of residence time modules, static mixers and fluid connectors (i.e. T- or Y-connectors). Therefore a variety of flow patterns can be defined, such as laminar flow, tunnel or pipe flow, [24] turbulent flow [25] and Stokes flow. [26]

In straight smooth tubes laminar and near laminar flow regimes and their corresponding residence time distributions are well investigated. [27] A problem which can appear in flow reactors is the lack of turbulent mixing in the polymer synthesis. A polymerisation reaction often involves an increase in viscosity. Polymers can therefore stick to the walls of the reactor distorting their progression and affecting the polymer distribution. Therefore, static mixers and agitators are still favoured when a polymerisation reaction is performed. To further solve this problem of wall fouling, flow pulsing in straight smooth tubes can be applied, [28] which narrows the residence time distribution. [20] To improve the reaction further and prevent the reactor from chocking, coiled tubing reactors can be used, which result in an increase in turbulent flow. The generated counter-rotating vortices increase mixing in a perpendicular direction to the main flow. The use of this type of reactor creates superimposed secondary flow patterns (Dean vortices) leading to enhancing mass and heat transfer over the cross-section of the tubular reactor (Figure 1.2). [20]

For emulsion polymerisation it is particularly important that the shear rates are distributed evenly and large heat exchange areas are of additional value to ensure homogeneous viscosity as the different phases do not mix. To take advantage of

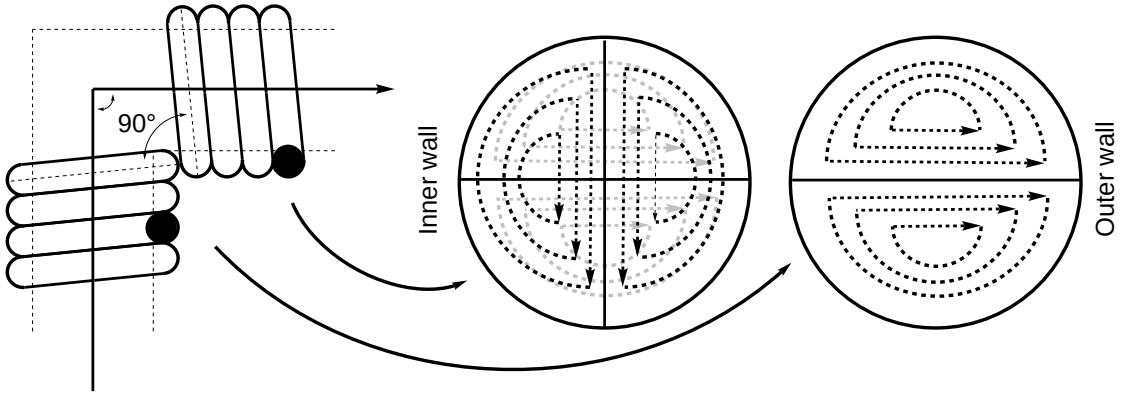

Figure 1.2: Dean vortices produced in a tightly coiled tube reactor.

secondary flow patterns Tanaka *et al.* were one of the first to propose the torus reactor as a suitable device for semi flow/batch suspension polymerisation. [29]

To perform successful suspension polymerisation droplet break-up is important as this determines the resultant particle size. The working principle of a torus reactor (Figure 1.3) is that the dispersion of the flow through the reactor is created by a mechanical stirrer. The stirrer not only moves the dispersion through the reactor, but also superimposes a secondary flow. The high symmetry and the forced

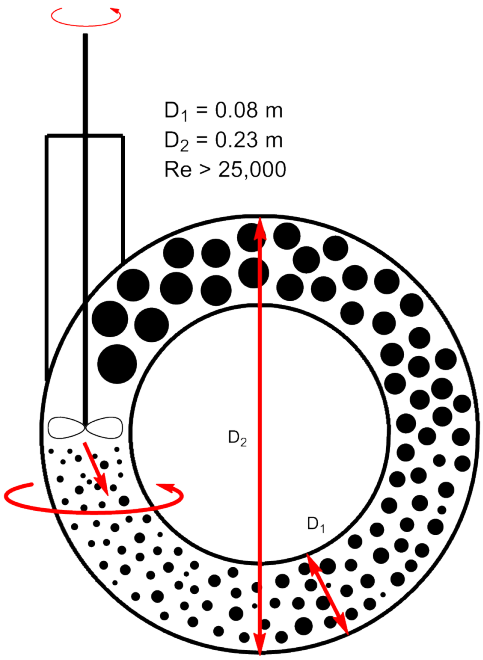

Figure 1.3: Torus reactor for semi flow/ batch emulsion polymerisation, dots are representing the emulsion.

circulation induced should therefore result in a uniform particle size distribution

as droplets will be continuously broken up. The reactor is characterised by a high Reynolds number (R_e) inherent to the improved small dimensional mixing zone but coupled with a potentially batch-like residence time and reactor volume. Of particular note is the higher surface area of this reactor which allows for greater heat transfer compared to an equivalent volume batch reactor.

This reactor type was used by Tanaka *et al.* to perform polymerisation in suspension of styrene and the results were compared to the same polymerisation in batch. [30] Table 1.1 shows the difference between the torus reactor and a normal stirred tank reactor. In this table the dispersity is used as a measure of the degree of uniformity of the droplet diameters. This is defined as the ratio between the standard deviation and the mean diameter (σ/d_p). Therefore, the smaller the dispersity, the higher the degree of uniformity of the droplet produced. Where N_r is the stirrer speed (rotations per second), $\emptyset$ is the styrene monomer volume fraction and C_T is the concentration of the stabilizer (wt-%).

Table 1.1: Comparison of dispersity between torus and stirred tank reactors.

Torus reactor				**Stirred tank reactor**			
N_r	$\emptyset$	C_t	σ/d_p	N_r	$\emptyset$	C_t	σ/d_p
20	0.5	0.3	0.19	4.2	0.5	0.3	0.55
25	0.5	0.3	0.18	5.0	0.5	0.3	0.60
30	0.5	0.3	0.20	6.0	0.5	0.3	0.62
40	0.5	0.3	0.21	7.5	0.5	0.3	0.65
50	0.5	0.3	0.24	8.2	0.5	0.3	0.66

The particle size distribution (σ/d_p) in the Torus reactor is more consistent when compared to the stirred tank reactor (Table 1.1). This can be explained by the rotatory stirrer which induces gravitational forces and thus a more even density gradient. As a result, the dispersed phase is homogeneously distributed and therefore a better option for suspension polymerisation. [30]

Mass transport limitations are not an issue for slow polymerisation processes. Unfortunately, there is very little literature describing the mass transfer coefficients of different monomers. Furthermore, the solubility of the monomer in the polymer

matrix will differ for different monomers.

To perform emulsion polymerisation in flow, a Couette-Taylor vortex reactor was selected by Imamura *et al.* [31] The reactor consists of a rotating inner cylinder and fixed outer cylinder with an inlet at the bottom and an outlet at the top. [32–34] The rotation speed of the inner cylinder influences the mixing of the material (see Figure 1.4). A threshold needs to be overcome before the reactor will have the desired effect (flow). This threshold is given by the dimensionless Taylor number (T_a) and can be calculated by equation 1.1. The threshold, also known as the critical Taylor number, needs to exceed the value of 60 to perform as a flow device.

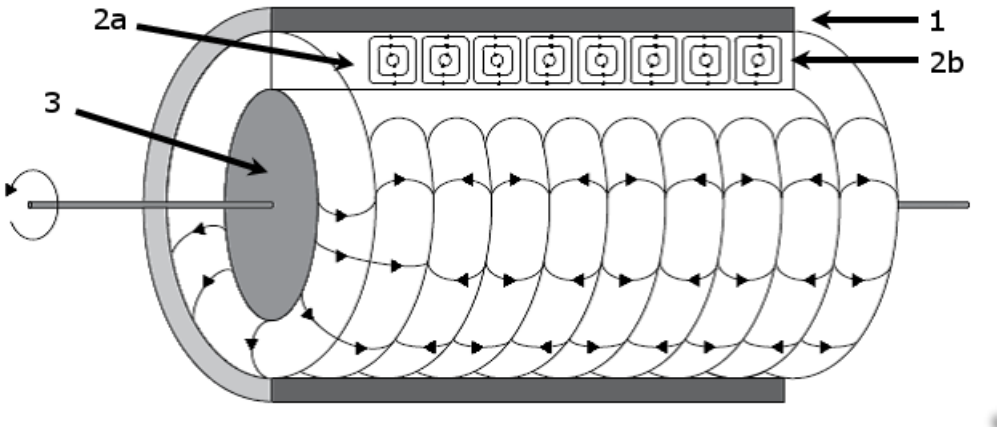

Figure 1.4: Couette-Taylor vortex reactor with 1, stationary outer cylinder; 2, Taylor vortices clock wise (2a) and anti-clock wise (2b); and 3, rotating inner cylinder. [32–34]

$$T_a = \left(\frac{\omega b R_i}{\nu}\right)\left(\frac{b}{R_i}\right)^{1/2} \tag{1.1}$$

R_i = inner cylinder radius (cm), b = radial clearance between concentric cylinders, ν = kinematic viscosity ($cm^2\ s^{-1}$) and ω = angular velocity of inner cylinder (s^{-1}).

Nomura *et al.* compared a Couette-Taylor vortex reactor, a pulse flow system and a continuous stirred tank reactor to perform the emulsion polymerisation of styrene. [35] Specifically the effects of initiator concentration and emulsifier feed, the Taylor number (rotation speed of inner cylinder) and the reactor mean residence time on

the steady-state monomer conversion and particle number were screened.

Using a pulse flow reactor a high monomer conversion was obtained. The continuous stirred tank reactor resulted in significantly less polymeric particles and a lower monomer conversion (approximately 60% for pulse flow reactor and 40% for continuous stirred tank reactors). The emulsion polymerisations performed in the Couette-Taylor reactor showed that all values between the range of the pulse flow reactor and continuous stirred tank reactors could be obtained. The dispersity of polystyrene particles obtained *via* batch emulsion polymerisation was 1.08 and *via* laminar vortex flow reactor 1.31. [31] This could be due to the laminar flow as perfect mixing is not achieved.

In comparison, the same polymerisation was performed using continuous seeded emulsion polymerisation of an aqueous solution of styrene (36 g L^{-1}) containing 0.4 g L^{-1} of the emulsifier (sodium lauryl sulfate), 1.0 g L^{-1} of initiator (potassium persulfate) and 8.9 g L^{-1} seeding material (polystyrene latex) was performed at 70 °C. The emulsion was measured using an electron microscope to determine the dispersity. The dispersity of the particles performed in the Couette-Taylor vortex flow reactor ($Đ = 1.05$) was similar to the dispersity found using the pulse flow reactor. A pulse flow reactor was preferred over a continuous stirred tank reactor, as the monomer conversion and amount of particles using a pulse flow reactor were higher.

A Couette-Taylor flow reactor was also used to study the continuous emulsion polymerisation of vinyl acetate. [36] In this process sodium lauryl sulfate was used as an emulsifier and potassium persulfate as the initiator. The results obtained were not consistent with the previous experiments conducted using styrene. The monomer conversions essentially mirrored the polymerisations performed in a continuous stirred tank reactor. However, the use of a pulse flow reactor was also evaluated for the same process and the conversion was found to be much higher. The continuous emulsion polymerisation of vinyl acetate was performed at 50 ± 0.5 °C, emulsion concentration of 700 g L^{-1} water, monomer concentration 200 g L^{-1}

water, initiator concentration 1,250 g L^{-1} water and a rotation speed of 45 rpm. Resulting in an approximate conversion of 91% in 32 minutes. A corresponding batch reaction gave conversion of 21% within 30 minutes. However, a potentially major problem for the plug flow reactor was the diffusion of material in the axial direction a phenomenon which has been described in several papers. [25, 26, 37–40] The drop of conversion for vinyl acetate compared to styrene can be explained by the stability of the obtained radical. Propagating styrene radicals can be stabilised by the phenyl ring. Vinyl acetate does not have stabilising groups and therefore termination will be more likely. For polymerisation in flow this means potentially less control over the molecular weight can be achieved.

1.3 Review of polymerisation techniques

1.3.1 Controlled radical polymerisation

The modern polymerisation techniques give greater control over polymers than they used to. It is now readily possible to tune polymers and design advanced structures having specific physical and chemical properties.

Controlled radical polymerisation (CRP) was first disclosed over thirty years ago [41] and has since been extensively used to prepare a variety of polymers in both academic and industrial settings. The value of CRP is simple; it enables the synthesis of macromolecules with complex architectures and well-defined microstructures. [42] These same macromolecules could alternatively be synthesised *via* ionic living polymerisation techniques but with much less precision. [43] CRP competes with both the high standard of ionic polymerisation (ionic polymerisation is relatively insensitive to temperature and could be performed at low temperatures, therefore, it will form more regular polymers) and the versatility of free radical polymerisation with regards to (chemical) impurities, process parameters (exothermic reactions), choice of monomer and operational conditions. It not only enables control over the polymeric architecture, which includes molecular weight, dispersity, functionality

and composition, it also minimises the occurrence of premature termination. Therefore, the dispersity is very narrow, allowing to use these polymers as standards for Gel Permeation Chromatography (GPC) in the measurements of molecular weights.

Despite the numerous benefits there are relatively few examples of CRP being used at large industrial scale compared to free radical polymerisation. The main reasons are that the polymerisation rate is significantly slower (the lifetime of growing chains is more than one hour) than compared to free radical polymerisation (the lifetime of growing chains is about one second), there is a need for the addition of an extra mediating or chain-transfer agent and the cost of these agents. [44, 45] This mediating or chain-transfer agent is often required in stoichiometric amounts relative to the number of chains being formed. These additives are often toxic and/ or harmful and so need removal before formulating the final product. This necessitates the purification of the material from the polymer; a potentially very costly process on an industrial scale. [46] This means there is room for improvement of the cost/ performance ratio.

Copper mediated CRP can be divided in three main categories, nitroxide mediated polymerisation (NMP), [47, 48] reversible addition fragmentation transfer (RAFT) polymerisation [49] and atom transfer radical polymerisation (ATRP). [50–53] Of these three techniques, ATPR has attracted most of the attention, resulting in substantial progress regarding increasing the polymerisation rate and decreasing the concentration of chain-transfer agent.

1.3.1.1 ATRP reactions

As a consequence of the body of work investigating ATRP has led to the development of several sub-categories such as activator regenerated by electron transfer (ARGET) ATRP, [54] initiators for continuous activator regeneration (ICAR) ATRP, [55] supplemental activator and reducing agent (SARA) ATRP, [56] single electron transfer living radical polymerisation (SET-LRP) [57] and photoinduced ATRP. [58] A specific discussion regarding the mechanisms of SET-LRP and SARA-ATRP will not

be examined within this thesis but can be found in the following citations (some terminology used in the cited articles is utilised herein). [57, 59, 60] Both reactions involve the same components but follow a different set of mechanistic steps (Figure 1.5).

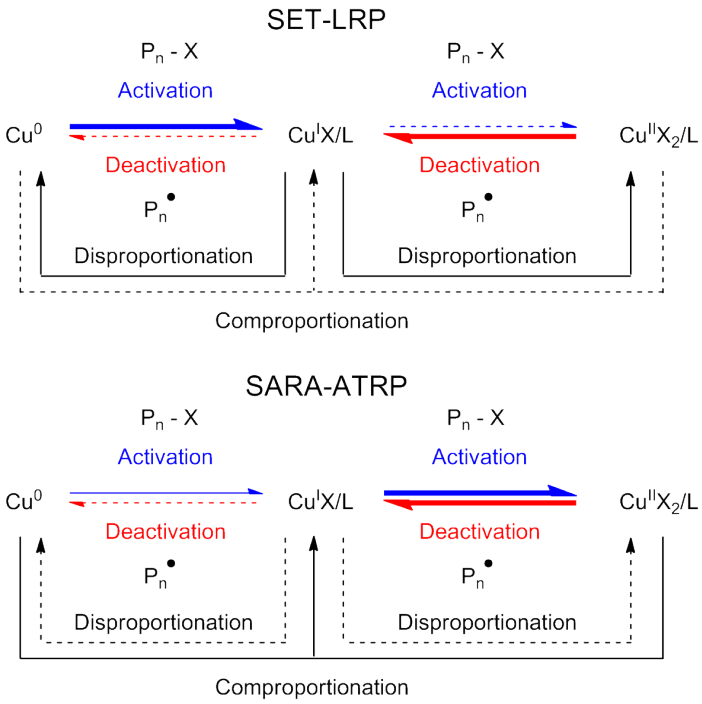

Figure 1.5: SET-LRP and SARA-ATRP mechanism.

These variations of ATRP all have reasonable polymerisation rates and therefore can be conducted with reduced levels of catalyst (Table 1.2) due to improved copper complexes. The reduction of catalyst is advantageous within industrial processes as it results in lower purification costs. Furthermore, these modified ATRP polymerisations utilise Cu(II) instead of Cu(I) which is known to be particularly air sensitive.

1.3.1.2 ATRP reactions performed in flow

The mechanism of ATRP has been studied extensively. [50–53] The individual steps for ATRP are shown in Figure 1.6. The polymerisation starts with the initiation of an alkyl halide or dormant polymer, in Figure 1.6 indicated with P_n – X. This species is often activated by a Cu(I) complex and forms an active polymer chain

Table 1.2: Catalyst amounts in ppm for different ATRP techniques.

Type of polymerisation	Amount of Cu(I) (ppm)	Amount of Cu(II) (ppm)
ATRP [61]	>10,000	variable
ARGET ATRP [62]	0	5
ICAR ATRP [55]	0	10
SARA ATRP [63]	0	100
Photoinduced ATRP [64]	0	100
Reverse ARTP [65]	0	1,000

and a Cu(II) complex which is now a deactivator. The active polymer chain then undergoes propagation, deactivation or termination. The dominant reaction process is deactivation promoted by the Cu(II) complex which upon reaction reforms the activator [Cu(I)] and a dormant chain. The kinetics of this step are highly dependent on the redox potential of the copper complex, as well as the stability of the radical formed. If the ratio between k_{act} and k_{deact} is small, control over the propagation step will be lost and a runaway reaction occurs.

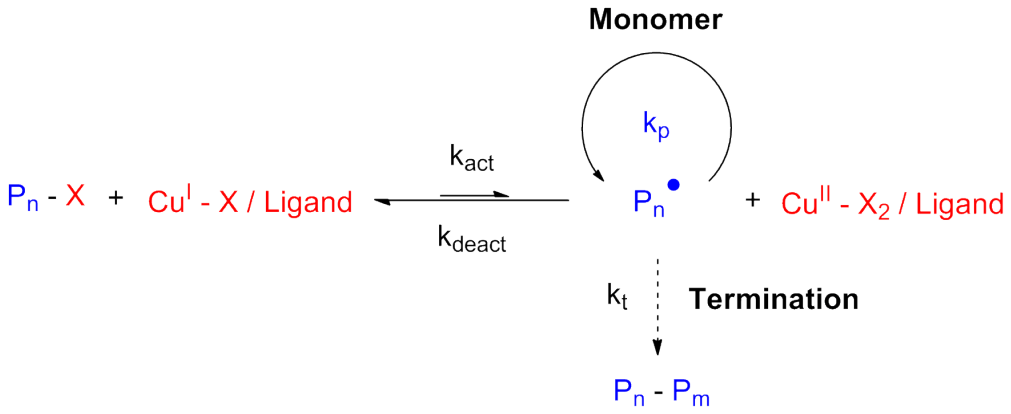

Figure 1.6: ATRP mechanism.

The first reported ATRP performed in flow was conducted on methyl methacrylate (MMA) by Zhu *et al.* in 2000. [66] The flow system was constructed from commercially available parts using a metering pump and a column packed with CuBr-hexamethyltriethylenetetramine (HMTETA). It was shown that when using low flow rates (long residence times) high conversions were obtained. The highest conversion (87%) was obtained using a flow rate of 1.2 mL h^{-1} equating to a resi-

dence time of 300 minutes. [NOTE: In the paper a flow rate of 1.2 mL min^{-1} was stated (page 957) [66] but also 1.2 mL h^{-1}. I have interpreted the results based upon a value of 1.2 mL h^{-1}, as this is more logical.] The conversion dropped to 23% at a higher flow rate of 9.6 mL h^{-1} (40 minutes residence time). Furthermore, the longer residence time also resulted in higher molecular weights (11,000 g mol^{-1} for 300 minutes and 5,000 g mol^{-1} for 40 minutes). Unfortunately, this reactor set-up was not competitive with traditional batch chemistry in terms of dispersity of the polymer molecular weights. [67] The molecular weight range in batch was 2,800 – 15,200 g mol^{-1} with conversions varying between 21% and 87%. Whereas for the flow system it was in the range of 3,400 – 11,000 g mol^{-1} with 23 – 87% conversion respectively. The dispersity in flow was around 1.80 (conversion 87%) compared with 1.15 (conversion 70%) in batch.

A tubular reactor (10 mL) has also been used to polymerise methyl methacrylate using ATRP by Haddleton *et al.* [68] High conversions and similar molecular weights were obtained to those achieved by Shen. [66, 67] For this flow reaction CuBr-*N*-*n*-octyl-2-pyridylmethanimine (CuBr-NOPMI) was used as the catalyst and *t*-butyl-2-bromoisobutyrate (*t*BiB) was used as initiator. The dispersity achieved using this set-up was considerably better, namely 1.06 at 90 °C, with a conversion of 60.7%, a residence time of 150 minutes and molecular weight of 11,000 g mol^{-1}.

The authors claimed good control over number average molecular weight, dispersity and conversion. As expected at higher flow rates, lower conversions were achieved (Table 1.3). Changing the ratio between monomer and initiator was also shown to influence the molecular weight with an increase in the ratio resulting in a corresponding rise in molecular weight (Table 1.3).

The reactor set-up was also modified to perform block co-polymerisation reactions. A second inlet was added after the first reactor (10 mL) and connected to a second reactor (10 mL) *via* a T-piece. A solution of methyl methacrylate dissolved in toluene was pumped through the first reactor (10 mL), at a flow rate of 3.0 mL h^{-1}, a block polymer of poly(methyl methacrylate) was obtained after 180 minutes

Table 1.3: Influence of flow rate and ratio on the polymerisation of methyl methacrylate.

Flow rate (mL h^{-1})	**Ratio** [MMA]/[*t*BiB]	**Conversion** (%)	M_n (g mol^{-1})	$Đ$
5.0	50	81.9	6,370	1.13
20	50	33.7	5,000	1.12
2.5	100	89.9	13,200	1.07
5.0	100	60.7	11,000	1.06
20	100	16.0	6,240	1.06
2.5	200	61.4	18,200	1.09
5.0	200	36.5	12,700	1.09

(conversion = 70%, M_n = 12,600 g mol^{-1}, $Đ$ = 1.12) (Figure 1.7). Addition of a second flow, containing *n*-butyl methacrylate (*n*BMA) also dissolved in toluene, with a flow rate of 1.8 mL h^{-1} and a residence time of two hours resulted in an 18% conversion of *n*BMA. The polymerisation was not completely selective as a gradient co-polymer of MMA (5%) and *n*BMA was formed. The value of M_n also increased to 16,000 g mol^{-1} with a corresponding dispersity of 1.2.

Further co-polymerisations with longer residence times for the second stage polymerisation were performed to improve the conversions and increase the molecular weight. This was realised by shortening the first reactor and decreasing the flow rate; from 10 mL reactor volume with flow rates of 3 mL h^{-1} to 5 mL reactor volume and a flow rate of 1.5 mL h^{-1}. The flow for the second reactor was 1.8 mL h^{-1}. Under these conditions the conversion of *n*BMA increased slightly (17 – 21%) and the molecular weight rose from 16,300 g mol^{-1} to 23,200 g mol^{-1} with a dispersity of around 1.10 for all experiments. In analogy, benzyl methacrylate was also successfully used to form a range of co-polymers in combination with MMA (M_n = 15,300 – 29,100 g mol^{-1} and $Đ$ = 1.22 – 1.49).

However, *n*-butyl acrylate (*n*BA) was not successfully co-polymerised with MMA. The reasons for this might be due to insufficient reaction time (80 minutes), using similar reaction conditions a conversion of 50% was reached [69] albeit after ten hours. Another reason might be the failure of the activation of the propagation reaction involved in the polymerisation. The rate constants of propagation are in the

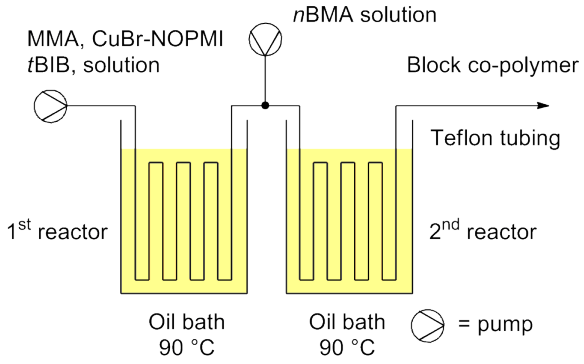

Figure 1.7: Block co-polymerisation set-up MMA and *n*BMA.

following order: methacrylates > styrene > acrylates, according to the literature. [70] The equilibrium constants for the activation of methacrylate polymerisation are much smaller than those of *n*-butyl acrylates. [71] A possible solution, which was presented in the paper, was the introduction of CuCl in the second step of the polymerisation to enable an halogen exchange. [72]

Serra *et al.* recently published on the polymerisation of 2-(dimethylamino)ethyl methacrylate (DMAEMA) using ATRP. [73] The paper highlighted an improved reactor design where, instead of a capillary spiral type coiled tube, a coil flow inverter reactor was used. [74] A coil flow inverter reactor contains four 90° angles in the coiled tube and therefore better mixing was obtained. The latter flow coil gave marginally improved monomer conversion (74 ± 1% versus 71 ± 1%) and was also associated with a marginally increase in molecular weight (22,874 g mol^{-1} versus 21,142 g mol^{-1}) and a decrease in dispersity (1.43 versus 1.53) using identical operating parameters. Independent of the reactor length and tube diameter the coil flow inverter reactor gave improved results over the coiled tube reactor.

Increasing the scale of a reaction in flow requires systems which can process larger volumes of fluid or the total collection time has to be increased, which is not always favourable in industry. This can, for certain processes, easily be achieved by increasing the diameter of the reactor tubing or increasing the length of the reactor which, in combination with higher flow rates, results in equatable residence times but greater throughput. However, often this changes critical reactor characteristics such as mixing or heat transfer that influence the quality of the polymers produced.

An example was shown by Serra *et al.* [73, 74], dispersity was considerably increased ($Đ = 1.43$ versus 1.59) moving from a small diameter tubular reactor (inner diameter = 876 μm) to a larger coil flow inverter reactor (inner diameter = 4,083 μm). [73, 74] Alternatively, multiple smaller systems can be combined to work in parallel (numbering-up principle). It is likely however, this will substantially increase the equipment costs. To operate systems in parallel fed by one inlet is technically challenging. This is due to the fact it is hard to evenly divide the flow stream.

Co-polymerisation of DMAEMA and benzyl methacrylate (BzMA) have been conducted in flow as reported by Parida *et al.* using ATRP conditions. [75] The reactor set-up comprised of two pumps, a micromixer and a coiled tube reactor (Figure 1.8). The study showed the importance of effective mixing by evaluating various mixing devices such as a simple T-junction, an interdigital multi-lamination (Figure 1.9) and an impact jet micromixer. Statistical co-polymers of DMAEMA and BzMA were synthesised in batch and in flow, containing 20% and 40% BzMA composition (by molecular weight). As an initial assessment the difference in conversion between batch and flow was determined and was established as +31% and +35% for BzMA and DMAEMA respectively, in favour of flow. The type of in-line flow mixer did not influence the total conversion. Interestingly, changing the composition of BzMA did have an influence on the total conversion using batch chemistry but not when evaluated using flow conditions. After one hour the viscosity was noticeably increased along with the dispersity (Table 1.4). This rise in viscosity affects the ongoing polymerisation, as it leads to slower mass diffusion and hence poor polymer growth and more termination. Here flow proved particularly valuable by allowing improved mixing using a multi-lamination mixer. Utilising this device improved control over the molecular weight and reduced dispersity was achieved (Table 1.4).

SET-LRP has been performed in flow using a simple set-up, as described by Haddleton *et al.* [77] SET-LRP is a robust and versatile method to polymerise vinyl monomers at ambient temperatures. To perform this type of polymerisation a Cu(0)

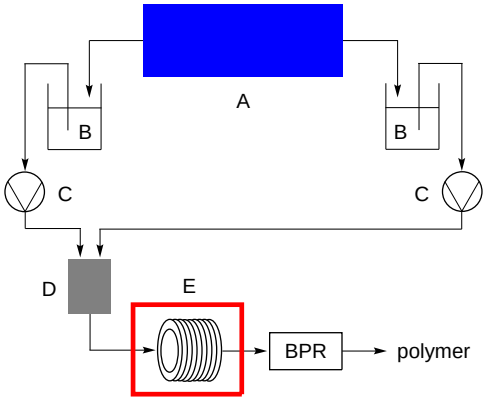

Figure 1.8: Reactor set-up for co-polymerisation of DMAEMA and BzMA. (A) Nitrogen generator, (B) reservoirs, (C) HPLC pump, (D) micromixer, (E) microreactor inside oven (60 °C).

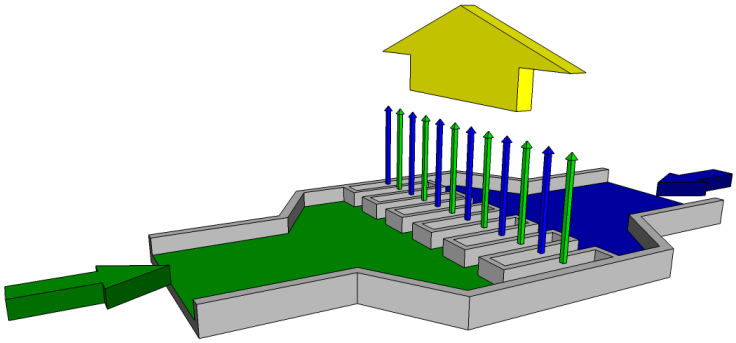

Figure 1.9: Operating principal of the interdigital micromixer. [76]

derived catalyst is used. The polymerisation sequence starts with the activation of the initiator or dormant polymer chain by Cu(0)/CuX_2 species (Figure 1.10). The solvent of choice is usually a polar solvent which is important. [78, 79] Solvents such as H_2O, alcohols, dipolar aprotic solvents, ethylene and propylene carbonate, and ionic liquids help disproportionate CuX into Cu(0) and CuX_2 species very rapidly in the presence of *N*-containing donor ligands. Therefore, *N*-containing donor ligands that destabilise Cu(I) species are used. Induction of the catalytic cycle is proposed to occur *via* the heterolytic dissociation of the C-X bond promoted by a Cu(0) mediated outer sphere electron transfer. Following this, CuX is generated but rapidly disproportionates to yield inactive CuX_2 and regenerating an active Cu(0) atom.

SET-LRP has a few inherent limitations, such as strong exotherms and long induction periods. However, if the reactor design is chosen carefully these limitations

Table 1.4: Influence of flow rate and ratio on the co-polymerisation of BzMA and DMAEMA.

Reactor	Sample BzMA	DMAEMA (%)[b]	BzMA (%)[b]	Theoretical M_n	M_n (g mol^{-1})	$Đ$
Batch	20%	44.75	41	14,315	11,095	1.62
Batch	40%	45.2	48	15,208	13,457	1.55
Flow[a]	20%	55.55	61.8	18,523	17,210	1.50
Flow[a]	40%	59.5	64.9	19,705	18,847	1.54

[a] Flow reactor, multi-lamination mixer.
[b] Conversion DMAEMA and BzMA as determined by ^{1}H NMR.

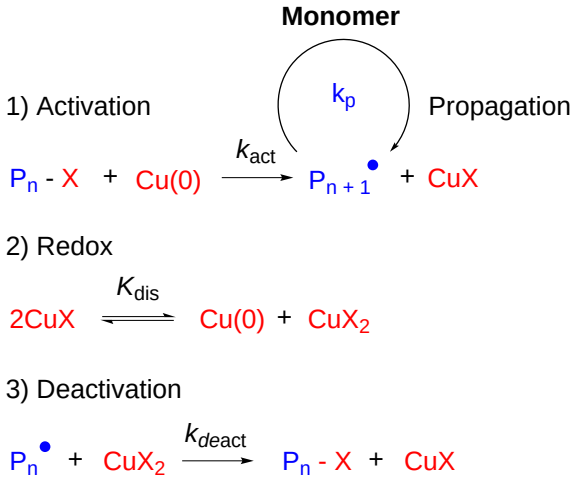

Figure 1.10: Mechanism SET-LRP.

can be mitigated against. Hutchinson *et al.* designed a flow reactor made from copper tubing. [80–82] This idea [81] was inspired by a prior paper [80] which instead of using a copper reactor comprised of PTFE tubing with a Cu(0) wire threaded insert. The results were remarkable for the simple set-up used. [81] It was noted that the flow rate greatly affected the molecular weight with longer residence time (thus longer contact time) leading to much higher molecular weight. Increasing the flow rate from 0.05 mL min^{-1} to 0.3 mL min^{-1} and therefore decreasing the residence time (80 to 13 minutes) decreased the molecular weight from 4,200 g mol^{-1} to 3,200 g mol^{-1}. A high 90% conversion was achieved at the low flow rate with a reasonable 69% conversion at the high flow rate. The dispersity was also reported as being very low (1.14 – 1.20) for all flow reactions performed. Overall the obtained results were comparable with equivalent batch procedures. [83] However, in the flow process

operation safety was increased as runaway reactions were prevented.

1.3.1.3 Nitroxide mediated polymerisations

Nitroxide mediated polymerisation (NMP) is controlled by the formation of a capped propagating chain. The chain extends through addition of a monomer to a reversibly generated radical (Figure 1.11). The nitroxide thus acts as a control agent mediating the reaction through the inert alkoxyamine as the predominant species. Homolytic cleavage is most often induced through thermolysis.

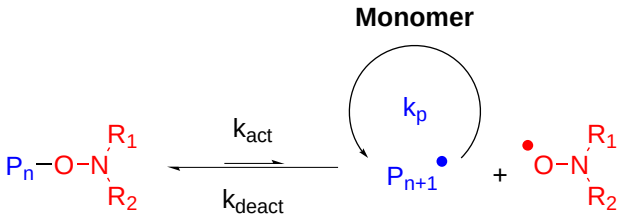

Figure 1.11: Nitroxide mediated polymerisation mechanism.

1.3.1.4 Nitroxide mediated polymerisations in flow

Nitroxide mediated polymerisations have also been performed in flow although not at the same scales as the related ATRP's. [84, 85] Cunningham *et al.* described the preparation of a latex polystyrene homo-polymer *via* nitroxide mediated polymerisation. [86] This research was published over two papers. In the first publication the initial step, the polymerisation of styrene in the presence of TEMPO, was performed in a batch reactor while the mini-emulsion styrene polymerisation was performed in a continuous tubular reactor. In the subsequent paper the total polymerisation process was fully conducted in flow.

The dispersity measured from both batch and flow polymerisations were similarly narrow being analysed as between 1.14 and 1.20. The major difference observed between the flow set-up and batch processing mode was a lower average molecular weight and reduced conversion in batch compared to in flow. This is most likely explained by the longer reaction times in batch provided by the extra time required to warm up and cool down the reactor. Additionally due to different temperature

regimes the associated rates of the polymerisation will differ. By contrast the flow reactor is essentially preheated and thermally balanced with a fixed temperature regime for the entire polymerisation.

The material obtained from the first stage flow polymerisation was further processed *via* mini-emulsion polymerisation in a continuous flow tube reactor to synthesise a latex polystyrene homo-polymer. The latex was formed by dispersing the 'living' polymer chains and styrene monomer into an aqueous phase. Using styrene as monomer, an average M_n of 15,500 g mol^{-1} with relatively narrow dispersity of 1.19 was obtained GPC. This stands well against an anticipated theoretical value of 17,211 g mol^{-1}.

As these experiments demonstrated that the polymer chains were still 'alive', it enabled their extended use in the formation of di-block co-polymers. Subsequently the synthesis of a di-block co-polymer with *n*-butyl acrylate was performed. A broader distribution compared to the mono-polymer was obtained (1.25 versus 1.19). In addition, the number-average molar mass for the di-block co-polymer was only 20,500 g mol^{-1}, indicating that only moderate conversion of *n*-butyl acrylate was achieved. To increase the reactivity ascorbic acid was dosed into the reaction as an additive. As a result it was found that higher conversion could be achieved but at the expense of the concentration of living polymer chains which had a corresponding negative influence on the dispersity (1.34 mono-polymerisation, 1.92 di-block co-polymerisation). The achieved M_n for homo-polymerisation was 24,300 g mol^{-1} where the theoretical M_n was 19,124 g mol^{-1} and for co-polymerisation the achieved M_n was 37,200 g mol^{-1} where the theoretical M_n was 28,366 g mol^{-1}. [86]

Finally, the di-block co-polymer was further processed to form a tri-block co-polymer using styrene. This second chain extension was also performed in the continuous tubular reactor resulting in a tri-block co-polymer with a number-average molar mass of 57,876 g mol^{-1} and dispersity of 2.30. This simple designed system shows the ability of flow reactors to perform multiple reactions in-line, resulting in a more continuous output of advanced polymer architectures.

1.3.1.5 RAFT polymerisation

Reversible Addition-Fragmentation chain Transfer (RAFT) is another controlled radical polymerisation method. With this polymerisation technique additional control over molecular weight, molecular weight distribution, composition and architecture is gained. This method is also suitable for a wide range of monomers. The most common functional polymerisation head is the trithiocarbonate group although benzyl benzodithioate, 1-(methoxycarbonyl)ethyl benzodithioate and many others can also be employed. [87]

1.3.1.6 RAFT polymerisation in flow

RAFT polymerisation in continuous flow was first reported by Seeberger *et al.* in 2010, [88] twelve years after its discovery at the Commonwealth Scientific and Industrial Research Organisation in 1998 (CSIRO, Australia, Melbourne). [49] It was demonstrated that, in general, a decrease in reaction time could be achieved from the traditional batch process. As an aside, an investigation into the use of microwave irradiation of reactions showed reaction times similar to the flow polymerisations. The flow set-up used to polymerise *N*-isopropylacrylamide was a very simple construction prepared from two syringe pumps, a T-piece, PTFE tubing and an oil bath for heating. With this set-up, Seeberger *et al.* managed to obtain good dispersity ($Đ = 1.11$) and molecular weights of ~20,000 g mol^{-1}. Rapid reaction screening was not possible as it took time to heat/ cool the oil bath and the size of the syringes placed a limitation on scale.

Hornung *et al.* only months later showed an interesting RAFT polymerisation using a commercial flow system (Vapourtec R2+/R4). [89] Their paper describes the polymerisation of various monomers, initiators, solvents and RAFT additives (Figure 1.12).

Several flow set-ups were tested before a suitable system was identified. It was highlighted that oxygen exclusion was very important to perform successful RAFT polymerisations. Initially the RAFT polymerisation was performed in a perfluo-

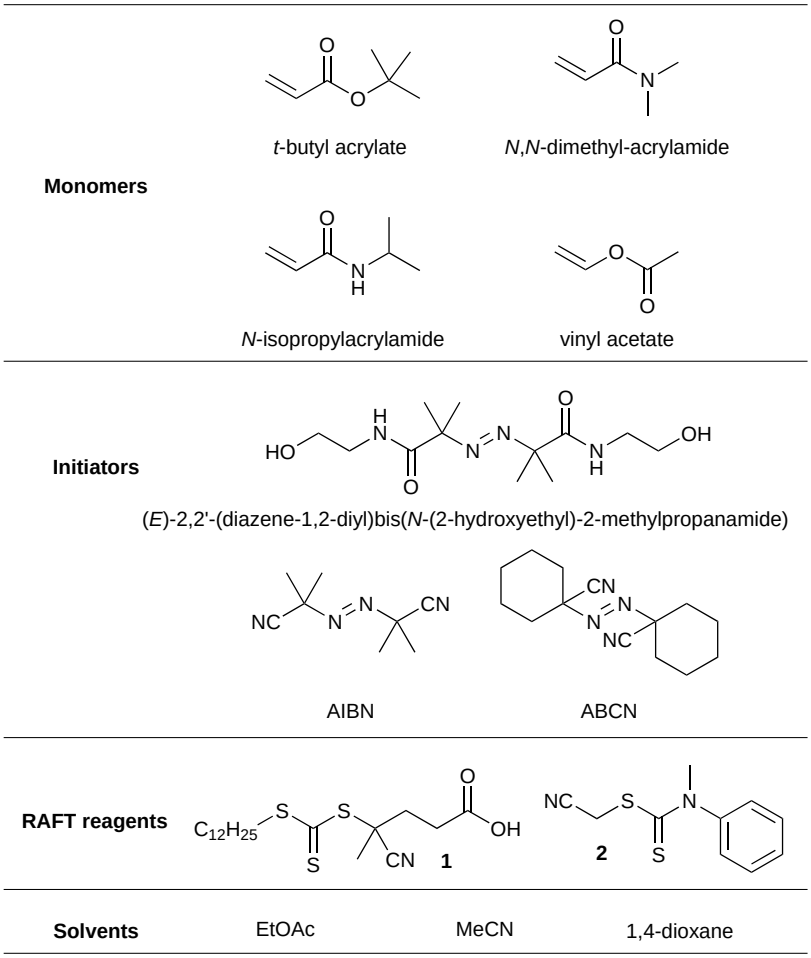

Figure 1.12: Monomers, initiators (AIBN = azobisisobutyronitril, ABCN = 1,1'-azobis(cyclohexane carbonitrile)), solvents and RAFT additives.

roalkoxy alkane (PFA) polymer reactor but failed to give good results. However, using a stainless steel reactor for the polymerisation gave much better result and thus it became clear that PFA polymer reactors were not suitable for oxygen sensitive processes. *N*-Isopropylacrylamide was used as a monomer to determine the preferred flow system (PFA or stainless steel coil) and polymerisation technique. The flow reactions were performed following a segmented flow procedure using a 2 mL loop. It was shown that increased control over the polymerisation could be gained using RAFT but as expected a major decrease in the number average molecular weight was also observed (Table 1.5), as the propagation rate is lower for RAFT compared to free radical polymerisation.

Little difference was observed in the percentage conversion of the monomer, average molecular weight or dispersity between the batch and segmented flow procedure

Table 1.5: Polymerisation of *N*-isopropylacrylamide at 90 °C using free radical polymerisation and RAFT in a batch reactor, PFA and stainless steel flow coil.

Parameters	**Batch**		**Flow PFA coil**		**Flow stainless steel coil**	
Polym. Tech.	free rad	RAFT	free rad	RAFT	free rad	RAFT
Conv. (%)	100	89	77	0	100	85
M_n(g mol^{-1})	316,000	19,500	233,000	-	327,000	20,500
$Đ$	1.78	1.14	1.88	-	1.77	1.17

for the different techniques. Free radical polymerisation in batch or in a stainless steel reactor both gave full conversion and similar number average molecular weight and dispersity. The difference between batch and segmented flow polymerisation is more noticeable when RAFT was used with shorter polymer chains being synthesised compared to batch. Initially due to the high levels of diffusion in the segmented flow the conversion and dispersity achieved was not as good as in batch. This was especially the case for reaction times of less than two hours. For reaction times of two hours, the difference in dispersity between batch and flow was approximately 0.08 higher. However, when a continuous flow polymerisation was performed and steady state was reached, conversion and dispersity were better at reaction times of 1.5 hours (Table 1.6) compared to batch or segmented flow polymerisation.

Table 1.6: Polymerisation of DMA for batch, segmented flow and continuous flow. 80 °C, [DMA] = 1.8 mol L^{-1}, [AIBN] = 5.4 mmol L^{-1}, RAFT additive **1** (Figure 1.12) = 9 mmol L^{-1} in MeCN.

Output	**Batch**	**Segmented flow**[a]	**Continuous flow**[a]
Conv. (%)	97	90	97
$Đ$	1.10 – 1.15	1.16[b]	1.09 – 1.16

[a] Polymerisation performed in stainless steel coil.

A main advantage of the flow set-up described, was the opportunity to perform rapid screening of various reaction conditions, especially as continuous operation was possible. If segmented flow is chosen to perform the screening, it has to be taken into account that diffusion is a major issue and steady state will not be reached. This is important as the concentration will not be the same in the entire plug of the

reaction mixture.

The by Hornung *et al.* designed system [89] was used to investigate other RAFT polymerisations evaluating both scale-up and modification of RAFT polymers in flow. [90–93]

Another report was published on a two stage process involving a RAFT polymerisation of selected monomers (Scheme 1.1). [94] The RAFT polymerisation was followed by aminolysis by polymer-supported or solution phase amines (Scheme 1.1). A UV spectrometer placed in-line allowed for direct analysis of the aminolysis reaction. Following aminolysis conjugate addition to form thioether terminated polymers was conducted which did not have any influence on the dispersity.

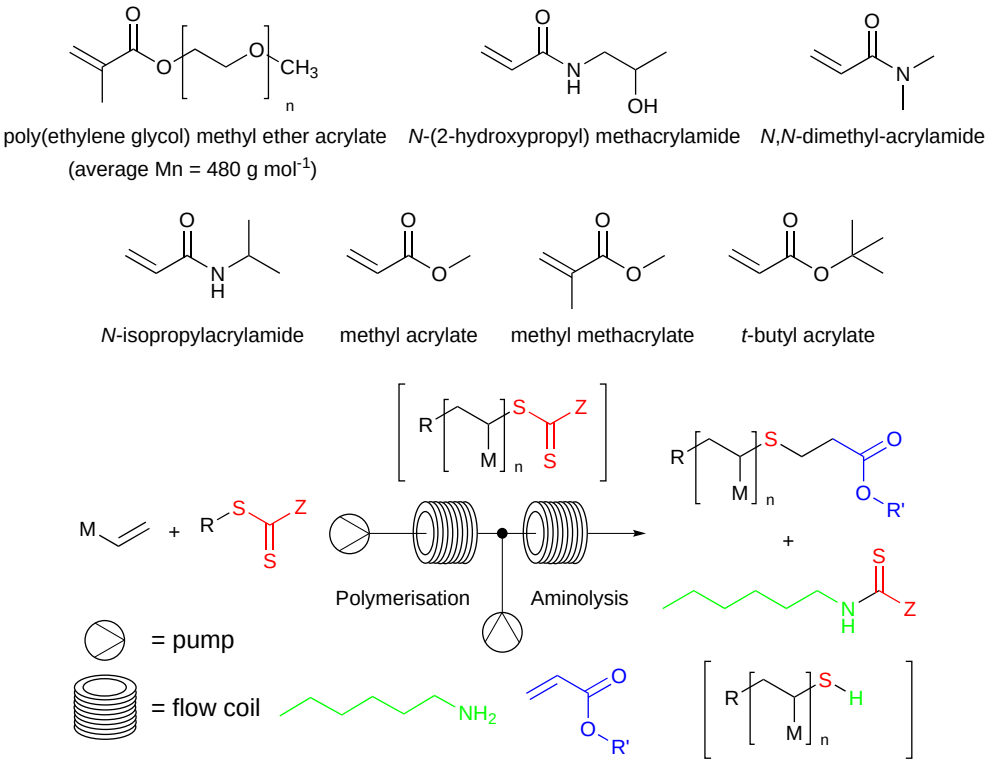

Scheme 1.1: Multi-step RAFT polymerisation and aminolysis.

Thermolysis is an approach used for desulfurisation of RAFT polymers. This has also been described by Hornung *et al.* starting from different RAFT polymers prepared in flow from acrylamides, acrylates, methacrylates and styrenes. [95] The polymer backbone needs to be stable at high temperatures as the thermolysis was carried out between 220 and 250 °C. To perform thermolysis in flow a continuous

set-up was designed (Figure 1.13).

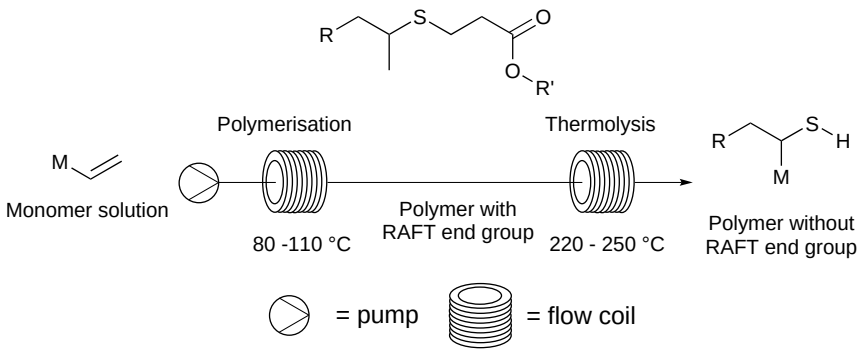

Figure 1.13: Polymersiation and thermolysis in flow.

A comparison between a batch and a flow process for the preparation of poly(methyl acrylate) (pMA) was conducted. The polymer produced was then used for the thermolysis (Table 1.7). The dispersity did not increase significantly and good control was achieved over the two steps. The synthesis of RAFT end group polymers in flow allows for a process to synthesise colourless and non-odorous polymers.

Table 1.7: Polymerisation and thermolysis of pMA.

Type	**Conversion**[a] **(%)**	$\boldsymbol{M_n}$ **(B)**[b] **(g mol^{-1})**	$\boldsymbol{M_n}$ **(A)**[b] **(g mol^{-1})**	$\boldsymbol{Đ}$ **(B)**[c]	$\boldsymbol{Đ}$ **(A)**[c]
Batch	97 / 54	9,900	9,100	1.33	1.33
Flow	96 / 87	8,300	7,400	1.24	1.25

[a] Conversion of monomer / thermolysis
[b] Number average molecular weight Before (B) and After (A) thermolysis
[c] Dispersity Before and After thermolysis

A continuous RAFT polymerisation was conducted as a scale up process by Micic *et al.* [93] They describe the differences between large scale batch processing and scale-up *via* flow. Acrylic acid and 2-acrylamido-2-methylpropane-1-sulfonic acid (AMPS) were used as monomers in an aqueous solution RAFT polymerisation. Conversion in the flow RAFT polymerisation was >90% at a temperature of 80 °C and a reaction time of 40 minutes. In comparison, the batch process showed non-stable temperature profiles. This was particularly noticeable at larger scales with exotherms reaching 98 °C for a 500 mL scale and 17.7 wt-% of the monomer. The same issue was noticed performing the polymerisation in a microwave. Although

the volume was limited to 20 mL instead of 500 mL the temperature rose to 94 °C. This overheating caused higher proportions of radicals resulting in a loss of control over the polymerisation process. The exotherm was not encountered in flow, the temperature profile was stably held at 80 °C. Conversion, number average molecular weight and dispersity for batch and flow polymerisation of acrylic acid were obtained (Table 1.8). A disadvantage of the flow set-up was the requirement for an increase in reaction time. Based on the throughput of the reactor described, it would take about five times longer to process the total volume equating to a single batch. Although it could be argued that this 'lost' time could be recouped during the purification of the polymer produced.

Table 1.8: Conversion, M_n and dispersity of poly(acrylic acid) (**8**) in batch and flow, polymerised at 80 °C, 500 mL scale and 17.7 wt-% acrylic acid.

Type	**Conversion (%)**	$\boldsymbol{M_n}$ **(g mol^{-1})**	$\boldsymbol{Đ}$
Batch	97.4	21,600	1.45
Flow	94.7	23,200	1.53

Junkers *et al.* developed a flow protocol for the synthesis of acrylate multi-block co-polymers using RAFT polymerisations. [96] Poly(*n*-butyl acrylate) (P*n*BuA) was synthesised in flow using different RAFT reagents. By tuning the reaction parameters various molecular weights could be produced. The key parameters controlling the molecular weight were the reaction time and ratio of monomer to RAFT reagent. The dispersity of the P*n*BuA polymers was retained within the expected limits (1.10 - 1.13) for this type of polymerisation. The functionalised material was subsequently used in co-polymerisations with different acrylates (ethyl hexyl acrylate, *tert*-butyl acrylate and *n*-butyl acrylate) in a microreactor. Ultimately a co-polymer with five different acrylate blocks was synthesised with a number average molar mass of 32,000 g mol^{-1} and a dispersity of 1.46. Directly comparing flow and batch co-polymerisations indicated better results for the flow process. For example, the co-polymer P*n*BuA-b-P*t*BuA-b-PEHA had a number average molar mass of 10,700 g mol^{-1} in flow and 9,300 g mol^{-1} in batch with dispersity of 1.28 and

1.93 respectively. This provides a highly convincing case as to the strength of flow chemistry for polymer synthesis.

1.3.2 Free radical polymerisation

Continuous free radical polymerisation of acrylic acid was performed by Qui *et al.* [97] As part of this work, a study of the kinetics of free radical polymerisation of acrylic acid in a micro reactor device, using potassium persulfate as initiator, was performed. The designed reactor allowed different reaction times as a switch-on valve (5-way tap) was introduced to alter the reactor length. Quick screening was possible allowing rapid access to kinetic parameters. The kinetic orders of acrylic acid and potassium persulfate were determined as 1.5 and 0.5 respectively, which were in line with the literature values. [98, 99] The measured activation energy was 67.4 kJ mol^{-1} which was in line with the previous literature. [99] Different polymers with variable molecular weights were synthesised, ranging from 103,326 g mol^{-1} to 176,052 g mol^{-1}. The dispersity was slightly broader compared to controlled radical polymerisation, but still good for a free radical process. Poly(acrylic acid) with the smallest molecular weight (103,326 g mol^{-1}) had a dispersity of 2.42 and poly(acrylic acid) with the highest molecular weight (176,052 g mol^{-1}) had a dispersity of 2.03. This design is particularly suitable for screening multiple parameters. The residence time could be increased easily by adding additional residence loops without changing the flow rate. Other free radical polymerisations in flow were performed by Yoshida *et al.* involving the polymerisation of butyl acrylate, benzyl methacrylate, methyl methacrylate, vinyl benzoate and styrene using AIBN as initiator for the reaction. [100] Similar molecular weights were obtained. The dispersity in flow for butyl acrylate was much lower compared to batch (3.14 versus 9.61), which was explained by the efficient removal of heat. Benzyl methacrylate (dispersity in flow 1.98 versus dispersity in batch 2.71) and methyl methacrylate (dispersity in flow 1.83 versus dispersity in batch 2.21) showed a smaller improvement for the dispersity. Vinyl benzoate (dispersity in flow 1.16 versus dispersity in batch 2.16) and styrene (dis-

persity in flow 1.76 versus dispersity in batch 1.76) gave similar dispersity for batch and flow. These reactions indicate flow chemistry could be used for a variety of free radical polymerisations.

1.3.3 Ionic polymerisation

The advantage of ionic polymerisation over radical polymerisation is the higher control over dispersity and molecular weight. The main drawback of ionic polymerisation is its sensitivity to impurities in the solvents and starting materials and high variation response to even small changes in processing parameters. Flow chemistry has also demonstrated its value to ionic polymerisation processes. Recently Nyrop *et al.* published an article comparing flow and batch polymerisation for the synthesis of vinyl ether terpolymers. [101] Their report focused on the preparation of polymer-siRNA (small interfering ribonucleic acid, siRNA is double stranded RNA and has a typical length of 20 - 25 base pairs) conjugates for utilisation in biomedical and medicinal chemistry. Specifically for such medicinal applications the ability to accurately control the polymeric structure was critical. A cationic polymerisation was chosen to generate vinyl ether terpolymers using BF_3OEt_2 as a Lewis acid catalyst. The polymers derived from flow processing were shown to be reproducibly more consistent and therefore better starting materials for formulation of the polymers – siRNA conjugates. This was highlighted through the better *in vivo* performance of the prepared conjugates (Figure 1.14).

Living anionic polymerisation was first comprehensively performed in flow as a means to study polymerisation kinetics. This research was undertaken by Szwarc *et al.* and Schulz *et al.* in the mid-sixties. [102–107] The technique then lay dormant for a time before being expanded upon recently by Müller *et al.* who investigated the living anionic polymerisation of 2-vinylpyridine and styrene in continuous flow. [76] Two different flow set-ups were compared. The first used an interdigital micromixer, resulting in laminar mixing. The second set-up used a tangential four-way jet mixing device resulting in a more turbulent flow regime (Figure 1.9 and 1.15). It quickly

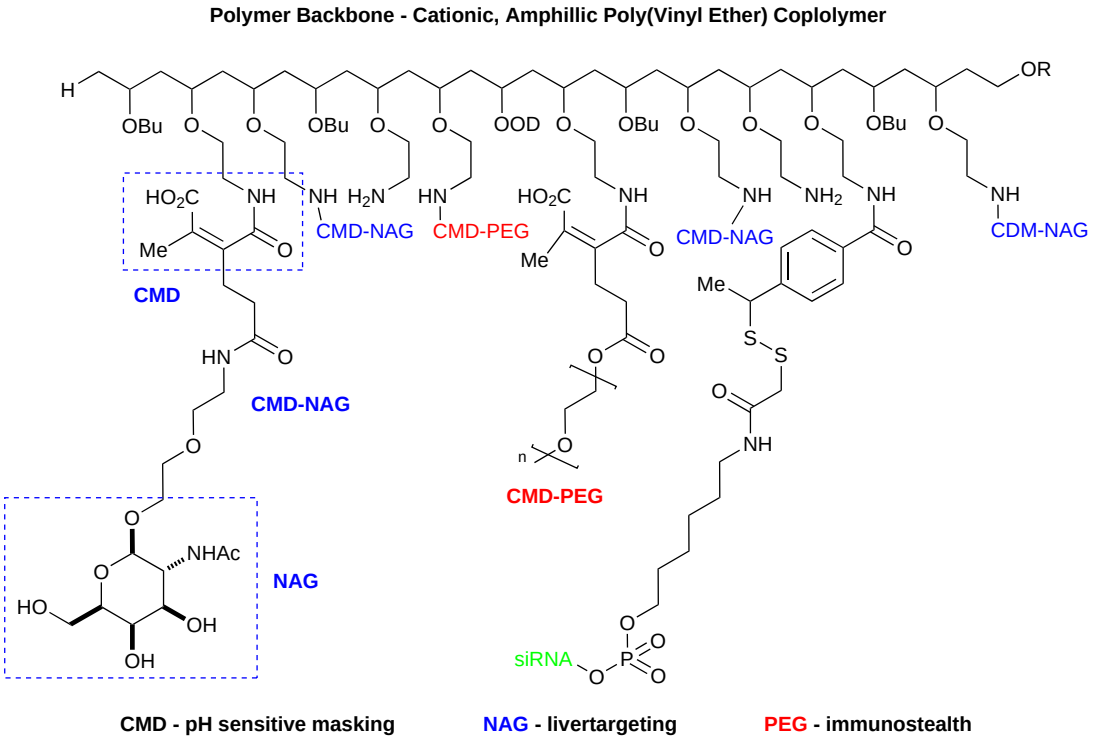

Figure 1.14: Polymer – siRNA conjugate.

became clear the turbulent four-way jet mixing device produced more defined dispersity and highlighted the importance of mixing. Normally anionic polymerisations in batch need to be performed at low temperatures (e.g. -78 °C) to allow control. Beneficially due to the high surface to volume ratio in the flow reactor, these reactions could instead be performed at room temperature.

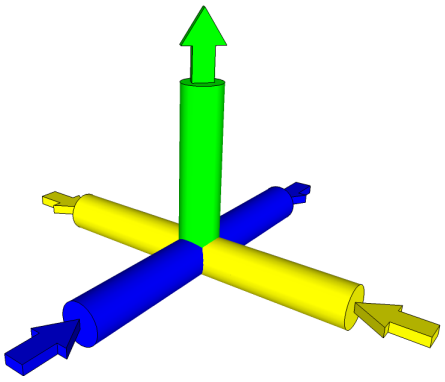

Figure 1.15: Operating principal of the four-way jet mixing device. [76]

The cationic ring-opening polymerization of 2-oxazolines in flow has been conducted by Baeten *et al.* [108] The general mechanism for the polymerisation is shown in Scheme 1.2. The synthesis of such polymers is mainly conducted only at a labora-

tory scale as polymerisation times in batch have extend reaction times of ten hours and problems regarding the scale up, like the strong exotherm of the reaction exist. [109–111] A reduction in the reaction time could be obtained *via* microwave assisted polymerisation (< 1 minute, 200 °C; although side reactions occurred above 140 °C) [111–113] and in pressurised batch reactors. [114] Flow chemistry was used to overcome these problems and mono-, di- and tri-block (co-)polymers were synthesised.

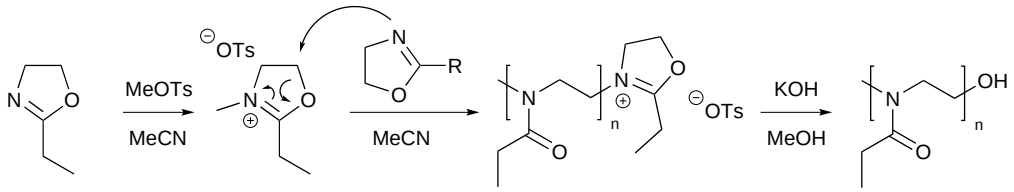

Scheme 1.2: Cationic ring-opening polymerizations of 2-oxazolines.

The polymerisation of 2-ethyl-2-oxazoline (EtOx) and *n*-propyl-2-oxazoline (*n*PropOx) show a high influence of temperature on the conversion and to certain extent on the average number molecular weight. The dispersity remained essentially constant for the various temperatures for both monomers (Table 1.9 and 1.10). Furthermore, no significant side reactions were observed. These results showed that flow chemistry is a valuable technique and opened a new route to homo-polymerised 2-oxazolines. Di-block polymerisation and tri-block polymerisation gave similar results compared to the mono-polymerisation (Table 1.11).

Table 1.9: 2-Ethyl-2-oxazoline homo-polymerisation achieving full conversion.

Temperature (°C)	**Residence time (min)**	**Conversion (%)**	$\boldsymbol{M_n}^{\mathbf{app}}$ **(g mol^{-1})**	$\boldsymbol{Đ}$
140	12.5	100	9,760	1.15
160	5	100	10,240	1.11
180	2	100	10,280	1.12

1.3.4 Photo-polymerisation

Over the last decade photochemistry has become increasingly popular with its apparent reclassification as a 'green' chemistry approach. This popularisation of the

Table 1.10: *n*-Propyl-2-oxazoline homo-polymerisation achieving full conversion.

Temperature (°C)	Residence time (min)	Conversion (%)	M_n^{app} (g mol^{-1})	$Đ$
140	12.5	99.3	8,950	1.24
160	5	100	8,170	1.23
180	2	99.5	9,240	1.16

Table 1.11: Block co-polymerisation of 2-ethyl-2-oxazoline and *n*-propyl-2-oxazoline at 160 °C and 5 minutes residence time.

Polymer	M_n^{app} (g mol^{-1})	$Đ$	M_p^{app} (g mol^{-1})	Ratio
EtOx	3,510	1.10	3,740	-
EtOx-b-*n*PropOx	6,140	1.12	7,130	1 / 1.18
EtOx-b-*n*PropOx-b-EtOx	7,400	1.25	10,910	2 / 1.02
*n*PropOx	3,940	1.09	4,210	-
*n*PropOx-b- EtOx	5,540	1.17	6,490	1 / 0.85
*n*PropOx-b-EtOx-b-*n*PropOx	7,320	1.21	9,660	2 / 1.11

M_n^{app} apparent molecular weight
M_p^{app} apparent proposed molecular weight

activation of reactions with photons has also been seen through the adoption of more photo-polymerisation. [115] The advantage of adopting a flow set-up to conduct this type of photo chemistry is generated by the reactor geometry. In a batch reactor a light gradient will occur due to the absorption of light by the preceding outer volume (Beer-Lambert law). Consequently scaling up the reaction may prove difficult and produce unpredictable results as reaction kinetics vary widely due to the type, shape and size of reaction vessel chosen. It has been shown that many different reactions can be performed more consistently using photo-flow reactors. [116] In many cases resulting in improved yields/ conversions and a reduction in processing times in certain cases from days to minutes. Furthermore, using this technique polymers with high precision have been obtained. [117]

Junkers *et al.* recently published a paper describing their efforts in the area of photo-polymerisation. [118] A photo-induced copper mediated radical polymerisation (UV SET-LRP) of methyl acrylate was conducted in DMSO at a reaction temperature of 15 °C (Scheme 1.3)

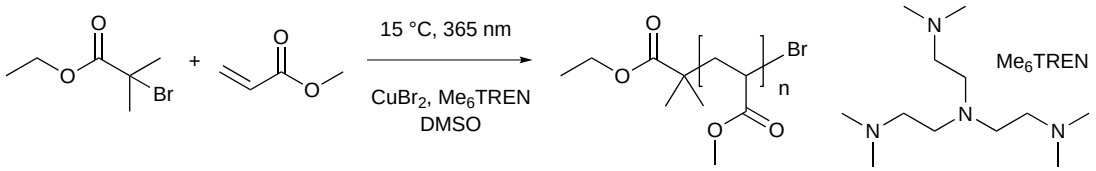

Scheme 1.3: UV-induced copper-mediated polymerization of methyl acrylate.

The photo-polymerisation was performed in both a tubular milli-flow reactor and a glass chip fabricated micro reactor. The reaction time reported using the milli-flow reactor was much shorter than for comparative batch experiments. A residence time of only 20 minutes (90 minutes batch) resulted in high conversions of the monomer (> 90%). Due to the short residence time and consequently much reduced irradiation time photo induced side reactions were also minimised. It was stated that the increase in polymerisation rate resulted from enhanced light absorption and also the use of a more powerful UV-lamp (3.0 mW cm^{-2} versus 400 W medium pressure, λ_{max} = 365 nm). However, it is hard to compare the light sources and therefore the results of the polymerisations due to limited information in the publication. A low dispersity was achieved which dropped from 1.3 to 1.1 when higher monomer conversion and longer residence times were used. Increasing the monomer to initiator ratio resulted in higher initial dispersities. A drop in dispersity was noticed at 40% conversion and a second drop at 60% conversion. All target molecular weights investigated (2,000 g mol^{-1}, 4,000 g mol^{-1}, 9,800 g mol^{-1}) yielded a similar trend. To access the specific target molecular weights, different ratios of monomer and initiator were used ($c_{monomer}/c_{initiator}$), 23, 47 and 116 respectively. Unfortunately, the target molecular weights were not achieved but the reason for this was unclear (Table 1.12). For comparison, batch polymerisations under equivalent conditions gave dispersity in the range of 1.11 to 1.05, with consistent molecular weight to the polymers synthesised in the tubular reactor. [119]

The same UV SET-LRP reaction of methyl acrylate was also performed in a micro-flow device (Scheme 1.3). A M_n of 4,000 g mol^{-1} was targeted and a maximum conversion of 80% was achieved with a residence time of 20 minutes. The produced polymers had similar average molecular weight and dispersity for the polymerisa-

Table 1.12: Targeted and obtained molecular weight.

Entry	Target M_w (g mol^{-1})	Approximate obtained M_w (g mol^{-1})	Conversion (%)
1	2,000	1,550	86
2	4,000	2,600	78
3	9,800	5,000	68

tions performed in the micro-flow reactor and the milli-flow reactor. The results were used to scale up the polymerisation, the described set-up was able to produce approximately 60 gram of polymer per day in the tubular reactor. The PFA tubing (1/16" x 0.75 mm, $V_{\text{tubing}} = 11$ mL) was wrapped tightly around a UV-lamp (400 W medium pressure, $\lambda_{\text{max}} = 365$ nm), and an HPLC pump was used to deliver the reaction mixture.

Block co-polymerisation of methyl acrylate and butyl acrylate was also performed using the same (previously mentioned) micro-flow set-up. First methyl acrylate was polymerised (M_n = 3,100 g mol^{-1}, $Đ$ = 1.10). Next, the butyl acrylate was co-polymerised with the active poly(methyl acrylate) chains with a M_n of 7,700 g mol^{-1} being formed if full conversion of butyl acrylate was obtained. Good control over the polymerisation was achieved, with a dispersity of 1.16 and a number average molecular weight of 4,990 g mol^{-1} at was for a conversion of butyl acrylate of 51%. This indicates a corresponding theoretical M_n of 5,400 g mol^{-1}.

To extend the scope other monomers were tested. Previous batch polymerisations had shown a large variety of monomers could be used to form block co-polymers using copper mediated photo-polymerisation. However, not all monomers tested gave good results in block co-polymerisation in flow. Attempts to prepare a block co-polymer of poly(metyl acrylate) with styrene for instance did not show significant secondary polymerisation, where methyl methacrylate gave a poor conversion (35%) beyond 20 minutes (M_n = 2,100 g mol^{-1}, $Đ$ = 1.45). The reaction times were not extended above 20 minutes. It is known methyl methacrylate is harder to polymerise due to the stability of the radical. Therefore, extended reaction time could increase the conversion.

1.3.5 Enzymatic polymerisation

Only a few papers have been published on the area of enzymatic polymerisations in flow. One of the most recent was disclosed by Beers *et al.* describing the synthesis of polycaprolactone from ε-caprolactone. [120] The enzyme *CAL B* was immobilised on solid beads (macroporous polymethyl methacrylate) and packed into a column reactor which enabled a higher local concentration than can be achievable in batch. Although good performance was demonstrated at lab scale the reactor set-up was not deemed suitable for scale-up due to its small volume. The residence time range was short (15 to 240 seconds) and the flow rate coverage low (30 to 640 μL min^{-1}).

1.4 In-line purification and analysis

An advantage of flow chemistry is that work-up and purification can be linked and performed in-line ideally as part of an integrated process. There are several literature reported examples of conducting purification and in-line analysis of small molecules, although four papers have been published relating to polymers. There are however known practices suitable for achieving the separation of polymeric reaction mixtures as part of a flow sequence. [121]

A demonstration of the use of in-line analysis and purification was reported by Hornung *et al.* [94] based upon the aminolysis of the end group of RAFT polymers into a thiol or thioether. The aminolysis of the end groups was followed using in-line UV spectroscopy (Scheme 1.1). Residual monomer could act as a Michael acceptor in the aminolysis allowing for the elimination of the thiol (intermediate of reaction with hexylamine). To prevent formation of the disulfide by-product a polymer supported packed column of Amberlite IR-120 (particle size: 300 - 1,180 μm, 14 - 52 mesh) was placed in-line after the aminolysis reactor to scavenge amine.

One possible reason for the low number of papers published relating to direct in-line analysis of polymerisation reactions might be the requirement for sample preparation prior to analysis, which is often a time consuming process. Especially

if a pure sample is required for analysis (i.e. by GPC). It can be difficult to simply inject a sample straight from the flow line into a GPC. The sample would at a minimum need dilution to a known concentration and probably require filtration before injection. Alternatively, mass spectrometry could be used to determine the molecular weight, although this will become problematic for high molecular weights due to detector limitations. On-line monitoring of the RAFT polymerisation of *n*BA, using 2-(dodecylthiocarbonothioylthio)propionic acid (DoPAT) and 2-2'-azoisobutyronitrile (AIBN) as the thermal initiator (Scheme 1.4) was performed by Junkers *et al.* [122] An electrospray ionization mass spectrometry (ESI-MS) was coupled with a Labtrix Start R2.2 system. The reactor was a glass micro chip with an internal volume of 19.5 μL. A variety of molecular weights was obtained. At 100 °C molecular weights of 1,100 g mol $^{-1}$ to 2,700 g mol $^{-1}$ were obtained for residence times between 1 and 5 minutes.

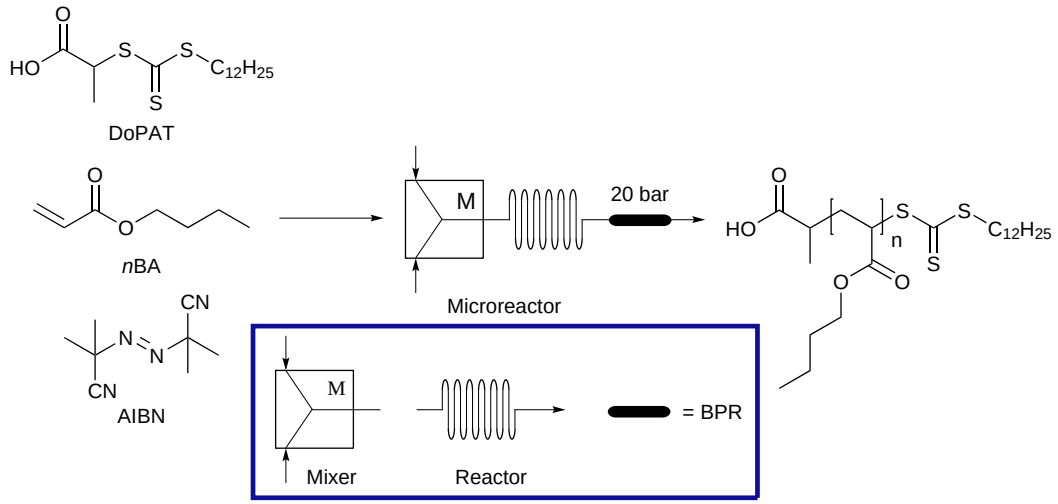

Scheme 1.4: RAFT polymerisation for on-line monitoring.

Other techniques such as in-line NMR are hard to realise and often again samples need to be purified to obtain meaningful results. Following polymerisation, a non-invasive technique such as UV or infra-red spectroscopy is easiest as it does not require sample preparation but does require access to authentic samples of the target polymer to allow calibration of the readings.

1.5 Polymer particles

An interesting and promising development area within the Material Sciences is the manufacture of precise polymer particles or spherical polymer capsules. [123] These materials are used in a wide range of products, such as drug delivery, [124] tissue replacement, [125] packaging [126] and electrochemical energy [127]. The desired properties are largely governed by their shapes, sizes and morphologies. Particles with core-shell or multi-layer structures are mainly used in coatings, spherical dielectric resonators and data storage technology. Whereas particles with liquid cores are mainly used for drug delivery, pesticides, liquid inks, paints and perfumes. [128, 129] These particles are most often produced *via* controlled phase separation, [130, 131] layer-by-layer deposition of polyelectrolyte multilayers, [132] interfacial polymerisation reactions [133] and Shirazu porous glass monomer emulsification accompanied by polymerisation [133–136]. Unfortunately, these methods all have drawbacks, such as expensive starting materials, time consuming procedures and in many instances the particles produced do not have a narrow distribution or lack defined morphology. Flow chemistry has proven its strength to overcome these problems. Therefore, it has been picked up as a powerful technique to synthesise precise polymer particles or spherical polymer capsules. Like with many chemicals, it depends on the application what the level of accuracy has to be.

Many different types of devices can be used to form droplets in flow. The two most common devices are capillary and micro-structured chip based systems. The capillary-based devises are mostly self-assembled bespoke reactor set-ups. The working of these devises is based on two capillaries (usually made from glass) of different outer diameter which are coaxial aligned. Using capillaries, there are two designs which are mainly used, the co-flow (Figure 1.16) and flow focussing design (Figure 1.17). The co-flow configuration has the continuous and dispersed phase flowing in the same direction. The flow focussing design has the continuous and dispersed phase flowing in opposite directions, with the output flow in the same direction as the dispersed phase.

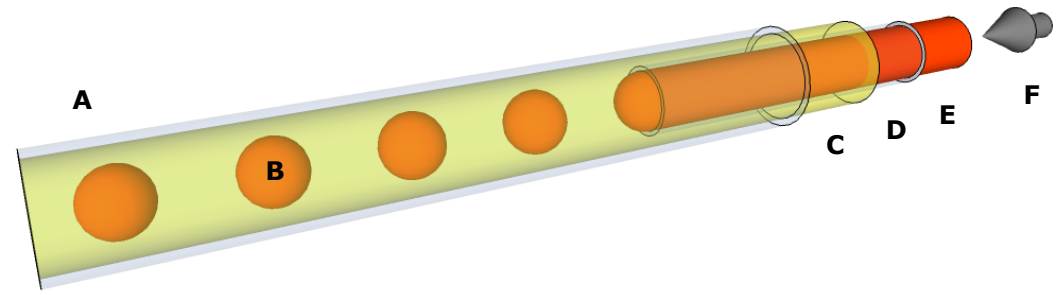

Figure 1.16: Co-flow design, A: outer capillary, B: formed droplet, C: continuous phase, D: inner capillary, E: dispersed phase, F: flow direction of continuous and dispersed phase.

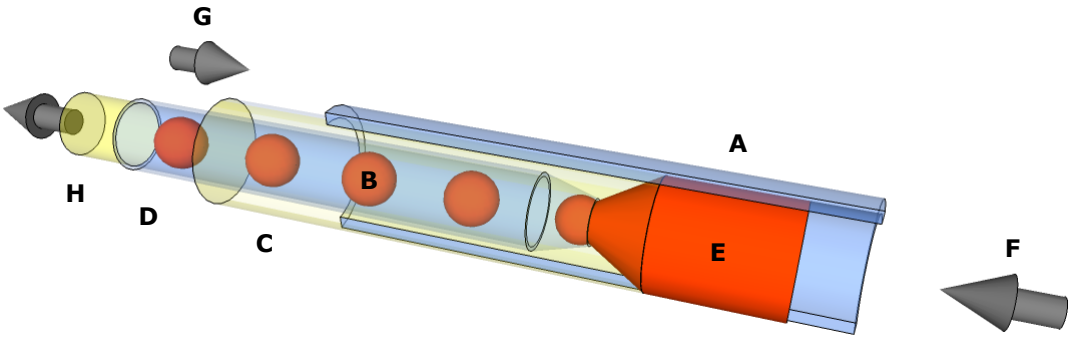

Figure 1.17: Flow focussing design with one inlet for dispersed phase, A: outer capillary, B: formed droplet, C: continuous phase, D: inner capillary, E: dispersed phase, F: flow direction dispersed phase, G: flow direction continuous phase, H: outlet of droplets and continuous phase.

The micro-structured chip based design can also be split into three divisions. First, a T-junction is used to mix the dispersed phase into the continuous phase (Figure 1.18). The flow rate of the dispersed phase, perpendicular to the continuous phase, will be low and the slowly growing droplet will emerge into the continuous phase and break off due to the shear forces imparted by the continuous phase. For polymeric particles a higher flow rate is used to form droplets through a higher shear force. The particles formed are smaller than the channel diameter, droplets which are in contact with the tube will deform or stick to the reactor walls.

Secondly, the use of split or intersections are also possible (Figure 1.19). A continuous phase can be introduced perpendicular to the output and added from two sides. The dispersed phase will move linearly towards the output. Consequently,

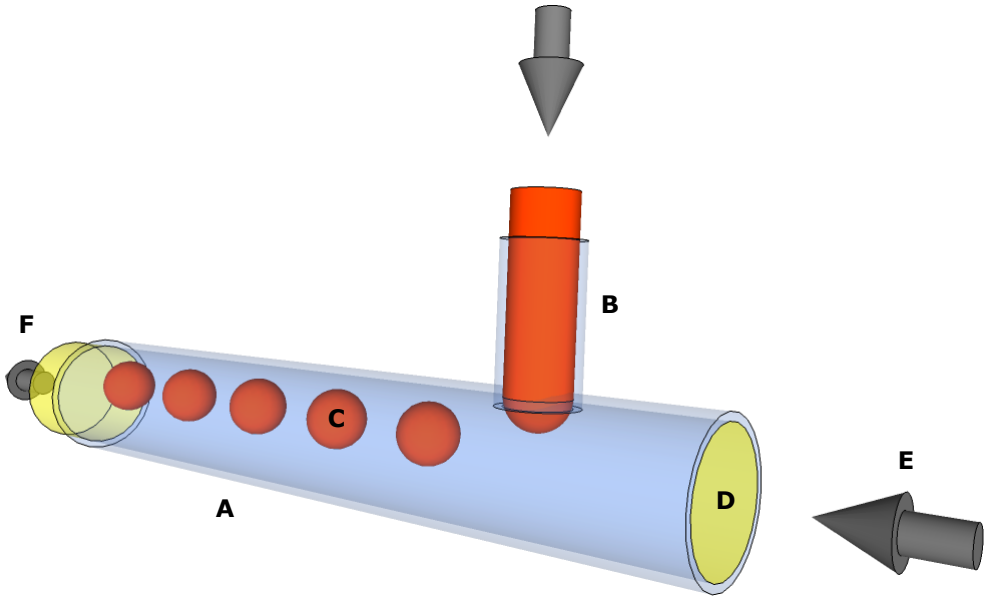

Figure 1.18: T-Junction design, A: capillary, B: dispersed phase, C: formed droplet, displace from equatorial possition in the flow, D: continuous phase, E: inlet and flow direction of continuous phase, F: outlet of droplets and continuous phase.

the droplets will be formed by the shear force of the dispersed phase. The advantage of this approach compared to the T-junction is the alignment of the droplets. The droplets are produced more in the middle of the channel and have as a result less interaction with the walls.

Finally, particles can be formed using flow focussing. The set-up is similar to the intersection configuration but has a narrow orifice at the exit of the channel. This set-up is most widely used as the droplets formed are of high quality.

One of the first papers describing the full continuous flow synthesis of polymeric particles was published in 2005. [137] Prior to this, particles were synthesised *via* a two stage process. The first step required emulsification of the monomer or a liquid polymer to obtain droplets ideally with a narrow size distribution. The second step produces the hardening of the particle shells.

As highlighted, Kumacheva *et al.* published their work on the continuous and scalable synthesis of core-shell droplets, polymer capsules and polymer particles with nonspherical shapes. [137] They describe the importance of creating initial droplets of uniform size. This was achieved by the use of a capillary instability-driven break-up of the liquid, which resulted in a good control of the emulsification

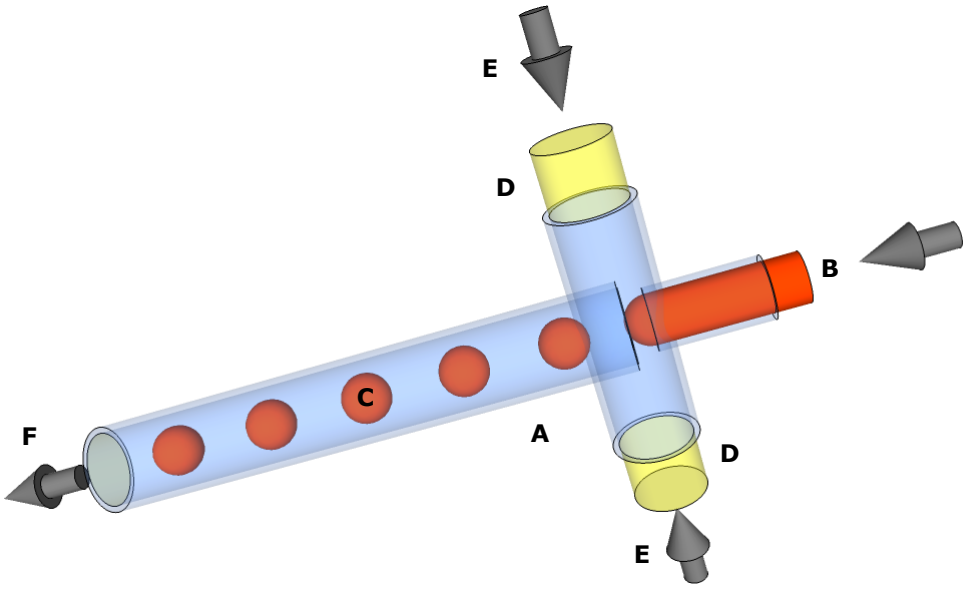

Figure 1.19: Intersection design, A: capillaries, B: inlet and flow direction dispersed phase, C: formed droplet, D: continuous phase, E: inlet and flow direction of dispersed phase, F: outlet of droplets, continuous phase and flow direction.

of immiscible liquids. Laminar flows of three liquid streams were pumped through the device producing a coaxial stream of silicon oil and monomer in an aqueous phase. The control of the break-up of the coaxial liquid was important as this led to the formation of highly mono disperse droplets (Figure 1.21). The production of these droplets gave good control over the size of the liquid core, the thickness of the shell, the number of core droplets and the size of the particles produced. This was achieved by changing the flow rate of each liquid and maintaining the other two flow rates constant (Figure 1.21).

In the next stage the freshly prepared droplets were continuously photo-polymerised under UV irradiation (360 nm, 200 mW m^{-2} intensity at sample location) to generate polymer capsules with different shapes (i.e. speres, truncated spheres and hemispheres). The polymerisation was performed using tripropylene glycol (TPGDA) or ethylene glycol dimethacrylate (EGDMA) as the monomer and 1-hydroxycyclohexyl phenyl ketone (HCPK) as initiator.

Multiple core particles could be produced using this design (Figure 1.21), including the formation of particles with different shapes. An increase in control over the morphology (size, 20 μm to 200 μm) was gained by variation of the flow rates of the

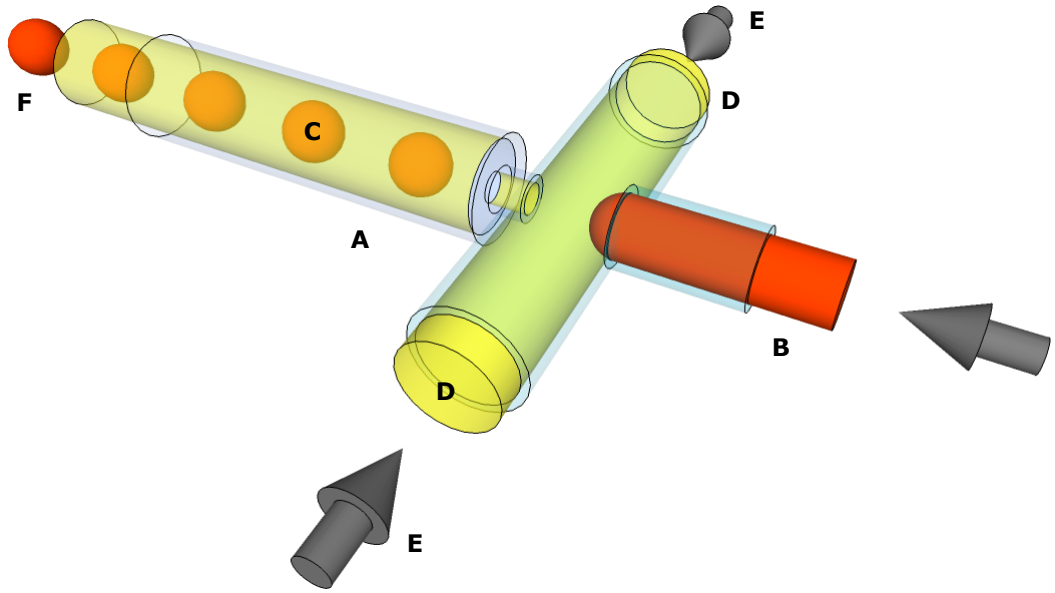

Figure 1.20: Flow focusing design with two inlets for dispersed phase, A: capillaries, B: inlet and flow direction dispersed phase, C: formed droplet, D: continuous phase, E: inlet and flow direction of dispersed phase, F: outlet of droplets, continuous phase and flow direction.

different compounds (liquid A to C) (Figure 1.21).

Kumacheva *et al.* published another paper in 2006 describing the synthesis of Janus particles and three phase particles in flow. The Janus particles were produced in a microfluidic device through the union of two liquid monomers in the presence of a photo initiator. To form the particles, an aqueous solution of sodium dodecylsulfate was injected to break up the organic flow. The formed particles were then irradiated to promote polymerisation. The shape of the Janus particles could be influenced as well as the ratio of the volume fractions in the Janus droplets. For the ratio of the volume fractions the interface of the adjacent phases is approximately flat. In this way the properties of the particles could be tuned. [138] It is clear from Figure 1.22 different concentrations of the two phases forming the Janus particles are used (A to D), which results in Janus particles with different physical properties.

These examples show that good control over the synthesis of particles is possible in flow enabling the preparation of particles with the same size and shape. Following on from the publication of Kumacheva *et al.*, several patents disclosed the formation of droplets using multiple parallel flow-focusing devices. [139–141] A variety

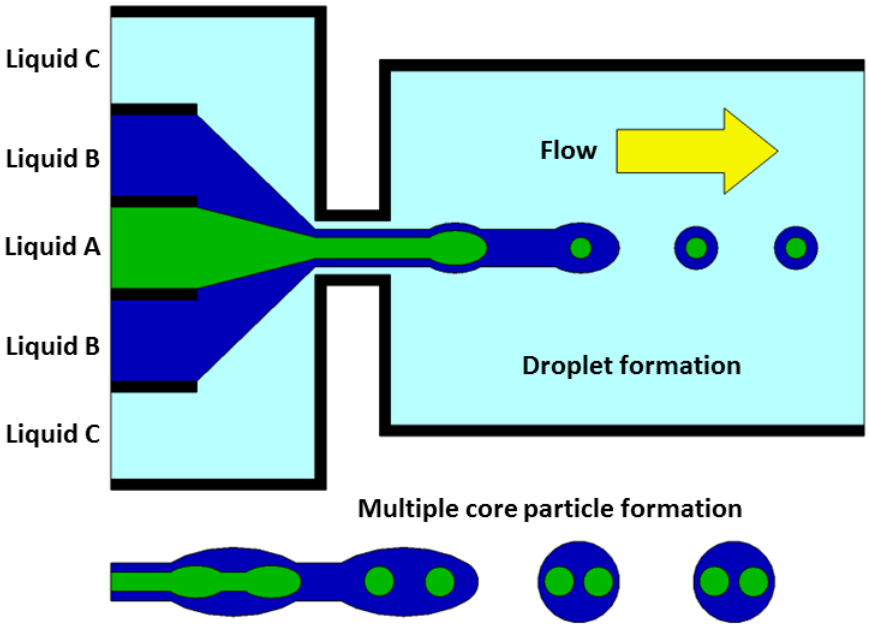

Figure 1.21: Schematic view of flow streams for the formation of droplets, laminar co-flow of silicone oil (A), monomer (B) and aqueous phase (C). Formation of multiple core particle.

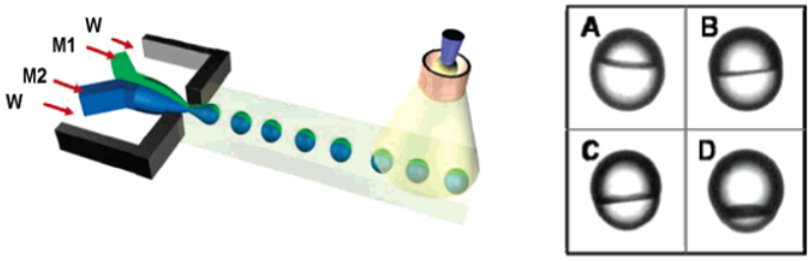

Figure 1.22: Flow pattern of Janus particle synthesis and droplet interface with different ratios for the volume fraction. [138]

of reactor geometries could be used, resulting in droplets with a variety of dimensions, shape, morphology and composition. Flow synthesis has thus opened up the possibility to achieve fast and scalable syntheses of polymer spherical capsules.

Semiconducting polymers are another type of macromolecule receiving increasing interest due to their use in lighting, solar cells and visual displays. [142–144] For these applications the polymers must be reproducibly prepared and their synthesis needs to be scalable. In addition, molecular weight distributions, defects in the conjugated backbone, control over end groups and impurity levels needs to be strictly controlled. [145, 146]

A method for the controlled synthesis of semiconducting polymers at large scale

using a droplet based flow reactor was reported by de Mello *et al.* [146] The polymer studied was the commonly used poly(3-hexylthiophene) and was synthesised *via* Kumada cross-coupling (Scheme 1.5). Flow processing resulted in exceptional control over the polymer properties, comparable with the best commercially available material.

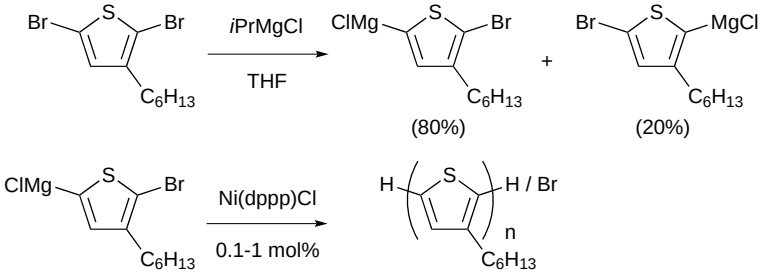

Scheme 1.5: Synthesis of poly(3-hexylthiophene).

The authors found the synthesised polymers were consistent with a quasi-living polymerisation model. [147] In this model each catalyst molecule is predominantly but not exclusively linked with a single polymer chain. [148] Therefore a better understanding of the polymer growth/ kinetics was obtained. This resulted in polymers with a variety of M_n and M_w which were flattening out at M_n = 27,000 g mol^{-1} and M_w = 46,000 g mol^{-1}. The technique of using droplets resulted in an effective way of controlling molecular weight distributions.

The process was also extended by including in-line preparation of the Grignard precursor. A continuous flow reactor with a four way mixer was inserted for the Grignard reaction in front of the droplet flow reactor. The continuous flow reactor (2 meter long PTFE tube) was supplied with 2 M ^{i}PrMgCl (5.33 μL min^{-1}), THF (28.33 μL min^{-1}) and 2,5-dibromo-3-hexylthiophene (2.35 μL min^{-1}) and heated to 55 °C. The intermediate was mixed with 1,3-bis[diphenyl-phosphinopropane]nickel(II) chloride (Ni(dppp)Cl$_2$) catalyst in perfluorinated polyether (180 μL min^{-1}) and droplets were formed by a droplet generator. The droplets were processed further in the droplet flow reactor (1.1 meter long PTFE tube) at 55 °C. This set-up enabled high production rates whilst maintaining low dispersities and high regio-selectivities. Although this demonstrated potential, the set-up has a few drawbacks. For example,

the system is not commercially available and cannot be operated continuously which makes it less attractive for industry. In the described system the use of syringes was a limiting factor.

Serra *et al.* described the formation of microfluidic droplets using a co-flow system in which the droplets comprising of monomer [(tri(propyleneglycol) diacrylate], initiator (aromatic ketone) and fluorescent dye were polymerised under photo-activation (366 nm, Lightningcure LC8, Hamamatsu) resulting in the formation of highly porous poly tri(propylene glycol) diacrylate particles if diethylene glycol was added. [149] The well-defined hydrodynamic conditions maintained in the reactor generated droplets with a narrow particle distribution. The same process was also run under thermal activation by mixing the monomer with a silver salt ($AgNO_3$) and adding a strong reducing agent (ascorbic acid). Thermally initiated polymerisation occurred at room temperature after 15 minutes. This could be a disadvantage as polymerisation of the mixture before the droplets are formed could lead to reactor blockage. However, changing the mixing order suppressed premature polymerisation and accumulation of silver nano-particles. It was not commented upon whether cooling the system prevented polymerisation. In my opinion a cooling mechanism should be in place. The set-up was used to quickly screen conditions for particle polymerisations and indicated that other polymer matrices beyond tri(propylene glycol) diacrylate could also be formed.

The synthesis of poly tri(propylene glycol) diacrylate particles has also performed by Visaveliya *et al.* in order to produces size-tuned fluorescent microparticles of broad size-spectrum. [150] Particle sizes between 40 μm and 500 μm were achieved by using various surfactants and changing the concentration along with flow rate ratios of the two immiscible phases. The possibility of mixing monochromatic fluorescent particles and multi-coloured particles of different sizes created a wide range of combinations for multi-fluorescence labelling. Therefore, the designed system has a wide applicability as a suitable combination could be found for specific applications.

1.6 Summary

Over the last three decades flow chemistry has been used in all areas of chemistry. Although this technique is still not fully incorporated in polymer chemistry, it is finding its way into various laboratories. It is understandable flow chemistry has not been fully adapted by the polymer chemistry community as introducing flow chemistry can be a costly endeavour. Another problem is the scalability, the investment in equipment to achieve scale up is currently higher compared to batch chemistry. Especially if a process developed in academia is scaled up to industrial scale. It is not possible to use 'small' laboratory scale equipment to scale the reaction.

To perform polymerisation in flow various devices have been used. The majority is based on plastic tubing. This kind of tubing is fairly cheap compared to glass or stainless steel devices and therefore easily to replace. All the advantages of flow chemistry discussed in this chapter are summarised in Table 1.13. This table proves polymer chemistry can benefit from flow chemistry.

Table 1.13: Properties batch versus flow.

	Batch	**Flow**
General applicable procedure	+	+
Automated pre- and post conditioning	+	+
In-line pre- and post conditioning	-	+
Atom-efficiency	+/-	+
Efficient heating	-	+
Optimisation	-	+
Reproducibility	+/-	+

The reasons to apply flow chemistry are different for academia and industry. The ability to perform in-line and on-line analysis is a strong advantage of flow polymerisations. This is a driving force for industry as products should be studied in detail before allowed to be used by pharmaceutical, healthcare and cosmetic product manufactures. Academia has started to use flow chemistry mainly as a tool in the process to optimise results. Unfortunately, it will take a long time before flow chemistry will be fully adapted in the synthesis of large molecules, even that the

reported results are very promising. Overall, the possibility that polymers are not well-defined macro structures is the driving force to find synthetic routes to generate more predictable polymer architectures. Usually polymers synthesised *via* advanced polymerisation techniques are well-defined. Unfortunately these polymers are of less interest for industry as the production costs will be too high.

Chapter 2

Polymers in Flow

2.1 Precis

Polymers are an important class of compounds used in many commercial products; for example, aqueous soluble polymers, are found in detergents and other cleaning products. Significant research has therefore been invested towards the synthesis of water soluble polymers using a variety of polymerisation techniques. One interesting approach used to synthesise aqueous soluble polymers is to apply flow conditions. A primary advantage of flow polymerisation is the ability to rapidly screen various parameters for the fast optimisation of the polymer synthesis conditions.

To synthesise aqueous soluble polymers at large scale, free radical polymerisation is the favoured process. This chapter will describe the synthesis and behaviour of an aqueous soluble polymer *via* free radical polymerisation using flow chemistry techniques.

2.2 Introduction

In this introduction the polymerisation of chain growth polymers in a top to bottom approach is described. In the first part the different polymerisation methods are mentioned in the context of poly(acrylic acid) (**8**). This is followed by a description of the different techniques used at industrial scale and a general background on

free radical polymerisation. In addition, the two main analytical techniques for analysis of polymers; GPC and NMR are described. The chosen monomer, acrylic acid (**7**) and initiator, 2,2'-azobis(2-methylpropionamidine) dihydrochloride (**4**) are introduced.

2.2.1 Types of polymerisation

Currently, the majority of commercially produced polymers are chain growth polymers. Chain polymers are generally synthesised *via* either free radical, cationic or anionic polymerisation. [151] If free radical polymerisation is chosen to synthesise a polymer, from an industrial stand-point, uncontrolled free radical polymerisation is preferred. A major virtue of uncontrolled free radical polymerisation is that it can typically be carried out under relatively undemanding conditions. The reaction also exhibits a tolerance for trace impurities, such as stabilizers and water; which are often present in monomers and solvents. [152] Other well-known related polymerisation techniques are controlled radical polymerisation; [153] condensation polymerisation; [154] plasma polymerisation [155] and photo-polymerisation. [156]

Staudinger was the first to propose the concept of chain growth polymerisation and defined the basic structure of the polymer molecules produced by such mechanisms. [157] He concluded that the monomer residues were connected in a head to tail way by covalent linkage (Figure 2.1).

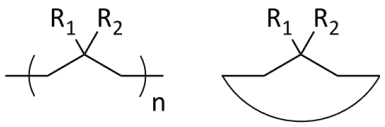

Figure 2.1: Staudinger proposed connection of monomer residues. [157]

The mechanism of chain growth polymerisation *via* free radical polymerisation is the fragmentation of an alkene π-bond to generate an extended carbon σ-bonded backbone. However, since the empirical formula of the synthesised polymer is the sum of the requisite number of monomers, these types of polymers are also called 'addition polymers' but better known as 'chain growth polymers'.

Polymers are widely used nowadays. Over the last four decades industry has invested heavily in new and greener synthesis techniques. One of the major outcomes of this ideological change has been the adoption of water as a highly favoured solvent. For example, water soluble polymers are used as detergent builders, flocculants, thickeners, scale inhibitors, paper sizing agents and emulsifiers. Related to this are products where water soluble polymers are used, such as soaps and shampoos, toothpaste, skin lotions, cleaning products, foods and textiles. One major drawback of water as a solvent is when purification of a water soluble polymer is necessary. Ideally, the polymer can be fully precipitated and the spent solvent can then be disposed of *via* the drain. Although the impact on the environment of the synthesis of these polymers is less compared to polymers synthesised *via* routes using non green solvents if the final water soluble polymers are not biodegradable such as poly(acrylic acid) (**8**) then the overall process is less green. [158] The long term environmental impact of this type of polymer is often hard to determine as they can persist in oceans, lakes, rivers, creeks and other water sources.

Nevertheless, water soluble polymers are a highly interesting group of polymers. The synthesis of this type of polymer has mainly been performed in batch. One principle reason for this is that synthesis in flow can cause problems due to the increase in viscosity with conversion [20], which in turn, can lead to pressure issues and potentially blocking the reactor. To overcome this problem different reactors have been designed, such as reactors with a secondary dilution flow stream, [20] or systems incorporating an ultrasonic mini mixing cell, [22] to create mini emulsions, or two phase systems including plug flow systems. [23]

A major problem when performing free radical polymerisation reactions is the lack of control over the different reaction steps compared to controlled radical polymerisation. As previously mentioned, flow chemistry could help to overcome some of these problems by providing a more regulated reaction environment. Radicals by nature are highly reactive and undergo reactions to extract an electron from another species or combine with another radical to obtain a full complement of electrons.

The obtained molecule can take many forms. As a consequence of the high reactivity of radicals, there is a lack of control regarding termination which can occur by either combination or disproportionation.

2.2.2 Polymerisation in an industrial setting

In an industrial setting, free radical polymerisation is usually carried out by one of four methods; bulk, solution, suspension or emulsion polymerisation. For bulk polymerisation, the initiator is soluble in the monomer which gives a high concentration of monomer. The dispersity will increase due to the increase in viscosity and poor heat and mass transfer in the sample. The polymerisation of certain monomers, for example acrylic acid (**7**), (undiluted or in concentrated solution) is accompanied by a marked deviation from first-order kinetics with an increase in reaction rate and molecular weight termed auto acceleration, or gel effect, as originally coined by Trommsdorf, Schulz and Norrish. [159, 160] Due to the exothermic nature of the reaction more initiator will be activated and therefore more chains will propagate. To overcome this problem, the reaction can be conducted at low conversion, or using chain transfer agents. These are species which have at least one weak bond, and for that reason, chain transfer reactions can occur, and are therefore commonly used. Besides controlling the auto acceleration, these agents are used for controlling the molecular weight of the polymer and/ or the polymer end groups. [161, 162]

The second method is solution polymerisation. In solution polymerisation, a solvent is used which reduces the viscosity and prevents the reaction from achieving auto acceleration. The reduction in the monomer concentration also gives rise to a proportionate decrease in the rate and degree of polymerisation. An issue with this approach can be chain transfer to the solvent; this results in a decrease in the degree of polymerisation and a reduction in the final molecular weight. Solution polymerisation is mostly applied to the preparation of polymers in which the polymer is used as a solution; normally the solution it is prepared in.

The third method is suspension polymerisation. This type of polymerisation is

often used on an industrial scale when the polymer easily separates from the reaction mixture. However, one of the major restrictions of suspension polymerisation is the solubility of the initiator in the monomer; the polymer must form a biphasic mixture with the bulk media. For this, water is often used as the inert bulk medium and surfactants are often required as dispersion stabilisers. The polymerisation takes place in created micelles and polymers are normally collected as particulates or beads. In industry this is the most important process for preparing materials for paints, coatings, latexes and adhesives.

The fourth method is emulsion polymerisation. This polymerisation technique is the most widely used commercial process for free radical diene and vinyl polymerisations. For these polymerisations the system contains water as solvent with a water soluble initiator, an immiscible monomer and often a surfactant. The surfactant is used to stabilise the formation of droplets in the solution. Emulsion polymerisation is preferred for the synthesis of polyacrylates over bulk polymerisations because of the high exothermicity, the increase in viscosity during solution polymerisation and the likelihood of soft particles binding together during suspension polymerisation.

2.2.3 Background on free radical polymerisation

Free radical polymerisation consists of three stages: initiation, propagation and termination. Each stage can be divided in two as shown in Figure 2.2. The first stage is the activation of the initiator. Usually this is *via* the formation of a radical by the elimination of a gas (N_2 from AIBN). The radical formed can then initiate the propagation step by reacting with a monomer. The main stage of free radical polymerisation is the propagation of the active chain. During propagation the chain reacts with an additional monomer to extend the chain (n + 1) or reacts to form a finished chain and a new reactive chain (Figure 2.2). The final stage of the polymerisation process is the termination. Termination occurs *via* the combination of two active chains or the exchange of radicals.

As polymerisation always starts with an initiation step the initiator is a key factor

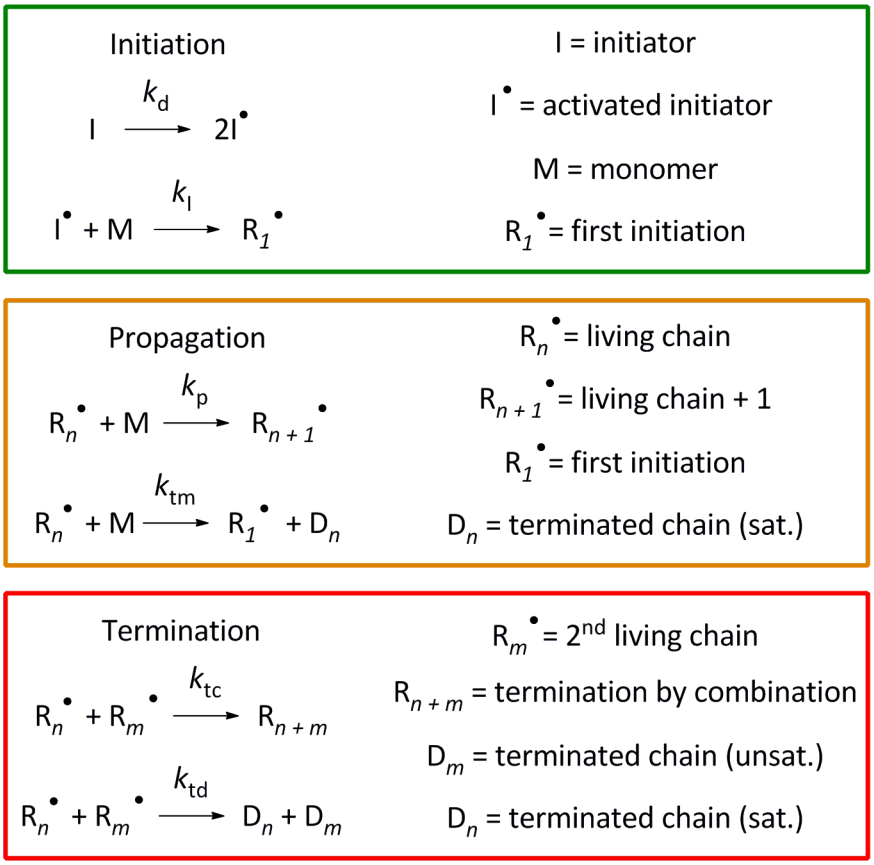

Figure 2.2: Different stages in polymerisation.

contributing to the success of the reaction. Many initiators are known to induce radical polymerisation and can themselves be activated through various stimuli such as by light, thermally, by ultrasound or by a combination of these three. When considering green processing chemistry, it is likely the polymer synthesis will occur neat or in a 'green' solvent. [163, 164] One of the key green solvents is water. This can however, also be problematic because only a small selection of initiators that are fully soluble in water. [165] The stability and behaviour of the initiators is something to consider during the radical polymerisation process. For instance, the hydrolysis rate of 2,2'-azobis(2-methylpropionamidine) (**2**) increases exponentially with increasing pH. A second important aspect is the half-life time of the initiator; especially for degradation under thermal conditions. Each initiator has its own half-life time specified for a given temperature. The initiation under thermal conditions should occur *via* a first order reaction for all initiators. The rate of the reaction will therefore follow equation 2.1 in terms of a decrease in initiator concentration. The

gas potentially formed in the process is not part of equation 2.1. Here, the initiator and activated initiator refer to the reaction illustrated in Figure 2.2.

$$-\frac{d[\text{Initiator}]}{d\text{t}} = 2\,\frac{d[\text{activated Initiator}]}{d\text{t}} \tag{2.1}$$

The complete cycle of a free radical polymerisation is around one second (initiation, propagation and termination). The rate limiting step in the synthesis of polymers *via* free radical polymerisation is the formation of the initial radicals. The decomposition of an initiator seldom produces a quantitative yield of initiating radicals. Degradation of an initiator molecule will provide two active centres. Most thermal and photochemical initiators generate radicals in pairs. Since not all the active centres will be involved in activating the monomer, some radicals may undergo recombination as consequence of the so called 'cage effect'. The cage effect is substantial even at low conversion when the medium is essentially mainly monomer. This shows the importance of diffusion rate for these species to break away from each other. This means the chemical environment is very important for initiator activity and the efficiency of the overall radical polymerisation reaction. Every initiator has an efficiency number which is dependent on the chemical environment and the initiator itself. The production of active radical centres follows equation 2.2, where f represents the initiator efficiency ($0 < \text{f} < 1$), typically this value lies between 0.3 and 0.8, and k_i, the rate constant of the initiation.

$$\frac{d[\text{active radical}]}{d\text{t}} = 2\text{f}k_\text{i}\frac{d[\text{Initiator}]}{d\text{t}} \tag{2.2}$$

Furthermore, the initiation step (radical generation from the initiator) should follow the Arrhenius equation (equation 2.3) and because nearly all radical formations are first order, equation 2.4 is valid for thermal decomposition of the initiator and gives the half-life time. With A being the frequency factor, E_a the activation energy, R the gas constant, T the absolute temperature, $t_{1/2}$ the half-life time and

k_d the decomposition rate.

$$k_\mathrm{d} \;=\; A\, e^{-E_\mathrm{a}/RT} \tag{2.3}$$

$$t_{1/2} \;=\; ln(2) \;/\; k_\mathrm{d} \tag{2.4}$$

Once the initiator has fragmented, rapid combination of the monomer units occurs (propagation, Figure 2.2). The rate constant k_p (middle panel Figure 2.2) for reaction with the monomer, is independent of chain length. During propagation both intramolecular and intermolecular chain transfer can occur. For example, 'back-biting' is an intramolecular reaction which produces a mid-chain radical and a terminated end chain and leads to branched polymers.

The final stage is the termination of the polymerisation which, despite the often drawn mechanisms, starts occurring to some extent as soon as the initiator fragments. Examples of termination events are combination where two chains combine to form one chain and disproportionation where two chains transfer an electron, but stay independent. Unsaturated chains are formed in both cases.

Besides homo-polymerisation, polymerisation of two (or more) monomers can be performed and usually leads to co-polymers. The extent of incorporation of each monomer unit into the final polymer is rarely equal as the reactivity ratio of the different monomers is rarely the same. Four main factors influence co-polymerisation, relative stoichiometry of each monomer species, reactivity of each monomer, reactivity of intermediate radical chains and conversion of the monomers. Normally, each monomer is consumed at a different rate due to their intrinsic reactivities. Therefore, the co-polymer composition changes as the polymerisation progresses. This is called a compositional drift. In a system with two monomers four propagation reactions are possible, two times self-propagation and two times cross-propagation. To determine the composition of the polymer it is important to know the reactivity ratio (r) of the different monomers. These can be calculated by dividing the rate constant for self-propagation (k_{11}) over the rate constant for cross-propagation (k_{12})

(see equation 2.5).

$$r_1 \; = \; k_{11} \; / \; k_{12} \tag{2.5}$$

If $r_1 > 1$, then there is a strong preference for homo-polymerisation, whereas if $r_1 < 1$ there is a strong tendency for co-polymerisation. Random co-polymerisation will occur if $r_1 = r_2 = 1$, alternating polymerisation will occur if $r_1 = r_2 = 0$ and block co-polymers will be formed if $r_1 >> 1$ and $r_2 << 1$.

Temperature and pressure can also influence chain growth polymerisation. By applying the Arrhenius equation (equation 2.3), the temperature dependence of the rates of the various steps in the radical chain growth polymerisation can be separated into different energies of activation representing the amount of energy that the reactant molecules must have to be able to react on collision. Enthalpies of polymerisation are readily measured and may also be calculated from bond dissociation energies. [152] The difference between these values also provides an indication of the amount of steric hindrance in the polymer.

2.2.4 Gel permeation chromatography

Gel permeation chromatography (GPC), also known as size exclusion chromatography (SEC), is a commonly used technique employed to analyse polymers. The two main characteristic attributes of polymers, molecular weight and dispersity, are determined by GPC. The analysis of polymers by GPC is based on the hydrodynamic volume of each individual chain when fully dissolved. The solvent of choice depends on the polymer being evaluated. The solution is passed through a set of columns packed with immobile porous material. This immobile material is often itself made of a cross-linked polymer. The immobile matrix has various pore sizes, resulting in a gradient of affinity for the polymer chains in solution passing through it. Smaller polymers can enter the pores whilst large polymers cannot. Therefore, large polymer chains have shorter retention times than the corresponding small polymer units. The range of pore sizes across the column and the elution times allows determination

of a distribution of various polymer weights.

The exact method used to analyse the polymer can vary as with most other analytical techniques. For instance, a GPC can have a single, double or triple detector. For GPC with triple detection, the detectors are commonly, but not restricted to: laser light scattering detector, refractive index detector, and viscometer (merged as detector(s) in Figure 2.3). With this set-up molecular weight, intrinsic viscosity and molecular size can be determined across the entire distribution. The three detectors combined provide not only the above mentioned numbers, but also direct information on the molecular structure (branching, conformation and aggregation). The analyses of samples described in this thesis were performed using GPC with triple detection.

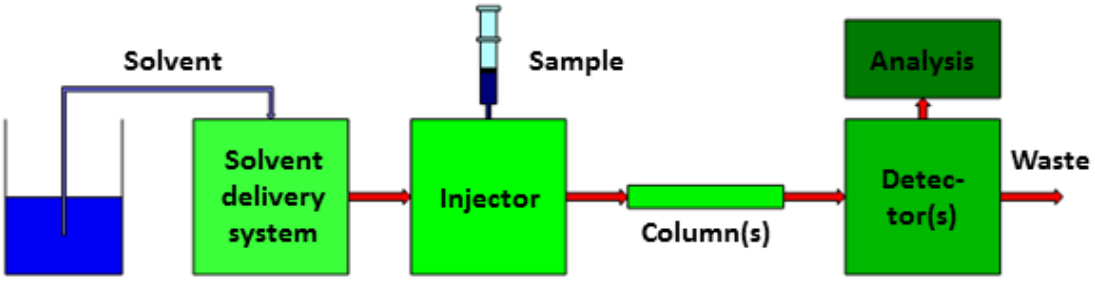

Figure 2.3: Schematic explanation of GPC system.

Usually the first detector of a GPC is the light scattering detector. Essentially, a laser beam is focussed into a cell that the sample passes through. The incident beam will be scattered by the polymer particles that are in solution. The design of the light scattering detector (small angle or multi-angle) will influence the measurement. Depending on this, the weight average molecular weight can be measured accurately with or without the radius of gyration of the polymeric solution.

The refractive index detector is usually the second detector in line. This detector is concentration sensitive and measures the difference in refractive index between the eluent in a reference chamber and the eluting sample. If the signal is poor, usage of a different solvent system can improve the sensitivity of the spectra.

The viscometer, usually the third detector, measures a difference in pressure.

The most common design of the viscometer for a GPC is known as the four capillary bridge. It consists of four linked capillaries, two are in series and two are in parallel. The flow is split and moves equally through the first capillaries of both parallel paths. Both flow paths are identical in length and can be combined after the measurement. The only difference for the flow paths is that these are not symmetrical. The difference is the placement of an elution delay column in one of the paths. This column has a large internal volume packed with glass beads. Therefore, the polymer sample will be hold-up by the delay column. In analogy with an electrical circuit the bridge becomes unbalanced, this scheme is very similar to a Wheatstone bridge; a well-known electrical circuit, and results in a pressure differential which can be measured and relates to the viscosity of the sample. Note, the pressure is measured across the entire bridge (inlet pressure) and between the two flow paths (differential pressure) (Figure 2.4).

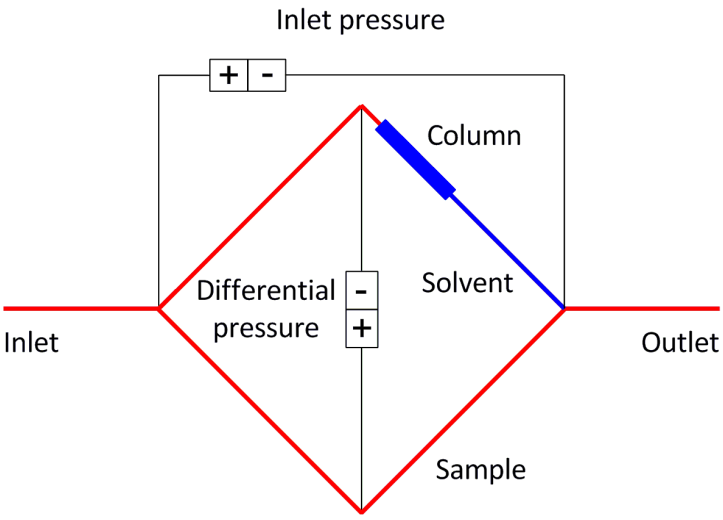

Figure 2.4: Principle of viscometer.

The benefit of measuring the intrinsic viscosity along with the differential refractive index is that it allows the determination of molecular weights *via* Benoit's Universal Calibration concepts. Regardless of the chemistry of the standards employed in the calibration, calculations of accurate molecular weights are permitted. A change of the intrinsic viscosity implies a change in structural architecture (Table 2.1). [166–170]

Table 2.1: Relation between intrinsic viscosity and polymer structure.

Structural or conformational change	**Effect on viscosity**	**Effect on intrinsic viscosity**
Increase chain length (M_w) of linear molecule	Decrease	Increase
Increase mass of chain segments, keeping chain length constant	Increase	Decrease
Increase stiffness of chain	Decrease	Increase
Add branches to chain, keeping M_w constant	Increase	Decrease
Collapse chain into solid particle (natural protein or aggregate)	Increase greatly	Decrease greatly

Aqueous samples are very challenging to characterise by GPC. The packing is made of hydrophilic methacrylate gels with residual carboxylate groups resulting in an overall anionic charge. It is therefore important to keep in mind that charge interaction between the sample and packing material can occur. To regulate this issue an electrolyte is often added, such as 0.10 M $NaNO_3$. Even for neutral samples, this electrolyte is satisfactory for use as a solvent. Some additional problems which may need to be overcome for aqueous GPC are given in Table 2.2.

Table 2.2: Interactions which could influence an aqueous GPC.

Interaction	**Effect on**
Hydrophobic Interactions	Non-ionic component of polyelectrolyte sample interacts with non-polar sites of packing material (addition of organic modifier)
Intramolecular Electrostatic Interactions	The expansion of polyelectrolytes due to the charges on the molecule itself
Ion Inclusion	The sample will stick to the column when the charge of the polyelectrolyte is opposite to that of the packing
Ion Exchange	This might occur in the case of ion inclusion, an ion exchange reaction occurs (adjusting pH)
Ion Exclusion	Packing material and sample polyelectrolyte have the same charge

2.2.5 Nuclear magnetic resonance

Nuclear magnetic resonance (NMR) was first performed in 1945 by Purcell *et al.* [171] who detected weak radio-frequency signals generated by the nuclei of atoms in one kilogram of paraffin wax. Almost simultaneously Bloch et al. [172, 173] performed a similar experiment where radio-frequency signals were observed from the atomic nuclei in water. It is of no surprise that these experiments opened up a wide range of opportunities to analyse all sorts of molecules and has become an incredible analytical tool for investigating matter. The list would be too long to name all types of material where NMR played a crucial role in discoveries, which exemplifies it expansive use.

All matter is made of atoms, and so are polymers. The atoms are made up of electrons and a nucleus which has four important physical properties: mass, electric charge, magnetism and nuclear spin. The last two are particular important for NMR, nuclear magnetism and nuclear spin can provide valuable information about the analysed material. To have a sample which is suitable for NMR analysis, it should contain nuclei with spin $I = ½$ or a multiple thereof. If an atom has an odd number of protons and/or neutrons it has non-zero spin, if both are odd it has integer spin (such as deuterium), if one is odd and the other even it is spin half (^{13}C has odd neutrons, ^{15}N odd protons). Nuclei with spin $I = 0$ are not suitable, because they have no intrinsic magnetic moment and angular momentum. Most chemical elements do not have a nucleus with spin $I = ½$. However, isotopes with this spin state are represented in organic materials (^{1}H, ^{13}C, ^{15}N, ^{19}F and ^{31}P) and therefore this analytical technique is extensively used in organic chemistry and thus in polymer chemistry. This does not implicitly imply nuclei with other spin states are not suitable for NMR. Quadrupolar nuclei with half-integer or integer spin can also be used, but in general they are harder to analyse.

The most common nucleus for NMR is ^{1}H. This nucleus is almost always present in organic molecules, NMR analysis of hydrogen is relatively short (four minutes) and does not require concentrated samples (approximately 20 μmol). Other nuclei

are less prevalent in organic molecules, for instance ^{19}F and ^{31}P have similar analysis times as ^{1}H (four minutes and seven minutes, respectively) thus are not routinely measured, and for other atoms the natural atomic abundance is low. This is the case for carbon, where the atomic abundance of ^{13}C is 1.1% and ^{12}C is 98.9%. Therefore, to analyse a sample using ^{13}C NMR a concentrated sample is required, also its analysis takes longer (around 40 minutes).

Another advantage of ^{1}H NMR is that the solvent can be suppressed. Suppression of a signal overcomes the dynamic range problem, which means the signals of interest are not digitized. The suppression of water has been extensively researched due to the solubility of proteins and other biologically important molecules in this media. Proteins are dissolved usually in 90% H_2O/ 10% D_2O rather than 100% D_2O in order to investigate exchangeable protons. Suppression techniques can be used to determine the conversion of an aqueous polymerisation or polymers which form a gel. Consequently, samples can be screened without requiring solvent removal or purification.

The process for the suppression of water requires first that all signals are excited. Following this, the water signal region is selectively inverted and then 'destroyed' using a field gradient. The suppression of water in the NMR signal is not without risk. Other signals could be influenced or in a worst case scenario lost if the notch (the frequency used to suppress the signal) is too wide. The notch used for the suppression of water (4.79 ppm) in this thesis was 500 Hz. This will not only influence the signal at 4.79 ppm, but will suppress signals roughly plus or minus 0.5 ppm of 4.79 ppm. Additionally, residual H_2O is distorted in the baseline and the integral of peaks close to the suppressed signal cannot always be calculated correctly.

2.2.6 A different approach used for polymerisation in flow

In polymerisation reactions, it is typical that the viscosity increases during polymerisation. Reactor designs need to take this into account. It can be expensive to overcome these problems and therefore low cost agitators or static mixers are widely

used. For many reactions the Reynolds number is important as it indicates mixing and diffusion: this is a non-dimensional parameter defined by the ratio of dynamic pressure and shearing stress (equation 2.6).

$$R_e = \frac{VL\rho}{\mu} = \frac{\text{inertial forces}}{\text{viscous forces}} = \frac{VL}{\nu} \tag{2.6}$$

In this equation V = velocity (m s^{-1}), L = length (m), ρ = density (kg m^{-3}), μ = dynamic viscosity (N.s m^{-2}) and ν = kinematic viscosity (m^2 s^{-1}). The dynamic viscosity is defined by the tangential force per unit area required to move one horizontal plane with respect to another at unit velocity when maintained at a unit distance apart by the fluid (Figure 2.5). Low Reynolds number (< 2,000) indicates

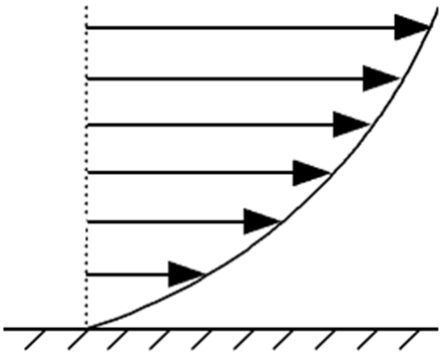

Figure 2.5: Dynamic viscosity.

laminar flow. The characteristics of the flow are a constant and smooth fluid motion. Fluid particles are moving in straight lines with low velocity and viscous forces are dominant. The mixing is not optimal when laminar flow is achieved. Medium Reynolds number (2,000 > R_e < 4,000) indicates transitional flow. The fluid particles have a medium velocity. High Reynolds numbers (> 4,000) indicates turbulent flow. The characteristics of the flow are an irregular and chaotic fluid motion with high velocity. The average motion is in the direction of the flow and cannot be seen by the naked eye. Turbulent flow is the most common type of flow as the viscosity is low.

2.2.7 Acrylic acid, initiators and poly(acrylic acid)

The synthesis and behaviour of poly(acrylic acid) (**8**) is well-known and various papers have been published on the synthesis of this polymer. [174–176] The monomer used for the polymerisation of poly(acrylic acid) (**8**) is acrylic acid (**7**) (Figure 2.6). Poly(acrylic acid) (**8**) has multiple applications, for example in soaps and shampoos, skin lotions, cleaning products and in textiles. In combination with the solubility in water poly(acrylic acid) (**8**) is a polymer Unilever is highly interested in, furthermore this is the most commonly used water soluble polymer. Therefore, acrylic acid (**7**) was the monomer of choice. Compared to other polymers, for example like poly(ethylene glycol) and poly(glycidol), poly(acrylic acid) (**8**) is harder to analyse and to work with as acrylic acid (**7**) is a very reactive monomer.

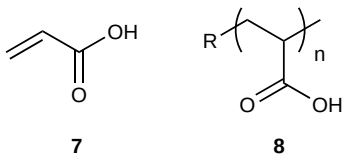

7 **8**

Figure 2.6: Acrylic acid (**7**) and poly(acrylic acid) (**8**).

To synthesise poly(acrylic acid) (**8**) different initiators can be used, however these need to be water soluble as most syntheses are performed in water. Cyanovaleric acid (**3**), methylpropionamidine (**4**) and imidazolin propane (**5**) are a selection of initiators which fulfil this criteria, as does to some extent the less soluble 2,2'-azobis(2-cyanopropane) (**6**) (Figure 2.7). In addition, peroxyl radical β-scission can proceed at appreciable rates, especially in the case of stabilized carbon-centred radicals.

The radicals formed are stabilized by either α-cyano or α-amidino groups (Figure 2.7). The radical is a mechanistically significant species. [177–179] Instead of initiating the polymerisation it can react with other organic molecules in competition with polymerisation reactions. This is important when the initial carbon-centred radicals are generated in the aqueous phase. The radicals can react with each other as a result of the cage-effect.

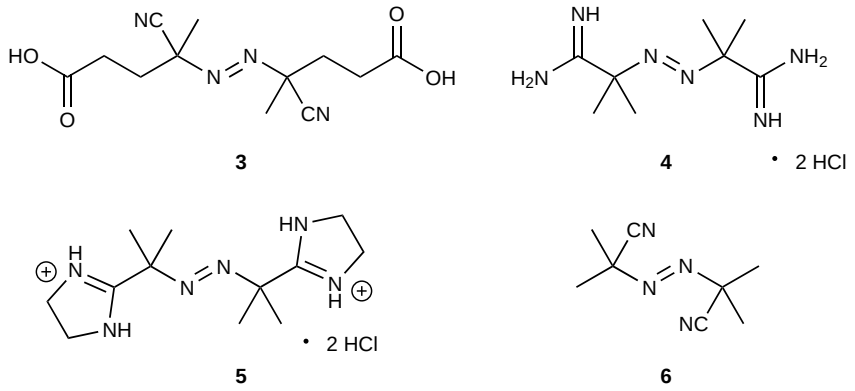

Figure 2.7: Azo initiators: 4,4'-azobis(4-cyanovaleric acid) (**3**), 2,2'-azobis(2-methylpropionamidine) dihydrochloride (**4**), 2,2'-azobis[2-(2-imidazolin-2-yl)propane] dihydrochloride (**5**) and 2,2'-azobis(2-cyanopropane) (**6**).

The half-life time of the initiator is important for the polymerisation; if the concentration of radicals formed is too high, many chains will propagate. The resulting polymer will have a low molecular weight. Changing the temperature of the reaction will affect the initiation step according to the Arrhenius equation (equation 2.3). [23] It should be noted that the temperature can also increase due to the intrinsic exothermic nature of most polymerisation reactions (auto catalytic runaway).

The pH can also influence the activity of the initiator. A study by Seybert *et al.* regarding lipid peroxidation using water soluble azo initiators (Figure 2.7) showed that the pH influences the rate of the peroxidation. [165] The rate increased at higher pH when initiators **4** and **5** were used. No reaction was observed at pH $<$ 5 using initiator **4** and a plateau was reached for pH $>$ 8. Initiator **5** gave similar results, over a pH range of 4.5 to 8.5. The use of cyano valeric acid (**3**) showed an inverse pH response with maximum reactivity obtained at low pH (pH $<$ 3) and no reactivity for high pH (pH $>$ 8). By contrast initiator **6** did not show any pH dependence. To the best of our knowledge, no research has been conducted regarding the influence of pH on initiation in free radical polymerisation. It is anticipated that pH will also influence free radical polymerisation using an initiator such as **4**. As the monomer being polymerised is acrylic acid (**7**), the reaction will be at low pH. As there was no pH influence found by Seybert *et al.* at low pH, a similar effect in free radical polymerisation was anticipated for.

2.2.8 Proposed mechanism poly(acrylic acid) polymerisation

RAFT polymerisation [49] has proven to be a very useful technique for the direct polymerisation of acidic monomers including acrylic acid (**7**). RAFT polymerisation of acrylic acid (**7**) has been performed in many solvents including ethanol, 2-propanol, dioxane, methanol, water, and dimethylformamide [49, 176, 180] and has shown to affect the end product. Investigation of these RAFT polymerisations provided understanding of the limits of acrylic acid (**7**) and indicated water could be used successfully as a polymerisation solvent.

As mentioned previously, water is a 'green' solvent and for this reason the solvent of choice. The most suitable initiator for polymerisation in water is 2,2'-azobis(2-methylpropionamidine) dihydrochloride (**4**), outlined in Scheme 2.1.

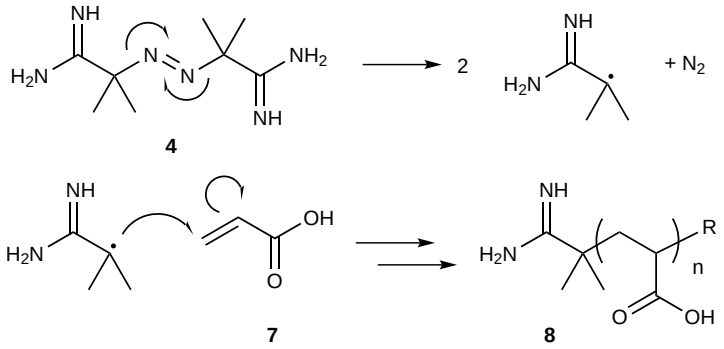

Scheme 2.1: Initiation and propagation of free radical polymerisation of poly(acrylic acid) (**8**).

The polymerisation of acrylic acid (**7**) in water has a disadvantage in that the poly(acrylic acid) (**8**) formed is very hydroscopic as it can form multiple hydrogen bonds. Additionally, due to the presence of the tertiary hydrogen adjacent to the carbonyl group, acrylic polymers tend to be 'branched'. This hydrogen can be abstracted by a radical species, the formed tertiary radical is stabilised by the adjacent carbonyl group (A in Figure 2.8). This radical can then lead to branching which is the replacement of a substituent for a covalent bond of a 'new' polymer chain. Branching can generate multiple side chains (B in Figure 2.8). [176] It is likely during the polymerisation cross-linking will occur, resulting in a gel, which can be

a disadvantage. A covalent network of poly(acrylic acid) (**8**) is formed.

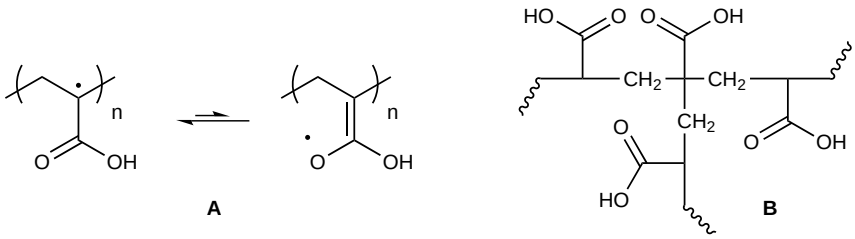

Figure 2.8: Stabilised radical (A) and branched poly(acrylic acid) (**8**) (B).

2.3 Research objectives

The aim of the work described in this thesis chapter was to perform polymer synthesis in flow *via* free radical polymerisation. To allow for comparisons to be made and increase the understanding of free radical polymerisation of poly(acrylic acid) (**8**) we have performed synthesise in both batch and flow. However, batch polymerisation conditions cannot easily be reproduced in flow. Reactor blockage can occur when conditions, especially concentrations, are transferred directly to flow. Because flow chemistry provides higher levels of control over reaction parameters, and can be applied to enable controllable polymerisation resulting in polymers with narrower dispersity, a second aim was develop methods to provide polymers with tuneable molecular weights.

It is highly probable that, due to different flow mixing characteristics inside the reactor, the outcomes comparing flow will differ significantly to batch. Therefore, the influences of different reaction parameters will be discussed. For example, it was assumed a priori that high temperatures should initialise high concentrations of initiator resulting in likely narrower dispersities. This is because the higher the initiator input, the shorter the formed polymers should be, as the monomer concentration would be insufficient.

2.4 Methodology

2.4.1 General

Different commercially available molecular weights of poly(acrylic acid) (**8**) are available from 1,800 g mol^{-1} to 3,000,000 g mol^{-1}, with a corresponding range of dispersity from 1.28 to 1.82. In the literature a wider range of molecular weights can be found, from 820 g mol^{-1} to 4,860,000 g mol^{-1}, with corresponding dispersity values between 1.2 and 4.6, however these were obtained using different polymerisation techniques. [176, 181, 182] The above numbers are used as reference guides in this chapter.

Polymerisation of acrylic acid (**7**) has been performed in the past using both batch (see Supporting information 1) and semi flow chemistry (a continuous feed of monomer and initiator) [183]. The general procedure used of Unilever [184] for polymerising aqueous soluble polymers in batch was used with minor modifications (as noted in the text).

2.4.2 Polymerisation in flow

To terminate a free radical polymerisation in batch, often the reaction is treated with an additional dose of initiator (up to a stoichiometric amount). As a result, the dispersity can be increased if the sample is not purified properly. To avoid unnecessary purification, a radical scavenger can be added to the reaction mixture. An advantage of adding a radical scavenger is that polymerisation will stop immediately. This enables premature cessation of the reaction and a real time projection of the conversion of the monomer can be achieved. Unfortunately, the scavenger has to be chosen carefully in order to not interfere with the polymer.

The polymerisation of acrylic acid (**7**) is performed in an acidic environment due to the natural acidity of the acrylic acid (**7**) monomer. Therefore, background anionic polymerisation has a low probability to occur. This makes sodium selenite a suitable radical scavenger because of its water solubility and, in addition, it does not interfere with the final polymer.

Aqueous stock solutions of acrylic acid (**7**) and 2,2'-azobis(2-methylpropionamidine) dihydrochloride (**4**) were prepared at known concentrations (Table 2.3). The solutions were degassed by sonification, bubbling nitrogen through and sonification for a second time, each performed for twenty minutes. The FlowSyn (Uniqsis Ltd, Shepreth, United Kingdom) system was set up using two independently controlled HPLC pumps (channels A and B). Flow rates were maintained at a 1:1 ratio. An in-line poly(ether ether ketone) (PEEK) cross assembly (1.30 mm through hole and 22.8 µL swept volume connector fitted with a pressure transducer (obtained from Uniqsis Ltd., Shepreth, United Kingdom)) was used to combine the flows into a single stream and then pass the flow into the coil reactor. The flow path was configured so that channel A and B entered laterally and the mixed flow exited at right angle, which passed into a 52 mL fluorinated ethylene propylene (FEP) coil which was heated at different temperatures. A back pressure regulator (BPR, 100 psi) was placed at the exit of the coil reactor. The exiting solution of poly(acrylic acid) (**8**) was collected in a stirred flask containing the sodium selenite as a radical quencher (Scheme 2.2).

Table 2.3: Screened parameters for acrylic acid (**7**) polymerisation.

Temperature (°C)	**[Acrylic acid] (mM)**	**[Initiator] (mol%)**	**Residence time (min)**
60	0.4, 0.7, 1.0	1.25, 2.50, 3.75	10, 20
70	0.4, 0.7, 1.0	1.25, 2.50, 3.75	5, 10, 20, 30
80	0.4, 0.7, 1.0	1.25, 2.50, 3.75	5, 10, 20, 30
90	0.4, 0.7, 1.0	1.25, 2.50, 3.75	5, 10, 20, 30

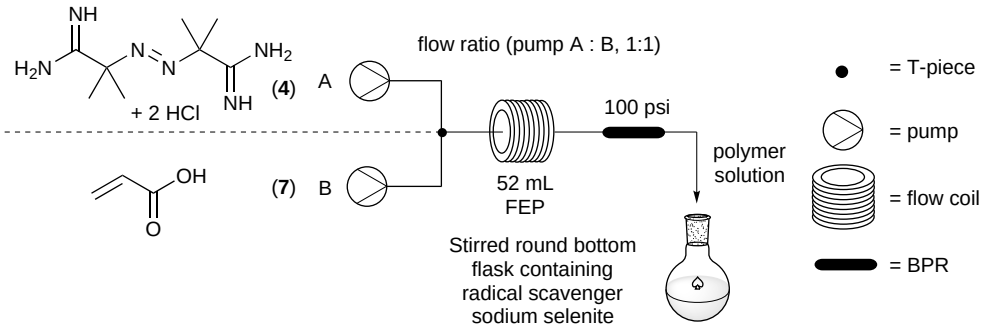

Scheme 2.2: Flow synthesis scheme poly(acrylic acid) (**8**).

2.4.3 Characterisation

^{1}H NMR spectra using water suppression were recorded on either a Bruker-Avance 400 or Varian VNMRS-600 instruments using D_2O to lock the signal and 1,2-dimethoxyethane (DME) as internal standard. The technique used was based on the Watergate [185] suppression technique and described in an article by Morris *et al.* [186] and further optimised by Aguilar *et al.* [187] GPC analysis of poly(acrylic acid) (**8**) was recorded on a Malvern Viscotek instrument performed in aqueous solution (0.05 mol/L $NaNO_3$, 2.81 mmol L^{-1} NaOH and MeOH [ratio 4:1]) using 2 x A6000M + guard column set (all purchased from Malvern Instruments Ltd., Malvern, United Kingdom)). The column and detector temperature was 50.00 °C, flow rate was 1.0000 mL min^{-1}, injection volume was 50 μL and volume increment was 0.00333 mL.

2.4.4 Analysis

The analyses of the samples are, if possible, based on the average of at least two measurements.

Extreme values of conversions were removed from the data-set if these values deviate more than 5% points of from the average value and only if three or more measurements were present. The conversion of monomer into polymer was determined by adding DME as internal standard (either 5 μM or 10 μM) to the monomer stock solution.

This was not possible for the GPC data. Extreme values were eliminated on the quality of the spectra, the baseline was used as the main guide. Spectra without smooth baseline were eliminated, therefore, certain outputs based upon GPC analysis are based on a single analysis, the average numbers were used for further analysis.

2.5 Results and discussion

2.5.1 Initiator and half-life time

Two major changes were made to the original protocol obtained from Unilever for the synthesis of aqueous polymers. [184] First, the adoption of flow conditions to investigate the free radical polymerisation of acrylic acid (**7**). And second, an alternative initiator, 2,2'-azobis(2-methylpropionamidine) dihydrochloride (**4**), because it was more soluble at room temperature compared to cyanovaleric acid (**3**), originally used by Unilever. It is important that the initiator is fully soluble at high concentration at room temperature as solubility is crucial to perform the polymerisation in flow. Heating the initiator stock solution to increase solubility is not an option as this will result in decomposition of the initiator. Therefore, 2,2'-azobis(2-methylpropionamidine) dihydrochloride (**4**) was the preferred initiator. To understand better the initiator's decomposition in water, a series of ^{1}H NMR kinetic experiments were carried out at 80 °C, with ^{1}H NMR spectra recorded every five minutes. The results show the initiation step follows the Arrhenius equation (equation 2.3) which is important for determination of temperature dependency and estimation of the half-life time (Figure 2.9 and 2.10). The peaks used for Figure 2.9 are enclosed in a rectangle in Figure 2.10.

The half-life time of this initiator was calculated for various temperatures by making one assumption, because the decomposition rate, and therefore the half-life time, cannot be calculated without having at least one full entry. The data for entries 1 and 4 Table 2.4 were obtained from the Polymer Handbook. [188] The activation energy is 128 kJ mol^{-1}. Using equations 2.3, 2.4 and 2.7 gives the half-life (Table 2.4). The half-life for entries 2, 3, 5 and 6 were calculated as these temperatures were used for the free radical polymerisation of acrylic acid (**7**) in flow.

$$E_{\mathrm{a}} \;=\; R\,\frac{T_1\,T_2}{(T_1 - T_2)} \;\times\; \ln\frac{k_1}{k_2} \tag{2.7}$$

The values for the half-life time decrease as the temperature increases. A short

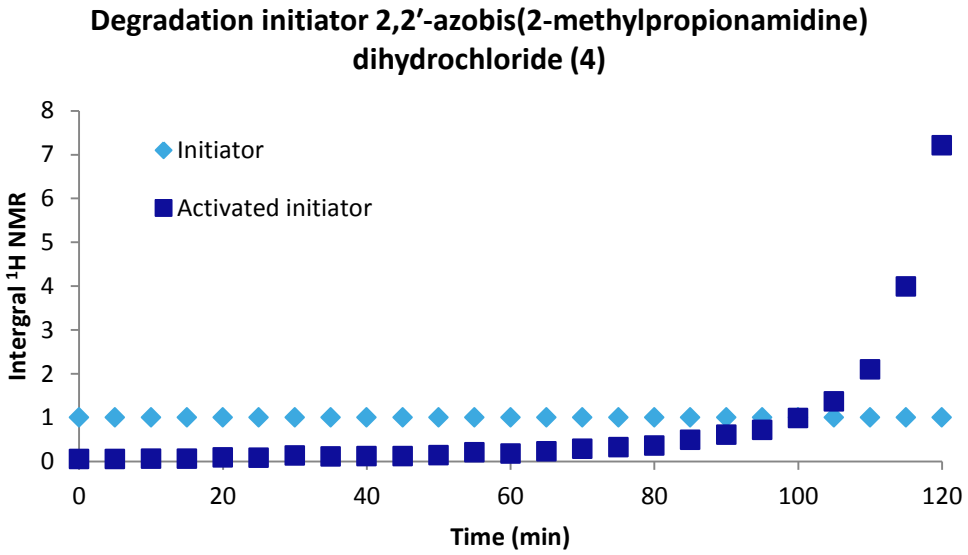

Figure 2.9: Degradation of 2,2'-azobis(2-methylpropionamidine) dihydrochloride (**4**) measured *via* kinetic ^{1}H NMR.

Table 2.4: Half-life time 2,2'-azobis(2-methylpropionamidine) dihydrochloride (**4**) for different temperatures.

Entry	T (°C)	T_{abs} (K)	Decomposition rate (s^{-1})	$t_{1/2}$ (min)
1	56	329.15	1.93×10^{-5}	599
2	60	333.15	3.33×10^{-4}	347
3	70	343.15	1.30×10^{-4}	88
4	78	351.15	3.61×10^{-4}	32
5	80	353.15	4.63×10^{-4}	25
6	90	363.15	1.54×10^{-3}	7.5

half-life time is important to match the short residence times achievable in flow. Although the calculated half-life times are extrapolated from literature values (entries 1 and 4, Table 2.4), the value calculated for 80 °C (half-life time is 26.2 min) is similar to the result determined empirically (Figure 2.9 and 2.10). Using knowledge of the half-life time of 2,2'-azobis(2-methylpropionamidine) dihydrochloride (**4**) at various temperatures, a batch polymerisation was performed using acrylic acid (**7**) as the monomer. Initial batch experiments, following the protocol provided by Unilever [184] for comparison, resulted in gel formation. In batch a gel can be handled, however it should ideally be avoided in the flow equipment. As the half-life time of the initiator should be extensive at 40 °C (equations 2.3, 2.4 and 2.7) a batch reaction

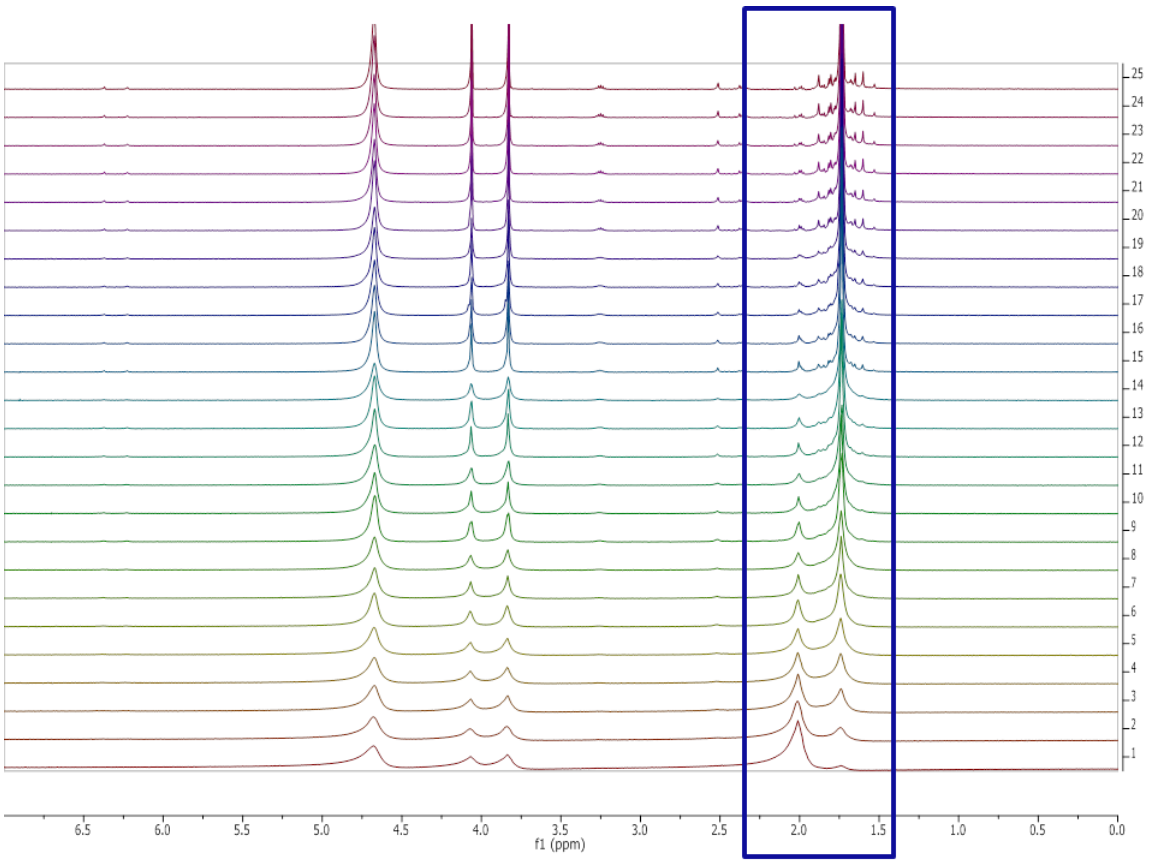

Figure 2.10: Degradation of 2,2'-azobis(2-methylpropionamidine) dihydrochloride (**4**) measured *via* kinetic ^{1}H NMR.

was performed at this temperature using the modified Unilever protocol [184] (page 197) to analyse the influence of the monomer and initiator mixing. A round bottom flask was loaded with 40 mL deionised water containing 3.47 mM acrylic acid (**7**) and 0.36 mmol 2,2'-azobis(2-methylpropionamidine) dihydrochloride (**4**). The internal temperature increase upon mixing was also measured and reached 61 °C, far above the set temperature and a gel was formed. To study the polymerisation, the reaction was repeated and the temperature in the reaction mixture was monitored while slowly heating the reaction mixture. At $t = 0$ the water bath was 13 °C and heated slowly to 65 °C. An increase in temperature and a corresponding increase in viscosity were observed. A resultant temperature above the set temperature occured at $t = 15$ minutes (Figure 2.11). At $t = 15$ minutes, the reaction mixture was no longer a stirring solution but a gel. The drop in temperature (15 to 17 minutes) inside the reaction mixture could be easily explained as heat transfer in a gel or very

viscous solution is poor. These experiments imply the polymerisation of acrylic acid (**7**) is an exothermic reaction, and creates a runaway generation of initiation.

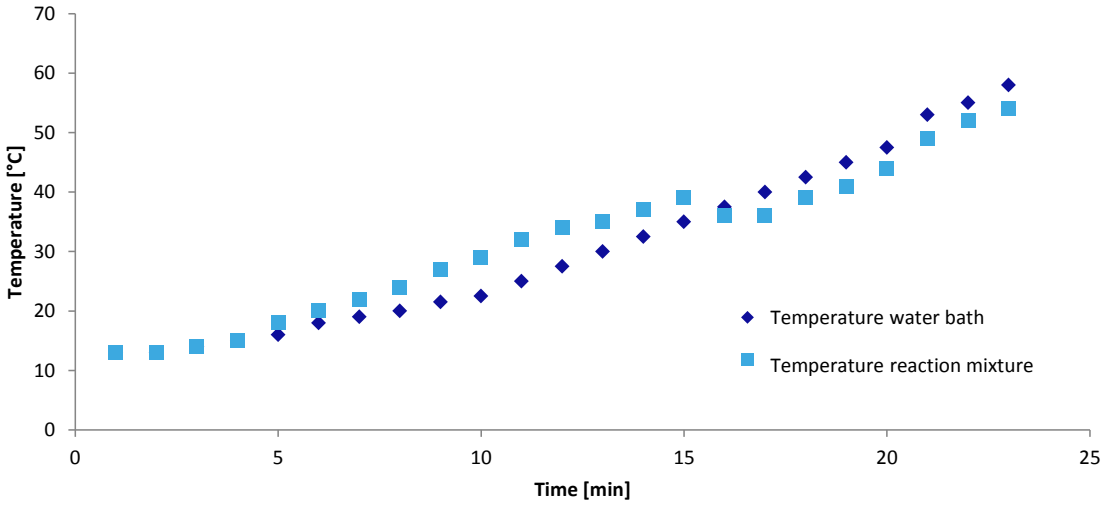

Figure 2.11: Temperature measurement of acrylic acid (**7**) polymerisation using 2,2'-azobis(2-methylpropionamidine) dihydrochloride (**4**) as the initiator performed in water.

2.5.2 Batch polymerisation

The formation of gel was not unexpected. Methyl acrylate, a monomer which is similar to acrylic acid (**7**), is known to be prone to gel formation, as described in 1970 by Cameron *et al.* [189] It is known that gel formation occurs as a result of cross-linking. [190] To avoid gel formation the reaction mixture should be diluted. This will minimise the absolute temperature increase (exothermic) and therefore it is less likely to produce a gel. Tuning the protocol by diluting the reaction mixture by a factor of 2.5 resulted in a polymer which did not gel. However, the viscosity increased but did not reach the point that it could not be progressed in flow. The resulting polymer solution was analysed by ^{1}H NMR spectroscopy without purification using water suppression (Figure 2.12). [186, 187] The conditions used are different to the conditions earlier mentioned. It is clear that the majority of acrylic acid (**7**) is consumed (near 6 ppm, inside rectangle). The peaks between 2.75 and 1.5 ppm are assigned to poly(acrylic acid) (**8**).

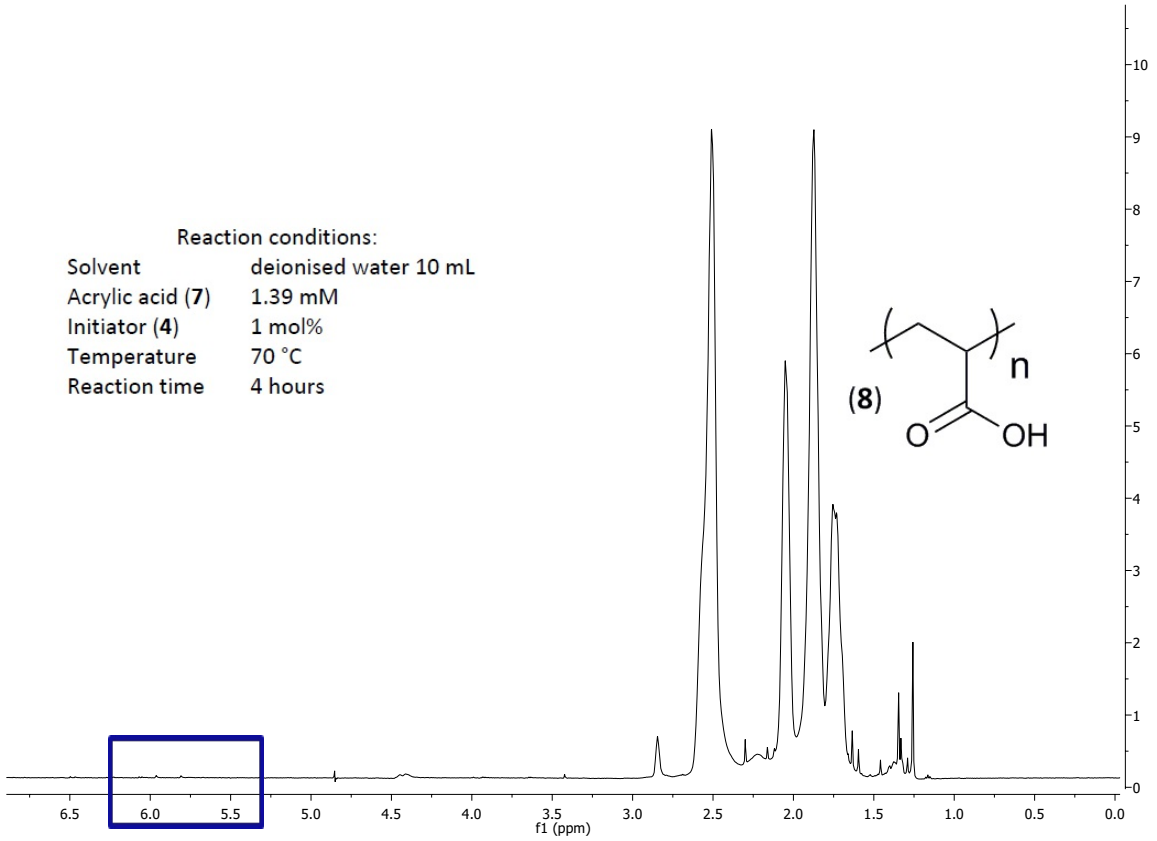

Figure 2.12: Batch polymerisation, ^{1}H NMR spectra with water suppression.

2.5.3 Flow polymerisation

The modified batch procedure clearly worked well, and was therefore used as a starting point for the flow synthesis. Polymerisation in flow was performed using a FlowSyn system, commercially available from Uniqsis. The flow system design was simple: involving two HPLC pumps, a T-piece for mixing, a reaction coil and back pressure regulator. Avoiding complex designs made the set-up more cost effective, should parts need to be replaced, as well as simple to use in its application. The parameters which were screened for the flow polymerisation were temperature, reaction time, and stoichiometry (Table 2.3). Stoichiometry was screened for by using various stock solution concentrations. Potentially in flow a different way to generate various concentrations is to tune the flow speed of two independent flow channels.

To determine the conversion of acrylic acid (**7**) to poly(acrylic acid) (**8**) dimethoxyethane was used as an internal standard. The internal standard needs

to meet the following requirements: it needs to be water soluble, inert and the ^{1}H NMR chemical shift(s) cannot overlap with peaks from acrylic acid (**7**) or the water signal. Dimethoxyethane meets the requirements for this reaction system. The corresponding conversion of acrylic acid (**7**) could therefore be calculated from the ^{1}H NMR; an example spectrum of a polymerisation in flow is shown in Figure 2.13. The peaks indicated with one and six are respectively the guanidine and

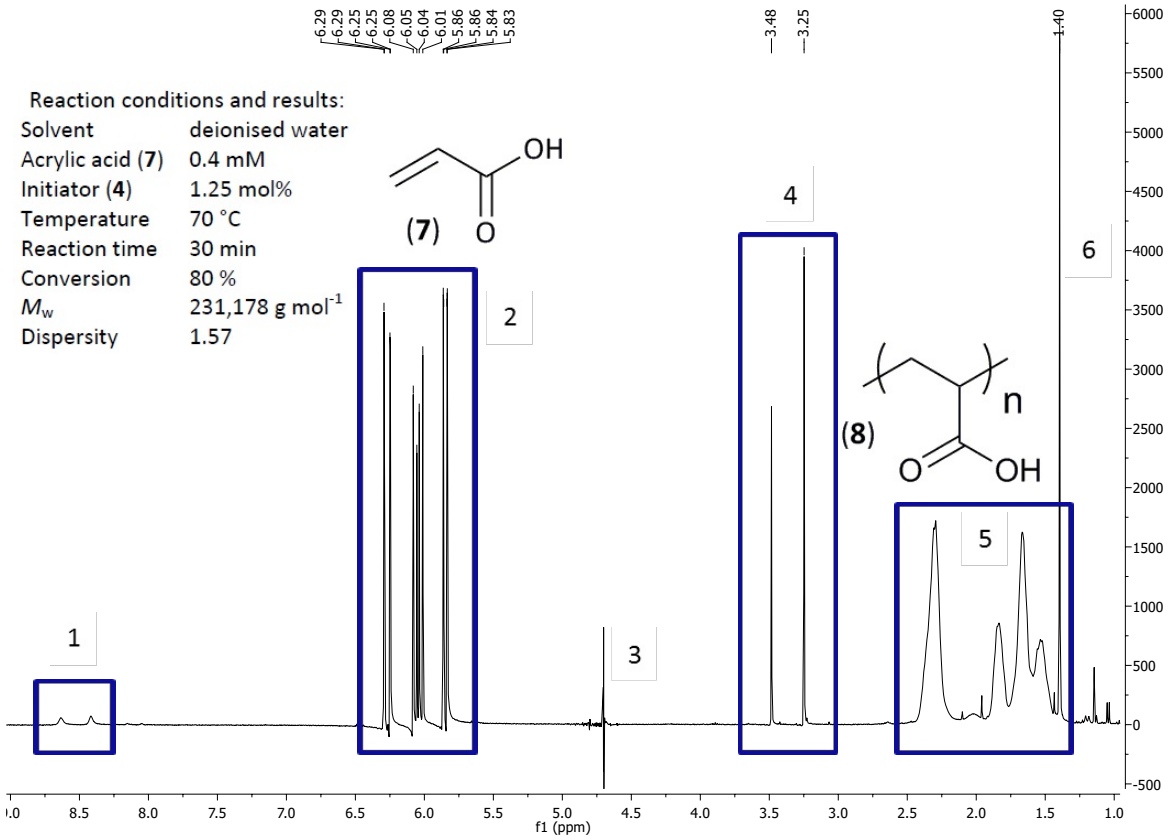

Figure 2.13: ^{1}H NMR poly(acrylic acid) (**8**) obtained under flow procedure conditions.

methyl groups of the initiated 2,2'-azobis(2-methylpropionamidine) dihydrochloride (**4**). The peaks in box two corresponds to residual acrylic acid (**7**), peak three corresponds to the suppressed water signal, the peaks in box four corresponds to the internal standard dimethoxyethane and the peaks in box five corresponds to poly(acrylic acid) (**8**).

The purification of the poly(acrylic acid) (**8**) has been performed using the Vivaflow membrane from Sartorius Stedim Biotech. The membrane used in the reactor had a molecular weight cut off (MWCO) of 2,000 g mol^{-1}, therefore molecules with

a molecular weight lower than 2,000 g mol^{-1} should have been removed from the sample within 60 minutes (bottom spectra Figure 2.14). No internal standard was used for this sample as it was not clear if the dimethoxyethane would damage the membrane. A calibrated mirror experiment (with internal standard) was therefore performed using exactly the same conditions, resulting in 28% residual acrylic acid (**7**).

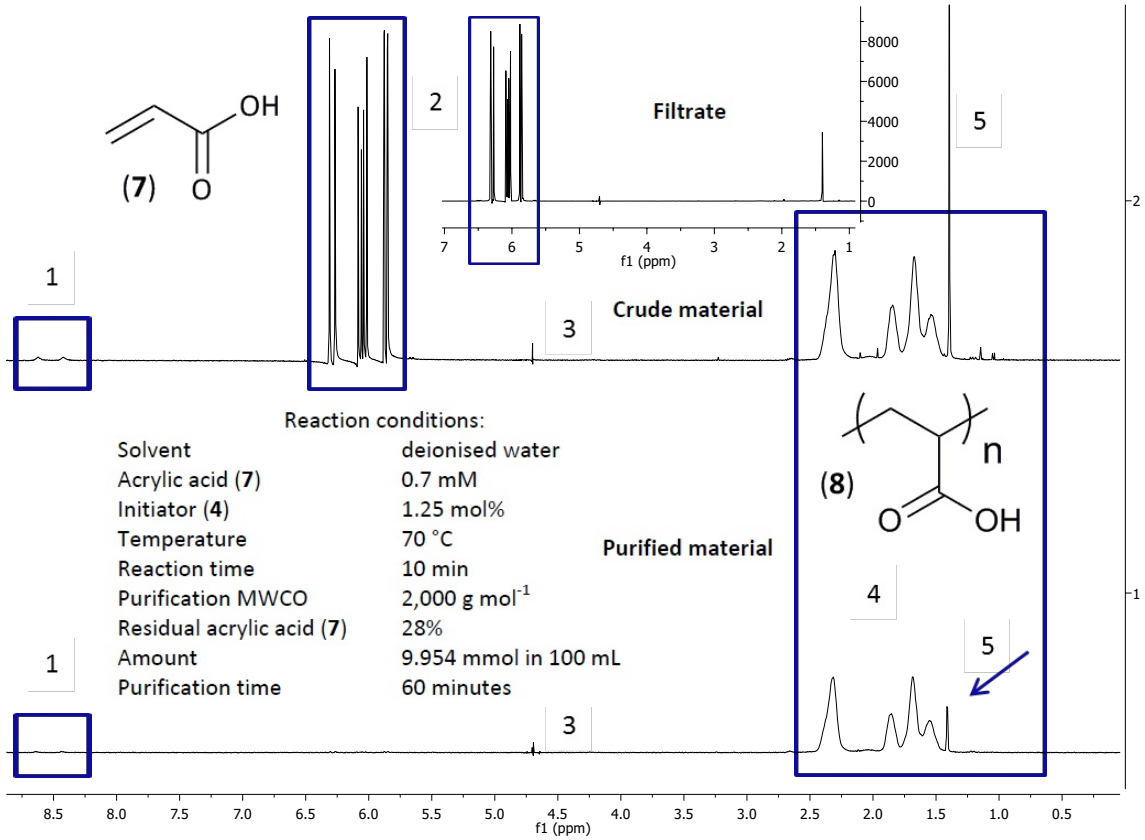

Figure 2.14: Purification of polymeric sample without internal standard; top initial sample, bottom purified sample after 60 minutes.

It is anticipated that the peaks in box one and peak five in Figure 2.14 represent end groups (initiated 2,2'-azobis(2-methylpropionamidine) dihydrochloride (**4**)) of poly(acrylic acid) (**8**), see Scheme 2.1. The signals in highlighted box one correspond to the guanidine group and peak five to the two methyl groups. These characteristic signals of the initiated initiator decrease in the spectrum of the purified poly(acrylic acid) (**8**) (peaks in box four), and is an indication this is an end group of a polymer chain. If these signals were part of molecules with low molecular

weight, for example residual initiator, combined initiator or oligomers, these signals should have disappeared. Unfortunately, it could not be determined if the guanidine protons exchanged with deuterium and peak five overlapped with the polymer peaks. Therefore, from the integral of poly(acrylic acid) (**8**) (peak five in Figure 2.13, peak four in Figure 2.14) and initiated 2,2'-azobis(2-methylpropionamidine) dihydrochloride (**4**) (peaks one and six in Figure 2.13, one and five in Figure 2.14) it was not possible to calculate the molecular weight. The peaks in box two correspond to residual acrylic acid (**7**) and peak three corresponds to the suppressed water signal.

When using 4,4'-azobis(4-cyanovaleric acid) (**3**) as the initiator, the broad peaks at 8.5 ppm are, as suspected, not present in the ^{1}H NMR spectrum (Figure 2.15). The signals in box one corresponds to the residual acrylic acid (**7**), the signals labelled two are assigned to poly(acrylic acid) (**8**) and the two signals labelled as three and the peak at 1.60 ppm are for 4,4'-azobis(4-cyanovaleric acid) (**3**).

2.5.4 Conversion in flow

The screening of various parameters showed that a reaction temperature below 70 °C led to poor conversion (Figure 2.16), especially at low initiator concentrations. Furthermore, an increase in residence time (from 10 to 20 minutes) did not cause a substantial difference in the overall conversion. Therefore, polymerisations with temperatures at or below 70 °C were not investigated further.

Screening of reaction temperatures showed that nearly full conversion was reached at 90 °C (Figure 2.17). The graphs in Figure 2.17 show conversion versus temperature (70 °C, 80 °C and 90 °C) for the four different residence times (5, 10, 20 and 30 minutes) evaluated. The acrylic acid (**7**) concentration was 0.4 mM, 0.7 mM and 1.0 mM for 70, 80 and 90 °C, respectively. From the plots it becomes evident that temperature is an important parameter in order to obtain full conversion. At 70 °C the half-life time of the initiator is 88 minutes (Table 2.4) and therefore, there is insufficient initiator activated to convert all of the acrylic acid (**7**). This is particularly

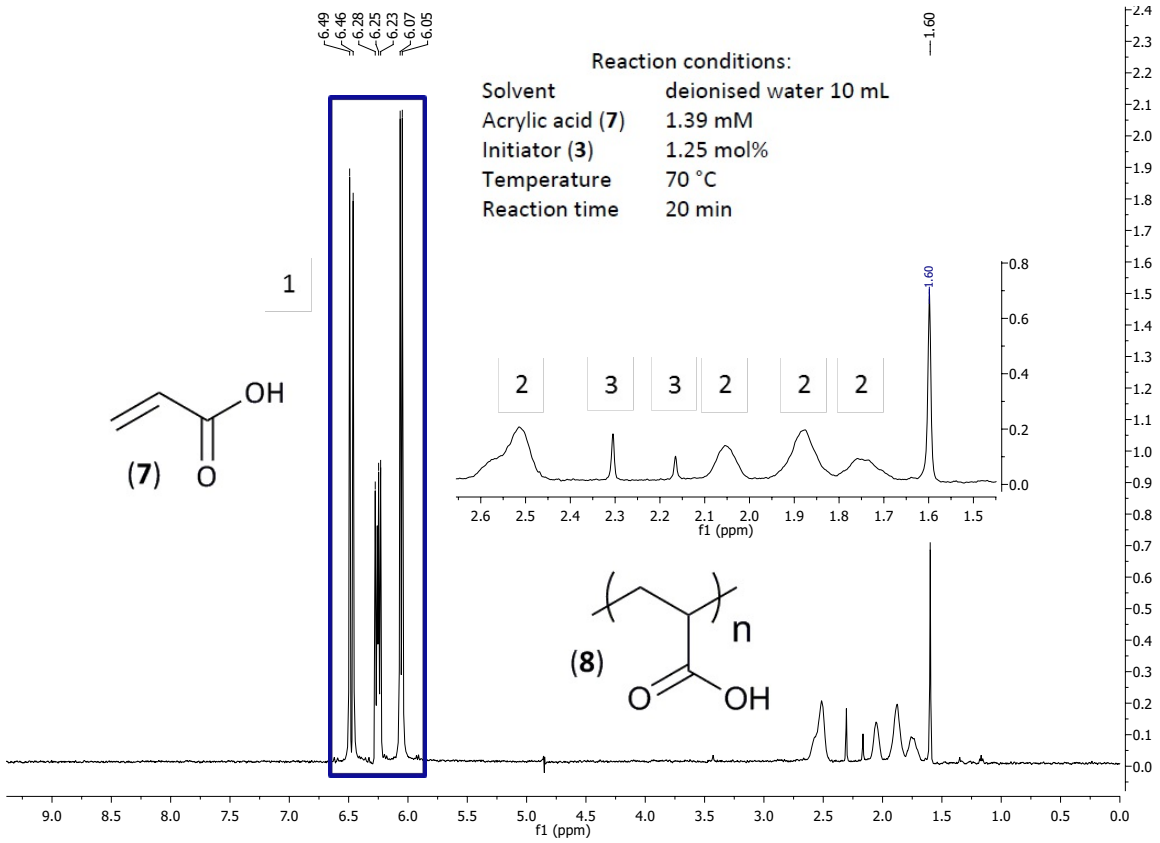

Figure 2.15: ^{1}H NMR with water suppression using cyanovaleric acid (**3**) as radical initiator.

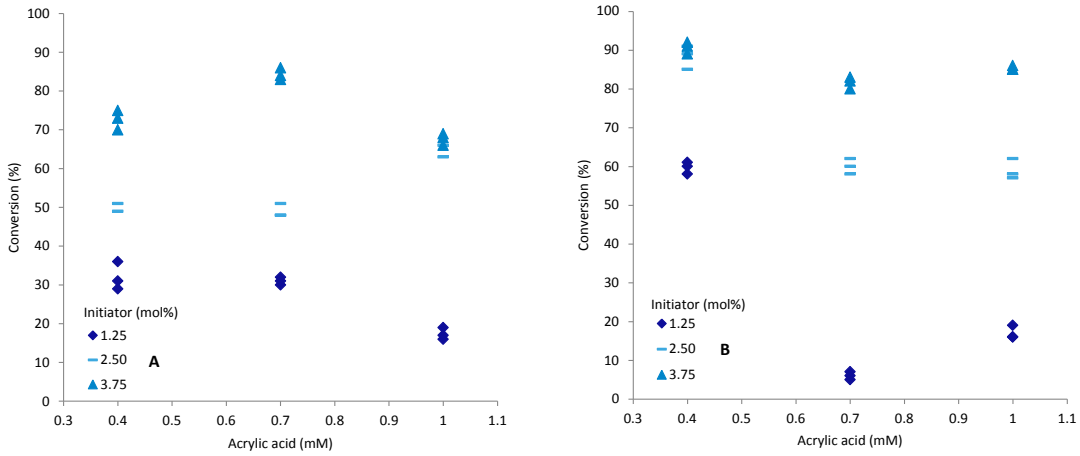

Figure 2.16: Conversion (%) versus concentration acrylic acid (**7**) (mM) at 60 °C. A: polymerisation with 10 minutes residence time, B: polymerisation with 20 minutes residence time.

the case for short residence times. Consequently, the acrylic acid (**7**) conversion can be increased at short residence time by increasing the initiator concentration (note, that the scale of the y-axis in Figure 2.17 runs from 50-100% (A), 60-100% (B) and

80-100% (C)). Conversely for short residence times variable conversions are achieved at low initiator concentrations. In general it is hard to achieve full or close to full conversion when temperatures are below 80 °C.

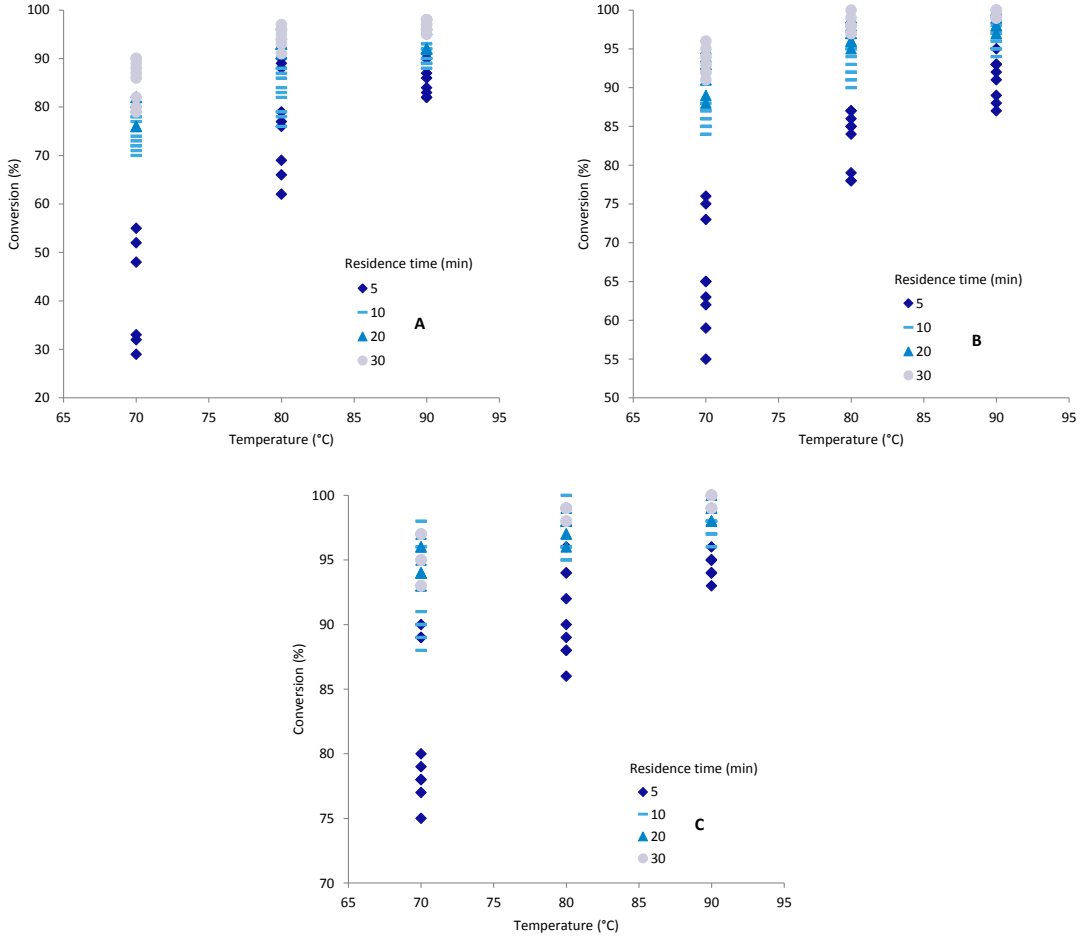

Figure 2.17: Conversion (%) versus Temperature (°C). A: 1.25 mol% of initiator, B: 2.50 mol% of initiator, C: 3.75 mol% of initiator.

The data in Figures 2.17 and 2.18 shows similar trends, with higher temperatures resulting in an increase in conversion. Furthermore, longer residence time produce an increase in conversion. The difference between figure 2.17 and 2.18 is, however, the number of the data points for acrylic acid (**7**) concentration. Figure 2.18 contains only the data obtained from the reactions performed with 2.50 mol% of initiator. The plots for 1.25 mol% and 3.75 mol% initiator concentrations show similar trends. In general, the conversion of acrylic acid (**7**) at 70 °C increases for higher concentrations of the monomer, which can be explained by its increased availability. With a higher concentration of monomer it is more likely that propagation will occur due

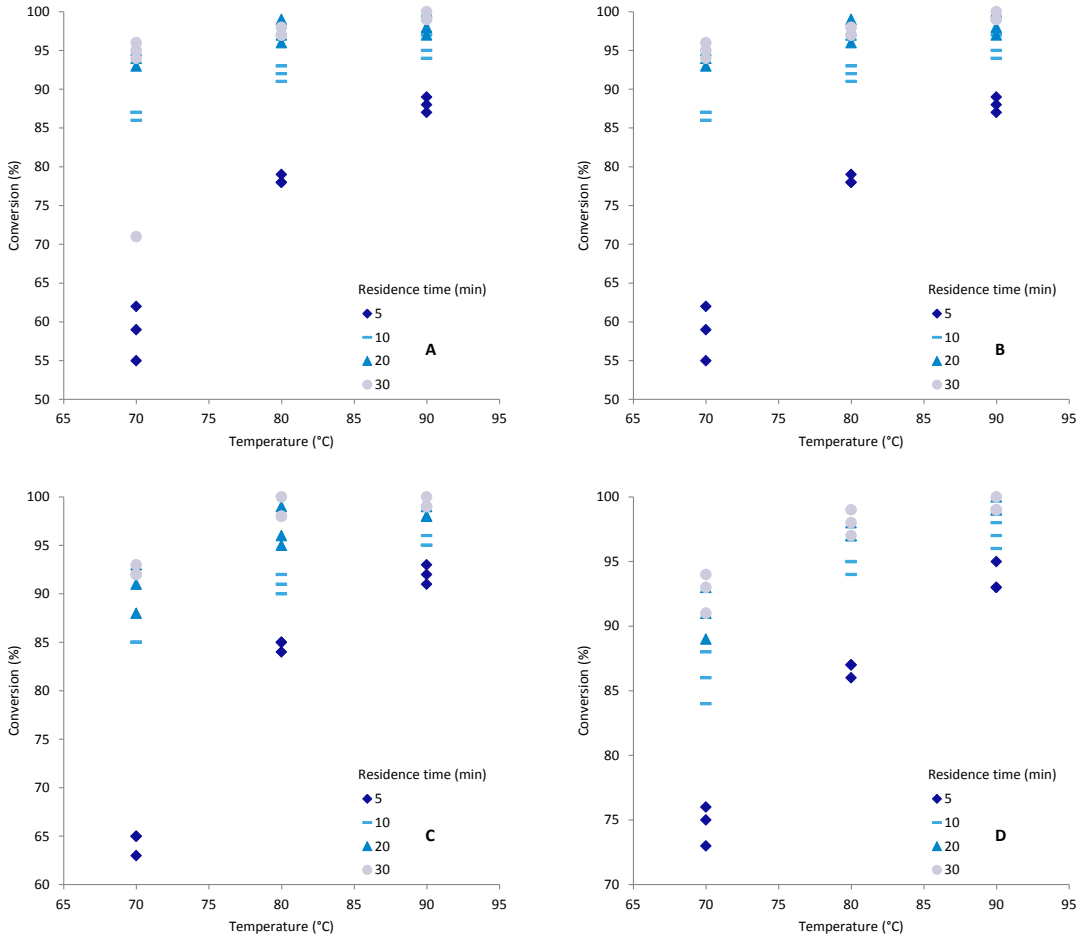

Figure 2.18: Conversion (%) versus Temperature (°C). The initiator amount is 2.50 mol% and A: 0.4 mM acrylic acid (**7**), B: 0.4 mM acrylic acid (**7**), C: 0.7 mM acrylic acid (**7**) and D: 1.0 mM acrylic acid (**7**).

to the favourable interaction of an active polymer chain and a monomer unit. As concentration decreases, the likelihood of termination increases. Longer residence times do not show this trend due to the increase of active initiator. For example, at a lower concentration only a small amount of radicals are formed during the course of the process, where as at high concentration large amounts are formed during the experiment. Furthermore, short chains are statistically more likely to propagate, and higher temperatures will result in more activated initiator. The determined dispersity and molecular weight also support this theory (Table 2.5). Dispersity and molecular weight both slightly increase with higher monomer concentration.

Conversion, molecular weight and dispersity are all based on an average of at least two separate experiment measurements. The range of conversion is ± 10%

Table 2.5: Conversion, molecular weight and dispersity for 0.4 mM, 0.7 mM and 1.0 mM at 70 °C, 5 min and 2.50 mol% initiator.

Temperature (°C)	**Acrylic acid (7) (mM)**	**Conversion (%)**	$\boldsymbol{M_w}$ **(g mol^{-1})**	$\boldsymbol{Đ}$
70	0.4	59	245,000	1.14
80	0.7	65	366,000	1.30
90	1.0	75	384,000	1.38

when the extreme values of all data points are taken into account. For example, graph A in Figure 2.18 shows an odd bend for a residence time of 30 minutes. The conversion of this particular point has therefore been measured four times. Without the extreme value of these four measurements the average conversion for 70 °C, 30 min residence time, 0.4 mM acrylic acid (**7**) and 2.50 mol% initiator would have been 95% (graph B Figure 2.18), which is in line with the expected value. Therefore, the assumption was made that a data point that deviates more than 5% from the initial average conversion is an extreme value and should therefore be removed from the data to obtain better fits (graph B Figure 2.18). Reducing the extreme values resulted in an average conversion with a maximum range of ± 4%. All data points were still based on a minimum of three measurements. For example, the average conversion was 80%, the obtained conversion were between 76% and 84% (both rounded to the nearest whole unit). The outliers were removed from the data in order to be able to create a predictive model.

2.5.5 Molecular weight in flow

To determine the average molecular weight and dispersity a minimum, if possible, of two measurements were used. For example (using imaginary values), the molecular weights of 135,000 g mol^{-1} and 165,000 g mol^{-1} gave a calculated average molecular weight of 150,000 g mol^{-1} and a deviation of 10%. Similarly, an average dispersity was calculated from 1.48 and 1.72 giving an average dispersity of 1.60 with a deviation of 8%.

Having analysed in full detail, the results show a maximum deviation of 7% on

molecular weight and 5% on dispersity. This indicates a relatively high robustness to the protocol. For example (using imaginary values), the calculated average average molecular weight was 150,000 g mol^{-1}, the obtained molecular weights were between 139,000 g mol^{-1} and 161,000 g mol^{-1} (rounded to the nearest thousand). The calculated average dispersity was for example 1.60, the obtained dispersity were between 1.52 and 1.68 (rounded to two significant digits).

A more complex element from this screening is the relationship between molecular weight and dispersity of the synthesised polymer. The recorded GPC spectrum reveals more information about the polymer sample than the single numbers representing average molecular weight and dispersity alone. Figure 2.19 to 2.21 show the influence of temperature, residence time, concentration of monomer and initiator on the average molecular weight. A residence time of five minutes results in less consistent results. This can be explained by the fact that the initiator half-life time for 70, 80 and 90 °C is much higher than the residence time. Therefore, fewer chains will be formed and, as result, the average molecular weight will increase for lower amounts of initiator and higher concentrations of monomer. From these figures it becomes clear that, as expected, higher monomer concentrations increase the average molecular weight, with a constant concentration of initiator. Temperature also has a pronounced influence on the average molecular weight. An increase in temperature results in lower average molecular weight. This can be explained by the impact on initiator half-life time, with higher temperature resulting in smaller half-life times and therefore more radicals are formed per unit time. Unfortunately, some of the data point are out of sync. For example, Figure 2.19 A [initiator] (**4**) = 1.25 mol% and [initiator] (**4**) = 3.75 mol% were expected to be linear and in the same order as Figure 2.19 B. It was anticipated low initiator concentration would result in higher molecular weight. These samples could not be measured again due to GPC failure.

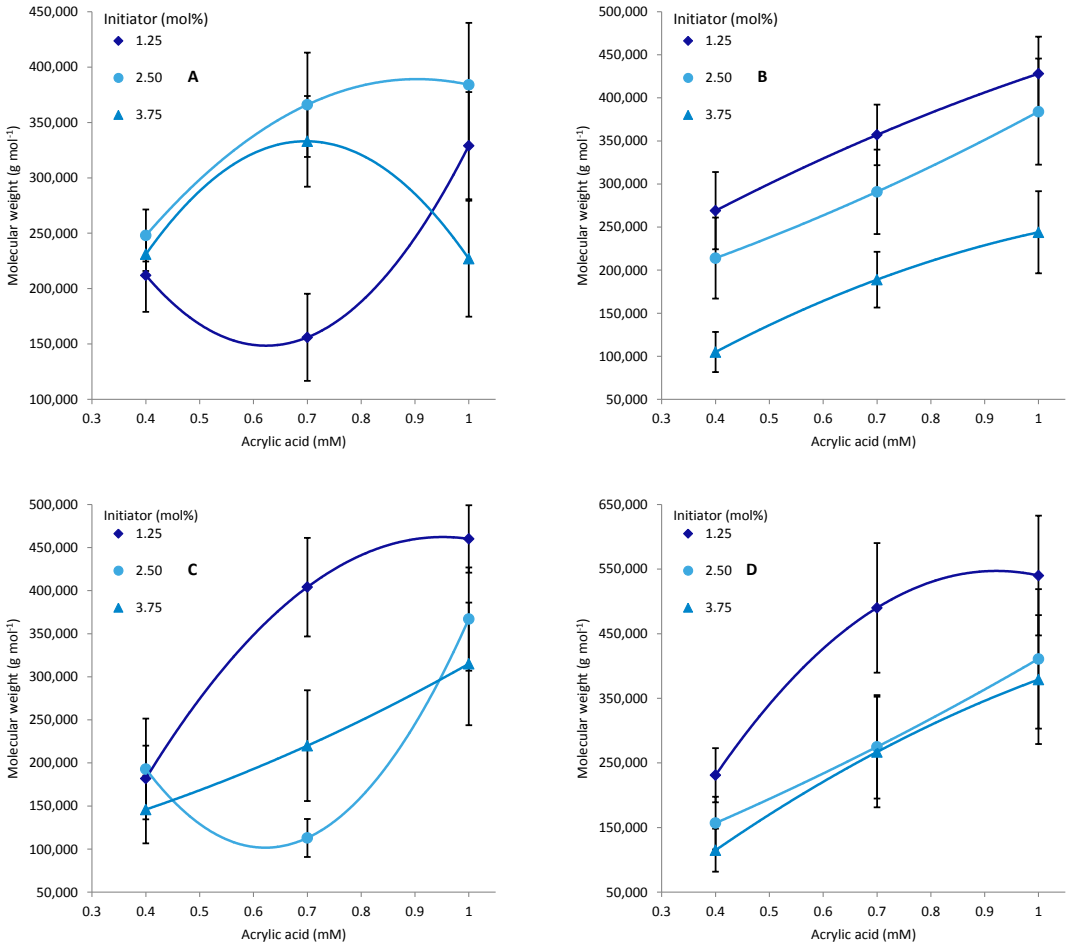

Figure 2.19: Molecular weight (g mol^{-1}) versus concentration acrylic acid (**7**) (mM) at 70 °C. A: polymerisation with 5 minutes residence time, B: polymerisation with 10 minutes residence time, C: polymerisation with 20 minutes residence time, D: polymerisation with 30 minutes residence time.

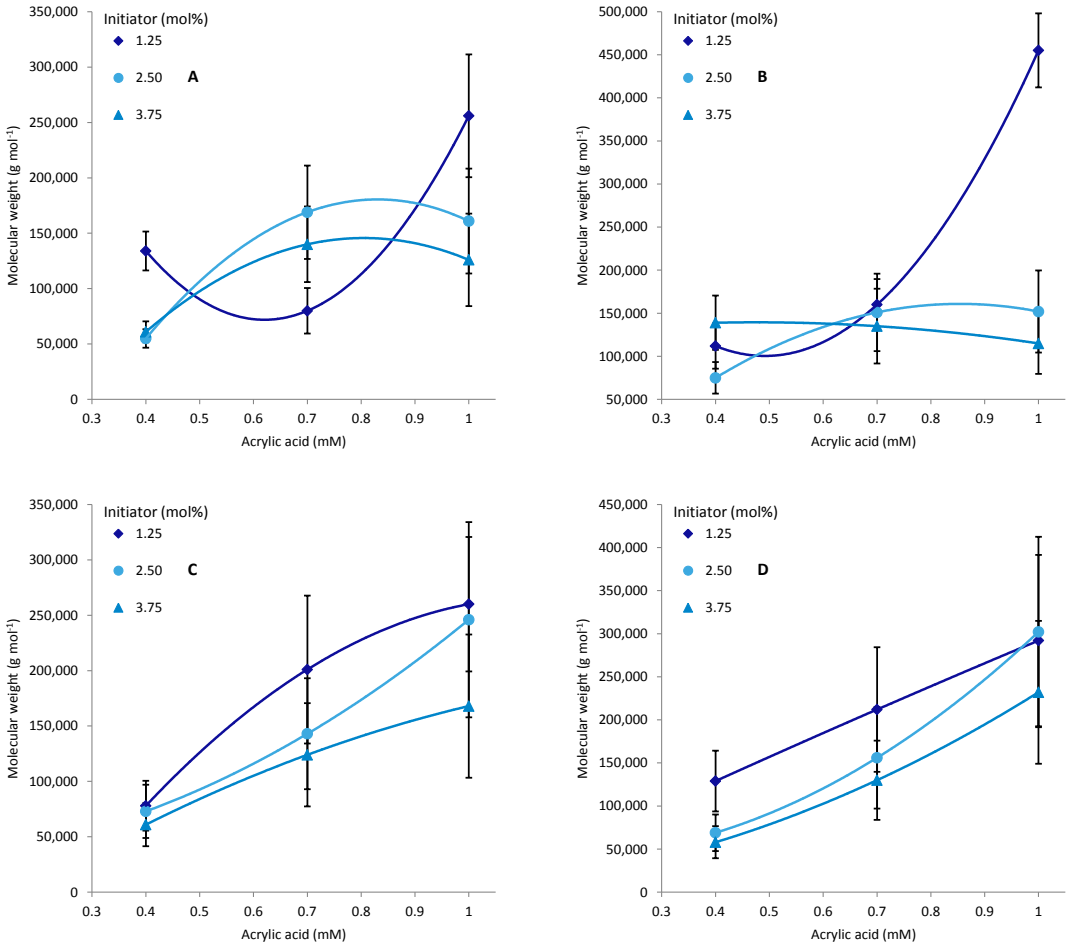

Figure 2.20: Molecular weight (g mol^{-1}) versus concentration acrylic acid (**7**) (mM) at 80 °C. A: polymerisation with 5 minutes residence time, B: polymerisation with 10 minutes residence time, C: polymerisation with 20 minutes residence time, D: polymerisation with 30 minutes residence time.

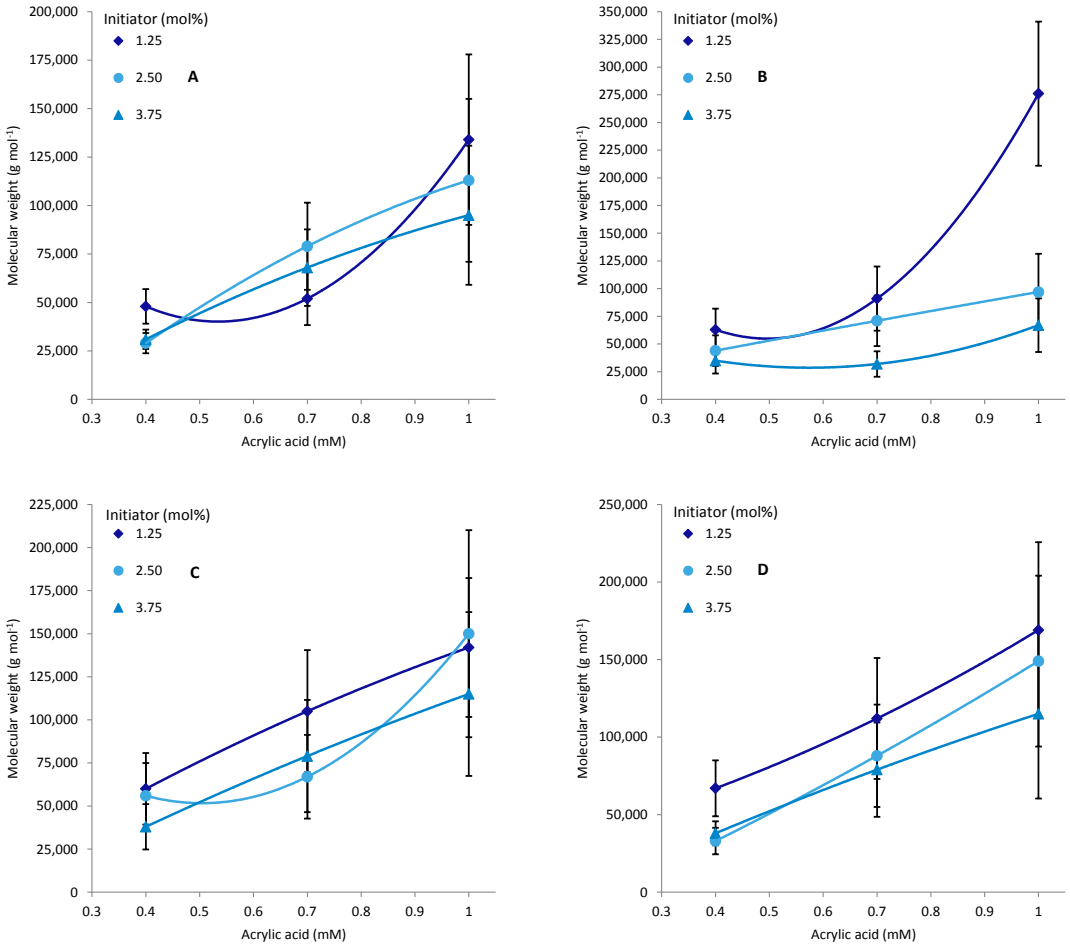

Figure 2.21: Molecular weight (g mol^{-1}) versus concentration acrylic acid (**7**) (mM) at 90 °C. A: polymerisation with 5 minutes residence time, B: polymerisation with 10 minutes residence time, C: polymerisation with 20 minutes residence time, D: polymerisation with 30 minutes residence time.

The data shown in Figures 2.19 to 2.21 shows the influence of various parameters on the resulting average molecular weight of the polymer. Although these graphs support a basic hypothesis, more information can be retrieved from in-depth analysis of the individual GPC spectra. GPC spectra usually do not have a perfect symmetrical distribution. A peak could potentially have no bias (no skew) or a negative or positive skew (Figure 2.22). A negatively skewed peak in GPC spectra implies more polymer chains with low molecular weight, whilst a positively skewed peak implies polymer chains with relatively more high molecular weights. The peak shape therefore gives further information about the dispersity. In addition if a small shoulder appears on either side, this can also influence the average dispersity significantly.

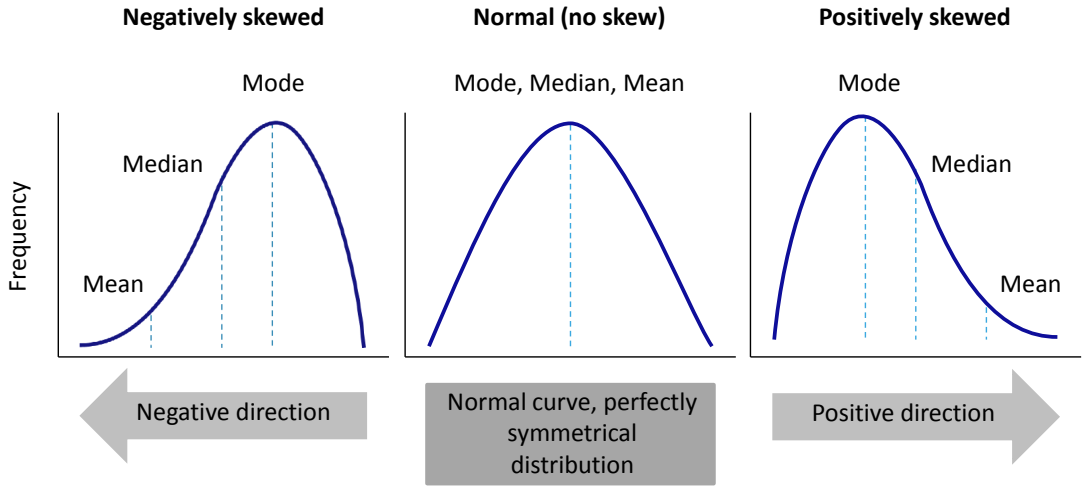

Figure 2.22: Skewness of distribution.

2.5.6 Analysis of GPC data

In Figure 2.23 the refractive index versus retention volume (mL) is plotted. The parameters of the different spectra are [acrylic acid] = 0.4 mM, [I] = 1.25 mol%, Rt = 30 minutes, T = 70 °C (red), 80 °C (purple), 90 °C (green). The principle peak is shifted with respect to retention volume. This is most likely due to changing molecular weight of the polymers. Smaller polymers elute with a longer residence time due to greater interaction with the column. The smaller auxiliary peaks do not show the same shifts and therefore the conditions used did not affect the components these correspond with. The peak having a retention volume of 19.7 mL (peak 2 in Figure 2.23) corresponds to residual acrylic acid (**7**). As the overall conversion is low at 70 °C (80%) compared to 80 °C (93%) and 90 °C (96%) the intensity of the residual monomer signal (peak 2 in Figure 2.23) will be proportionally higher. It is not possible to calculate the conversion from the data in Figure 2.23 as there is not a clear separation between the peaks. Acrylic acid (**7**) is visible in the refractive index but not in the RALS detector. The peaks at retention volumes 21.6 mL (peak 3) and 24.0 mL (peak 4) are from the solvent. The tailing of the peak which corresponds with the trace for 70 °C (red) is slightly shifted to the right, where the other two have a more equal distribution. This does not have a negative effect on the dispersity (Table 2.6). Although the peaks are relatively equally distributed, the

dispersity of the peaks is not as low as was targeted. Higher temperatures resulting in a higher concentration of active initiator and, therefore, shorter polymer chains are produce. This will increase the dispersity. The analysed sample contained also oligomers, which is shown in Figure 2.24.

Table 2.6: Conversion, molecular weight and dispersity for Rt = 30 min, [acrylic acid] = 0.4 mM and [I] = 1.25 mol%.

Temperature (°C)	Conversion (%)	M_w (g mol^{-1})	$Đ$
70	80	231,000	1.57
80	93	129,000	2.19
90	96	67,000	2.17

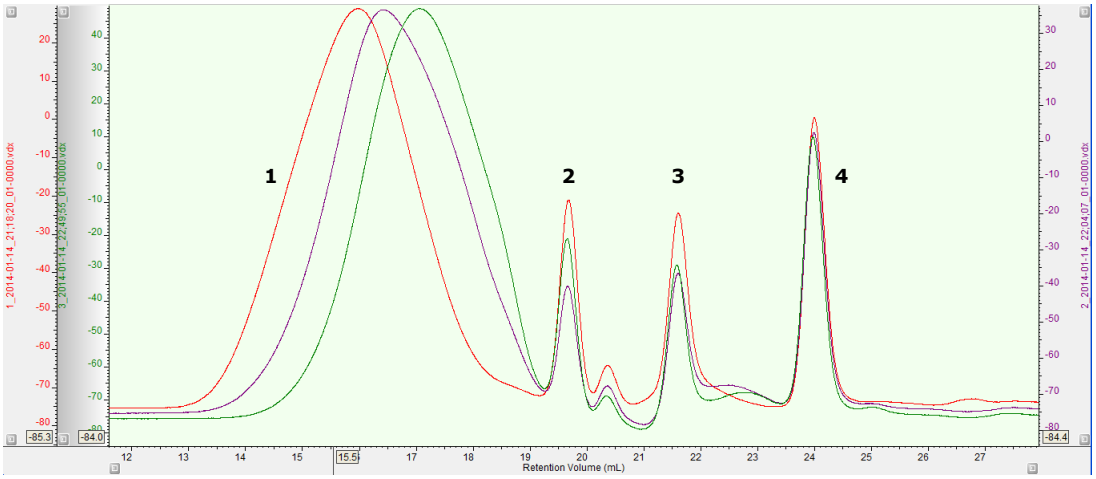

Figure 2.23: Comparing temperature 70 °C (red), 80 °C (purple) and 90 °C (green) for refractive index (Rt = 30 min, [acrylic acid] = 0.4 mM, [I] = 1.25 mol%).

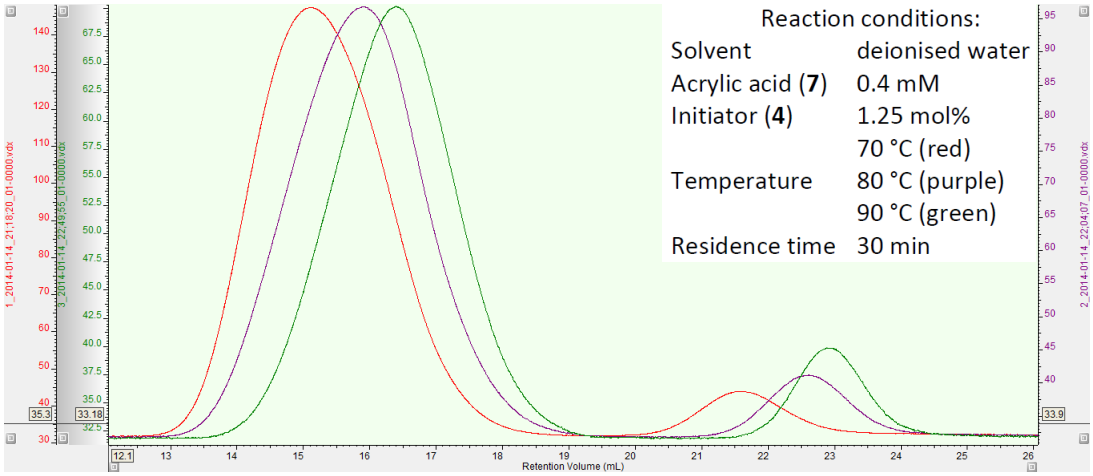

Figure 2.24: Comparing temperature 70 °C (red), 80 °C (purple) and 90 °C (green) for RALS (Rt = 30 min, [acrylic acid] = 0.4 mM, [I] = 1.25 mol%).

Comparing the results obtained from a residence time of 30 minutes (Table 2.6, Figure 2.23 and 2.24) and 5 minutes (Table 2.7, Figure 2.25 and 2.26) show a similar trends. The refractive index versus retention volume (mL) is plotted in Figure 2.25. The red, purple and green spectra correspond respectively with reaction temperatures of 70 °C, 80 °C and 90 °C. It is clear from Figure 2.25 the monomer conversion is lower at 70 °C than at 80 °C and 90 °C (Table 2.7). Both the spectra obtained from the refractive index (Figure 2.25) and RALS (Figure 2.26) show a negative skewing for 70 °C, normal distribution for 80 °C and positive skewing for 90 °C. The skewing however does have an impact upon dispersity. The results for 5 minutes show a lower dispersity. This can be explained due to the shorter residence times at given temperatures resulting in lower overall amount of active initiator being produced.

Table 2.7: Conversion, molecular weight and dispersity for Rt = 5 min, [acrylic acid] = 0.4 mM and [I] = 1.25 mol%.

Temperature (°C)	**Conversion (%)**	$\boldsymbol{M_w}$ **(g mol^{-1})**	$\boldsymbol{Đ}$
70	32	378,000	1.44
80	66	134,000	1.35
90	82	48,000	1.58

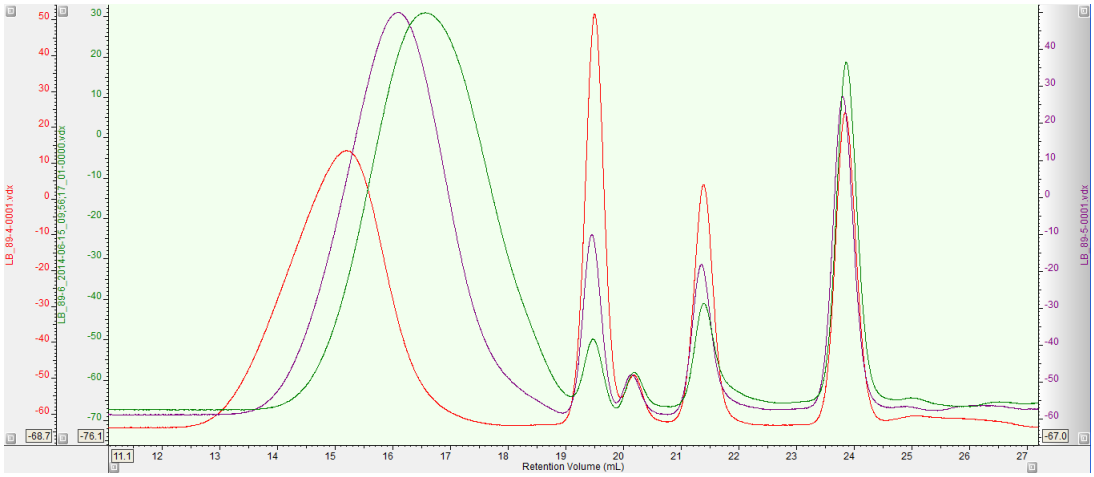

Figure 2.25: Comparing temperature 70 °C (red), 80 °C (purple) and 90 °C (green) for refractive index (Rt = 5 min, [acrylic acid] = 0.4 mM, [I] = 1.25 mol%).

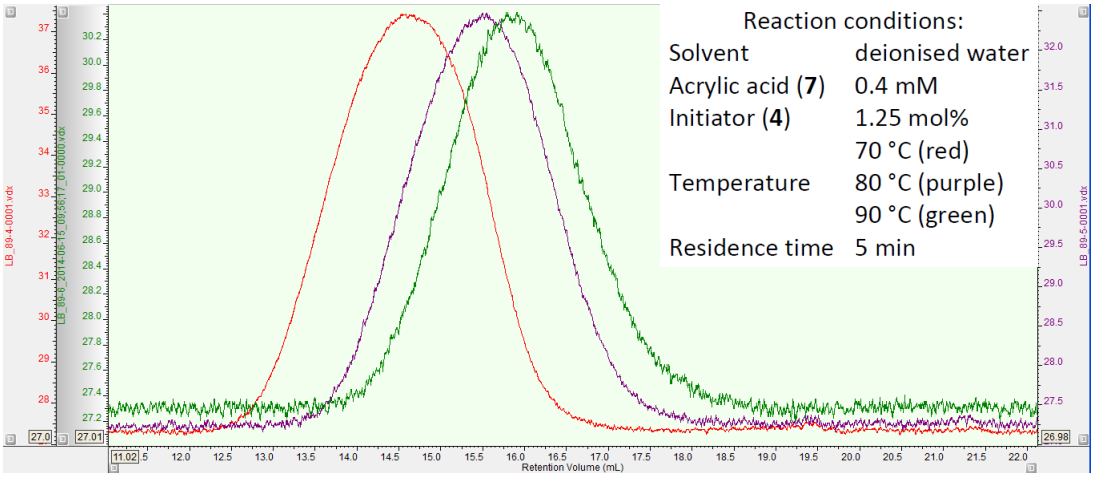

Figure 2.26: Comparing temperature 70 °C (red), 80 °C (purple) and 90 °C (green) for RALS (Rt = 5 min, [acrylic acid] = 0.4 mM, [I] = 1.25 mol%).

A monomer concentration of 1.0 mM and initiator concentration of 1.25 mol% resulted in a similar trend as changing from 5 to 30 minutes with regards to conversion (increase for higher temperatures), molecular weight (decrease for higher temperatures) and dispersity (increase for higher temperatures) (Table 2.8). The conversion of monomer is higher at higher temperatures and the molecular weight approximately halves for every temperature increase of 10 °C. The dispersity also increased when the temperature was raised above 70 °C but changed little between 80 °C and 90 °C. The refractive index (Figure 2.27) shows an equal distribution for the spectrum corresponding with 70 °C (red), whereas both spectra for 80 °C (purple) and 90 °C (green) show slight shoulders. The RALS (Figure 2.28) spectra for 80 °C (purple) and 90 °C (green) are positively skewed which indicates polymer chains with high molecular weights are dominant.

Table 2.8: Conversion, molecular weight and dispersity for Rt = 30 min, [acrylic acid] = 1.0 mM and [I] = 1.25 mol%.

Temperature (°C)	**Conversion (%)**	$\boldsymbol{M_w}$ **(g mol^{-1})**	$\boldsymbol{Đ}$
70	88	540,000	1.52
80	96	292,000	3.14
90	98	169,000	3.04

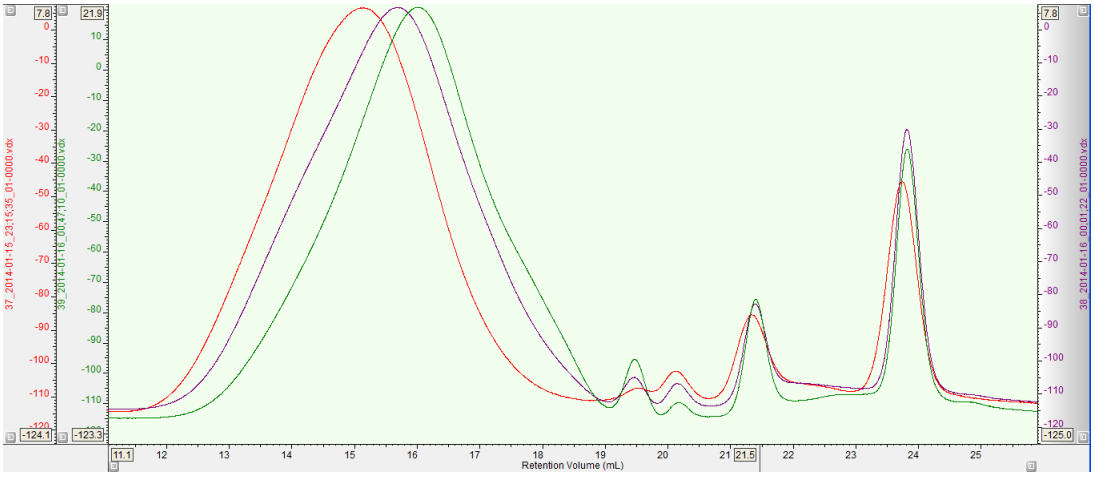

Figure 2.27: Comparing temperature 70 °C (red), 80 °C (purple) and 90 °C (green) for refractive index (Rt = 30 min, [acrylic acid] = 1.0 mM, [I] = 1.25 mol%).

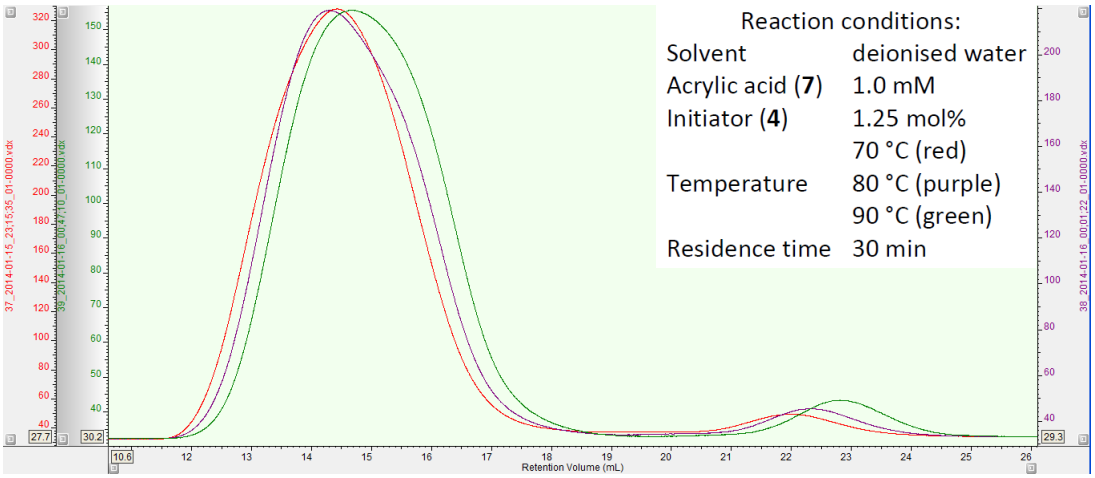

Figure 2.28: Comparing temperature 70 °C (red), 80 °C (purple) and 90 °C (green) for RALS (Rt = 30 min, [acrylic acid] = 1.0 mM, [I] = 1.25 mol%).

The polymerisation of acrylic acid (**7**) (1 mM) with a residence time of 5 minutes and initiator concentration of 1.25 mol% gave the results mentioned in Table 2.9. The trend in the results is similar to Table 2.8, although the molecular weight decreases less with changing temperature. The dispersity increases for higher temperatures (Table 2.9 and Figure 2.29 and 2.30). This trend holds true for 70 °C (red) and 80 °C (purple) (Table 2.8, Figure 2.27 and 2.28) at longer residence time (30 min). The dispersity increases for higher conversion (2.31) and this is the case for all concentrations of acrylic acid (**7**). Thus, the dispersity of the reaction at 80 °C (purple) (Table 2.8) would be expected as full conversion was not obtained. The dispersity at 90 °C is high as there is overlap at the right tail of the main peak in

the refractive index (Figure 2.29), indicating the presence of polymers with a low molecular weight.

Table 2.9: Conversion, molecular weight and dispersity for Rt = 5 min, [acrylic acid] = 1.0 mM and [I] = 1.25 mol%.

Temperature (°C)	**Conversion (%)**	M_w **(g mol^{-1})**	$Đ$
70	52	329,000	1.42
80	77	256,000	1.77
90	89	134,000	2.91

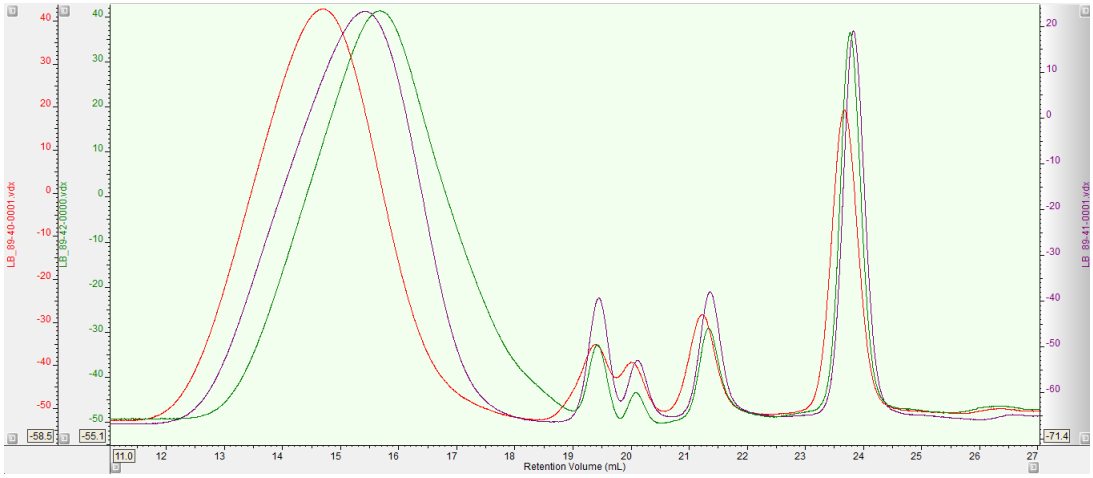

Figure 2.29: Comparing temperature 70 °C (red), 80 °C (purple) and 90 °C (green) for refractive index (Rt = 5 min, [acrylic acid] = 1.0 mM, [I] = 1.25 mol%).

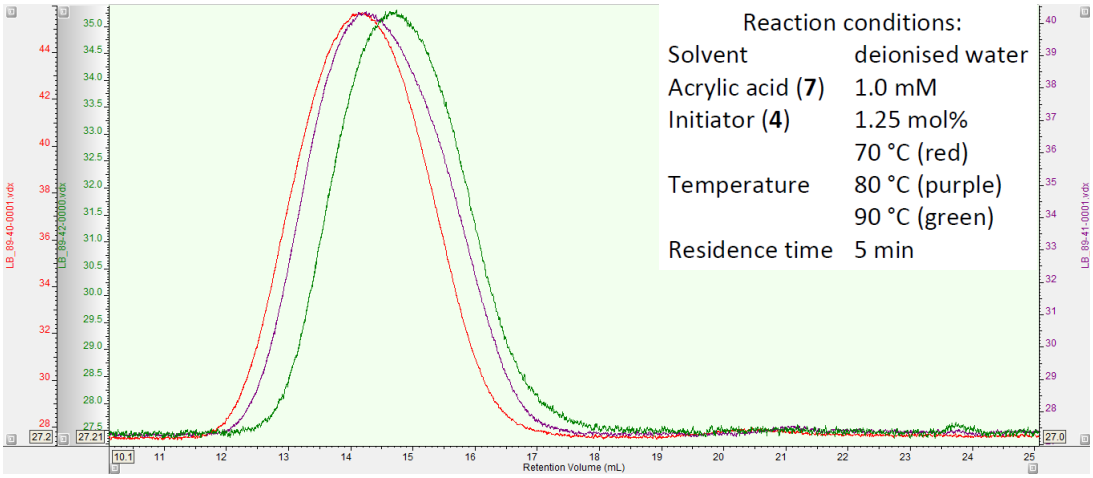

Figure 2.30: Comparing temperature 70 °C (red), 80 °C (purple) and 90 °C (green) for RALS (Rt = 5 min, [acrylic acid] = 1.0 mM, [I] = 1.25 mol%).

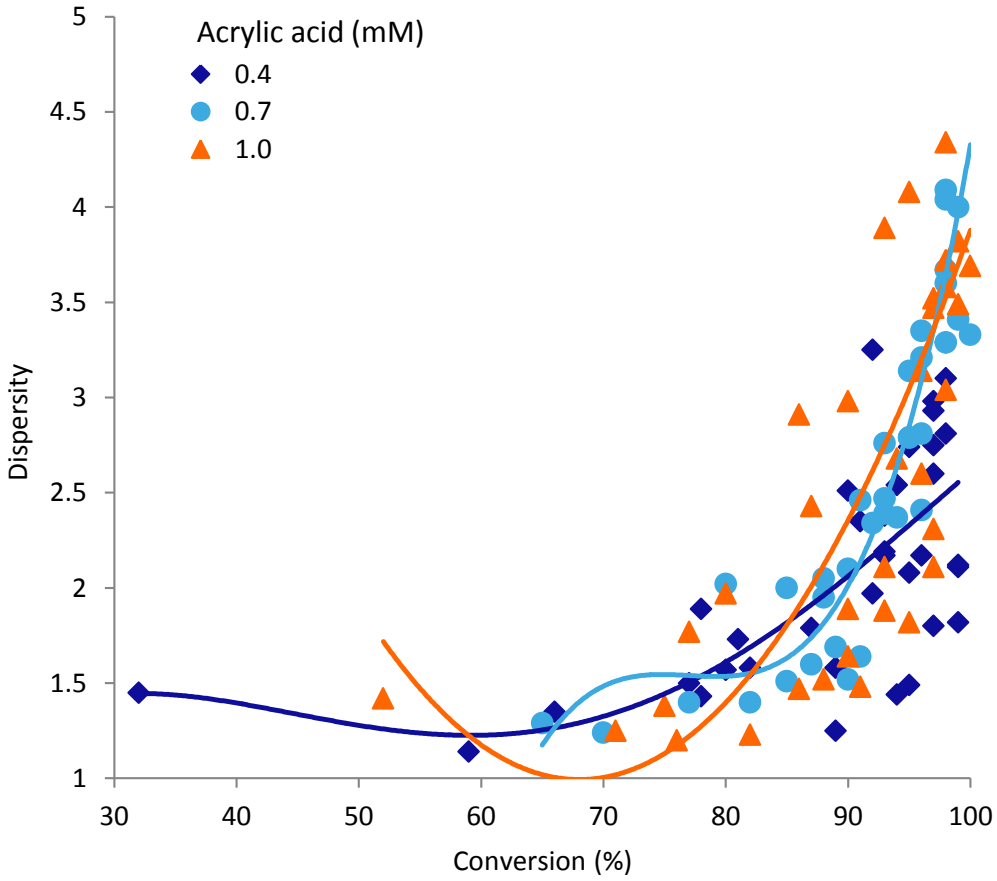

Figure 2.31: Dispersity versus conversion.

Increasing the amount of initiator to 3.75 mol% and maintaining the concentration of acrylic acid (**7**) constant (1.0 mM) and residence time (5 minutes) produced the output as shown in Table 2.10. Increased conversion was observed at higher temperatures (Figure 2.17 and 2.18), which was accompanied by a decrease in molecular weight. This was expected as more active initiator is produced at higher temperatures (Table 2.4). The refractive index spectrum (Figure 2.32) at 90 °C indicates a slight shoulder at a retention volume of 18 mL. This negatively influences the dispersity. The refractive index (Figure 2.32) for 70 °C is slightly negatively skewed and the RALS (Figure 2.33) is slightly positively skewed. The refractive index and RALS for 80 °C are both normal in form. The increase in dispersity can be rationalised by the small shoulder visible in the refractive index spectra at a retention volume of 18 to 19 mL (Figure 2.32) which represents polymers with a low molecular weight.

Table 2.10: Conversion, molecular weight and dispersity for Rt = 5 min, [acrylic acid] = 1.0 mM and [I] = 3.75 mol%.

Temperature (°C)	Conversion (%)	M_w (g mol^{-1})	$Đ$
70	80	227,000	1.97
80	90	126,000	2.98
90	95	95,000	4.08

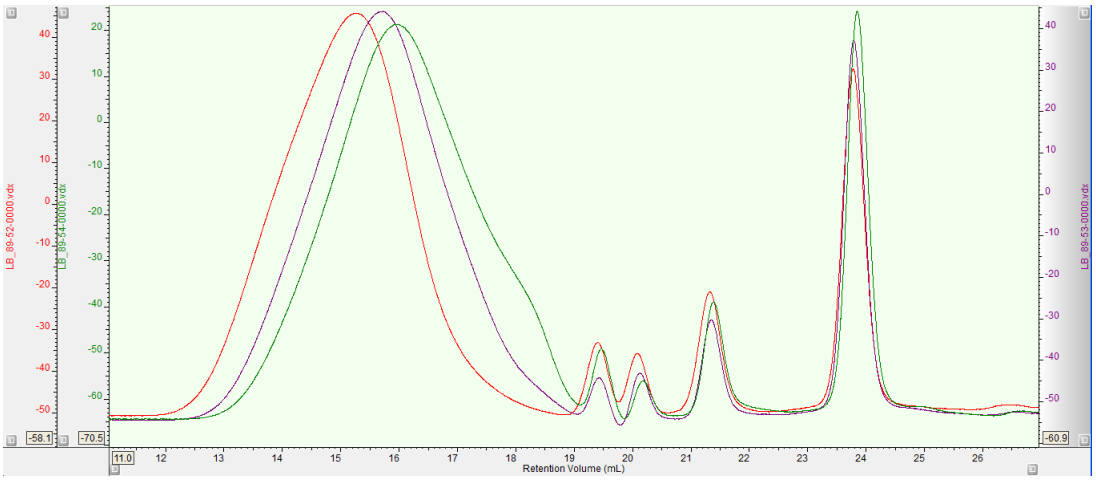

Figure 2.32: Comparing temperature 70 °C (red), 80 °C (purple) and 90 °C (green) for refractive index (Rt = 5 min, [acrylic acid] = 1.0 mM, [I] = 1.25 mol%).

For long residence times nearly full conversion was achieved and did not drastically influence the molecular weight. The difference between the polymer molecular weights obtained at a residence time of 5 minutes and 20 minutes was only an increase of 15%. This difference can be rationalised as being due to the different batches of starting material used or the difference in the column condition whilst running the GPC measurements (same model was used). For reference, the difference between the molecular weight of the polymers obtained at a residence time of 20 minutes and 30 minutes was 8% (Table 2.11).

Dispersity is expected to increase for longer residence times and this is also supported by the GPC measurements (Figure 2.34 and 2.35). The spectra for 20 minutes (green) and 30 minutes (black) residence time are positively skewed, especially the 30 minutes plot (black) which has a shoulder in the spectra of the refractive index detector (Figure 2.34). The positive skew and shoulder indicate a large amount of polymers with a low molecular weight. Having analysed all the given data sets,

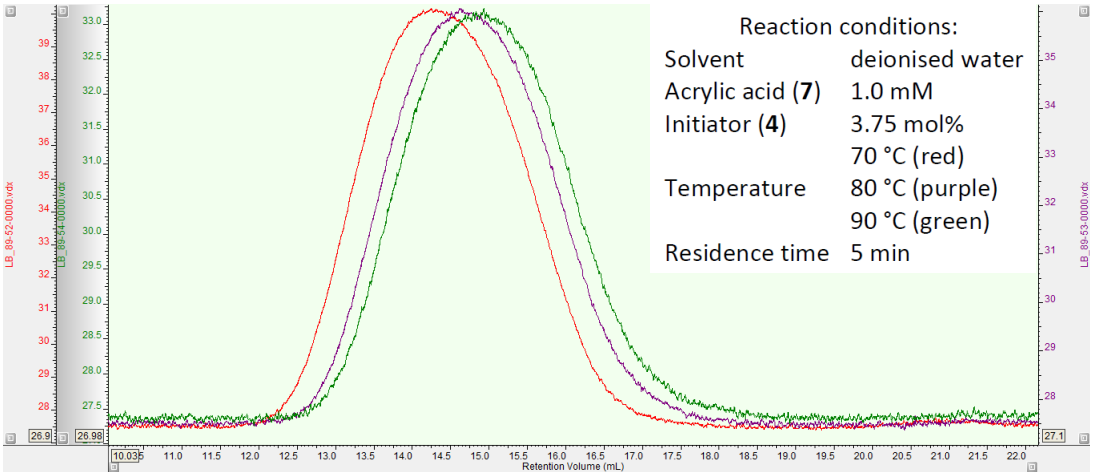

Figure 2.33: Comparing temperature 70 °C (red), 80 °C (purple) and 90 °C (green) for RALS (Rt = 5 min, [acrylic acid] = 1.0 mM, [I] = 1.25 mol%).

Table 2.11: Conversion, molecular weight and dispersity for T = 80 °C, [acrylic acid] = 0.7 mM and [I] = 2.50 mol%.

Residence time (min)	**Conversion (%)**	$\boldsymbol{M_w}$ **(g mol^{-1})**	$\boldsymbol{Đ}$
5	85	169,000	2.00
10	91	151,000	2.46
20	96	143,000	3.35
30	98	156,000	4.09

Table 2.3 gives a predictable trend. Temperature has a significant effect on the conversion, which will increase for higher temperature. The molecular weight of the polymer increases for higher monomer concentrations, lower initiator concentration and longer residence time. The molecular weight decreases for higher temperature. Dispersity increases when the conversion increases.

2.5.7 Termination

In general, the termination of the polymeric chains was not by combination, otherwise, bimodal peaks would appear in the GPC spectra, but these were not observed. Termination by combination involves two polymeric chains of different molecular weights and will most often result in a bimodal peak (Figure 2.36). Also, the coupling of two radicals together is by far less energetically favourable, requiring approximately 20 kJ mol.

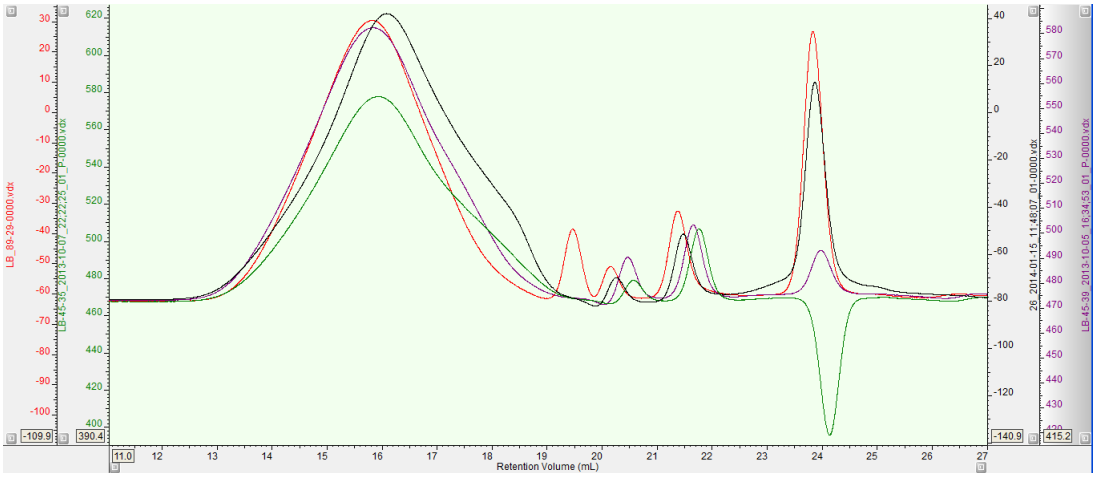

Figure 2.34: Comparing residence time (5 min (red), 10 min (purple), 20 min (green) and 30 min (black)) for refractive index (T = 80 °C, [acrylic acid] = 0.7 mM, [I] = 2.50 mol%).

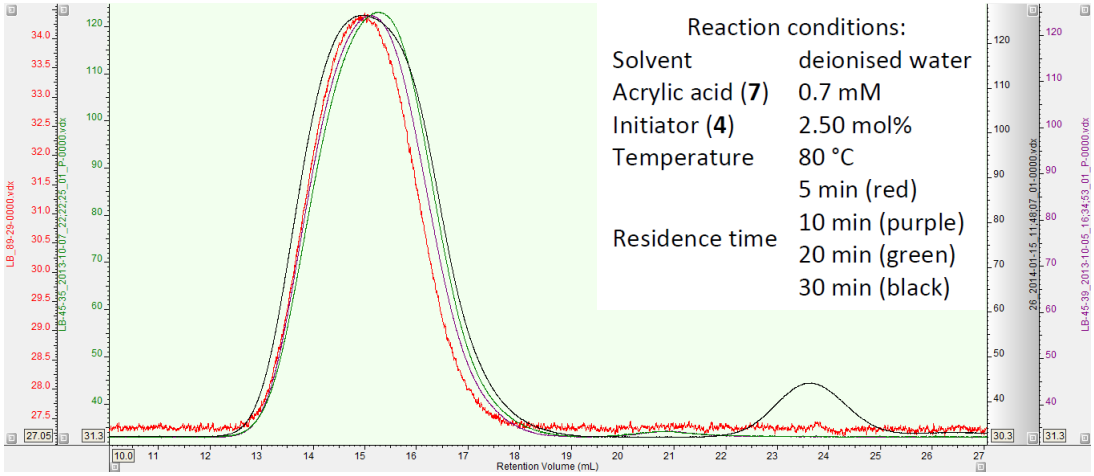

Figure 2.35: Comparing residence time 5 min (red), 10 min (purple), 20 min (green) and 30 min (black) for RALS (T = 80 °C, [acrylic acid] = 0.7 mM, [I] = 2.50 mol%).

If termination were exclusively by combination a bimodal peak in the GPC spectra would not necessarily be expected. Polymers with high molecular weight will most likely combine with polymers with low molecular weight as movement is limited.

Several spectra, for example Figure 2.34, have peaks which possess shoulders especially at higher retention volumes (17 to 20 mL) indicating an increase in the amount of polymer chains of low molecular weight. The combination of an active chain with an active initiator radical is also possible but less likely as sufficient monomer would still be available especially at short residence times. The Arrhenius

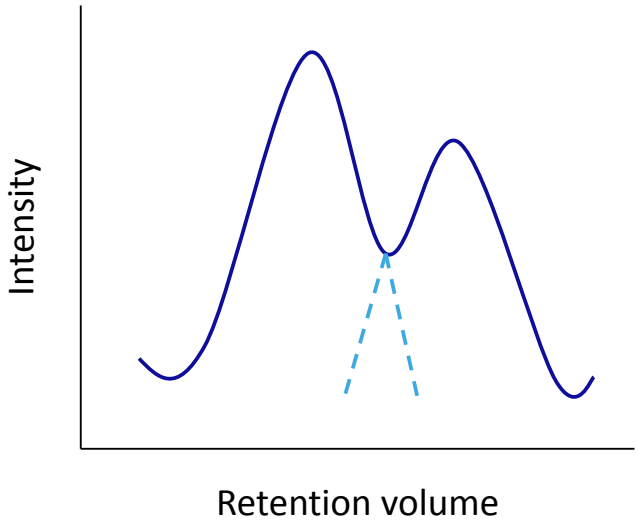

Figure 2.36: Theoretical example of bimodal peaks.

equation (equation 2.3) shows propagation is favoured until the monomer concentration become insufficient, which is near full consumption of the monomer (conversion $> 95\%$). Two other possible terminations are with impurities or *via* radical disproportionation. Although it is possible impurities could have been present, it is still an unlikely termination event. All starting solutions were fully degassed as oxygen had to be removed. Oxygen is a reactive gas and will therefore interfere with the formed radicals and act as a radical scavenger. This will influence the molecular weight and dispersity. Furthermore, the flow system was purged six times by eluting the reactor volume with degassed solvent before each run. This leaves radical disproportionation as the most likely termination mechanism. The termination process will accelerate over time due to the decrease in monomer concentration.

2.5.8 Targeted polymers

The combined data permitted a model to be created to predict a molecular weight for a given set of parameters. The predicted conditions were derived from a $3x3x3x4$ Full Factorial Design and Least Square Fit model using JMP Pro 12.1.0 software. Therefore a set of target molecular weights were selected at random from across three different ranges (rounded to the nearest ten thousand; Table 2.12). The ranges were set at a low, medium and high molecular weight as 80,000 g mol^{-1} – 200,000 g mol^{-1},

210,000 g mol^{-1} – 350,000 g mol^{-1} and 360,000 g mol^{-1} – 500,000 g mol^{-1} respectively.

When the reactions were run and analysed the obtained molecular weights and dispersities were not exactly as predicted. A difference of 1.4% for target M_w = 120,000 g mol^{-1}, 7.6% for target M_w = 310,000 g mol^{-1} and 5.9% for target M_w = 450,000 g mol^{-1} were obtained. The deviation is largest for the targeted molecular weight of 310,000 g mol^{-1}, this could be due to a miscalculation of the concentrations or possibly steady state operation was not reached in the flow reactor. Unfortunately, this experiment was only analysed once due to critical GPC failure. It should also be noted that the spectra were not recorded on the same GPC system as previously used to create the model data (Figure 2.37 to 2.39). Due to fatal system failure these test samples had to be sent away to be screened, using a GPC system with single detection only. Furthermore, the spectra could not be calibrated. In general, the dispersity of all samples analysed were much higher than anticipated. However, the same general trend could still be recognised. The dispersity increases for longer residence times. No final explanation can be made based upon this data in the time remaining in this project.

Table 2.12: Reaction conditions, obtained molecular weight and dispersity for targeted molecular weight.

Target	**Predicted conditions**						**Obtained**	
M_w (g mol^{-1})	T (°C)	R_t (min)	[a](7) (mM)	[I] (4) mol%	M_w (g mol^{-1})	$Đ$	M_w (g mol^{-1})	$Đ$
120,000	72	19.5	0.764	2.60	120,000	3.22	118,000	6.69
310,000	79	10.0	0.785	1.26	311,000	1.48	333,000	2.43
450,000	72	29.0	1.100	1.27	449,000	2.10	477,000	7.53

[a]Acrylic acid concentration

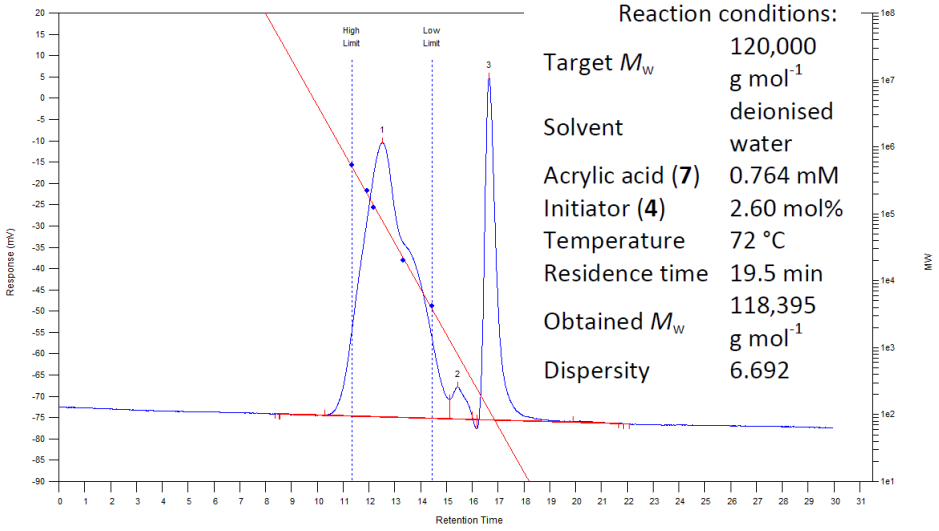

Figure 2.37: Refractive index detector spectrum target M_w = 120,000 g mol^{-1}.

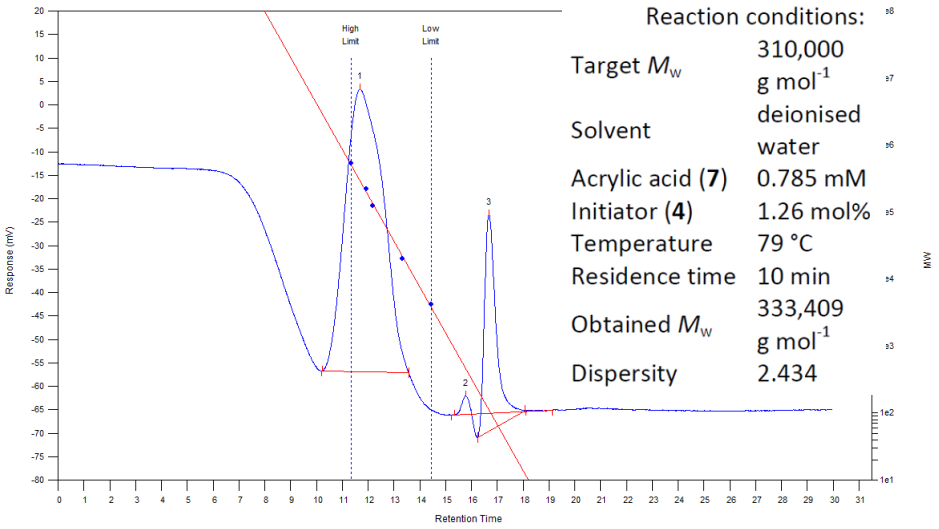

Figure 2.38: Refractive index detector spectrum target M_w = 310,000 g mol^{-1}.

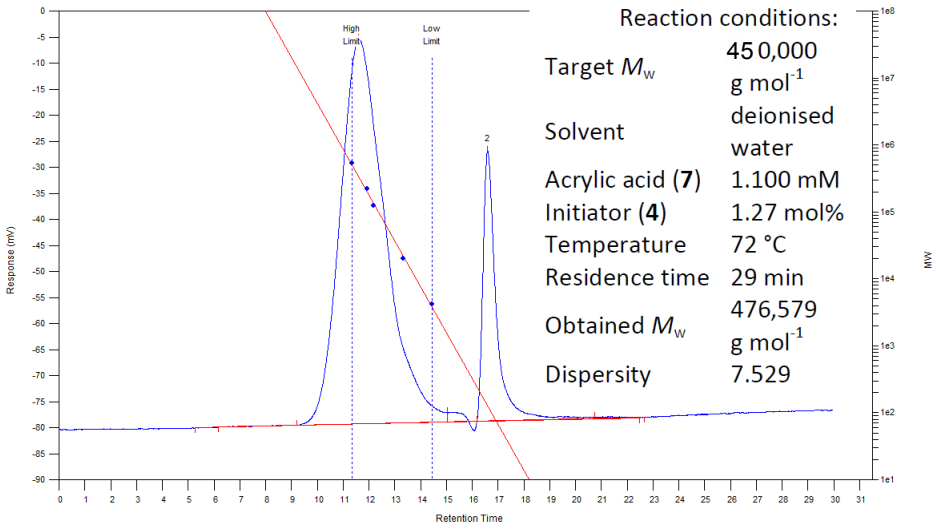

Figure 2.39: Refractive index detector spectrum target M_w = 450,000 g mol^{-1}.

2.6 Conclusion

The aim of the work described in this chapter was to develop a process which could rapidly, safely, efficient and repeatedly perform free radical polymerisation in flow. The designed system was easy to operate and the polymerisation of poly(acrylic acid) (**8**) with different molecular weights proved free radical polymerisation could be performed in flow.

It was determined that residence time has a major influence on the dispersity and molecular weight of the polymers prepared in flow. In addition higher temperature causes higher dispersity as more initiator is activated and thus chains will propagate. For the synthesis of polymers with a low molecular weight high concentrations of initiator should be used in the flow reaction. Conversely low concentrations of initiator should be used to obtain polymers with correspondingly high molecular weight.

As in general the polymer product is more valuable than the starting monomer, conversion is of less importance compared with molecular weight and dispersity. Therefore, although temperatures above 75 °C gave nearly full conversion, if full conversion cannot be reached to obtain a given molecular weight and dispersity due to limitations of the application, the conversion should be taken for granted.

The amount of initiator is one of the keys to influence conversion but is a secondary linked variable associated with residence time and temperature. If the concentration of the acrylic acid (**7**), 2,2'-azobis(2-methylpropionamidine) dihydrochloride (**4**), and residence time are maintained constant, the temperature will influence the molecular weight. An increase in temperature results in a decrease in molecular weight. As a rule of thumb: high temperature, large dispersity and lowering of the molecular weight; high amount of initiator, low molecular weight and termination is residence time dependent.

In summary, a range of polymers from low to high molecular weight (28,608 g mol^{-1} - 540,213 g mol^{-1}) have been synthesised under continuous flow conditions. To obtain polymers with low molecular weight short residence times and high temperatures were used. For polymers with high molecular weight long residence times, high temperatures were used along with low initiator concentration. These polymers were obtained in a conversion between 32% to 100% and disperities between 1.14 and 5.74.

Unfortunately the targeted molecular weights were not achieved as accurately as expected. The difference of 120,000 g mol^{-1} was small but the difference of 310,000 g mol^{-1} and 450,000 g mol^{-1} were more spread.

Instead of freeze drying the samples after the polymerisation, the materials could be purified before analysis by GPC. Unfortunately, whilst working on a system to purify the samples easily, the GPC did not give consistent data.

Chapter 3

Polymer Purification

3.1 Precis

A principle advantage of performing polymerisation reactions in flow is the ability to rapidly screen various parameters for the optimisation of the polymer's synthesis. As accelerated synthesis has shown (see Chapter 2), the subsequent purification also needs to be quick to avoid the generation of a new bottle neck. Purification already constitutes the most time consuming step, performed off-line, in the process of generating a pure polymer sample.

The purification of water soluble polymers can be conducted *via* either dialysis or ultrafiltration. Dialysis is classically the most common procedure, but it is inherently time consuming and volume dependent. Alternatively, ultrafiltration can be conducted and it is possible to perform this process as a flow-through sequence. This takes advantage of the expanded surface area and operational pressure, as a result the purification time can be significantly reduced when compared to traditional dialysis operation.

As described, we have developed methodology to synthesise water soluble polymers in flow, possessing a variety of molecular weights. However, full conversion was not always achieved without significantly increasing the dispersity and therefore, purification is necessary. In the following research the flow polymerisation

reaction was successfully coupled with a direct in-line purification to obtain purified polymer within a processing time of one hour.

3.2 Introduction

3.2.1 Polymer purification

The purification of polymers is often the slowest step in the sequence of converting starting materials to polymer and obtaining analysis especially when uncontrolled free radical polymerisation is performed. This is often, as less control is achieved over the polymerisation compared to other, earlier mentioned, polymerisation techniques. The technique used to purify the synthesised polymer is highly dependent on several factors such as the polymerisation technique used, the resulting chemical structure of the polymer and critically the final specification and application of the polymer. For some applications, a very high purity is required, such as in medicinal applications [191] or organic photovoltaic devices [192]. Other applications, such as thickeners or food packaging do not necessarily require polymers possessing narrow dispersity but may need exhaustive removal of any residual monomers.

Polymers can be separated from the reagents (residual monomer(s), catalyst, etc.) but can also be separated by molecular size. Polymers with various molecular weights can be filtered, using membranes with different pore molecular weight cut-offs. [193] To perform analysis, it is preferable to have a clean sample, especially for GPC analysis.

In the area of flow chemistry different terminology is often used to describe the way analysis is performed. In this thesis we will use three different terms: off-line, on-line and in-line analysis. The characteristics are described in Table 3.1. [194]

Over the last few decades, much research has been undertaken to automate processes such as the synthesis of polymers at large scale. This has also influenced the way of approaching chemical reactions at laboratory scale. Flow chemistry has therefore become more embedded in organic chemistry laboratories. One of the

Table 3.1: Characteristics of off-line, on-line and in-line analysis.

Process analysing	Sampling method	Sample transport	Analysis
Off-line	Manual	Remote	Automated Manual
On-line	Automated	Integrated	Automated
In-line	Integrated	No transport	Automated

drivers has been the aspiration that a reaction performed at laboratory scale could be screened, purified and analysed directly in-line or on-line and the data evaluated to enable a rapid improved secondary synthesis. [92, 195, 196] The major advantage of flow then becomes the ability to monitor the reaction and effect change to the processing conditions in essentially real time.

Polymer synthesis has also benefited from in-line monitoring, for example, techniques like IR and Raman spectroscopy have been applied to monitor the polymerisation process in real time. [197] However, to the best of our knowledge, polymer synthesis has not been performed in a system containing in-line or on-line GPC analysis for the determination of molecular weight and dispersity in combination with flow chemistry. On-line GPC has been peformed by Reed *et al.* using the automatic continuous on-line monitoring of polymerisation reactions (ACOMP) system. ACOMP is based on batch reactor system with continuous sampling. It measures the development of average molar mass, intrinsic viscosity and monomer conversion kinetics. In case of co-polymerisation ACOMP measures in addition the average composition drift and distribution. ACOMP is applicable to free radical polymerisation, controlled radical homo- and co-polymerisation, emulsion polymerisation, polyelectrolyte synthesis. [198] This system has great potential but unfortunately it is not easily accessible. Therefore, 'traditional' GPC-SEC will be used for the majority of the measurements. To analyse these sample it is highly recommended to first purify the sample especially when full conversion has not been achieved. This is where the need for rapid purification arises.

3.2.2 A brief review of purification techniques

3.2.2.1 Anti-solvent

One way of purifying a polymer sample is to find a solvent or solvent mixture where the monomer or polymer is soluble but the other component is not. This methodology is probably most preferred, especially at an industrial scale, as it is the easiest to perform. Ideally, the polymer component would precipitate but it may also form a gel. It should be acknowledged that the addition of certain solvents (anti-solvents) can add issues relating to contamination depending on the specific application (i.e. medical). In addition, it is often difficult to be selective regarding molecular weight cut off in terms of precipitation methods and yields of recovered material can be variable.

3.2.2.2 Dialysis

The principle of dialysis is based upon diffusion of material from a high concentration zone towards a low concentration zone across a porous membrane (Figure 3.1). [199] Unfortunately, not all polymerisation reactions can be purified using dialysis. The tubing or membranes used are not always compatible with the full range of organic solvents or polymers produced. However, this technique has been shown to be a viable method for the efficient purification of a broad range of natural products such as enzymes, [200, 201] proteins, [201, 202] polysaccharides, [203] lignin sulfonates, [204] polymers in semi-aqueous systems [205–207] and polymers in aqueous systems [208]. Alternatively and for a completely different application, dialysis tubing has been used to grow bacteria as described by Millner. [209] All these applications have one thing in common: that the purifications are (partly) performed in water. Residual monomer and reagents (especially inorganic compounds) are readily removed from the solutions by transport across a semipermeable membrane. The strength/ efficiency of the dialysis varies with the surface area and pore size of the membrane. Dialysis membranes are generally made of regenerated cellulose, cellulose acetate, polysulfone, polyethersulfone or collagen. Polymers with various molecular weights

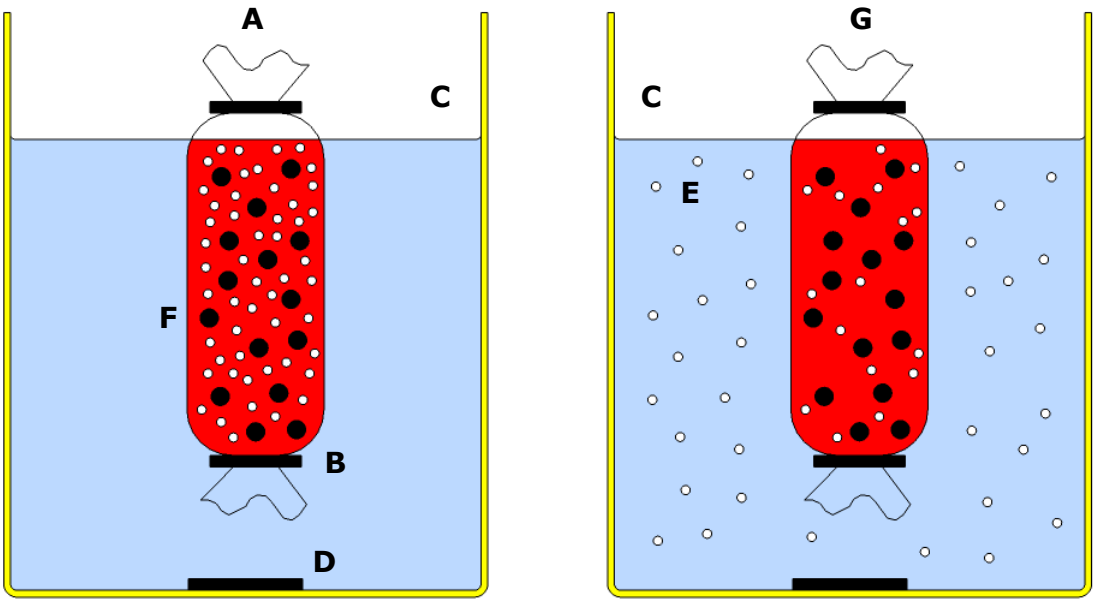

Start dialysis
(high concentration gradient)

End dialysis
(equilibrium)

A: Dialysis tubing filled with crude sample. **B**: Clips to seal dialysis tubing.
C: Beakers filled with water. **D**: Stirrer bar. **E**: Small size particles.
F: Large size particles. **G**: Dialysis tubing purified sample.

Figure 3.1: Principal of dialysis.

can be separated by iteratively increasing the pore size of the membrane. [210] A major advantage of the use of dialysis tubing is that it has low initial investment costs, and can be performed with only a beaker and the dialysis tubing.

A disadvantage of using dialysis tubing is its passive mode of action, meaning it can take a long time to purify a sample. Indeed, purification can easily take in excess of 24 hours. In addition, the dialysis tubing has to be handled with care as the storage solutions often contain toxic compounds (e.g. sodium azide). Furthermore, it can be hard to process large samples as it quickly becomes diluted due to the initial influx of water making the process less efficient (gradient ratios). Thus to drive the equilibrium shifting the monomer/ impurity concentration towards the bulk water source, a significant amount of water is needed. To improve the sequence, variations have been developed in a dialysis approach, such as *counter-flow dialysis*. [211] Counter-flow dialysis is based on the principle of two flow streams traveling in opposite directions to each other (Figure 3.2). A membrane is positioned between the

streams allowing diffusion between them. Kidney dialysis is a well known example of counter-flow purification.

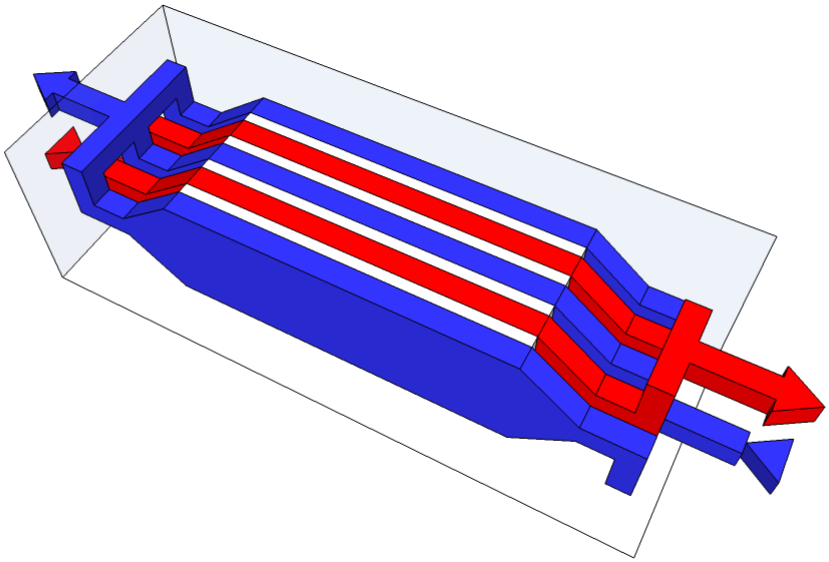

Figure 3.2: Counter-flow device, the membranes (white) separate the two flows from each other. The flow of red and blue are in the opposite direction.

3.2.2.3 Ultrafiltration

As an alternative to dialysis, ultrafiltration can be considered. There are multiple variations of ultrafiltration, for example *centrifugal ultrafiltration*, [212, 213] and *tangential/ crossflow ultrafiltration*. [214] In general, the advantage of ultrafiltration is it is *faster* compare to dialysis *via* tubing and also includes the ability to concentrate samples. Furthermore, as with dialysis, different molecular weights can be separated as membranes with various molecular weight cut off (MWCO) are commercially available. Finally, it is also easier to recover residual monomer compared to dialysis, as the volume of filtrate is considerably smaller and therefore easy to concentrate aiding isolation and re-use.

A drawback of ultrafiltration systems is their limited compatibility with various solvents. For example, the commercial Vivaflow 200 produced by Sartorius Stedim Biotech can only be used with a limited set of solvents. A summary of the compatible and non-compatible solvents can be found in Table 3.2.

Table 3.2: Compatibility of solvents with ultrafiltration membrane.

Compatible solvents	Non-compatible solvents
water	ethyl acetate
ethanol (70%) in water	acetone
methanol (60%) in water	*n*-hexane
n-butanol (70%) in water	dichloromethane
formaldehyde (30%) in water	toluene
formic acid (5%) in water	

The membranes will additionally degrade or become blocked rapidly if the sample is too concentrated as the polymer will form clusters. To avoid this issue, a solvent should be added constantly to maintain the samples dilution. Purification of a polymeric sample *via* this technique can therefore be more labour intensive compared to using simple dialysis tubing. This drawback can however be overcome by installing an external pump delivering the solute to the main tank with a speed similar to the withdrawn rate from the sample mixture. This balances the system and facilitates continuous throughput operation.

3.3 Research objectives

The aim of this area of research was to develop *a method to conduct a sequence that delivered a pure polymer sample from a monomer as rapidly as possible.* This chapter constitutes an extension of the work described in Chapter 2. As purification is often the most time consuming step in the cycle from monomer to analysis, it is desirable to develop a method to synthesise and then purify the polymer in as short a time as possible. This would be a major advantage for screening reaction conditions. Parameters that impinge upon the time needed for purification are flow design (connectivity of the multiple membranes), conversion (concentration of residual monomer) and sample concentration.

In our work the purification of polymers was conducted by dialysis tubing and ultrafiltration membranes. The membranes used for the purification of poly(acrylic acid) (**8**) samples, a water soluble polymer, had a MWCO of 2,000 Da. The rea-

son for using membranes with a MWCO of 2,000 Da was the removal of residual monomer and oligomers. Therefore, a membrane with the smallest possible pore size was chosen. Additionally, dialysis tubing with high MWCO takes less time to purify polymeric samples compared to low MWCO, dialysis is driven by passive diffusion and is therefore a passive purification technique. Membranes with a high MWCO will also take less time to purify, but for different reasons compared to dialysis tubing. Ultrafiltration is driven by convective purification, and is therefore an active purification technique. Using the membrane with the lowest possible MWCO, a compromise had to be made between speed and what was removed (e.g. impurities, residual monomer). Conducting the purification using a membrane with the lowest possible MWCO would result in the longest purification time.

The amount of remaining monomer will have a large influence on the time it takes to purify the sample. A low monomer conversion will result in an increased purification time for the sample. Additionally, the polymers concentration will play an important role defining the required time. A sample of high concentration will be purified faster compared to a sample of low concentration assuming they contain the same amount of polymer/ monomer. Finally, sample size is also an important parameter, as a larger volume of sample will take longer to cycle through the purification system. For example, 10 mL (0.5 mM) will generate a shorter purification time compared to 20 mL (0.25 mM).

3.4 Methodology

As most commercially-sold membranes have a fixed path length, it is necessary to link multiple membranes together to generate sufficient path length to achieve purification. Using multiple membranes can lead to a variety of different path shapes. Membranes can be positioned in series, parallel or a combination of these two as highlighted in Scheme 3.1 to 3.3. Each membrane requires an optimal pressure differential of about 3 bar to operate efficiently. Lower pressures will not facilitate

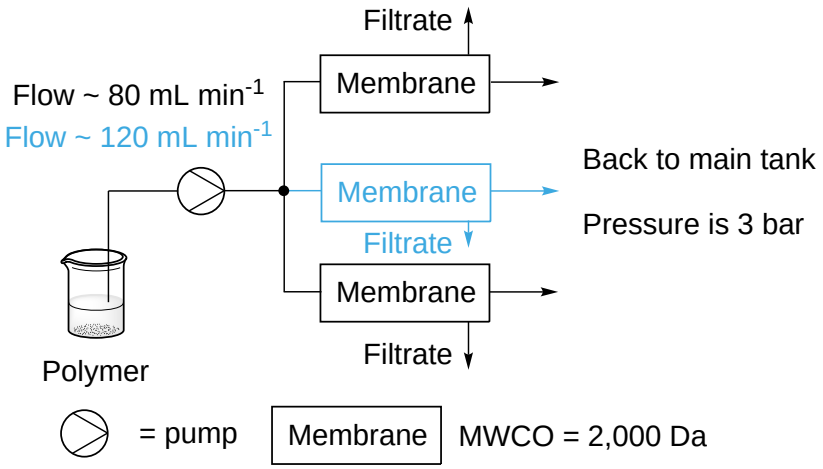

Scheme 3.1: Membranes in parallel.

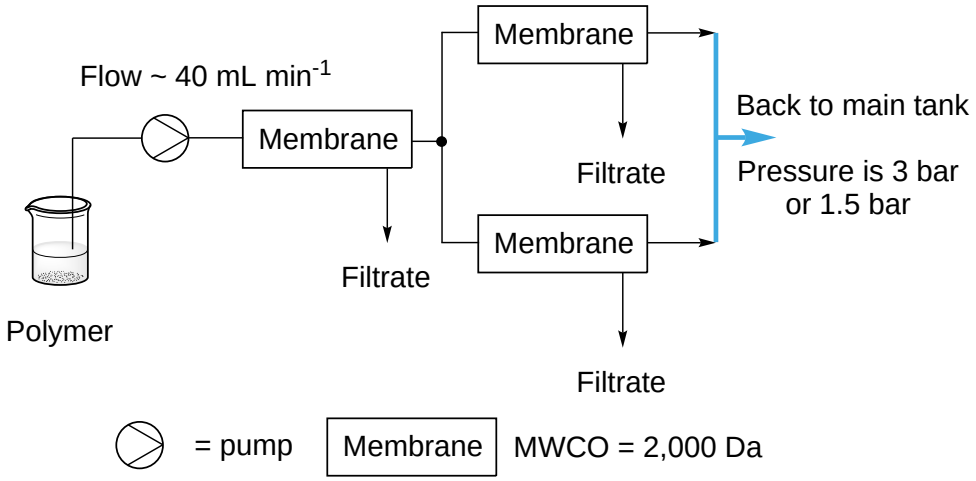

Scheme 3.2: Membranes in series/ parallel.

filtration of the sample, and higher pressures will over time degrade the membrane. The necessary pressure can be achieved by a flow rate of around 40 mL min^{-1} per membrane. The membrane outlet is then connected back to the main tank to form a recycling loop and the concentration of the sample is kept constant during the purification by the continuous addition of water to the stock tank. During the purification low molecular weight impurities are withdrawn *via* the filtrate and directed to waste.

The membranes in Scheme 3.1 are positioned in parallel. When two membranes were used the flow rate was set at 80 mL min^{-1}. The addition of a third membrane to the set-up (shown in blue) increased the flow rate to 120 mL min^{-1} to maintain a similar pressure and membrane extraction efficiency.

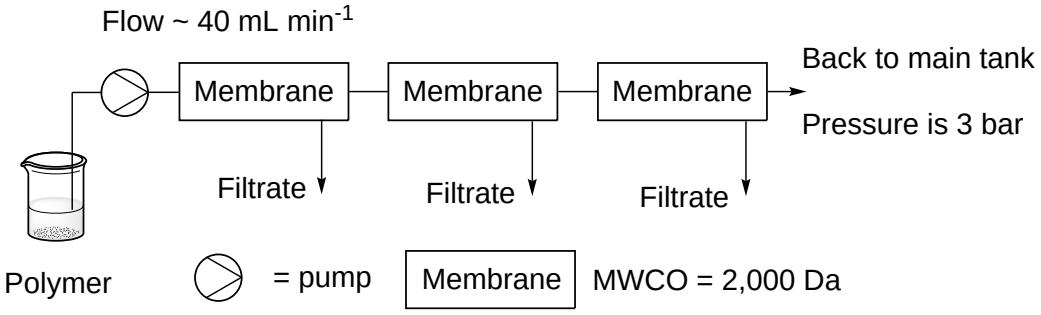

Scheme 3.3: Membranes in series.

In an alternative configuration the membranes were positioned in a combination of parallel and series as shown in Scheme 3.2. Two pathways are possible; with the outlets collected separately or combined into a bulk collection (blue line). The flow rate used was 40 mL min^{-1} as higher flow rates would have damaged the first membrane. The pressure will be divided equally over the two membranes configured in parallel, resulting in a pressure of approximately 1.5 bar.

A third membrane set-up (Scheme 3.3) was also evaluated where the three membranes were placed in series. The flow rate was again 40 mL min^{-1} to generate a pressure of 3 bar.

To test the purification process in each described membrane configuration poly-(acrylic acid) (**8**) was synthesised containing different amounts of residual acrylic acid (**7**) monomer as an impurity. The procedure for the synthesis of poly(acrylic acid) (**8**) is described in Chapter 2. The conditions for 22%, 30% and 70% residual acrylic acid (**7**) were determined experimentally (using ^{1}H NMR) in Chapter 2 and are summarised in Table 3.3.

Table 3.3: Conditions residual acrylic acid (**7**).

Res. acrylic acid (7) (%)	**[Acrylic acid] (7) (mM)**	**[Initiator] (4) (mol%)**	***T*** **(°C)**	***Rt*** **(min)**
22	0.14	0.70	2.50	70	10
30	0.20	0.70	1.25	70	10
70	0.49	0.70	1.25	70	5

Various concentrations of aqueous polymer solution were then used for the purification process (Table 3.4). These concentrations were obtained by diluting a

standard 50 mL sample of 0.2 mM equating to ∼30% residual acrylic acid (**7**). Each measurement was performed on the same amount of acrylic acid (**7**) at different concentrations and therefore a different volume in each purification cycle (3.4).

Table 3.4: Used concentrations for purification.

Concentration (mM)	Dilution factor	Total volume (mL)
0.2	1	50
0.1	2	100
0.05	4	200
0.033	6	300
0.0025	8	400

3.5 Results and discussion

To compare the efficiency of dialysis tubing to ultrafiltration, four samples of 25 mL, with 30% residual monomer, were loaded in twenty centimetres long and four centimetre wide dialysis tubing packets. These samples were then placed in individual beakers containing four litres of water with stirring for various amounts of time. The MWCO of the dialysis tubing was 3,000 Da as this was the closest available to the MWCO of the ultrafiltration membranes (2,000 Da). The amount of acrylic acid (**7**) (between 6.3 ppm and 5.8 ppm) decreased over time whilst the amount of poly(acrylic acid) (**8**) (between 2.5 ppm and 1.6 ppm) remained constant as determined using ^{1}H NMR analysis of the filtrate. The filtrate did not contain any polymer. The singlets around 3.5 ppm represent the internal standard dimethoxyethane (which was in the polymer to be purified). As the molecular weight of dimethoxyethane is 90.12 g mol^{-1} it was also separated from the polymer. Due to the small quantity of the internal standard, this will not affect the membranes, connectors or tubing but makes it possible to calculate the residual monomer concentration at $t = 0$. With this set-up full purification was not achieved even after four hours (Figure 3.3). A very small quantity (∼1%) of acrylic acid (**7**) was still present in the final sample. This indicates the purification takes over four hours.

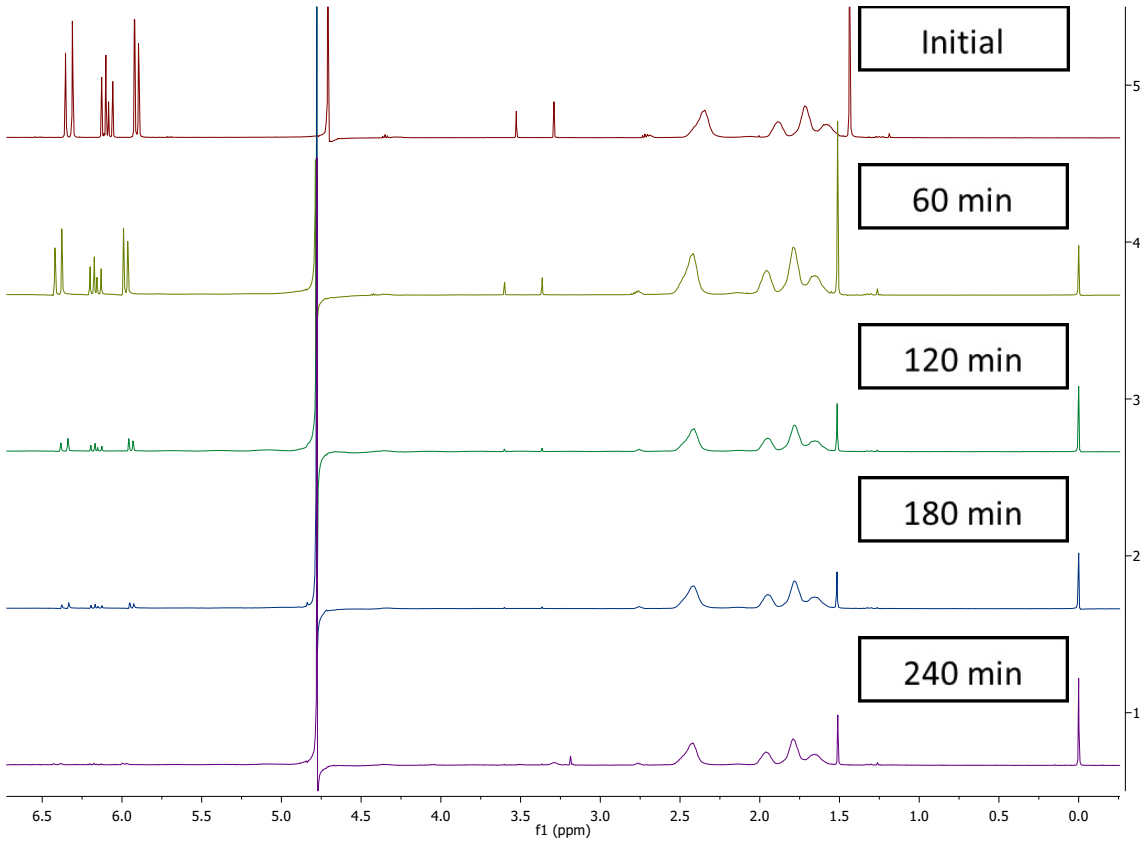

Figure 3.3: ^{1}H NMR spectroscopy of residue of the dialysis, using dialysis tubing with a MWCO of 3,000 Da.

3.5.1 Evaluation using ultrafiltration in flow

As the overall conversion to poly(acrylic acid) (**8**) can be easily tuned as described in Chapter 2 and briefly mentioned in Table 3.3, various monomer/ polymer concentrations can be quickly evaluated by simply diluting the initial reaction mixture. Initially the various reactor configurations as described above were evaluated using 50 mL aliquots of polymer solution containing ~30% residual acrylic acid (**7**), which corresponds to a concentration of 0.2 mM.

Variations in purification time between the different path forms were found (Figure 3.4). The major difference in extraction time was attained by increasing the membrane surface area. For example, utilizing three membranes shortens the purification time compared to two membranes. However, it is hard to achieve an equal pressure at both outlets by splitting the flow streams equally and therefore, the membranes do not perform optimally. To highlight this, a full screening was per-

formed using two (Figure 3.5) and three (Figure 3.6) membranes in parallel (Scheme 3.1).

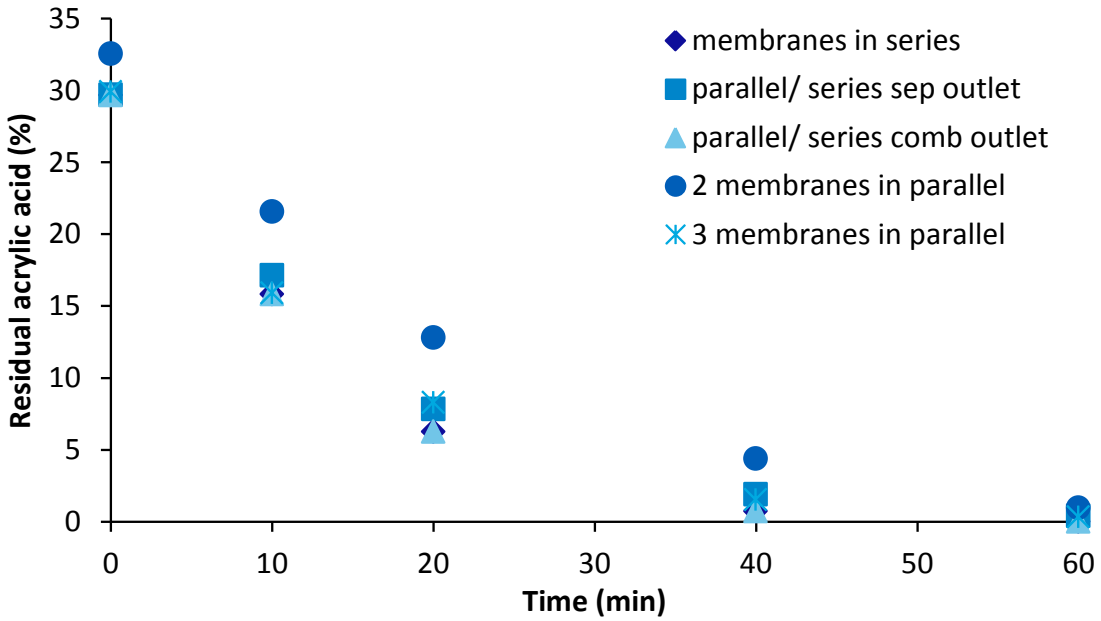

Figure 3.4: Influence of design (separate is sep and combined is comb).

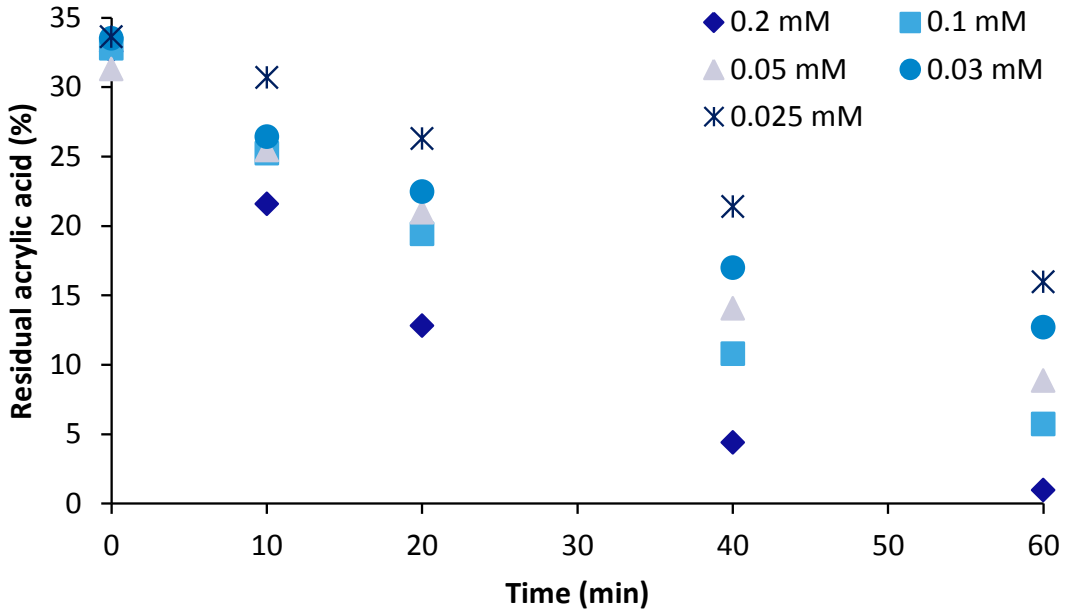

Figure 3.5: Influence of concentration on two membranes in parallel.

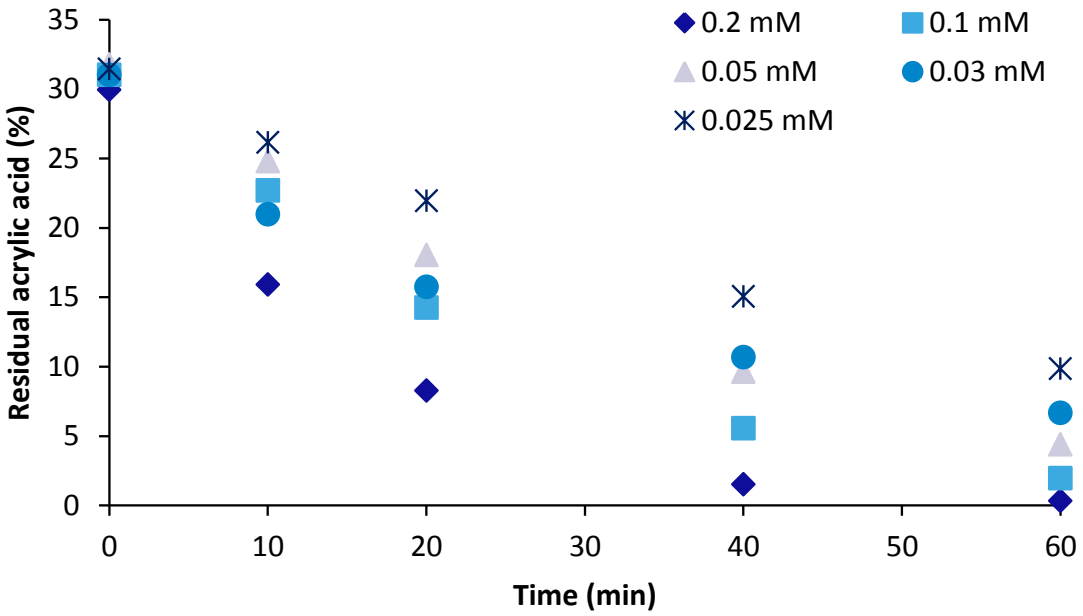

Figure 3.6: Influence of concentration on three membranes in parallel.

The screened concentrations varied from 0.2 mM to 0.0025 mM (Table 3.4). The processing time required for the purification of a polymer sample increases as the sample volume increases. Thus, using two membranes in parallel (Figure 3.5) a 50 mL (0.2 mM) sample was purified within one hour leaving less than 1% residual acrylic acid (**7**). By comparison, a sample diluted to 400 mL (0.0025 mM) still had 16% residual acrylic acid (**7**) after one hour processing time (Figure 3.5). Therefore, to increase efficiency, if a diluted sample is produced it needs to be concentrated first. This can be performed by the ultrafiltration membranes. The sample can be processed to achieve the desired concentration. However, the concentration of the polymer sample should not exceed concentrations which damage the membrane. This is not a fixed concentration but depends on the polymer and has to be determined empirically. For example, the macromolecular environment has to be taken into consideration, as well as whether a polymer is known to easily form a gel.

Similar results were obtained when three membranes were used in parallel (Figure 3.6). The difference compared to the system with two membranes in parallel (Figure 3.5) is the specific increase in membrane surface area and consequently the flow stream has to be proportionally divided three times. However, the increase in

membrane surface area reduced the required purification time. For comparison, a residual acrylic acid (**7**) value of 10% was obtained after one hour for a 400 mL (0.0025 mM) sample (Figure 3.6). The difference between a sample of high concentration (50 mL, 0.2 mM) and a sample of low concentration (400 mL, 0.0025 mM) was seen in the cycle time: the highly concentrated sample did not contain residual acrylic acid (**7**) after one hour. The separation efficiency for a polymeric sample of 50 mL is eight times higher compared to a sample of 400 mL.

Additional screening was performed using the set-up described in Scheme 3.3. The trend of decreasing residual acrylic acid (**7**) over time for three membranes in series (Scheme 3.3) (Figure 3.7) was similar to three membranes in parallel for all concentrations. The purification of a 50 mL (0.2 mM) polymer sample is also completed within one hour. This was also applicable for samples of volume 100 mL (0.1 mM). From the plot it is clear that the majority of the residual acrylic acid (**7**) is removed during the first twenty minutes; especially for the more concentrated samples.

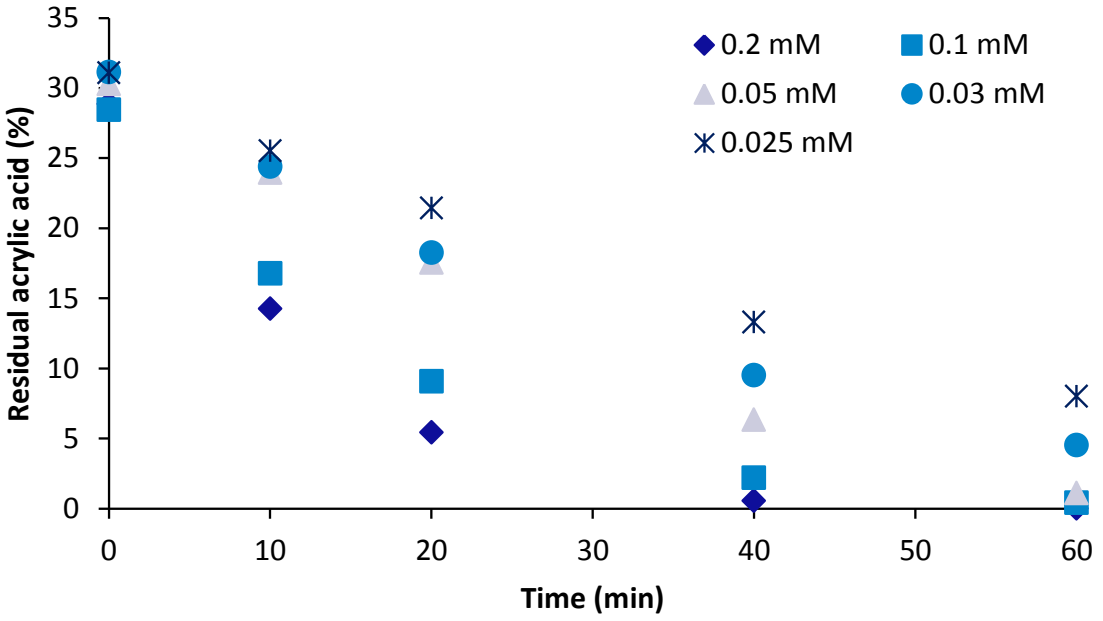

Figure 3.7: Influence of concentration on three membranes in series.

Employing three membranes in various configurations results in similar purification times and therefore there is no clear preference for a specific set-up. The

membrane efficiency should be equal for membranes in parallel (Scheme 3.1) and in series (Scheme 3.3) where only the membrane surface is considered. The flow rate per membrane is 40 mL min^{-1} but was lower for the set-ups shown in Scheme 3.2, where two of the three membranes have the polymer solution passing through at 20 mL min^{-1}. Difficulty in achieving equal splitting of the flow streams was a practical reason for why the membranes in series (Scheme 3.3) are favoured. The flow per membrane is decreased slightly over the membranes in series. The pressure was set at 3 bar and was measured at the outlet. Due to a decrease in the amount of fluid pumped through each membrane, a pressure gradient is present over the membranes. The pressure difference between the first and last membrane was $\sim$0.2 bar. This difference did not unduly affect the operation of the membranes nor caused decomposition. Having three membranes in series (Scheme 3.3) did not give any difficulties with reproducibility. When performing the purification of polymer sample using three membranes in parallel, which required a flow rate of 120 mL min^{-1}, different tubing had to be used in order to deliver the required flow rate. This tubing is less robust and needed to be replaced frequently.

Full monomer conversion is usually desirable in an industrial process as it removes a costly and time-consuming purification step. It is preferable therefore to use optimal reaction conditions to achieve full conversion unless it negatively influences the desired product. For example, physical property or purity and in such cases it may therefore be necessary to have high levels of residual monomer present. Post-reaction, this may need to be separated from the polymer sample. In our investigation to achieve a purified polymer sample in the shortest possible time, the influence of residual monomer concentrations was tested using various residual monomer concentrations (Figure 3.8). Samples with high residual monomer concentration required longer processing time to purify compared to samples with low concentration. This trend is clearly shown in Figure 3.8. Over twenty minutes the relative difference between the three graphs obtained decreases. The residual acrylic acid (**7**) is respectively 14%, 5% and 3% (Table 3.3). Full purification is achieved

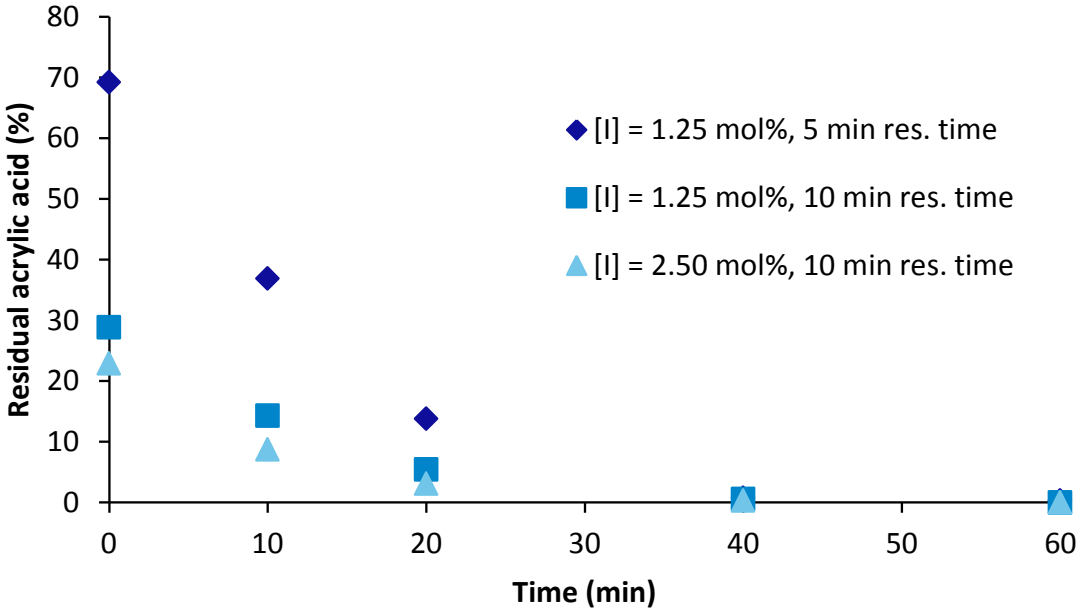

Figure 3.8: Influence of initial residual monomer concentration against purification time.

within sixty minutes (as shown in Figure 3.8; at 40 minutes the residual acrylic acid (**7**) amounts are 0.77%, 0.56% and 0.31% respectively). When the same data is plotted using a log function (Figure 3.9) it becomes clear the purification rate is similar for all concentrations if the volume is the same.

For the purification set-up used there is a maximum sample concentration which arises from the increasing viscosity which occurs upon purification and can, if too high, lead to blocking of the membranes. This means sample concentration must be kept reasonably low and large volume will need longer purification time.

Operating with small sample volumes is preferred when a full screening of parameters is aimed for. However, purifying small volumes can have drawbacks; the internal volume of the membrane separators could be larger than the volume of the sample, resulting in the need for dilution by an additional co-solvent such as water. The constant addition of water can be a labour intensive process, however this can be resolved by automatically filling the reservoir *via* an external pump at the same rate as the filtrate is withdrawn from the sample volume.

To conduct purification on a small scale, 5 mL of reaction mixture were collected and diluted to a total volume of 25 mL (Figure 3.10). It is possible to dilute even

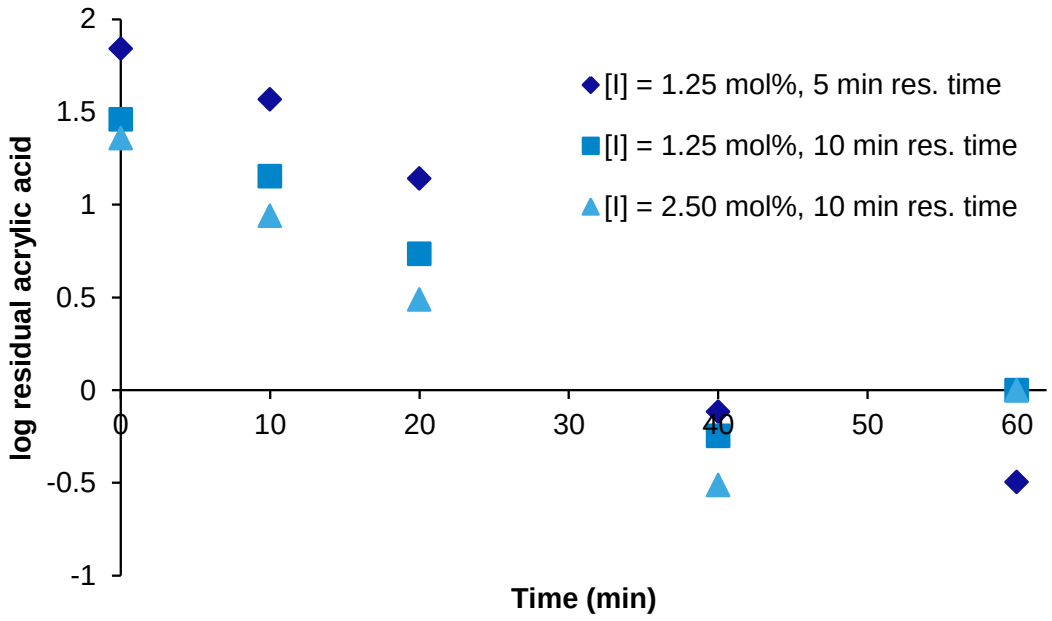

Figure 3.9: log function of influence of residual acrylic acid of residual acrylic acid (**7**), 50 mL sample was used.

smaller samples but the total amount of polymer in the sample should be taken into consideration. The test sample had 33% residual acrylic acid (**7**) content, which corresponds with at total acrylic acid (**7**) amount of 1.2 mmol. The purification was completed within 30 minutes (Figure 3.10) and generated 120 mg of dry poly(acrylic acid) (**8**) following water removal (30 minutes) *via* a high vacuum pump. This amount is sufficient for all analysis (liquid phase ^{1}H NMR spectroscopy, GPC, etc.).

By combining the purification and synthesis set-ups it is possible to create a system as shown diagrammatically in Scheme 3.4. This system, shown in real in Figure 3.11, can be used in a high throughput mode. With the capability to purify a sample within 30 minutes, potentially 16 samples can be fully processed during a standard working day (8 hours). Assuming a GPC measurement also takes on average around 30 minutes to conduct, all samples could be prepared and screened within 24 hours (48 samples per day). This includes the GPC measurements and running duplicates of the samples.

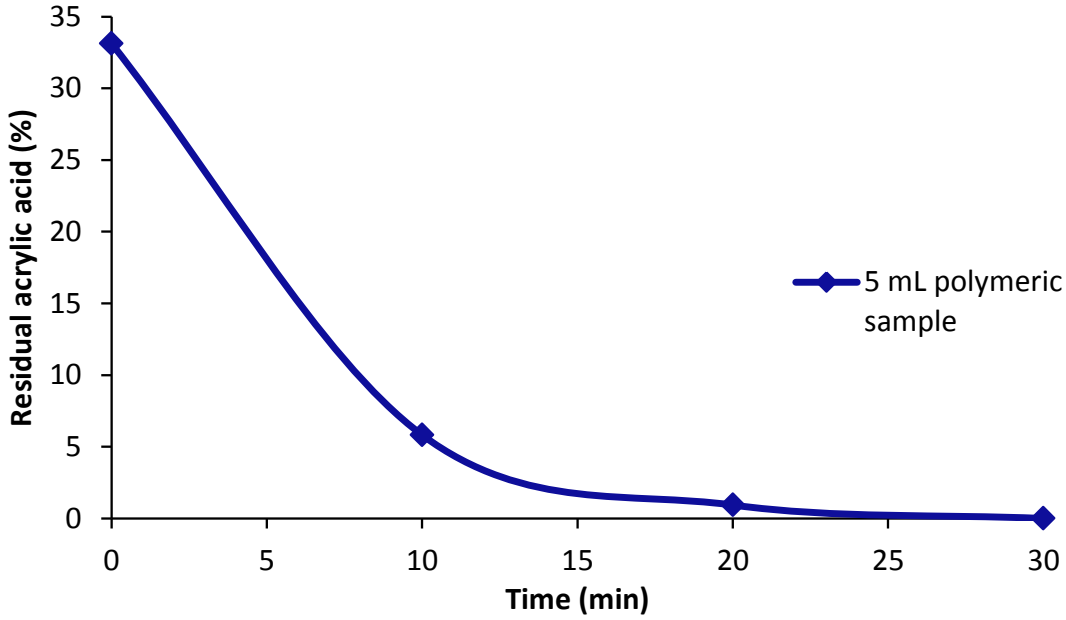

Figure 3.10: Purification of 5 mL sample diluted to 25 mL total volume.

3.6 Conclusion

The aim of the work described in this chapter was to develop a flow system for the rapid purification of polymeric samples. These results show how a simple flow system can be used to both synthesise and purify a water soluble polymer such as poly(acrylic acid) (**8**). With the designed set-up, poly(acrylic acid) (**8**) can be synthesised and purified within 60 minutes (maximum of 30 minutes synthesis time and 30 minutes purification time). After the first sample, the synthesis time will be similar to the purification time of the previous sample. To purify the sample, placing ultrafiltration membranes in series (Scheme 3.3) was found to be the easiest assembly as fewer problems were encountered. The flow stream did not have to be divided into equal feed streams.

The sample characteristics such as size and concentration influenced the time required for purification. In general, smaller volume samples will be purified quicker. However, a drawback is that the samples could not be too highly concentrated as the viscosity influences the operation of the membranes. High viscosity damages the membranes by blocking the pores or cracking the membrane structure. Polymer concentrations of up to 0.49 mM were successfully purified, higher concentrations

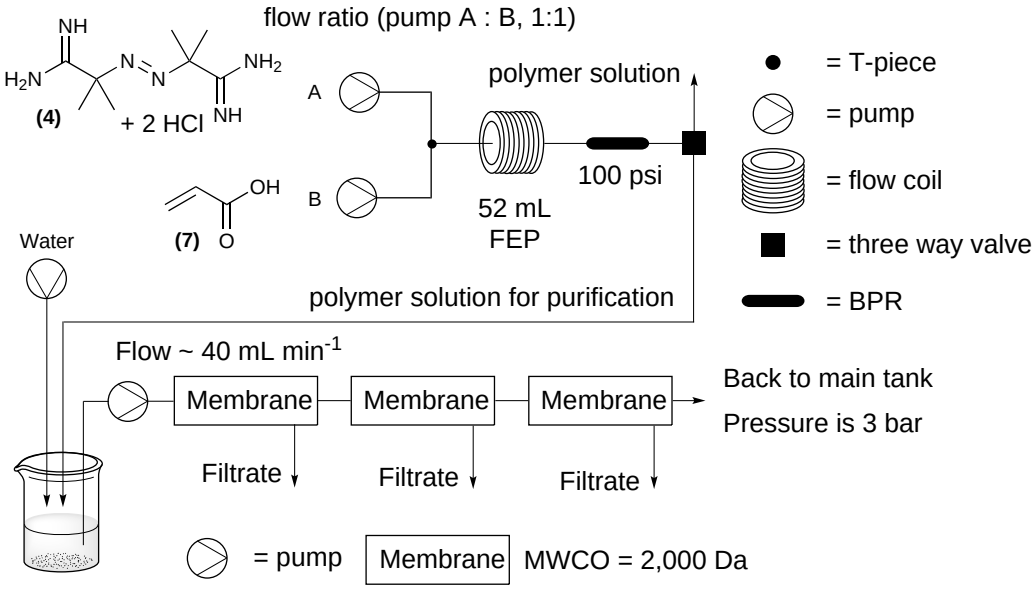

Scheme 3.4: High throughput system for the synthesis and purification of poly(acrylic acid (**8**)).

were not tested.

By demonstration the synthesis and purifications of poly(acrylic acid) (**8**) was conducted within one hour. This research shows it is possible to synthesise, purify and analyse up to 16 samples per day and has the potential to increase the throughput of many polymer laboratories as the investment costs are low.

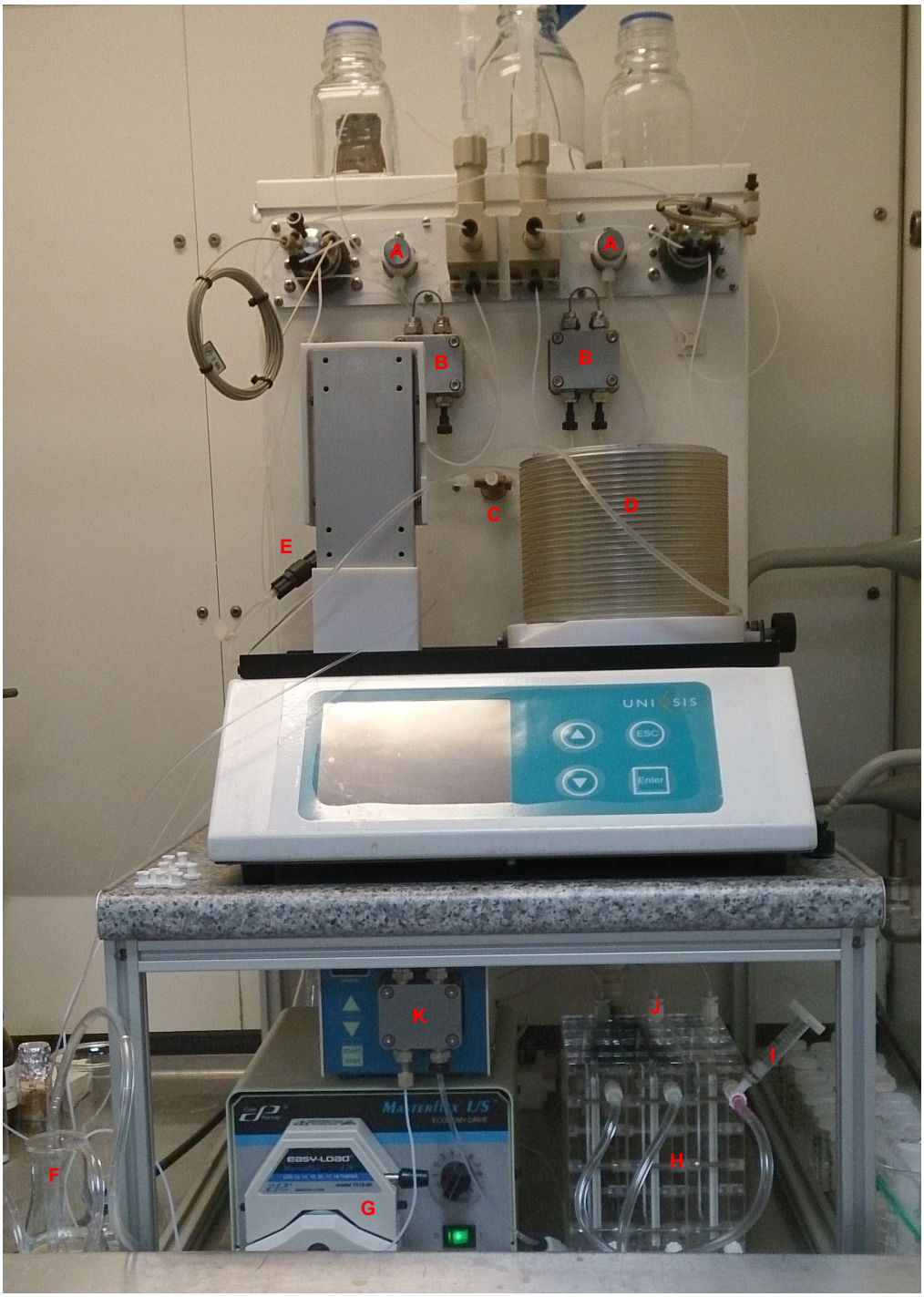

Figure 3.11: Flow system used to perform the synthesis and purification of poly(acrylic acid) (**8**) samples. **A**: Reagent feed lines, **B**: Piston pumps, **C**: Mixer, **D**: Reactor, **E**: BPR, **F**: Sample collection, **G**: Peristaltic pump to feed membranes, **H**: Ultrafiltration membranes, **I**: Pressure regulator, **J**: Filtrate of purification, **K**: Piston pump to maintain sample volume.

Chapter 4

Crystal Polymerisation

4.1 Precis

In this chapter the controlled assembly *via* topochemical polymerisation of conjugated alkyne species is investigated. Conducting a polymerisation *via* this fascinating route has great potential. Various dialkyne monomers have been synthesised and crystallised. The crystals were studied to test the potential for polymerisation in the solid state using either thermal or photochemical activation. The orientation and intermolecular distance of the monomeric layers within the crystals was deemed crucial to the success and has been determined empirically.

4.2 Introduction

Polymerisation is still considered very much a form of 'black box' chemistry. Much of this derives from the fact that the organic synthesis of small molecules has the advantage that the structures obtained can be fully characterised by numerous analytical techniques like NMR spectroscopy, X-ray, IR, etc. Polymers can also be characterised by various techniques (NMR spectroscopy, GPC, etc.) but there is always some degree of uncertainty about the structure, and the analytical results are based upon distributions. However, over the last few decades, many improvements have been made helping to unravel the delicacies of polymer chemistry. Several

chemical synthesis techniques have been developed to improve the control over the molecular weight and shape of the polymers.

As with all structurally viable molecules, stereochemical centres can be introduced into a polymer. Chirality can affect the physical properties of the polymer as predicted by Staudinger *et al.* in 1929. [215] To prove this, Staudinger *et al.* compared polystyrene with polyindene. However, it took until 1947 before the first synthetic stereoregular polymer was reported. Schildknecht *et al.* attributed the semicrystalline properties of a poly(isobutyl vinyl ether) to the ordered stereochemistry, or tacticity, of the polymer backbone. [216, 217] The field of research into tacticity became highly popular in the 1950s with many academic and industrial research groups benefiting from the discovery of heterogeneous titanium catalysts. [218] Dow Chemical employees discovered the reaction of propylene oxide in the presence of iron(III) chloride formed poly(propylene oxide). The reaction mixture could be divided into amorphous and semicrystalline material using solvent fractionation. [219–221] Soon after their discovery, Natta [222] and Price [223] provided evidence that the semicrystalline material was the isotactic polymer in which the methyl substituents had the same relative configuration (Figure 4.1). Epoxide ring opening polymerisation has gained a lot of attention since it was first discovered (1956). Recently, this area of research, has been extensively reviewed by Childers *et al.* [224] The main conclusion of this review was that current research has expanded into more defined homogeneous catalysts that give isotactic polyethers or polycarbonates from enantioselective epoxide polymerisation.

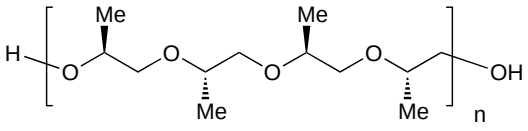

Figure 4.1: Isotactic poly(propylene oxide).

It is important to identify the tacticity in a polymer by defining the relative stereochemistry of adjacent chiral centres. Having control over the tacticity of a polymer results in an improvement in the understanding of the physical properties

of the polymer. Two adjacent monomeric units constitute a diad. A meso diad is present when both monomeric units have the same stereochemical assignment (R or S), and a racemo diad is present when both monomeric units have opposite stereochemical orientation (R, S). Various types of tacticity can be found in a polymer (Figure 4.2 and Table 4.1), here been labelled R and S to indicate the chirality.

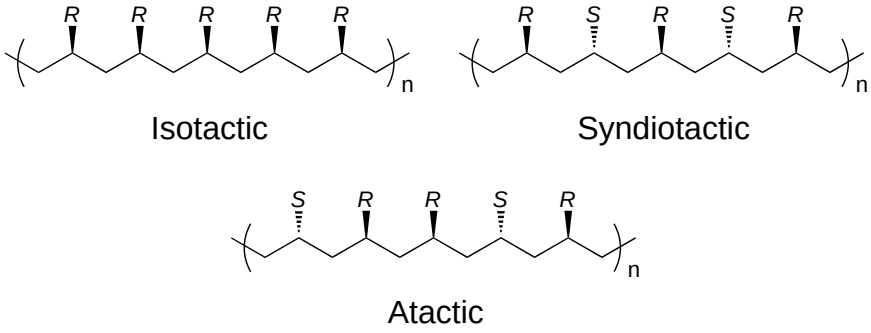

Figure 4.2: 2D configuration of polymers.

Table 4.1: Possible tacticity of polymers.

Tacticity	**Properties**
Isotactic	Stereocentres of monomeric units are all R or S. 100% meso diads
Syndiotactic	Stereocentres of monomeric units alternate between R and S. 100% racemo diads
Atactic	Stereocentres of monomeric units are randomly R or S.

Isotactic polymers contain only R or S stereocentres and are usually semicrystalline and often form a helixical configuration. Not all monomers are able to form isotactic polymers, as side groups can interfere with each other to prevent their assembly. Extensive research has been performed into methods for the synthesis of isotactic polymers. For example, for polylactides, an important synthetic biodegradable polymer, it took several years of intensive research to develop to a commercially viable protocol. In 2002 Feijen *et al.* managed to synthesise isotactic polylactide using the Jacobson ligand (Scheme 4.1). [225] The polymerisation of isotactic polylactide took into consideration that the starting organic ligands and substrates had to be inexpensive; the synthesis of the catalyst must be straightforward; the polymerisation should be conducted neat, and a high temperature would be essential

to initiate the polymerisation. Therefore, the catalyst had to be robust to survive the high temperature conditions. It was found that average molecular weight and conversion showed a parallel linear trend. All experiments resulted in the isolation of crystalline polylactide, an indication that long isotactic chains were generated.

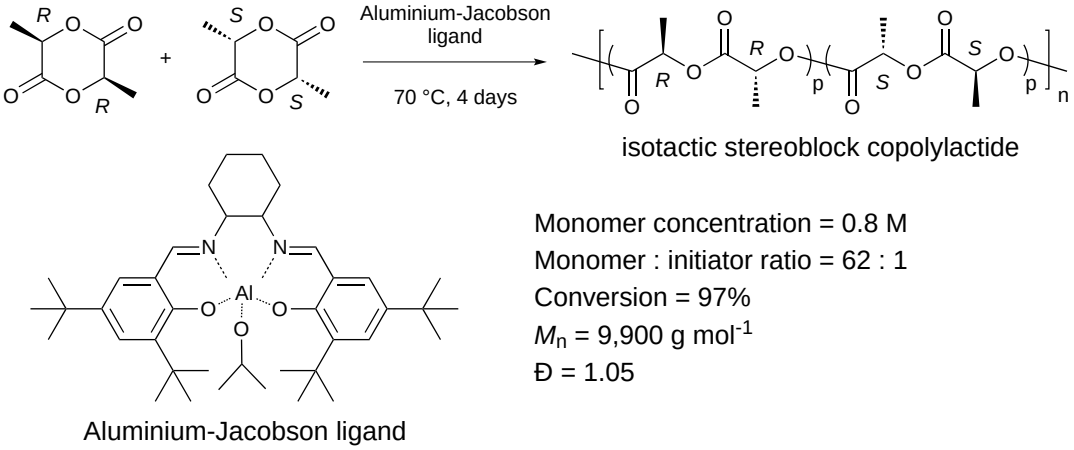

Scheme 4.1: Polymerisation of lactide.

Syndiotactic polymers containing alternating relative stereocentres form racemo diads. One polymer which has been extensively researched is syndiotactic polypropylene. Research towards this polymer started in the early 1950s (with the discovery of stereoselective olefin polymerisation) mainly as a scientific curiosity. [226] This was primarily due to the low crystallinity and melting temperature of the materials produced. In 1985 the discovery of new single-centre metallorganic catalysts was reported for the polymerisation of simple alkenes. [227] Some of these catalysts were able to produce highly stereo regular and regio regular syndiotactic polypropylene. Several of the polymers had high crystallinity and associated elevated melting temperatures. This makes it strong and at the same time still elastic. The formed syndiotactic polypropylene has shown interesting physical properties. The most important and unique property which relies on the fact that syndiotactic polypropylene is a high modulus thermoplastic elastomer, alongside a high crystallinity and relatively high glass transition temperature. The renewed interest has resulted in several papers over the last few decades. [228–231]

Atactic polymers contain random configurations of R and S stereocentres with

no control being imposed over the orientation. Atactic polymers could be produced by uncontrolled polymerisations. For example, the polymerisation of acrylic acid (**7**) as described in Chapter 2 is an atactic polymerisation. It is therefore not hard to appreciate that the synthesis of atactic polymers are in general less expensive and time consuming to prepare compared to isotactic and syndiotactic systems.

4.2.1 Historical setting

Before techniques were developed to install control over the stereoselectivity of the polymerisation, a monomer like ethene was polymerised by free radical processes using high pressures (1000 bar) and temperatures (300 °C). Polymers with a highly branched backbone were obtained as a result of backbiting. This process also formed polyethene which had moderate thermal and mechanical properties with limited crystallinity.

Ziegler found that polymerisation could occur at ambient temperature and atmospheric pressure in the presence of a variable valency metal catalyst ($TiCl_3$ and Et_2AlCl). [226] The resultant polyethene was a crystalline solid which was free from defects and branching. Natta applied similar conditions to the polymerisation of propene resulting in an isotactic polymer. [222, 232] This polypropene showed great thermal and mechanical properties (tougher and more robust) compared to polypropelene obtained *via* free radical polymerisation. Nowadays isotactic polypropelene can be found in many applications from artificial fibre ropes to car parts.

This polymerisation methodology is now more commonly known simply as Ziegler-Natta polymerisation. Ziegler-Natta catalysts have many variants which can be prepared by reacting an alkyl of a metal from group I-III (e.g. triethylaluminum) with a compound containing a transition metal from group IV-VIII (e.g. titanium tetrachloride). The catalyst is readily prepared by dissolving both components in a hydrocarbon solvent (e.g. *n*-hexane, *n*-heptane or tolune) at ambient temperature which results in an exothermic reaction in which gases are formed and the catalyst usually precipitates as a dark-coloured solid. Reduction of titanium(IV) to lower

valencies is the crucial step in the formation of the Ziegler-Natta catalyst. The key step in the catalysis is the co-ordination of alkene double bonds, the first step in the polymerisation when the monomer is exposed to the pre-prepared catalyst. Since the first proposal of this type of polymerisation, several mechanisms have been postulated. One of the earliest was Natta's bimetallic mechanism as highlighted in Scheme 4.2.

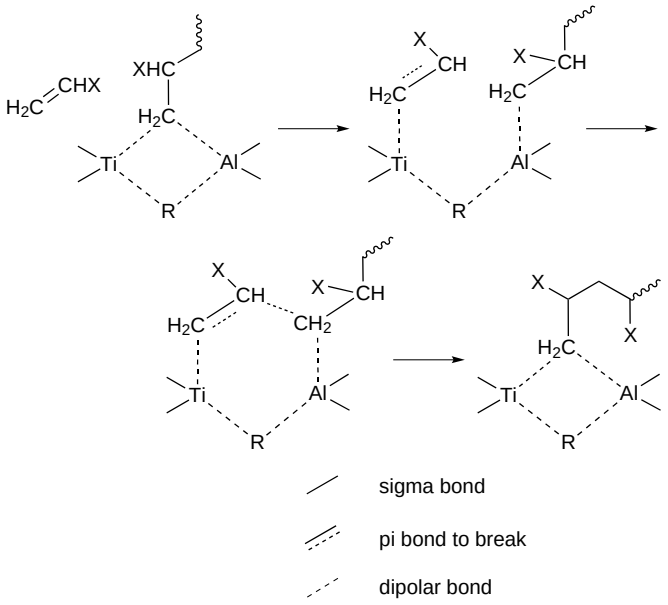

Scheme 4.2: Bimetallic mechanism proposed by Natta.

In 1964 Cossee proposed an alternative mechanism where the titanium(III) species has a vacant site in its co-ordination sphere (Scheme 4.3). [233] The alkene can co-ordinate at this position through a π-bond donation. In general the catalysts often contain metals with no or very few non-bonding *d*-electrons. [234–236] The anionic end of the alkyl unit re-orientates forming a σ-bond to titanium and creating a new vacant position where additional monomer units are able to bind and allow the chain to grow. The stereochemical control, which is necessary to form isotactic polymers, comes from the driving force (steric hindrance) of the R group of the monomer and the symmetry and geometry of the catalyst.

Ziegler-Natta catalysts based on titanium and aluminium do have some drawbacks. The most inconvenient is the intolerance of these catalysts to Lewis bases. Titanium halides and alkylaluminium co-catalysts are poisoned by monomers which

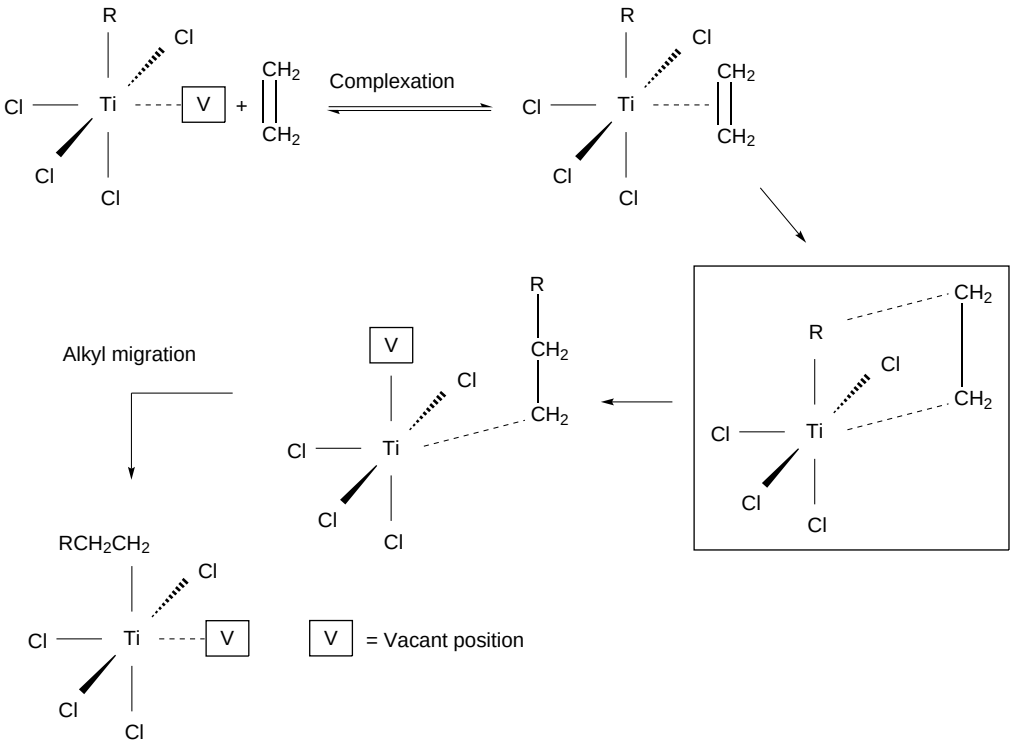

Scheme 4.3: Cossee's proposed mechanism for alkene polymerisation.

contain many functionalities including amines, carboxylic acids, ethers and esters. [237–244] This problem can be overcome by using alternative cationic, group IV metallocene catalysts (e.g. zirconium and samarium). Therefore, it is possible to polymerise olefins in the absence of alkylaluminium. [245, 246] Solvents which can be used are anisole, *N*,*N*-dimethylaniline, and chlorobenzene. Over the years multiple papers have been published describing improved polymerisation strategies as well as the preparation of specific catalysts. [247] Furthermore, bimetallic Schiff bases have been used for stereoselective polymerisations (Figure 4.3). For example, ring opening polymerisation of racemic lactide can be performed. [248]

A more delicate, less well known, and less used polymerisation route is to perform it in the solid state. A potential advantage of a solid crystalline form is that it already has a well-defined molecular structure packing. Molecules are 3D orientated and the structure of the crystal can be analysed by X-ray spectroscopy. The packing of the crystal is important for solid state polymerisation, which is also called topochemical polymerisation. This type of polymerisation has the advantage that the stereochemistry/ tacticity of the polymer can be determined (predicted) from

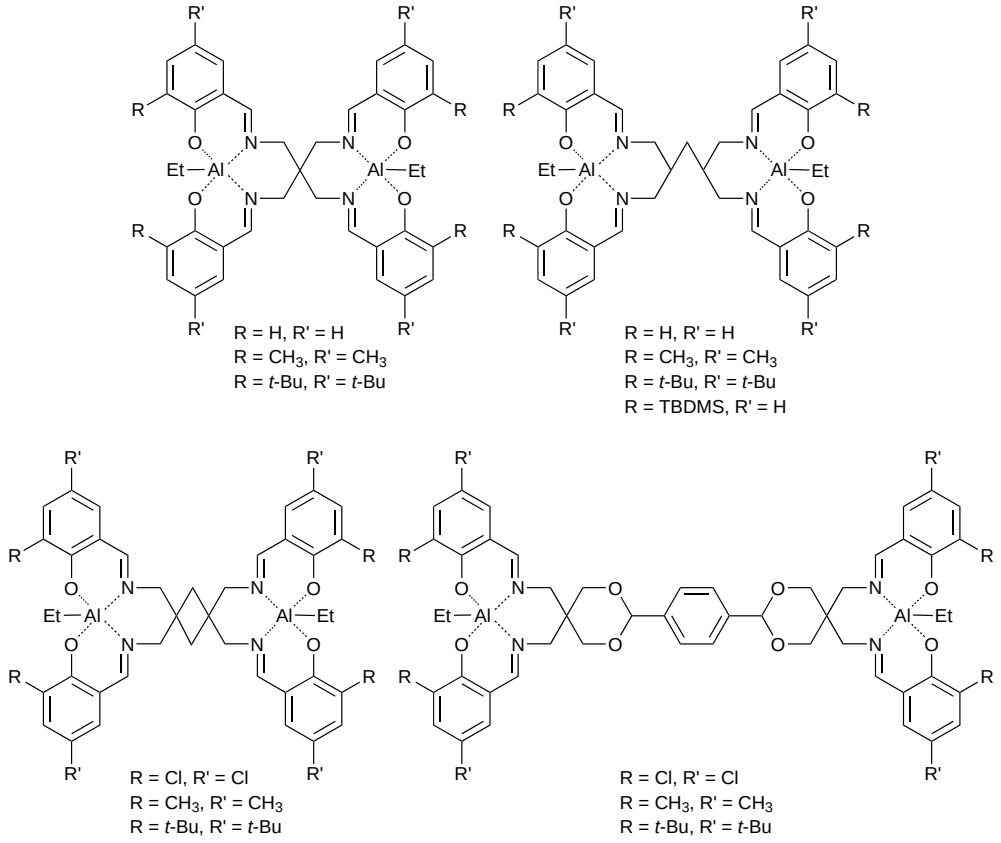

Figure 4.3: Schiff bases used for the synthesis of polylactide.

the crystal form. A disadvantage of topochemical polymerisation is potentially the scale at which it can be performed. There are currently no reported examples of this type of polymerisation performed at an industrial scale. However, with the recent advances in continuous processing techniques several options would be available for conducting such polymerisations.

The synthesis of polymers *via* a crystal, which needs to be nearly defect free, are usually derived and related to experimental observations like X-ray crystallography due to the difficulty of predicting the shape and packing of a crystal. Various crystal packings are known for crystals but not all are suitable for use in this type of solid state polymerisation. For example, some crystal structures will preferentially result in dimer formation whereas others can form an ordered network more suitable for polymer formation (Figure 4.4). All the depictions of crystal A-D packing shown in Figure 4.4 are viable for polymer assembly. The forms E and F, however, will result in dimer formation. The polymerisation process can in theory be performed

by other irradiation methods or by thermal induction.

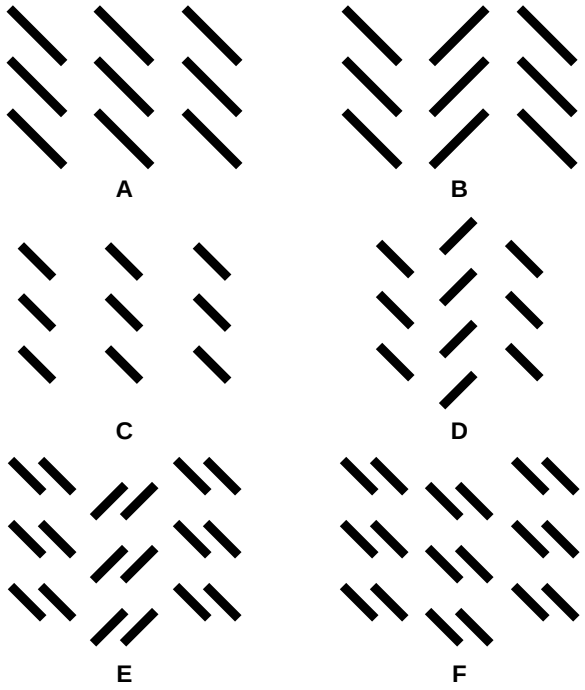

Figure 4.4: Different crystal packing.

A third way to promote the polymerisation in the solid state is by an external initiator in solution or in contact as a solid on the surface of the crystal. To initiate the polymerisation using an initiator in solution the crystals should be insoluble in the solvent. Again, the initiation process could be promoted either thermally or photochemically.

The first reported topochemical polymerisation was by Wenger [249–251] where a class of monomers was polymerised in the solid state to produce nearly defect-free polymer crystals. More specifically, diacetylene monomer crystals were induced thermally or *via* irradiation to perform *trans*-stereospecific 1,4-polyaddition along a unique crystal direction and was therefore inherently controlled by the crystal packing parameters. [252–254] As mentioned earlier (Figure 4.4) the packing of the crystal was important. If a distance of 3.5 Å $<$ d $>$ 6.0 Å between the monomer layers and an angle of around 45° of the monomer layers is established in the crystal, the molecules are positioned at a suitable distance and alignment to perform the polymerisation. Overall, the average distance of the polymer repeating unit is about 4.91 Å and therefore the polymerisation proceeds only with minimal rearrangement

of packing. [255, 256] The obtained conjugated polymers often have optoelectric properties. The displacement of the diacetylene carbons are accomplished by a shearing force of the diacetylenes and the side groups which requires a flexible linker. [251]

More recently Ronddeau-Gagné *et al.* performed topochemical polymerisation of phenylacetylene macrocycles to prepare organic nanorods. [257] These soluble organic nanorods were synthesised by polymerisation of butadiyne moieties placed both inside and outside the skeleton of the macrocycles (Figure 4.5). The macrocycle building block was obtained as an organogel in 38% overall yield over eight steps and irradiated with UV-light (253 nm). A blue material was obtained in 30 – 50 wt-% compared to the starting material (monomer units). The material was analysed by UV-Vis spectroscopy and the thermochromic properties determined in both the solid and liquid state. A broad absorption band at $\lambda_{max} = 654$ nm and the lack of thermochromism proved topochemical polymerisation (1,4-addition) had occurred.

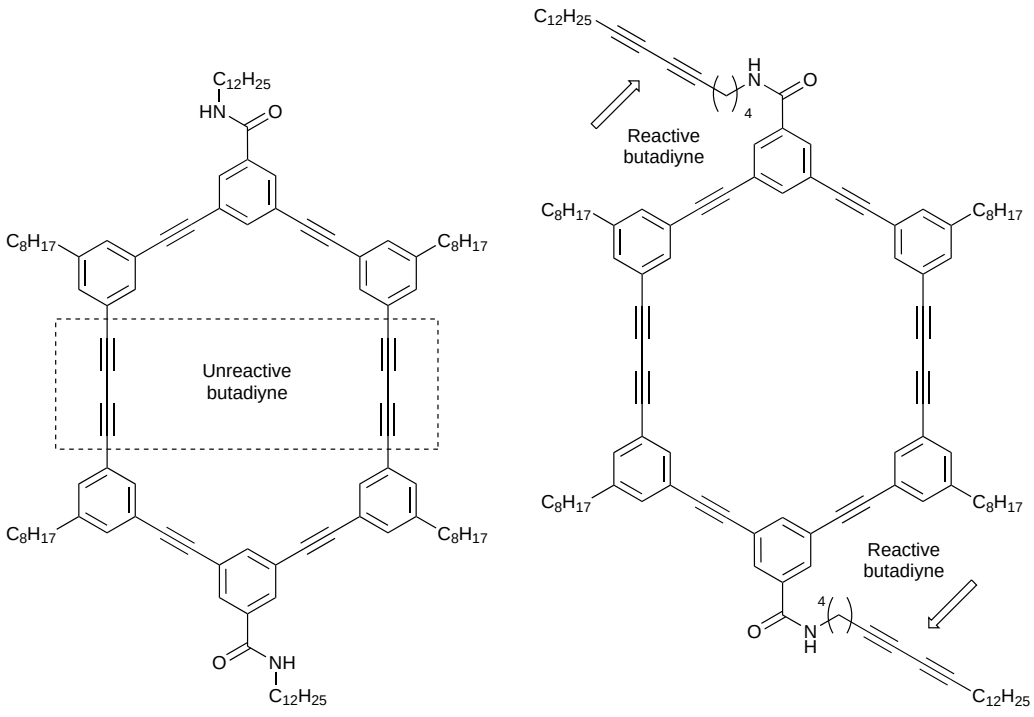

Unreactive butadiyne Reactive butadiyne

Figure 4.5: Reactive side phenylacetylene macrocycles building block.

4.2.2 Orbital alignment

Polymerising a crystalline diacetylene structure *via* a *trans*-stereospecific 1,4-poly-addition will result in structures as shown in Scheme 4.4. The equilibrium will be biased towards the mesomeric structure B in Figure 4.4 as this will result in the least strain in the molecule. This polymerisation can be achieved because of the alignment of the molecular orbitals.

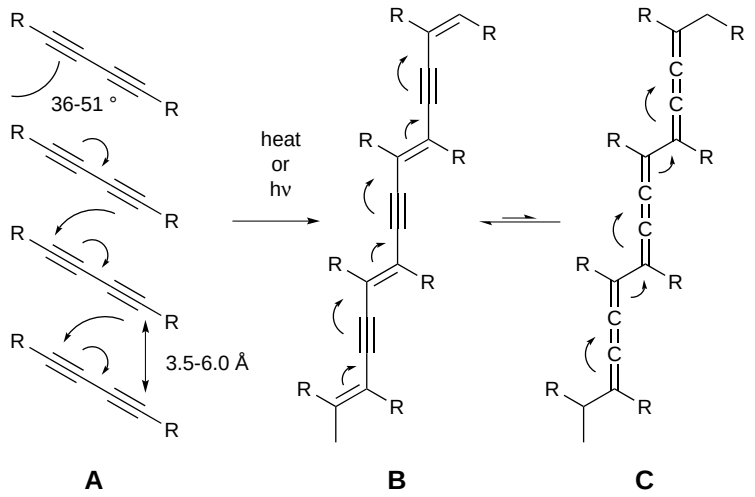

Scheme 4.4: Topochemical polymerisation of a diactylene compound.

The orbital interaction of a simple alkyne is shown in Figure 4.6 (A). A dialkyne will have an extended orbital alignment as shown in Figure 4.6 (B). Polymerisation in the solid state is only possible if the alignment of the orbitals allows a positive interaction. Therefore the interaction between the HOMO and LUMO of two molecules is crucial. The HOMO and LUMO level for the p_z orbital of a monoalkyne is showed in Figure 4.6 (C).

In a crystal the orientation of the HOMO and LUMO have to be in such a way that the fourth carbon (HOMO) of a dialkyne can overlap with the first carbon (LUMO) of a secondary dialkyne. As this is a cascade reaction the same LUMO can repeat the overlap with the next HOMO of an additional dialkyne (Figure 4.7); as this is a cascade reaction, standard Woodward-Hoffman rules do not apply. [258, 259]

Another similar polymerisation process which has also been performed in the

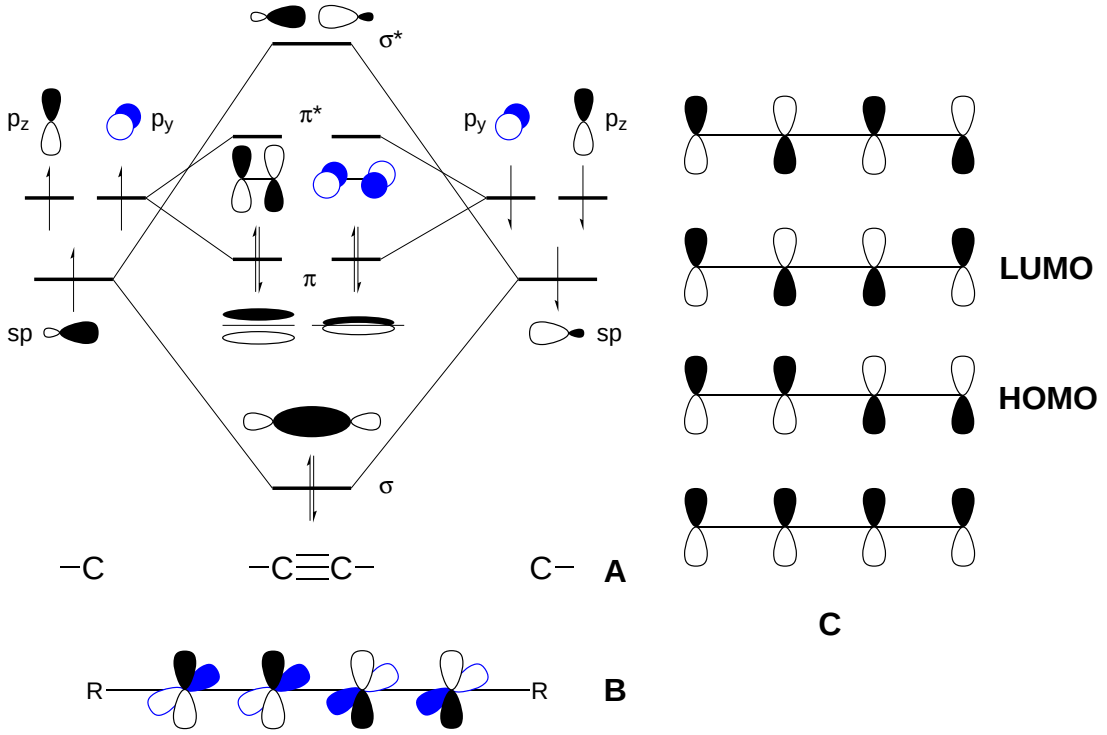

Figure 4.6: Orbital interaction and alignment of an alkyne (A), a dialkyne (B) and the orbital energy levels of a dialkyne (C).

solid state is 1,6-addition. The requirements for 1,6-additions are similar to 1,4- or 1,3-additions. The angle and distance between the reacting carbons of the monomers needs to be within specific values (ideally 27°and 7.5 Å). [260]

For example, polymerisation in solid state *via* 1,6-addition was performed by Hoang *et al.* [261] The basis for this topochemical polymerisation was a triene (Figure 4.8) derived crystal. The distance between carbon one and six of the triene in adjacent layers was 4.09 Å with a tilt angle of 34°and an orientation angle of 68°. For 1,6-addition topochemical polymerisation of trienes a distance between adjacent reacting carbons is preferably under 4.0 Å (Figure 4.8). The obtained crystals were heated for eight hours at 110 °C and resulted in the formation of the corresponding *meso*-diisotactic polymer.

4.2.3 Glaser coupling - Construction of monomers

The Glaser coupling of alkynes is a proven route to synthesise symmetrical dialkynes. Three mechanisms are proposed: an inner sphere mechanism, an outer sphere mech-

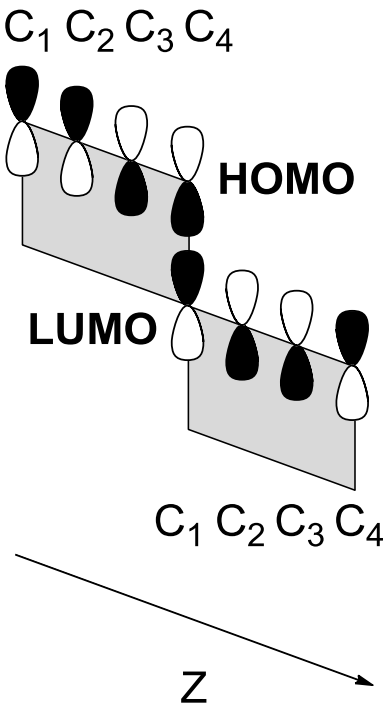

Figure 4.7: HOMO LUMO interaction of crystalline dialkynes.

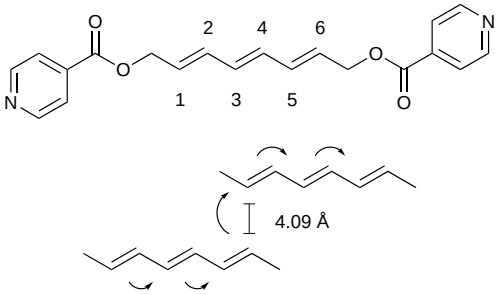

Figure 4.8: Monomer used to perform topochemical polymerisation.

anism and a bimetallic reductive elimination process. [262] In general, copper ligates with the alkyne bond, a base abstracts the alkyne proton and copper binds at the vacant sp hybridised position. Two alkyne copper species then form a complex together with electron donating ligands (Scheme 4.5). The alkyne species couple to form the dialkyne and the resulting Cu(0) is re-oxidised in the presence of oxygen.

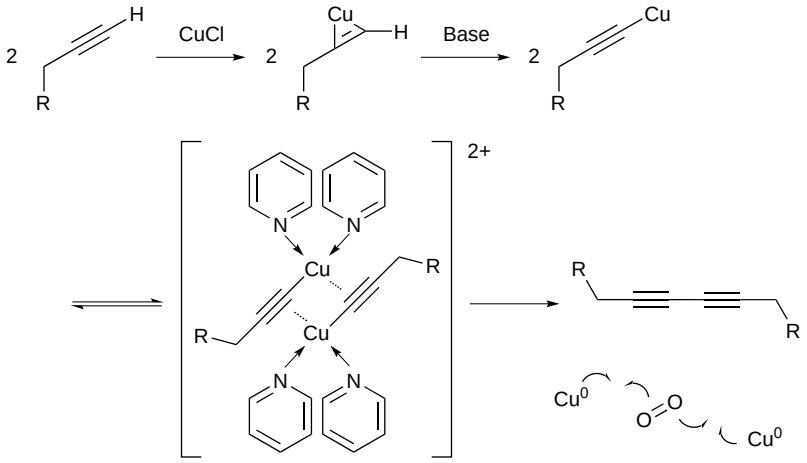

Scheme 4.5: General mechanism of Glaser coupling.

4.3 Research objectives

To perform topochemical polymerisation, 1,4-dialkyne derivatives were synthesised *via* a Glaser coupling of the corresponding mono substituted alkynes. The coupling was performed using various copper sources and different bases. The aim was to investigate whether the polymerisation of the crystal could be induced thermally or photochemically in the solid state.

4.4 Methodology

The protocols for the synthesis of the individual monomers can be found in Supporting Information Chapter 4.

The topochemical polymerisation was performed using a single crystal, which was induced thermally or photochemically. Thermal induction of the crystal involved the use of a radical initiator (2,2'-azobis-(2-methylpropionamidine) dihydrochloride) (**4**). The initiator was dissolved in a solvent which did not solubilise the crystal. The resulting suspension was then heated or the solvent was evaporated to obtain a crystal covered in the initiator, followed by heating.

Photochemical induction of a crystal was performed using different types of lamps, either a 125 Watt white light plasma lamp or a UV lamp (λ = 253 nm)

125 Watt. The crystals were irradiated for up to ten hours. The distance between the light source and the crystal was fixed at 2 cm - 6 cm depending on the light source.

4.5 Results and discussion

To gather experimental knowledge and understanding of topochemical polymerisations involving 1,4-additions, two examples previously published by Baughman were synthesised. [252] First, propargylic alcohol (**9**) was coupled *via* Glaser conditions (Scheme 4.6). The dialkyne was obtained as a powder in a good yield (86%) as an

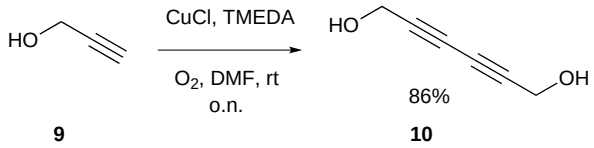

Scheme 4.6: Glaser coupling of propargylic alcohol (**9**).

off white solid. Over extended periods of time (30 days) the colour of the powder changed slowly to orange/ red. This process could be delayed (60 days) by storing the dialkyne in the dark and in the freezer. Electron rich dialkynes are known to decompose or react upon exposure to light. [263] A sample was stored in the dark at ambient temperature for over six months and still contained 83% dialkyne (**10**) as proved by ^{1}H NMR spectroscopic analysis. The sample was dissolved in acetonitrile, filtered and concentrated in order to remove the insoluble polymeric solid. The colour of the filtrate was deep red and the solid was insoluble. In the literature it was described that the excitation of dialkyne **10** produces a dark red powder. [264] A freshly purified sample was therefore treated with a plasma lamp (white light, 125 Watt) producing white light for twenty minutes. The solid sample changed colour, from off white to dark red and became insoluble in acetonitrile. Solid state NMR spectroscopy measuring cross polarisation (with and magic angle spinning and 60 seconds recycle delay) and broad lines were measured. This is an indicator of a polymeric structure as there is no isotropic molecular tumbling. Unfortunately, at-

tempts to crystallise dialkyne **10** were unsuccessful and therefore it was not possible to measure a single crystal.

However, knowledge gained was used to synthesise dialkyne **13** which was reported to be far easier to crystallise and less reactive. [252] The first step in the synthesis of dialkyne **13** was the substitution of benzoyl chloride (**11**) with propargylic alcohol (**9**) (Scheme 4.7). Ester **12** was obtained in an unoptimised yield of 78%. The purity of the starting compound is important to avoid difficult column chromatography at the end of the synthesis due to Glaser coupling products derived from left over propargylic alcohol (**9**). The coupled dialkyne **13** was obtained in a yield of 81% and was crystallized from *n*-hexane and ethyl acetate (5:1). The obtained crystals were light yellow in colour and proved to be stable over a long period of time (one year at room temperature on the bench).

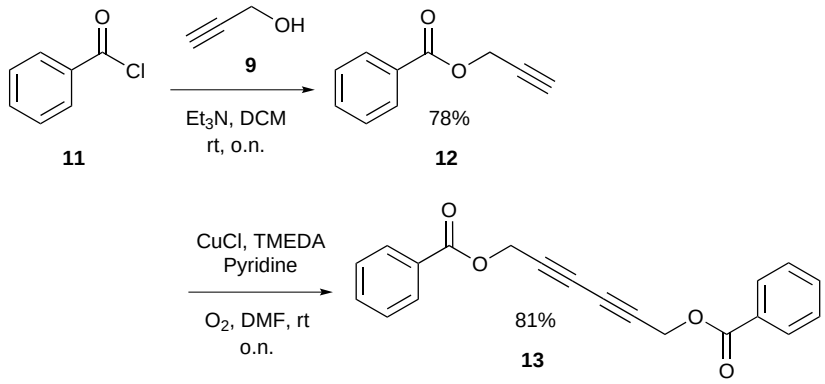

Scheme 4.7: Synthesis of dialkyne **13** starting from benzoyl chloride (**11**) and propargylic alcohol (**9**).

The packing of the crystal was shown to meet the requirements for 1,4-addition topochemical polymerisation. NOTE: The crystal was not fully resolved but the dimensions of the unit cell were exactly the same as the crystal previously submitted to the Cambridge Structural Database (Table 4.2). Therefore, the packing of the obtained crystal is the same as the crystal published by Xu *et al.* [265] as shown in Figure 4.9.

The obtained crystals were irradiated using an UV lamp (λ = 253 nm, 125 Watt) for twenty minutes. The white needles changed colour, from white to deep

Table 4.2: Literature and determined values of the unit cell of compound **13**.

Parameter	**Literature values** [265]	**Determined values**
Space group	P 2_1/n	P 2_1/n
a (Å)	14.038(2)	14.038(6)
b (Å)	4.3526(10)	4.3527(0)
c (Å)	14.864(2)	14.864(3)
α (°)	90	90
β (°)	117.055(16)	117.055(11)
γ (°)	90	90

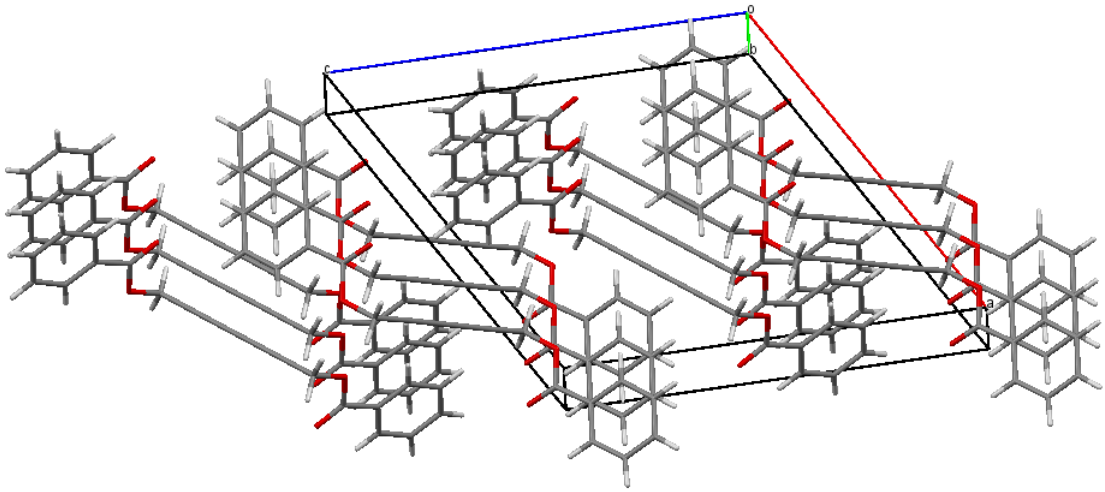

Figure 4.9: Crystal packing of dialkyne **13**.

red (Figure 4.10). Triturating the irradiated crystals in ethyl acetate yielded a dark red insoluble solid. Previous experiments and the literature [264] indicated the solid was polymerised material. The suspension was filtered and the yellow filtrate was analysed by ^{1}H NMR spectroscopy. As expected, the yellow solution was the unreacted starting material dialkyne **13**.

It was found it was hard to achieve full monomer conversion (a conversion of 26% was obtained) as irradiation of the crystals required long treatment times. The required time to obtain a conversion of 26% was 14 hours for a 10 mg sample. Raman spectroscopy was performed to follow the change in the crystal over time (Figure 4.11). Raman spectroscopy could be used to distinguish between alkyne and alkene bonds. A clear change in the spectra of the starting material was observed. At 1,460 cm^{-1} (alkene) and 2,150 cm^{-1} (alkyne stretch) peaks developed over time. Further-

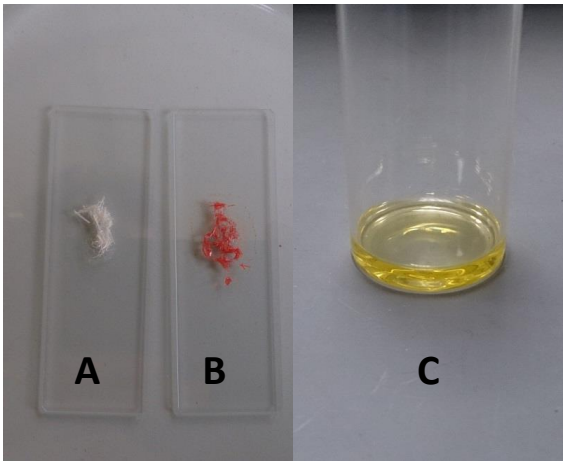

Figure 4.10: Irradiation of dialkyne **13**, before (white crystals (A)) and after (red crystals (B) and yellow solution (C)).

more, the peak at 2,290 cm^{-1} (dialkyne) decreases and completely disappeared after 90 minutes of irradiation. Irradiation longer than 90 minutes did not change the results.

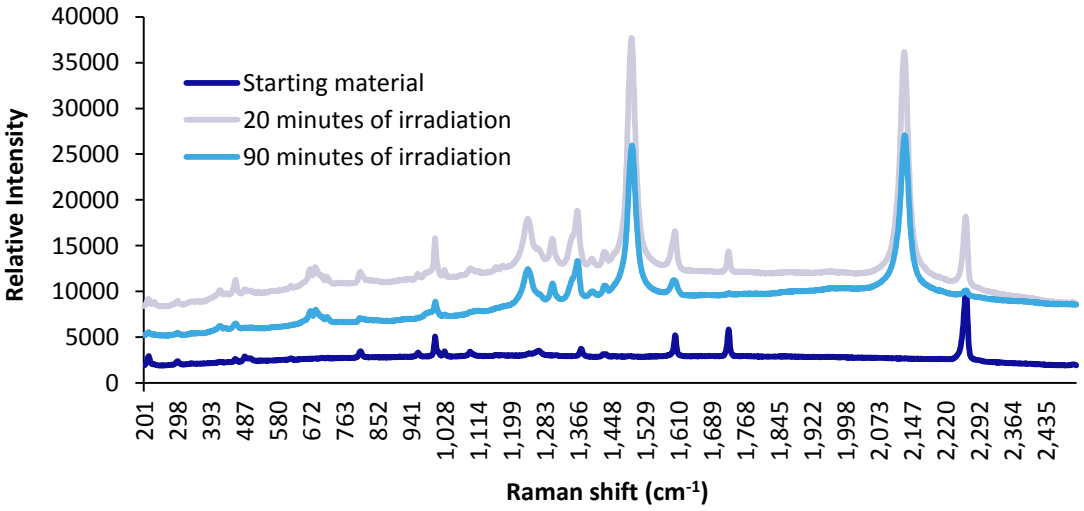

Figure 4.11: Raman spectroscopy of dialkyne **13**, irradiation of crystals with white light.

To extend the scope of this process various additional dialkynes were prepared, crystallised and then evaluated for suitability for topochemical polymerisation (Figure 4.12). The selection was based on known chemical compounds but ones that had not previously been investigated for topochemical polymerisation. The packing of the unit cells (**14**, **17**, **18**), and possibility to form a co-crystal (**15**, **16**) were selection criteria. Structure **19** was chosen because of its similarity to **14**. In the

literature the dialkyne **19** had been synthesised and analysed by X-ray diffraction; the packing of the unit cell did not show the proper stacking, the monomers were perpendicularly orientated. Changing the solvent or solvent system for this compound crystallisation could have generated a different packing of the crystal, but unfortunately this was not observed for dialkyne **19**.

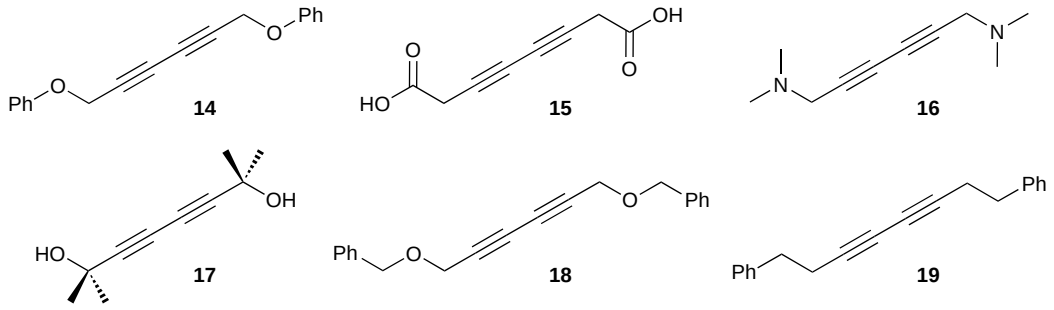

Figure 4.12: Selected dialkynes for topochemical polymerisation.

A co-crystal was also generated from dialkyne **13** and the fluorinated analogue **22** which had been published by Xu *et al.* [266] Compound **22** was prepared from pentafluorobenzoyl chloride (**20**) and propargylic alcohol (**9**) to obtain the corresponding ester **21** in 79%. A Glaser coupling using the previous conditions (Scheme 4.7) was used to form dialkyne **22** (Scheme 4.8), which was obtained in a yield of 61%.

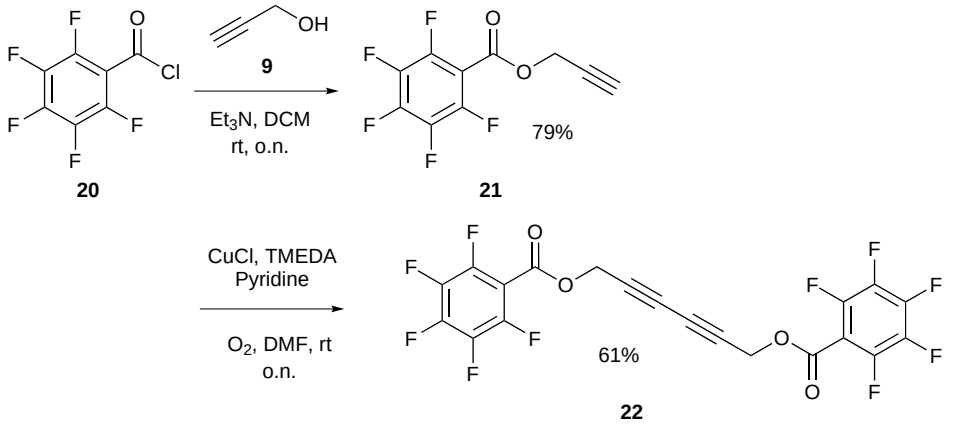

Scheme 4.8: Synthesis of fluorinated dialkyne **22**.

Co-crystals of dialkynes **13** and **22** were prepared by mixing both alkynes in a molecular ratio of 1:1 in a solvent mixture of ethyl acetate and *n*-hexane (1:4). Irradiation was performed using a UV lamp ($\lambda = 253$ nm, 125 Watt) for 90 minutes.

The starting crystals which were originally pale red turned dark red after irradiation. Figure 4.13 shows the Raman spectra of the starting crystal and irradiated crystal (the same single crystal was used for the Raman spectroscopy measurements). It is clear that the intensity is much higher for the irradiated crystal peaks appearing at 1,000 cm^{-1} (carbon carbon single bond (B in Scheme 4.4)), 1,210 cm^{-1} (alkene alkene bond (C Scheme 4.4)), 1,500 cm^{-1} (alkene (B in Scheme 4.4)) and 2,090 cm^{-1} (alkyne stretch (B in Scheme 4.4)). Further research was required to establish the proposed polymerisation although the colour and Raman spectra were good indications of an electron rich polymer.

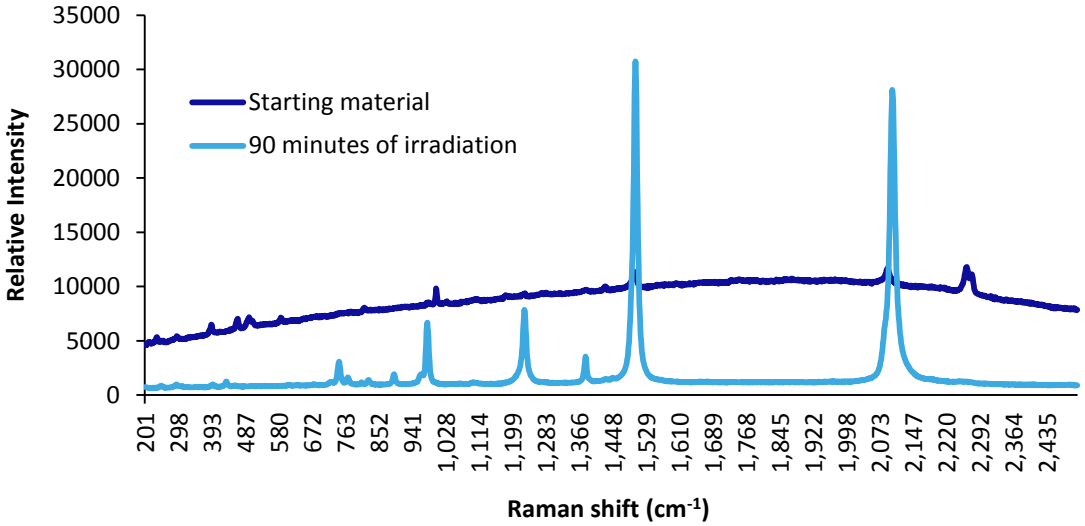

Figure 4.13: Raman spectroscopy of co-crystal containing dialkyne **13** and **22**.

Washing the crystals with ethyl acetate left a dark red solid which was further analysed by solid state NMR spectroscopy. The sample was first measured neat using cross polarisation measurement overnight with five seconds recycle delay and one millisecond contact time. This type of measurement polarises the protons into the carbon signals and the carbons can then be viewed. Unfortunately, the signals were too weak to perform a proper optimisation of the experimental conditions and therefore, the delay and contact time were approximately determined by the spectroscopist. The C-F signals do not show in spectra A of Figure 4.14 as these are most likely broadened through dipolar coupling to the fluorine. From this spectrum it is clear there are two groups, the aromatic groups at 65.17 ppm and CH_2 at 129.78

ppm. To improve the signal intensity and to record a fluorine spectrum, the sample was mixed with potassium bromide. The starting material and product were shown to be inert to potassium bromide. First a fluorine spectrum was recorded. The sample contains fluorine, spectrum B in Figure 4.14. The sample was further measured using cross polarisation and direct excitation. Direct excitation measurements will observe carbons directly. This was also applied to the starting material and a clear difference in the carbon spectra was observed. The peak at 131 ppm increased in intensity significantly. The starting material (spectrum C in Figure 4.14) shows two peaks which contain a second peak, the peaks at 131 ppm and 76 ppm. From these spectra it is clear the solid contains both monomer units.

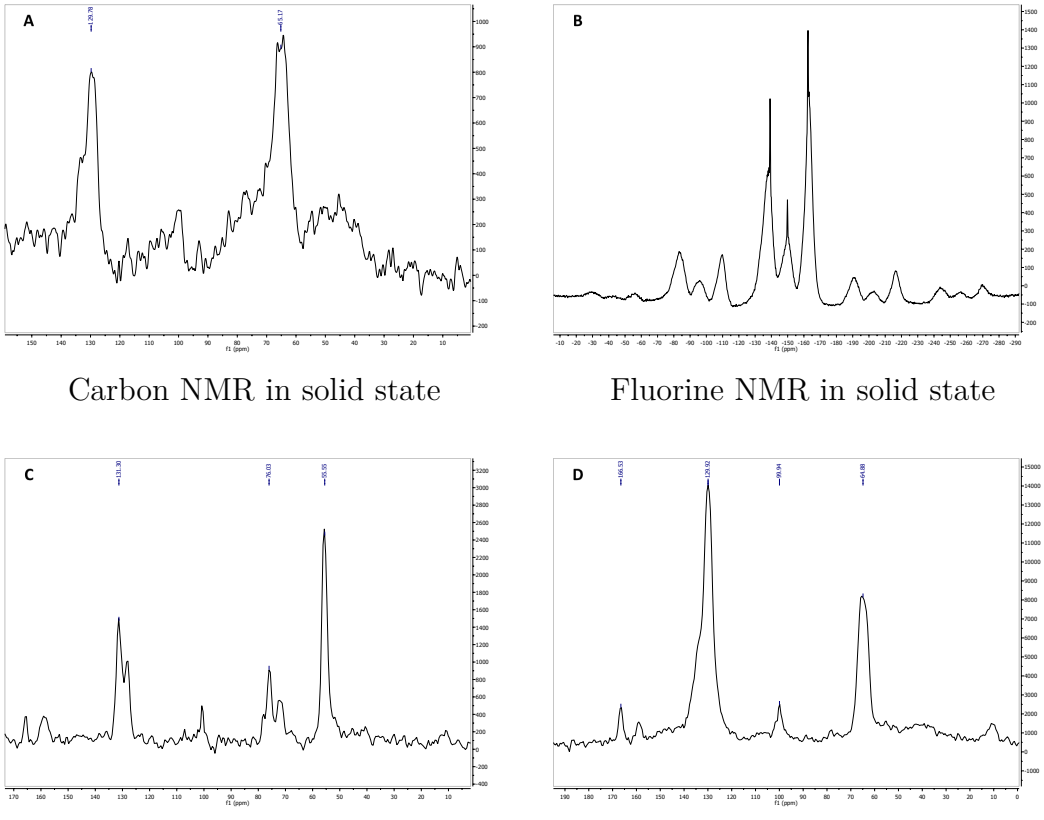

Carbon NMR in solid state | Fluorine NMR in solid state

Carbon NMR starting material | Carbon NMR product

Figure 4.14: Solid state spectra of dialkyne co-crystal (dialkyne **13** and **22**).

The synthesis of the molecules mentioned in Figure 4.12 was straight forward for compounds **14**, **16** - **19**. The synthesis of compound **14** started with the mesylation of propargylic alcohol (**9**) followed by nucleophilic substitution with phenol (**24**) resulting in an overall yield of 74% of compound **25** (Scheme 4.9). [267] The Glaser

coupling was then performed using a pre-made Hay catalyst. It was shown that the Glaser coupling was more efficient if the Hay catalyst was prepared separately and then added to the reaction mixture instead of mixing all the compounds together. Preparing the Hay catalyst separately resulted in an increase in yield of 29% for the same reaction time (overnight).

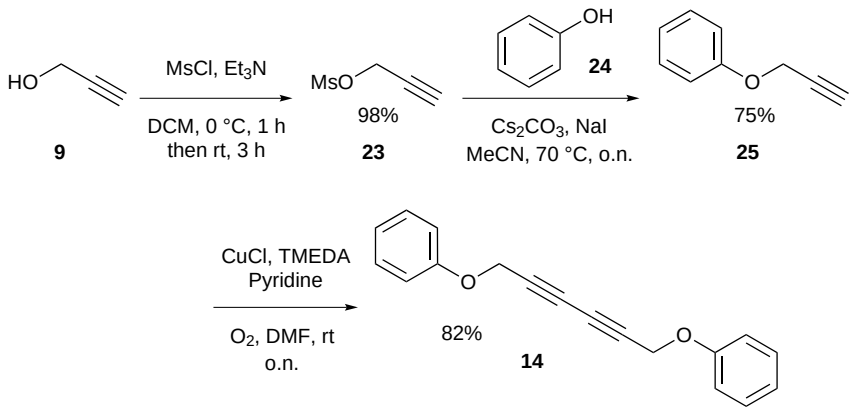

Scheme 4.9: Synthesis of dialkyne **14** from propargylic alcohol (**9**).

Unfortunately, despite multiple attempts to crystallise dialkyne **14**, conditions were not found to produce suitable crystal structures consistent with the known structure. [268] Therefore, the packing was as shown in Figure 4.15 with the distance between two molecules being insufficient.

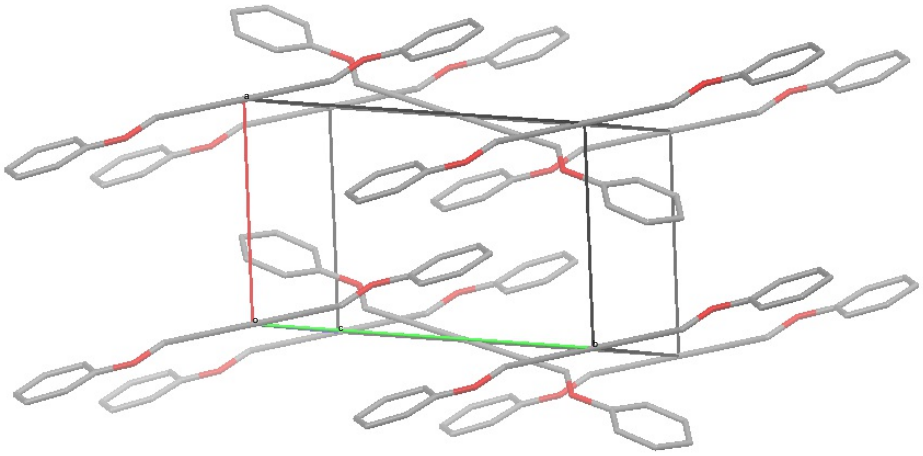

Figure 4.15: Crystal structure and packing of dialkyne **14**, (a = 7.469(3) Å, b = 11.368(12) Å, c = 8.591(9) Å). [268]

The synthesis of dialkyne **18** started from the commercial available alkyne **26** (Scheme 4.10). The Glaser coupling gave molecule **18** in an unoptimised 53% yield.

The reaction conditions were not further optimised as enough material was obtained for analysis of the compound however, the compound could not be crystallised despite various solvents and techniques being tested.

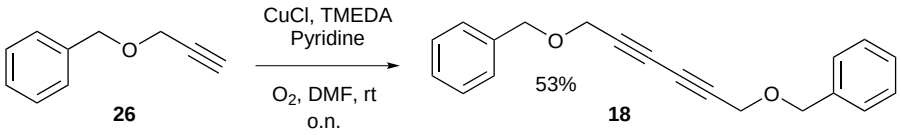

Scheme 4.10: Glaser coupling of alkyne **26**.

To determine the influence of the presence of heteroatoms, dialkyne **19** was synthesised in a yield of 81% starting from commercially available alkyne **27** (Scheme 4.11). The conditions used for this Glaser coupling worked well providing the product in 81% yield. The crystal structure did not however, meet the criteria for topochemical polymerisation. The packing of the crystal was unfortunately like E in Figure 4.4.

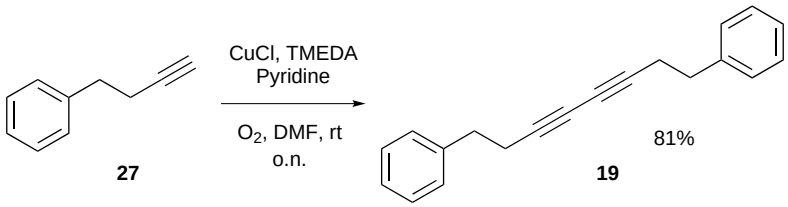

Scheme 4.11: Glaser coupling of alkyne **27**.

The reactivity of dialkyne **10** was too high and dark red samples were immediately formed. To investigate the influence of the CH_2, group 2-methyl-3-butyn-2-ol (**28**) was used as the substrate for the Glaser coupling (Scheme 4.12). The dialkyne **17** was obtained in 88% yield. The sample was off white and maintained this colour over several weeks, an indicative sign the sample is not polymerising/ decomposing. Furthermore, ^{1}H NMR spectroscopy did not show any change. Crystals were formed using a solution of *n*-hexane and isopropanol (4:1). Different crystal structures are known but are either a crystal structure containing mixed complexes or do not meet the criteria for topochemical polymerisation. The powder was irradiated using a plasma lamp (white light, 125 Watt) for 90 minutes. Irradiation of the crystals did not lead to topochemical polymerisation. The sample was still fully soluble in

dimethyl sulfoxide-d_6 and was identical to the starting material as determined by ^{1}H NMR spectroscopy.

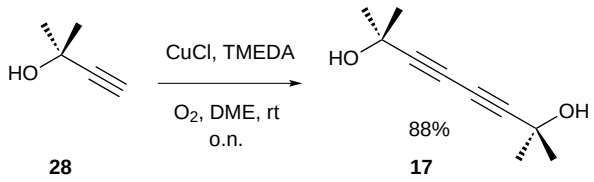

Scheme 4.12: Glaser coupling of 2-methyl-3-butyn-2-ol (**28**).

Co-crystallisation has been shown to present opportunities for topochemical polymerisation. Co-crystals could be made from a variety of different monomer compounds. One class is especially interesting, the formation of salt crystals. A possible combination of an organic salt formed from dialkyne **15** and **16** by Brønsted exchange. The working hypothesis was that the crystal will be formed around alternating pairs of the dialkynes (**15** and **16**). The synthesis of dialkyne **16** was straight forward and the compound was obtained as a yellow oil in 59% yield (Scheme 4.13). [269] Some material was lost during the purification, therefore, the yield was lower than expected. Compared to the previously described Glaser couplings, the solvent was changed to acetone to improve the solubility of propynamine **29**.

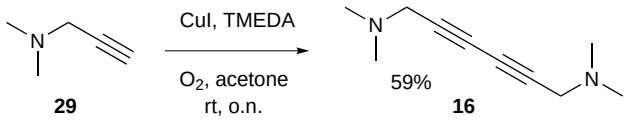

Scheme 4.13: Glaser coupling of propynamine (**29**).

The synthesis of dialkyne **15** had not previously been described in the literature. A proposed route (Scheme 4.14) starts with the oxidation of 3-butyn-1-ol (**30**) to form but-3-ynoic acid (**31**). [270, 271] Unfortunately, the Glaser coupling of substrate **31** was more challenging than anticipated. Various conditions were tested but without any success (Table 4.3). Different explanations could be given for the failure of this reaction. For example, the pH of the reaction mixture could have been too acidic due to the presence of the acid side group of the starting material. Therefore, the reaction was performed in trimethylamine or pyridine and used three

equivalents of TMEDA. The reaction mixture became a gum unless a few drops of solvent (DME, DMF or THF) were also added. Alternatively, the copper could be ligating with the acid inhibiting the coupling. To overcome this problem up to three equivalents of the Hay catalyst were added to the reaction mixture, unfortunately also without success.

Scheme 4.14: Synthesis of dialkyne **15** starting from 3-butyn-1-ol (**30**).

Table 4.3: Reaction conditions Glaser coupling but-3-ynoic acid (**31**).

Entry	Catalyst	Bases	Solvents	Time	T (°C)
1	CuI	Et_3N, TMEDA pyridine	Acetone, DME DMF, THF	on	rt - 60
2	CuCl	Et_3N, TMEDA pyridine	Acetone, DME DMF, THF	on	rt - 60
3	$Cu(OAc)_2 \cdot H_2O$	Et_3N, TMEDA pyridine	Acetone, DME DMF, THF	on	rt - 60

A precedent exists for a similar reaction in the literature which is the Glaser coupling of the corresponding alkyne methylester. [272] The methodology described is based on an immobilised copper complex. This approach was however not used to couple but-3-ynoic acid (**31**) as the formation of the immobilised copper complex was not reproducible. An alternative approach to the synthesis of dialkyne **15** started with the Glaser coupling of 3-butyn-1-ol (**30**) followed by the oxidation of intermediate **32** (Scheme 4.15). The second step in this synthesis was problematic as the starting material was not soluble in water, which is one of the preferred solvents. Using acetone instead did not result in the desired product formation.

As the synthesis of dialkyne **15** proved challenging, a different strategy was proposed. The synthesis of diphenyl prop-2-yn-1-ylphosphonate (**34**) and phosphonate salt **37** was straightforward and has been previously described in literature (Scheme 4.16). [273–276] However, the Glaser coupling of the monomeric units is to the

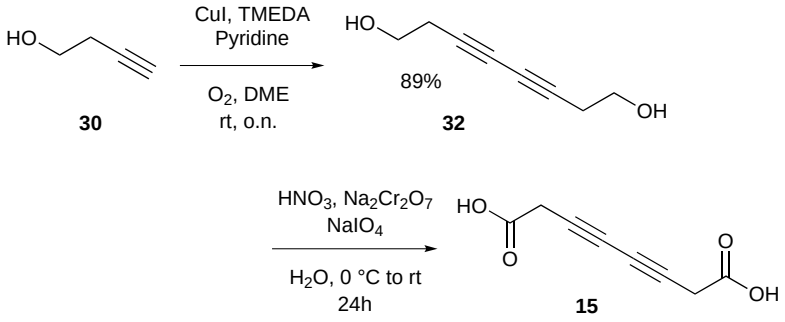

Scheme 4.15: Synthesis of dialkyne **15** *via* the oxidation of intermediate **32**.

best of our knowledge not described in literature. Various reaction conditions were screened (Table 4.4) without success. The reaction progress was followed by ^{31}P NMR spectroscopy and TLC but both indicated only starting material. As for the reaction mentioned in Scheme 4.14 different possibilities were given for the failure. The same arguments apply for the synthesis of dialkyne **38**. To rule out any possibilities the reaction was performed with up to three equivalents of base and catalyst. No clear explanation could be given for the fact the synthesis of dialkyne **35** did not work.

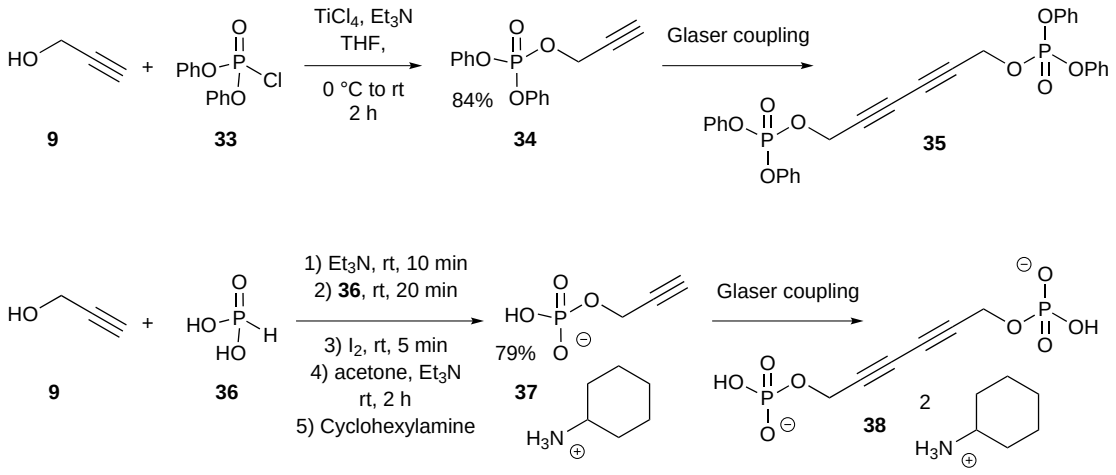

Scheme 4.16: Synthesis routes of dialkyne **35** and **38**.

Using an excess of dialkyne **10** to form the desired dialkyne phosphate salt **38** was performed (Scheme 4.17). Neither reaction worked, although the similar reaction which gave alkyne **37** (Scheme 4.16) gave a good yield. The only difference was the addition of acetonitrile in order to dissolve the starting material. Observations showed dissolving phosphorous acid (**36**) was hard to achieve in the given solvent

Table 4.4: Conditions screened for Glaser coupling to form dialkyne **35** and **38**.

Entry	Catalyst(s)	Bases	Solvents	Time	T (°C)
1	CuI	Et_3N, TMEDA pyridine	Acetone, DME DMF, THF	on	rt - 60
2	CuCl	Et_3N, TMEDA pyridine	Acetone, DME DMF, THF	on	rt - 60
3	$CuCl_2$	Et_3N, TMEDA pyridine	Acetone, DME DMF, THF	on	rt - 60
4	$Cu(OAc)_2 \cdot H_2O$	Et_3N, TMEDA pyridine	Acetone, DME DMF, THF	on	rt - 60
5	$Cu(OAc)_2 \cdot H_2O$ and $NiCl_2$	Et_3N, TMEDA pyridine	Acetone, DME DMF, THF	on	rt - 60

system.

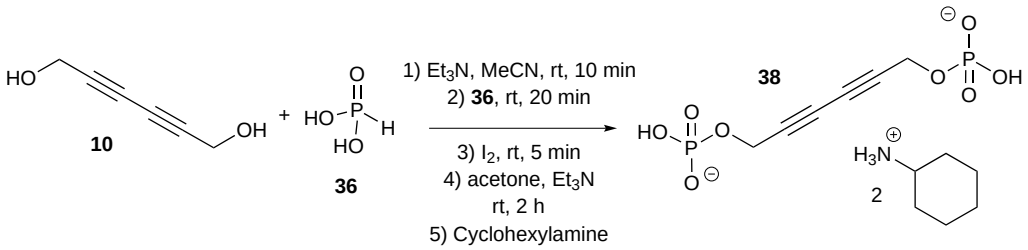

Scheme 4.17: Synthesis dialkyne **38**.

The synthesis of compound **40**, *via* a double Sonogashira coupling, was straightforward and had been published by Werner *et al.* [277] The desired product was obtained in a yield of 81% and was successfully crystallised from *n*-hexane and methanol (6:1). The X-ray structure of this compound revealed the packing of this compound did meet the criteria for topochemical polymerisation (Figure 4.16).

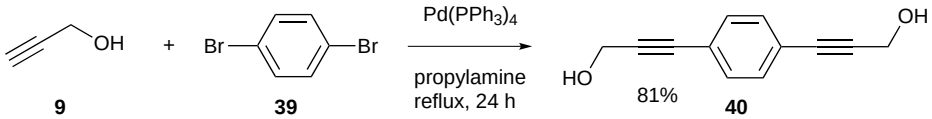

Scheme 4.18: Synthesis dialkyne **40**.

The phenyl rings were not stacked on top of each other, resulting in a distance of 4.910 Å between the carbons involved in the topochemical polymerisation. The space group of compound **40** is P 2_1/c, corresponding to orientation B in Figure 4.4. This type of crystal packing has the potential to polymerise. Therefore, it is either

due to the distance between the monomer layers (4.910 Å), the light source used or the orientation of the alkynes and phenyl ring, that dialkyne **40** was not able to polymerise.

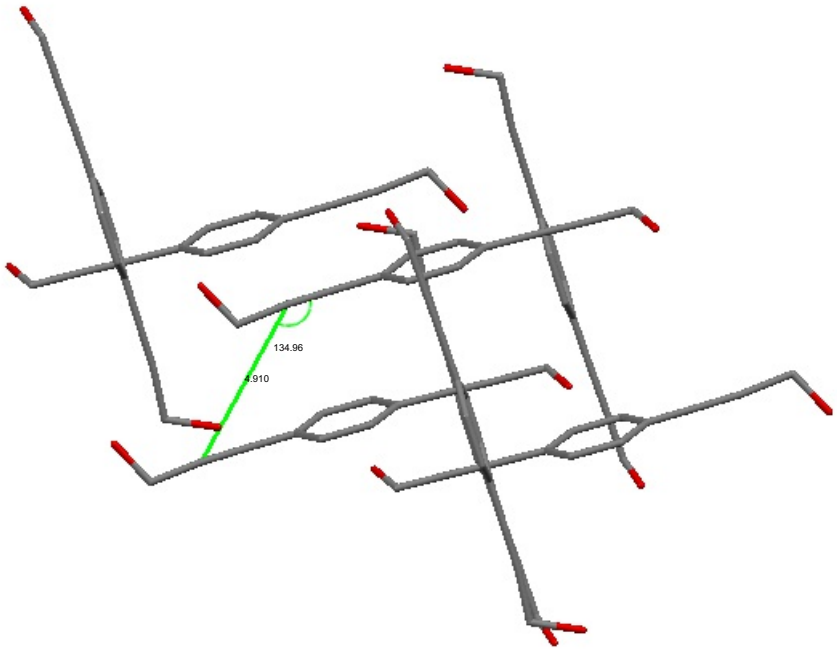

Figure 4.16: Crystal structure compound **40**, distance between reacting carbons is 4.910 Å and the angle between two adjacent layers is 134.96°.

If phenyl rings are present, these should align so they sit on top of each other in order to create space for the alkyne group of the molecule. It is most likely the phenyl rings will not align directly on top of each other but instead will be offset to get better molecular orbital interactions with the alkynes.

Therefore further research was performed determining the influence of the electronics of the system. Alkyne **40** was modified using benzoyl chloride (**11**) to obtain compound **41** in a good yield (73%) (Scheme 4.19). The obtained crystals, using ethyl acetate : *n*-hexane (1:4), were analysed by X-ray spectroscopy. Unfortunately, the packing of the crystal did not meet the preferred criteria (Figure 4.17). The distance between the monomer layers was 5.271 Å, but the angle was too wide (53.00 °). Analogue **41** is related to dialkyne **13** which was successfully used in polymerisation.

Alkyne **40** was also modified using pentafluorobenzoyl chloride (**20**) to obtain

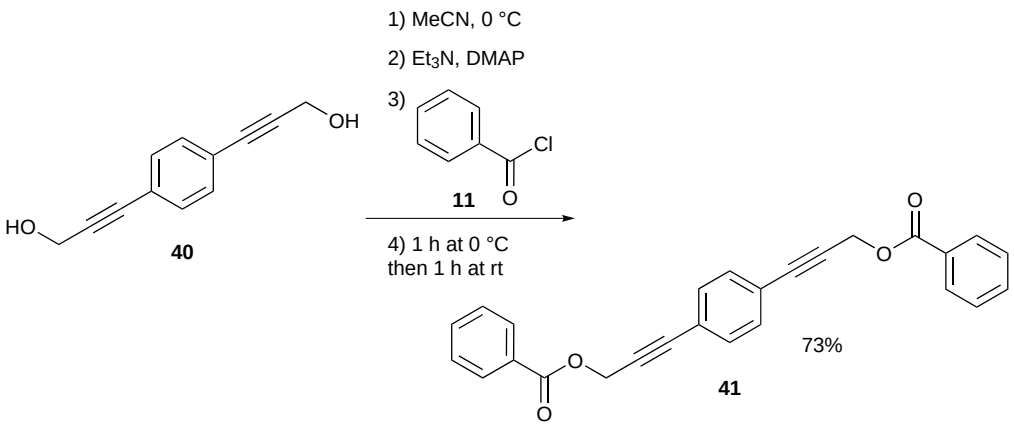

Scheme 4.19: Synthesis dialkyne **41**.

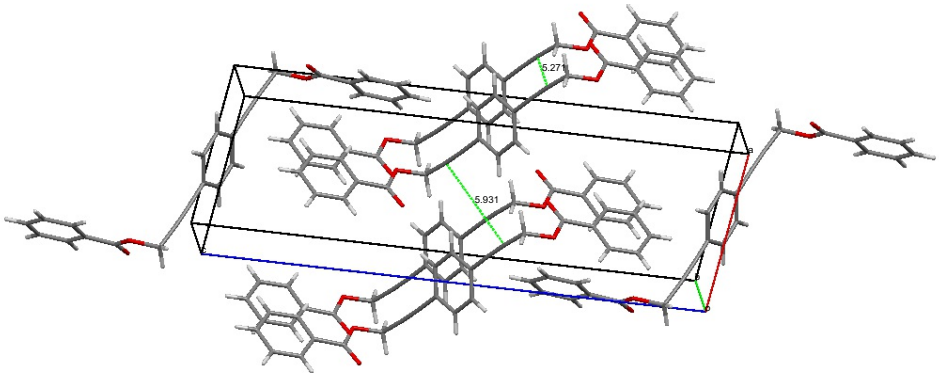

Figure 4.17: Crystal structure compound **41**, distance between reacting carbons is 5.271 Å and the angle between two adjacent layers is 53.00°.

ester **42** in a good yield (82%) (Scheme 4.20). The crystals obtaining using a mixture of ethyl acetate : *n*-hexane (1:4), were analysed by X-ray spectroscopy. Two different crystal structures were found for ester **42** depending on the temperature used for analysis (120 K and 230 K) (Figure 4.18). The packing of both crystal forms (D in Figure 4.4) did meet the criteria for topochemical polymerisation. This is interesting as ester **42** is related to dialkyne **22** which was successfully used in polymerisation. In the crystals of **42** the distance between the layers is 4.604 Å and the angle is 52.25 °for the crystal analysed at 120 K. The distance between the layers is 4.803 Å and the angle is 47.53 °for the crystal analysed at 230 K. The encounter temperature transition in the crystal was not expected as the related compound **41** did not show a similar change. Therefore, the fluorine interactions cause the change in crystal packing.

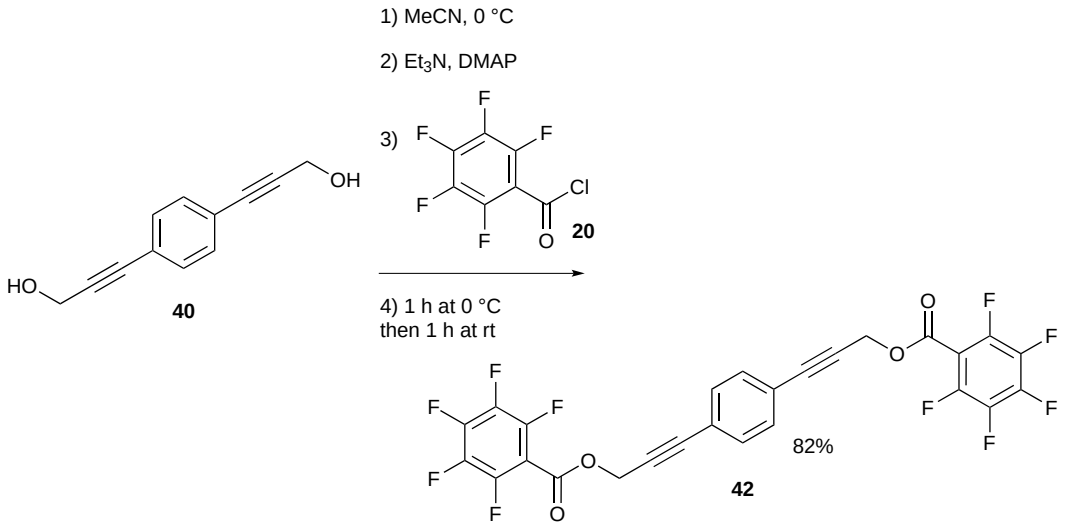

Scheme 4.20: Synthesis dialkyne **42**.

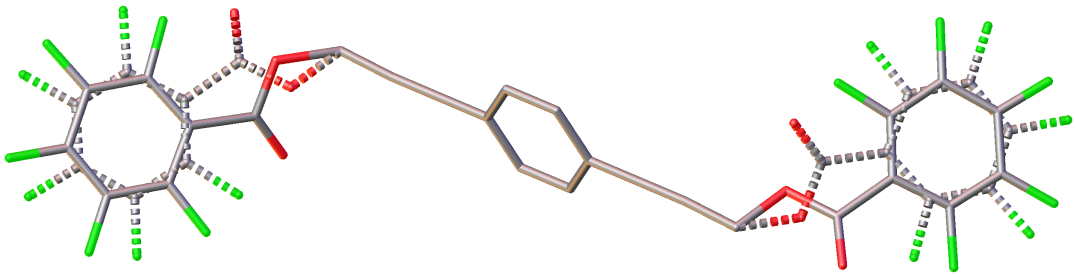

Figure 4.18: Different configurations crystal of compound **42** at 120 K (dashed line) and 230 K (solid line).

The crystal was irradiated, using a plasma lamp (white light, 125 Watt). However, as predicted, no change was observed and the irradiated crystals were still soluble in MeCN. Raman spectroscopy showed identical spectra for $t = 0$ min (Figure 4.19 A) and $t = 150$ min (Figure 4.19 B). Furthermore, mass spectrometry using the Atmospheric Solids Analysis Probe (ASAP) technique and TLC (ethyl acetate : *n*-hexane [1:4]) did not show any difference compared to the starting material. A possible reason that no polymerisation occurred could be, although unlikely, the power of the lamp.

A π extended compound **44** was synthesised following the general procedure using propargylic alcohol (**9**) and 1,4-dibromonapthalene (**43**) as starting material. [278] The Sonogashira coupling resulted in a moderate yield (43%) for compound **44**. Analysing compound **46** by X-ray spectroscopy revealed a unit cell with angles

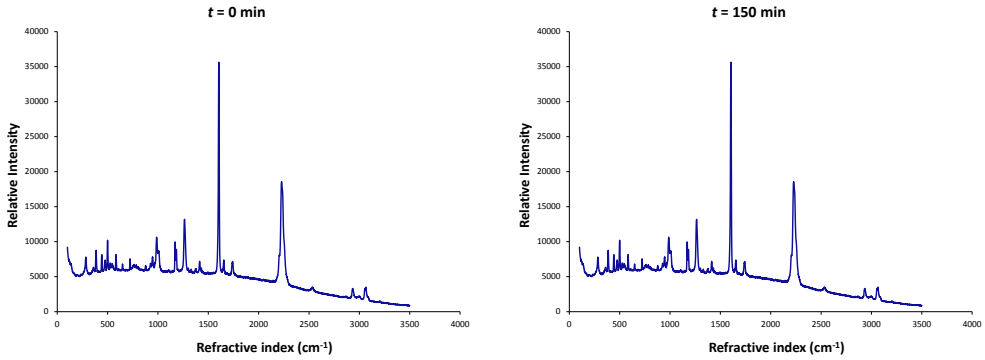

A: Raman spectra compound **42** at $t = 0$ min

B: Raman spectra compound **42** at $t = 150$ min

Figure 4.19: Raman spectra compound **42**, using a laser wavelength of 633 nm.

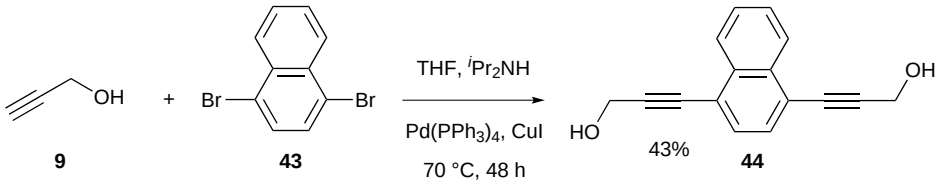

Scheme 4.21: Synthesis dialkyne **44**.

of 90°. The packing of the crystal did meet the criteria for topochemical polymerisation. The distance between the layers was 4.967 Å and the angle 49.04°(Figure 4.20).

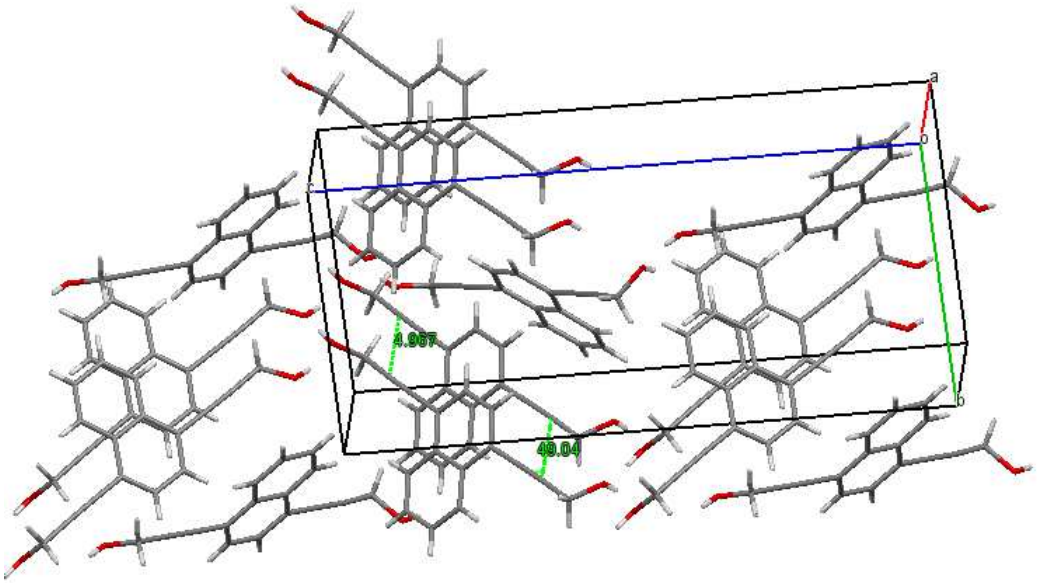

Figure 4.20: Distance and angle compound **44**.

Raman spectroscopy showed similar spectra for $t = 0$ min (Figure 4.21 A) and

t = 150 min (Figure 4.21 B). The peak at 2225 cm^{-1}, which is assigned to C≡C, did not disappear. The intensity of the peaks between 1200 and 1600 cm^{-1} changes due to the irradiation of the C=C bonds. Furthermore, ASAP and TLC (CH_2Cl_2) did not show any difference compared to the starting material. An explanation topochemical polymerisation is not observed could be the power of the lamp was not sufficient or the phenyl ring stops polymerisation from happening.

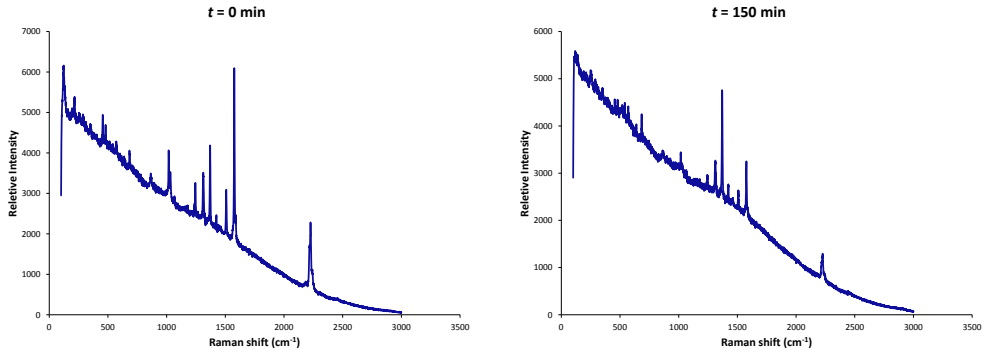

A: Raman spectra compound **44** at t = 0 min

B: Raman spectra compound **44** at t = 150 min

Figure 4.21: Raman spectra compound **44**, using a laser wavelength of 738 nm.

In a similar way compound **46** was synthesised *via* a double Sonogashira coupling on 9,10-dibromoanthracene (**45**). The reaction was performed using a solvent mixture of THF (10 mL), $^{i}Pr_2NH$ (10 mL) and Et_3N (5 mL). The use of the two bases were added in order to fully solubilise all the material.

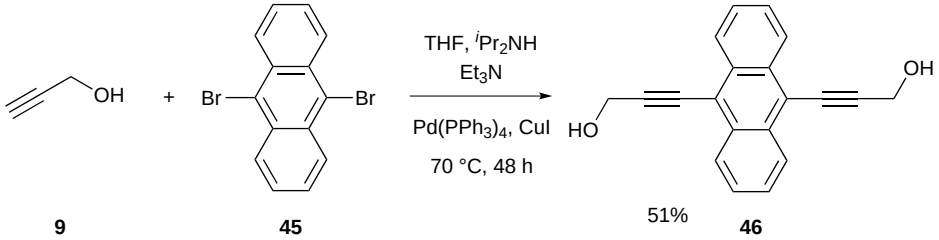

Scheme 4.22: Synthesis dialkyne **46**.

Analysing compound **46** by X-ray spectroscopy revealed a unit cell consisting of three halves of the molecule. Each half is orientated around the centre of symmetry. Hexamers were formed as the molecules are connected by hydrogen bonding (Figure

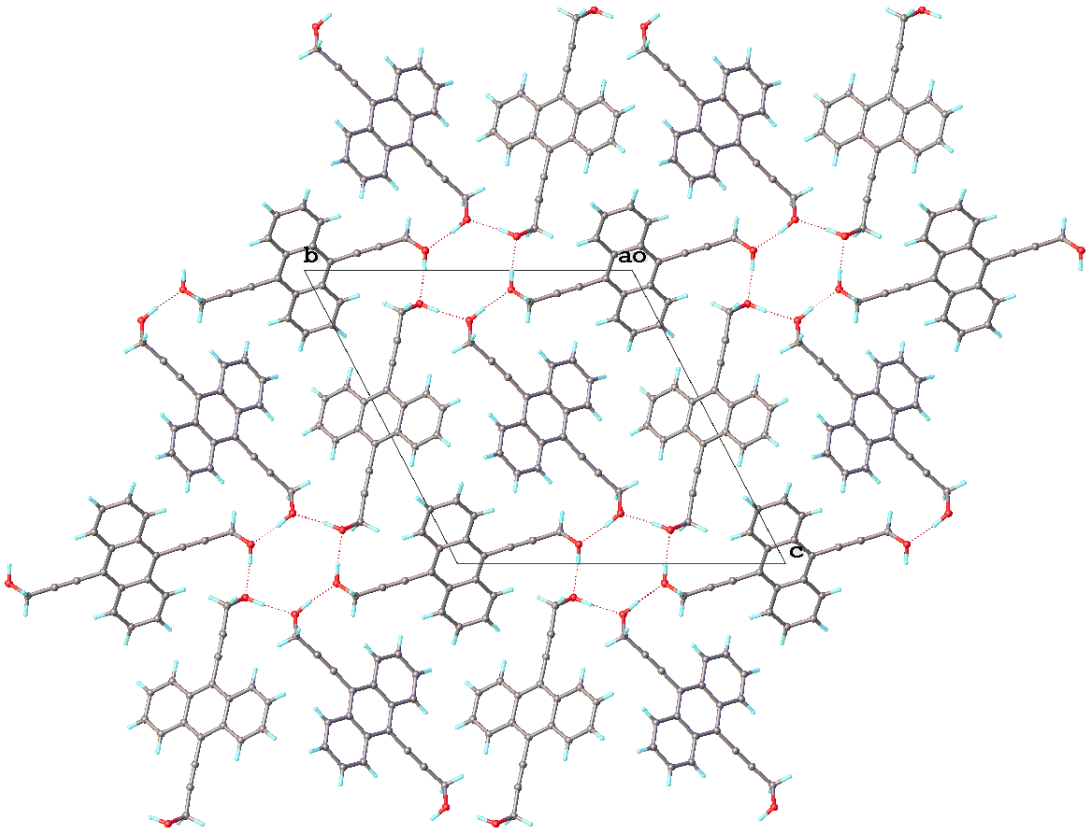

Figure 4.22: Hexamer orientation of compound **46**.

4.22). The packing of the crystal shows the slight rotation of the molecules does not interfere with the other molecules in the plane. Furthermore, the distance between the layers is 4.269 Å and the angle is 102.48°. The distance meets the criteria for topochemical polymerisation, but the angle is too wide (Figure 4.23). Despite the prediction the crystal was still irradiated, using a plasma lamp (white light, 125 Watt). As expected, no change was observed, the irradiated crystals were still soluble in DMSO. Raman spectroscopy showed identical spectra for $t = 0$ min (Figure 4.24 A) and $t = 150$ min (Figure 4.24 B). Furthermore, ASAP and TLC (CH_2Cl_2) did not show any difference compared to the starting material.

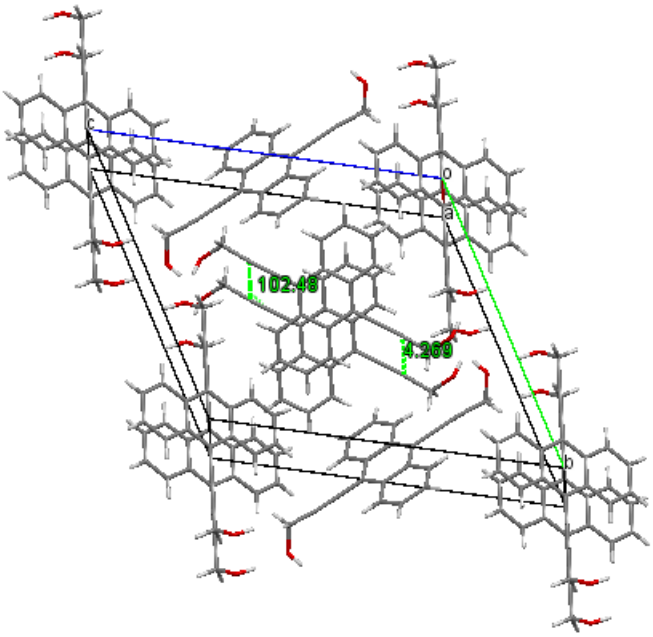

Figure 4.23: Distance and angle between layers **46**.

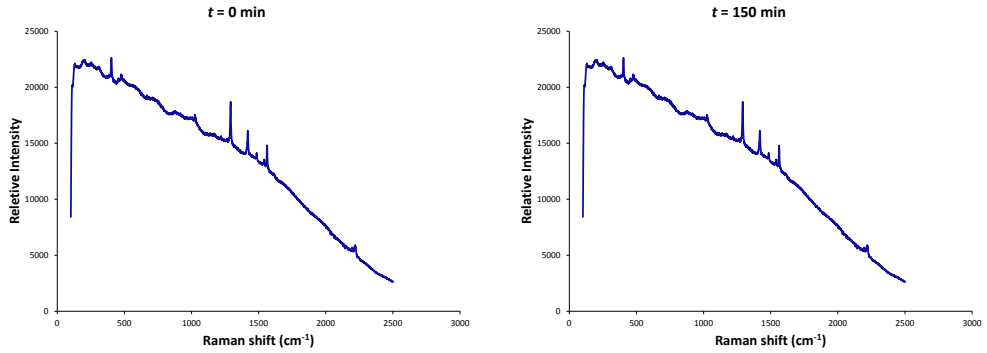

A: Raman spectra compound **46** at $t = 0$ min

B: Raman spectra compound **46** at $t = 150$ min

Figure 4.24: Raman spectra compound **46**, using a laser wavelength of 738 nm.

The dialkyne **48** was also synthesised following a procedure published by Paegle *et al.* using propargylic alcohol (**9**) and 2,5-dibromothiophene (**47**) as starting materials. [278] The Sonogashira coupling resulted in a good yield (80%) of dialkyne **48**. The crystallisation of dialkyne **48** was not successful as the compound became a powder instead of crystals. Different (combinations of) solvents have been used for the cristalisation (e.g. ethyl acetate : *n*-hexane [1:9], MeCN, acetone, DMSO : H_2O [25:1]).

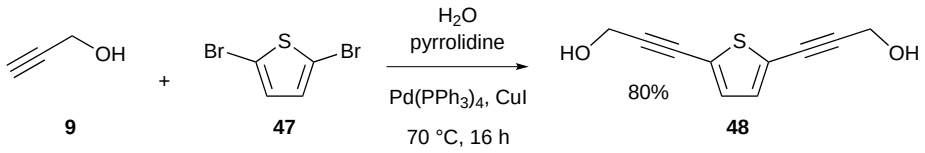

Scheme 4.23: Synthesis dialkyne **48**.

The corresponding oxygen derived compound **51** was synthesised starting from furan (**49**). Furan (**49**) was firstly dibrominated to produce 2,5-dibromofuran (**50**) as a yellow oil in a yield of 56%. This material was determined to be unstable over time. Therefore, the Sonogashira coupling was performed immediately upon its formation. Compound **51** was obtained as an oil in a yield of 46% and shown to decompose to multiple products over time.

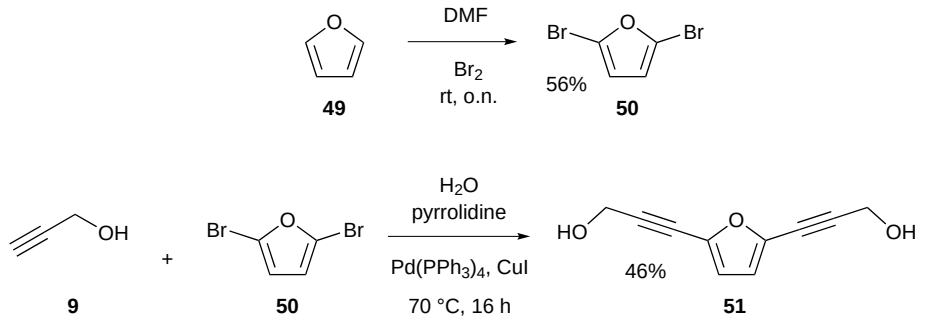

Scheme 4.24: Synthesis dialkyne **51**.

4.6 Conclusion

Free radical polymerisation does not always result in predictable tacticity. Therefore, topochemical polymerisation was aimed for using various substrates as this will always result in predictable tacticity. The synthesis of several different dialkyne compounds was successful accomplished. Unfortunately, topochemical polymerisation was not achieved for all monomers prepared. Although it is known molecules can have crystals with different space groups, this was not achieved for the dialkynes where the crystal did not match the desired criteria. The formation of alternative crystal forms is trial and error as it is hard to predict the outcome. Due to the lack of success with the topochemical polymerisation of the dialkyne systems, no time

was left to research molecules not containing alkyne groups.

Chapter 5

Future perspective

5.1 Polymers in flow

Several aspects of the work reported in this thesis provide opportunities for improvement and further work based upon the knowledge gained. The synthesis of poly(acrylic acid) (**8**) in flow was challenging, especially the analysis of the polymeric samples by GPC. To further verify the outcomes from this project another monomer could be used to perform polymerisations in flow. Preferably the monomer would be water soluble and the polymerisation could be initiated using 2,2'-azobis-(2-methylpropionamidine) dihydrochloride (**4**). Applying these conditions would be closest to the conditions applied to the flow polymerisation of acrylic acid (**7**). A potential example would be the polymerisation of *N*-vinylpyrrolidone (NVP). The advantages of this monomer and resultant polymer are their dual solubility in water and organic polar solvents like DMF. This will make the analysis by GPC much easier compared to acrylic acid. In general aqueous GPC is less stable compared to a GPC analysis based on THF or DMF. It can also easily be distinguished if the polymer is highly cross-linked as this leads to insoluble material.

To examine the potential for formation of poly(vinylpyrrolidone) in flow various flow conditions were investigated (Table 5.1). The experiments show full conversion could be obtained within twenty minutes under flow conditions. Lower residence

times influence the conversion which can be explained by the reactivity. The reactivity of NVP is lower compared to acrylic acid (**7**). The initial experiments show a similar trend with regards to conversion with the full data set described in Chapter 2. Unfortunately, the samples were not analysed by GPC. Therefore, no comments can be made upon obtained molecular weight or dispersity.

Table 5.1: Polymerisation of *N*-vinylpyrrolidone.

Entry	**Technique**	**[NVP] (mM)**	**[I] (mol%)**	***T*** **(°C)**	**Rt (min)**	**Conversion (%)**
1	Batch	0.7	2.50	70	120	100
2	Batch	0.7	1.25	70	120	100
3	Flow	0.7	2.50	70	20	100
4	Flow	0.7	2.50	80	20	100
5	Flow	0.7	2.50	90	20	100
6	Flow	0.7	2.50	70	10	88
7	Flow	0.7	2.50	70	5	79

Furthermore, acrylic acid (**7**) could be used under more controlled radical polymerisation for example using RAFT in the designed flow system. A difficulty which may arise would be the encountering of precipitates which will negatively influence the polymerisation for reasons mentioned earlier.

One of the main disadvantages of controlled radical polymerisation is that in general the reduction in molecular weight compared to uncontrolled polymerisation. If polymers with a high molecular weight are required, uncontrolled free radical polymerisation can be used and is therefore an important technique. On the other hand, controlled radical polymerisation will result in lower dispersity of the polymers. As proved in Chapter 2, using flow chemistry did not result in similar dispersity for uncontrolled free radical polymerisation compared to controlled radical polymerisation.

The designed flow set-up is not suitable for co-polymerisation or block co-polymerisation; nonetheless, it is a challenge to perform co-polymerisation or block co-polymerisation in flow. The design of the flow set-up needs to be changed in order to be able to perform co-polymerisation (Figure 5.1) or block co-polymerisation

(Figure 5.2). In addition, the reactivity ratios of the monomers have to be taken into account.

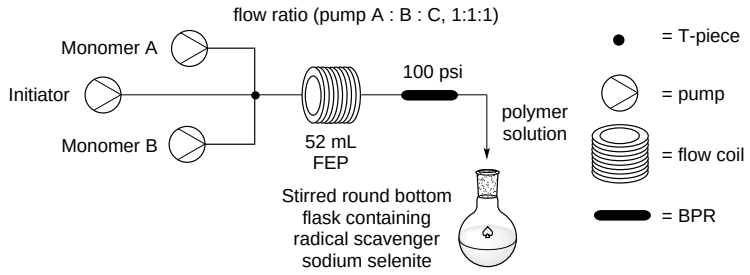

Figure 5.1: Co-polymerisation in flow, mixing of monomers and initiator before reactor.

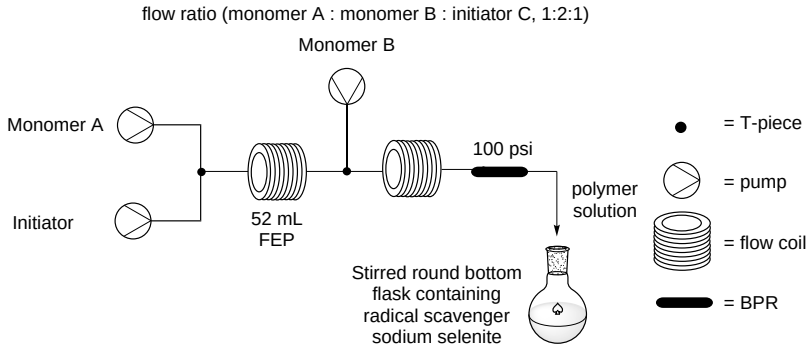

Figure 5.2: Block co-polymerisation in flow, mixing of monomer A and initiator before reactor, and addition of monomer B after first polymerisation.

5.2 Polymer purification

The purification of polymers in flow using ultrafiltration could be further extended. The membrane surface is very important to purify the sample, the time it takes to purify a polymeric sample correlates to membrane surface area and pore dimension. Increasing the surface will shorten the purification time. There is therefore potential to design a membrane which suits the purification purpose better. Currently it is not cost effective to increase the membrane surface to more than 600 cm^2, as the purification is not the time limiting step in the process from monomer to pure polymer if the residence time for the synthesis is larger then 10 min. A decrease in price or a custom designed membrane would be ideal and will open up opportunities to purify polymeric samples obtained with short residence times (< 5 min).

Unfortunately with the equipment available, it was not possible to assemble direct in-line purification and therefore on-line purification was performed. If the membrane(s) used for in-line purification work following the same principle as the Vivaflow 200, the out-let flow of the polymerisation has to be increased otherwise the membrane will not be operating properly. Therefore, extra solvent has to be added during the purification process as applying a back pressure will result in blocking and damage occurring to the membranes due to cluster formation of the polymers. Practical consideration will therefore be the dilution process of the polymeric sample and the size overall of the set-up.

Furthermore, it could be an option to sequentially process a sample using different MWCO membranes. This will help to understand how the polymer is formed and different fractions could be analysed. Also the purification of other monomers is an option. Unfortunately, the current membranes are not compatible with many organic solvents. This possibility could be researched further. For now, future projects will have to stick with polymers soluble in the membrane compatible solvents. For example, poly(vinylpyrrolidone) can be used and purified by ultrafiltration as it is water soluble.

Finally, the purification of other aqueous polymers can be performed. For example the purification of poly(vinylpyrrolidone). To prove this is possible, poly(vinylpyrrolidone) was purified using the same membrane set-up as for acrylic acid (**7**) (Figure 3.7). Poly(vinylpyrrolidone) was synthesised using the conditions mentioned in Table 5.1 entry 7. The residual NVP (21%, 0.15 mM) was reduced to ∼1% within 30 min purification time.

5.3 Crystal polymerisation

Topochemical polymerisation has great potential to become an important technique to determine the tacticity of polymers. The research conducted in this thesis on topochemical polymerisation can be extended. Different alkyne system can be syn-

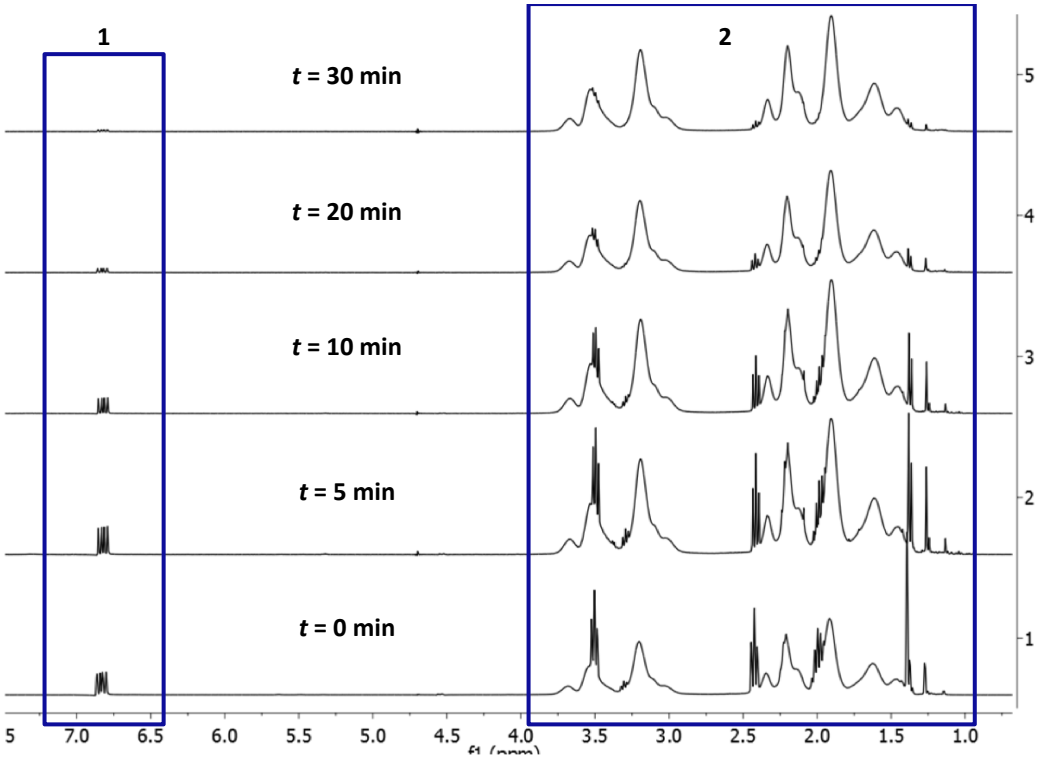

Figure 5.3: ^{1}H NMR spectroscopy of poly(vinylpyrrolidone) purification using the ultrafiltration membrane set-up (Figure 3.7), box 1 is residual NVP and box 2 is residual NVP and poly(vinylpyrrolidone).

thesised. One of the drawbacks is the predictability of the crystal structure. Currently a wide range of compounds have to be made in order to achieve crystals suitable for topochemical polymerisation. A second drawback is that not all monomers are crystalline. This will limit the possibilities for topochemical polymerisation. Further research should therefore be conducted. More alkyne systems have to be synthesised and plenty of opportunities can be found.

To extend the scope of this project, it would be advisable to modify dialkyne **10**. Although compound **41**, **42**, **44** and **46** showed promising results and unexpected crystal structures, none of the compounds were sensitive to topochemical polymerisation. Besides determining if a crystal is suitable for topochemical polymerisation empirically, modelling can be used to predict the crystal structures. Topochemical polymerisations described in literature and the results mentioned in Chapter 4 can be used to develop an algorithm for modelling.

Bibliography

1. Carter, C. F., Lange, H., Ley, S. V., Baxendale, I. R., Wittkamp, B., Goode, J. G. & Gaunt, N. L. ReactIR Flow Cell: A New Analytical Tool for Continuous Flow Chemical Processing. *Organic Process Research & Development* **14,** 393–404 (2010) (cit. on p. 1).

2. Park, J.-S., Park, K.-B., Shin, K.-S., Park, H.-D., Kim, M.-C., Kim, J.-R., Park, S.-J. & Song, Y.-H. Design, fabrication and characterization of an integrated micro ammonia analysis system (IMAAS) with microreactor and in-plane type optical detector based on the Berthelot reaction. *Sensors and Actuators B: Chemical* **117,** 516–522 (2006) (cit. on p. 1).

3. Wensink, H., Benito-Lopez, F., Hermes, D. C., Verboom, W., Gardeniers, H. J. G. E., Reinhoudt, D. N. & van den Berg, A. Measuring reaction kinetics in a lab-on-a-chip by microcoil NMR. *Lab on a Chip* **5,** 280–284 (2005) (cit. on p. 1).

4. Bart, J., Kolkman, A. J., de Vries, A. J. O., Koch, K., Nieuwland, P. J., Janssen, H. J. W. G., van Bentum, J. P. J. M., Ampt, K. A. M., Rutjes, F. P. J. T., Wijmenga, S. S., Gardeniers, H. J. G. E. & Kentgens, A. P. M. A Microfluidic High-Resolution NMR Flow Probe. *Journal of the American Chemical Society* **131,** 5014–5015 (2009) (cit. on p. 1).

5. Holmes, N., Akien, G. R., Savage, R. J. D., Stanetty, C., Baxendale, I. R., Blacker, A. J., Taylor, B. A., Woodward, R. L., Meadows, R. E. & Bourne, R. A. Online quantitative mass spectrometry for the rapid adaptive optimisation

of automated flow reactors. *Reaction Chemistry & Engineering* **1,** 96–100 (2016) (cit. on p. 1).

6. Browne, D. L., Wright, S., Deadman, B. J., Dunnage, S., Baxendale, I. R., Turner, R. M. & Ley, S. V. Continuous flow reaction monitoring using an on-line miniature mass spectrometer. *Rapid Communications in Mass Spectrometry* **26,** 1999–2010 (2012) (cit. on p. 1).

7. McMullen, J. P. & Jensen, K. F. An Automated Microfluidic System for Online Optimization in Chemical Synthesis. *Organic Process Research & Development* **14,** 1169–1176 (2010) (cit. on p. 1).

8. McMullen, J. P. & Jensen, K. F. Integrated Microreactors for Reaction Automation: New Approaches to Reaction Development. *Annual Review of Analytical Chemistry* **3,** 19–42 (2010) (cit. on p. 1).

9. Derboven, P., Steenberge, P. H. M. V., Vandenbergh, J., Reyniers, M.-F., Junkers, T., D'hooge, D. R. & Marin, G. B. Improved Livingness and Control over Branching in RAFT Polymerization of Acrylates: Could Microflow Synthesis Make the Difference? *Macromolecular Rapid Communications* **36,** 2149–2155 (2015) (cit. on p. 2).

10. Zaquen, N., Steenberge, P. H. M. V., D'hooge, D. R., Reyniers, M.-F., Marin, G. B., Vandenbergh, J., Lutsen, L., Vanderzande, D. J. M. & Junkers, T. Improved Mechanistic Insights into Radical Sulfinyl Precursor MDMO-PPV Synthesis by Combining Microflow Technology and Computer Simulations. *Macromolecules* **48,** 8294–8306 (2015) (cit. on p. 2).

11. Haven, J. J., Vandenbergh, J. & Junkers, T. Watching polymers grow: real time monitoring of polymerizations via an on-line ESI-MS/microreactor coupling. *Chemical Communications* **51,** 4611–4614 (2015) (cit. on p. 2).

12. Baxendale, I. R. The integration of flow reactors into synthetic organic chemistry. *Journal of Chemical Technology and Biotechnology* **88,** 519–552 (2013) (cit. on p. 3).

13. Baxendale, I. R., Brocken, L. & Mallia, C. J. Flow chemistry approaches directed at improving chemical synthesis. *Green Processing and Synthesis* **2,** 211–230 (2013) (cit. on p. 3).

14. Hartman, R. L., McMullen, J. P. & Jensen, K. F. Deciding Whether To Go with the Flow: Evaluating the Merits of Flow Reactors for Synthesis. *Angewandte Chemie International Edition* **50,** 7502–7519 (2011) (cit. on p. 3).

15. Serra, C. A. & Chang, Z. Microfluidic-assisted synthesis of polymer particles. *Chemical Engineering and Technology* **31,** 1099–1115 (2008) (cit. on pp. 5, 6).

16. Bally, F., Serra, C. A., Hessel, V. & Hadziioannou, G. Homogeneous polymerization: Benefits brought by microprocess technologies to the synthesis and production of polymers. *Macromolecular Reaction Engineering* **4,** 543–561 (2010) (cit. on pp. 5, 6).

17. Bally, F., Serra, C. A., Hessel, V. & Hadziioannou, G. Micromixer-assisted polymerization processes. *Chemical Engineering Science* **66,** 1449–1462 (2011) (cit. on pp. 5, 6).

18. Tonhauser, C., Natalello, A., Löwe, H. & Frey, H. Microflow Technology in Polymer Synthesis. *Macromolecules* **45,** 9551–9570 (2012) (cit. on p. 5).

19. Chan, N., Cunningham, M. F. & Hutchinson, R. A. Copper-mediated controlled radical polymerization in continuous flow processes: Synergy between polymer reaction engineering and innovative chemistry. *Journal of Polymer Science, Part A: Polymer Chemistry* **51,** 3081–3096 (2013) (cit. on pp. 5, 6).

20. Pauer, W. & Moritz, H.-U. Continuous reactor concepts with superimposed secondary flow - Polymerization process intensification. *Macromolecular Symposia* **243,** 299–308 (2006) (cit. on pp. 5, 6, 50).

21. Salice, P., Fenaroli, D., Filippo, C. C. D., Menna, E., Gasparini, G. & Maggini, M. Efficient functionalization of carbon nanotubes. *chimica oggi/Chemistry Today* **30,** 37–39 (2012) (cit. on p. 5).

22. Yadav, A. K., de la Cal, J. C. & Barandiaran, M. J. Feasibility of Tubular Microreactors for Emulsion Polymerization. *Macromolecular Reaction Engineering* **5,** 69–77 (2011) (cit. on pp. 6, 50).

23. Zargar, A. & Schork, F. J. Design of Copolymer Molecular Architecture via Design of Continuous Reactor Systems for Controlled Radical Polymerization. *Industrial & Engineering Chemistry Research* **48,** 4245–4253 (2009) (cit. on pp. 6, 50, 64).

24. Jullien, M.-C., Ching, M.-J. T. M., Cohen, C., Menetrier, L. & Tabeling, P. Droplet breakup in microfluidic T-junctions at small capillary numbers. *Physics of Fluids* **21,** 72001–72006 (2009) (cit. on p. 6).

25. Minsker, K. S., Zakharov, V. P. & Berlin, A. A. Plug-Flow Tubular Turbulent Reactors: A New Type of Industrial Apparatus. *Theoretical Foundations of Chemical Engineering* **35,** 162–167 (2001) (cit. on pp. 6, 11).

26. Stone, H. A., Stroock, A. D. & Ajdari, A. Engineering flows in small devices. *Annual Review of Fluid Mechanics* **36,** 381–411 (2004) (cit. on pp. 6, 11).

27. Trachsel, F., Günther, A., Khan, S. & Jensen, K. F. Measurement of residence time distribution in microfluidic systems. *Chemical Engineering Science* **60,** 5729 –5737 (2005) (cit. on p. 6).

28. Paquet, D. A. & Ray, W. H. Tubular reactors for emulsion polymerization: I. Experimental investigation. *AIChE Journal* **40,** 73–87 (1994) (cit. on p. 6).

29. Tanaka, M. & Hosogai, K. Suspension polymerization of styrene with circular loop reactor. *Journal of Applied Polymer Science* **39,** 955–966 (1990) (cit. on p. 7).

30. Tanaka, M. & O'Shima, E. Dispersing behaviour of droplets in suspension polymerization of styrene in a loop reactor. *The Canadian Journal of Chemical Engineering* **66,** 29–35 (1988) (cit. on p. 8).

31. Imamura, T., Saito, K., Ishikura, S. & Nomura, M. A new approach to continuous emulsion polymerization. *Polymer International* **30,** 203–206 (1993) (cit. on pp. 9, 10).

32. Couette, M. M. Tudes sur le frottement des liquides. *Annales de Chimie et de Physique* **21,** 433–510 (1890) (cit. on p. 9).

33. Taylor, G. I. Stability of a Viscous Liquid Contained between Two Rotating Cylinders. *Philosophical Transactions of the Royal Society of London A: Mathematical, Physical and Engineering Sciences* **223,** 289–343 (1923) (cit. on p. 9).

34. Coles, D. Transition in circular Couette flow. *Journal of Fluid Mechanics* **21,** 385–425 (1965) (cit. on p. 9).

35. Xue, W., Takahashi, H., Sato, S. & Nomura, M. Continuous emulsion polymerization of styrene in a single Couette-Taylor vortex flow reactor. *Journal of Applied Polymer Science* **80,** 1931–1942 (2001) (cit. on p. 9).

36. Xue, W., Yoshikawa, K., Oshima, A., Sato, S. & Nomura, M. Continuous emulsion polymerization of vinyl acetate. II Operation in a single Couette-Taylor vortex flow reactor using sodium lauryl sulfate as emulsifier. *Journal of Applied Polymer Science* **86,** 2755–2762 (2002) (cit. on p. 10).

37. Danckwerts, P. V. Continuous flow systems: Distribution of residence times. *Chemical Engineering Science* **2,** 1–13 (1953) (cit. on p. 11).

38. Wehner, J. F. & Wilhelm, R. H. Boundary conditions of flow reactor. *Chemical Engineering Science* **6,** 89–93 (1956) (cit. on p. 11).

39. Grabmüller, H. & Schädlich, H.-K. Residence time distribution of plug flow in a finite packed-bed chemical reactor. *Chemical Engineering Science* **38,** 1543–1553 (1983) (cit. on p. 11).

40. Houseworth, J. E. Shear dispersion and residence time for laminar flow in capillary tubes. *Journal of Fluid Mechanics* **142,** 289–308 (1984) (cit. on p. 11).

41. Otsu, T. & Yoshida, M. Role of initiator-transfer agent-terminator (iniferter) in radical polymerizations: Polymer design by organic disulfides as iniferters. *Die Makromolekulare Chemie, Rapid Communications* **3,** 127–132 (1982) (cit. on p. 11).

42. Barbey, R., Lavanant, L., Paripovic, D., Schüwer, N., Sugnaux, C., Tugulu, S. & Klok, H.-A. Polymer Brushes via Surface-Initiated Controlled Radical Polymerization: Synthesis, Characterization, Properties, and Applications. *Chemical Reviews* **109,** 5437–5527 (2009) (cit. on p. 11).

43. Szwarc, M. & Beylen, M. V. *Ionic polymerization and living polymers* (Springer Science & Business Media, 2012) (cit. on p. 11).

44. Braunecker, W. A. & Matyjaszewski, K. Controlled/'living' radical polymerization: Features, developments and perspectives. *Progress in Polymer Science* **32,** 93–146 (2007) (cit. on p. 12).

45. Destarac, M. Controlled Radical Polymerization: Industrial Stakes, Obstacles and Achievements. *Macromolecular Reaction Engineering* **4,** 165–179 (cit. on p. 12).

46. Perrut, M. Supercritical Fluid Applications: Industrial Developments and Economic Issues. *Industrial & Engineering Chemistry Research* **39,** 4531–4535 (2000) (cit. on p. 12).

47. Kang, S. H., Lee, S. G., Jung, W. M., Kim, M. C., Kim, W.-S., Choi, C. K. & Feigelson, R. S. Effect of Taylor vortices on calcium carbonate crystallization by gas-liquid reaction. *Journal of Crystal Growth* **254,** 196–205 (2003) (cit. on p. 12).

48. Georges, M. K., Veregin, R. P. N., Kazmaier, P. M. & Hamer, G. K. Narrow molecular weight resins by a free-radical polymerization process. *Macromolecules* **26,** 2987–2988 (1993) (cit. on p. 12).

49. Chiefari, J., Chong, Y. K. B., Ercole, F., Krstina, J., Jeffery, J., Le, T. P. T., Mayadunne, R. T. A., Meijs, G. F., Moad, C. L., Moad, G., Rizzardo, E. & Thang, S. H. Living Free-Radical Polymerization by Reversible Addition-Fragmentation Chain Transfer: The RAFT Process. *Macromolecules* **31,** 5559–5562 (1998) (cit. on pp. 12, 23, 65).

50. Kato, M., Kamigaito, M., Sawamoto, M. & Higashimura, T. Polymerization of Methyl Methacrylate with the Carbon Tetrachloride/ Dichlorotris-(triphenylphosphine) ruthenium(II)/ Methylaluminum Bis(2,6-di-tert-butylphenoxide) Initiating System: Possibility of Living Radical Polymerization. *Macromolecules* **28,** 1721–1723 (1995) (cit. on pp. 12, 13).

51. Wang, J.-S. & Matyjaszewski, K. Controlled/Living Radical Polymerisation. Halogen Atom Transfer Radical Polymerization Promoted by a Cu(I)/Cu(II) Redox Process. *Macromolecules* **28,** 7901–7910 (1995) (cit. on pp. 12, 13).

52. Wang, J.-S. & Matyjaszewski, K. Controlled/Living radical polymerization. atom transfer radical polymerization in the presence of transition-metal complexes. *Journal of the American Chemical Society* **117,** 5614–5615 (1995) (cit. on pp. 12, 13).

53. Ando, T., Kato, M., Kamigaito, M. & Sawamoto, M. Living Radical Polymerization of Methyl Methacrylate with Ruthenium Complex: Formation of Polymers with Controlled Molecular weights and Very Narrow Distributions. *Macromolecules* **29,** 1070–1072 (1996) (cit. on pp. 12, 13).

54. Jakubowski, W. & Matyjaszewski, K. Activators Regenerated by Electron Transfer for Atom-Transfer Radical Polymerization of (Meth) acrylates and Related Block Copolymers. *Angewandte Chemie* **118,** 4594–4598 (2006) (cit. on p. 12).

55. Matyjaszewski, K., Jakubowski, W., Min, K., Tang, W., Huang, J., Braunecker, W. A. & Tsarevsky, N. V. Diminishing catalyst concentration in atom

transfer radical polymerization with reducing agents. *Proceedings of the National Academy of Sciences* **103,** 15309–15314 (2006) (cit. on pp. 12, 14).

56. Wang, Y., Zhang, Y., Parker, B. & Matyjaszewski, K. ATRP of MMA with ppm Levels of Iron Catalyst. *Macromolecules* **44,** 4022–4025 (2011) (cit. on p. 12).

57. Percec, V., Guliashvili, T., Ladislaw, J. S., Wistrand, A., Stjerndahl, A., Sienkowska, M. J., Monteiro, M. J. & Sahoo, S. Ultrafast Synthesis of Ultrahigh Molar Mass Polymers by Metal-Catalyzed Living Radical Polymerization of Acrylates, Methacrylates, and Vinyl Chloride Mediated by SET at 25 °C. *Journal of the American Chemical Society* **128,** 14156–14165 (2006) (cit. on pp. 12, 13).

58. Ishizu, K. & Kakinuma, H. Synthesis of nanocylinders consisting of graft block copolymers by the photo-induced ATRP technique. *Journal of Polymer Science Part A: Polymer Chemistry* **43,** 63–70 (2005) (cit. on p. 12).

59. Konkolewicz, D., Wang, Y., Zhong, M., Krys, P., Isse, A. A., Gennaro, A. & Matyjaszewski, K. Reversible-Deactivation Radical Polymerization in the Presence of Metallic Copper. A Critical Assessment of the SARA ATRP and SET-LRP Mechanisms. *Macromolecules* **46,** 8749–8772 (2013) (cit. on p. 13).

60. Konkolewicz, D., Wang, Y., Krys, P., Zhong, M., Isse, A. A., Gennaro, A. & Matyjaszewski, K. SARA ATRP or SET-LRP. End of controversy? *Polymer Chemistry* **5,** 4396–4417 (2014) (cit. on p. 13).

61. Pintauer, T. & Matyjaszewski, K. Atom transfer radical addition and polymerization reactions catalyzed by ppm amounts of copper complexes. *Chemical Society Reviews* **37,** 1087–1097 (2008) (cit. on p. 14).

62. Nicolaÿ, R., Kwak, Y. & Matyjaszewski, K. A Green Route to Well-Defined High-Molecular-Weight (Co)polymers Using ARGET ATRP with Alkyl Pseudohalides and Copper Catalysis. *Angewandte Chemie* **122,** 551–554 (2010) (cit. on p. 14).

63. Costa, J. R. C., Mendonça, P. V., Maximiano, P., Serra, A. C., Guliashvili, T. & Coelho, J. F. J. Ambient Temperature "Flash" SARA ATRP of Methyl Acrylate in Water/Ionic Liquid/Glycol Mixtures. *Macromolecules* **48,** 6810–6815 (2015) (cit. on p. 14).

64. Konkolewicz, D., Schröder, K., Buback, J., Bernhard, S. & Matyjaszewski, K. Visible Light and Sunlight Photoinduced ATRP with ppm of Cu Catalyst. *ACS Macro Letters* **1,** 1219–1223 (2012) (cit. on p. 14).

65. Pan, K., Jiang, L., Zhang, J. & Dan, Y. Copper-based reverse ATRP process for the controlled radical polymerization of methyl methacrylate. *Journal of Applied Polymer Science* **105,** 521–526 (2007) (cit. on p. 14).

66. Shen, Y., Zhu, S. & Pelton, R. H. Packed column reactor for continuous atom transfer radical polymerization: Methyl methacrylate polymerization using silica gel supported catalyst. *Macromolecular Rapid Communications* **21,** 956–959 (2000) (cit. on pp. 14, 15).

67. Shen, Y., Zhu, S., Zeng, F. & Pelton, R. H. Atom Transfer Radical Polymerization of Methyl Methacrylate by Silica Gel Supported Copper Bromide/Multidentate Amine. *Macromolecules* **33,** 5427–5431 (2000) (cit. on p. 15).

68. Noda, T., Grice, A. J., Levere, M. E. & Haddleton, D. M. Continuous process for ATRP: Synthesis of homo and block copolymers. *European Polymer Journal* **43,** 2321–2330 (2007) (cit. on p. 15).

69. Zhang, H. & van der Linde, R. Atom transfer radical polymerization of *n*-butyl acrylate catalyzed by CuBr/*N*-(*n*-hexyl)-2-pyridylmethanimine. *Journal of Polymer Science Part A: Polymer Chemistry* **40,** 3549–3561 (2002) (cit. on p. 16).

70. Percec, V., Barboiu, B. & Kim, H.-J. Arenesulfonyl Halides: A Universal Class of Functional Initiators for Metal-Catalyzed "Living" Radical Polymerization

of Styrene(s), Methacrylates, and Acrylates. *Journal of the American Chemical Society* **120,** 305–316 (1998) (cit. on p. 17).

71. Matyjaszewski, K., Wang, J.-L., Grimaud, T. & Shipp, D. A. Controlled/Living Atom Transfer Radical Polymerization of Methyl Methacrylate Using Various Initiation Systems. *Macromolecules* **31,** 1527–1534 (1998) (cit. on p. 17).

72. Shipp, D. A., Wang, J.-L., & Matyjaszewski, K. Synthesis of Acrylate and Methacrylate Block Copolymers Using Atom Transfer Radical Polymerization. *Macromolecules* **31,** 8005–8008 (1998) (cit. on p. 17).

73. Parida, D., Serra, C. A., Garg, D. K., Hoarau, Y., Muller, R. & Bouquey, M. Flow Inversion: An Effective Means to Scale-Up Controlled Radical Polymerization Tubular Microreactors. *Macromolecular Reaction Engineering* **8,** 597–603 (2014) (cit. on pp. 17, 18).

74. Parida, D., Serra, C. A., Garg, D. K., Hoarau, Y., Bally, F., Muller, R. & Bouquey, M. Coil Flow Inversion as a Route To Control Polymerization in Microreactors. *Macromolecules* **47,** 3282–3287 (2014) (cit. on pp. 17, 18).

75. Parida, D., Serra, C. A., Bally, F., Garg, D. K. & Hoarau, Y. Intensifying the ATRP synthesis of statistical copolymers by continuous micromixing flow techniques. *Green Processing and Synthesis* **1,** 525–532 (2012) (cit. on p. 18).

76. Natalello, A., Morsbach, J., Friedel, A., Alkan, A., Tonhauser, C., Müller, A. H. E. & Frey, H. Living Anionic Polymerization in Continuous Flow: Facilitated Synthesis of High-Molecular Weight Poly(2-vinylpyridine) and Polystyrene. *Organic Process Research & Development* **18,** 1408–1412 (2014) (cit. on pp. 19, 30, 31).

77. Burns, J. A., Houben, C., Anastasaki, A., Waldron, C., Lapkin, A. A. & Haddleton, D. M. Poly(acrylates) via SET-LRP in a continuous tubular reactor. *Polymer Chemistry* **4,** 4809–4813 (2013) (cit. on p. 18).

78. Lligadas, G., Rosen, B. M., Bell, C. A., Monteiro, M. J. & Percec, V. Effect of Cu(0) Particle Size on the Kinetics of SET-LRP in DMSO and Cu-Mediated Radical Polymerization in MeCN at 25 °C. *Macromolecules* **41,** 8365–8371 (2008) (cit. on p. 19).

79. Lligadas, G., Rosen, B. M., Monteiro, M. J. & Percec, V. Solvent Choice Differentiates SET-LRP and Cu-Mediated Radical Polymerization with Non-First-Order Kinetics. *Macromolecules* **41,** 8360–8364 (2008) (cit. on p. 19).

80. Chan, N., Cunningham, M. F. & Hutchinson, R. A. Continuous Controlled Radical Polymerization of Methyl Acrylate in a Copper Tubular Reactor. *Macromolecular Rapid Communications* **32,** 604–609 (2011) (cit. on p. 20).

81. Chan, N., Cunningham, M. F. & Hutchinson, R. A. Continuous controlled radical polymerization of methyl acrylate with copper wire in a CSTR. *Polymer Chemistry* **3,** 486497 (2012) (cit. on p. 20).

82. Chan, N., Cunningham, M. F. & Hutchinson, R. A. Copper mediated controlled radical polymerization of methyl acrylate in the presence of ascorbic acid in a continuous tubular reactor. *Polymer Chemistry* **3,** 1322–1333 (2012) (cit. on p. 20).

83. Levere, M. E., Willoughby, I., O'Donohue, S., de Cuendias, A., Grice, A. J., Fidge, C., Becer, C. R. & Haddleton, D. M. Assessment of SET-LRP in DMSO using online monitoring and Rapid GPC. *Polymer Chemistry* **1,** 1086–1094 (2010) (cit. on p. 20).

84. Enright, T. E., Cunningham, M. F. & Keoshkerian, B. Nitroxide-Mediated Polymerization of Styrene in a Continuous Tubular Reactor. *Macromolecular Rapid Communications* **26,** 221–225 (2005) (cit. on p. 21).

85. Rosenfeld, C., Serra, C., Brochon, C. & Hadziioannou, G. High-temperature nitroxide-mediated radical polymerization in a continuous microtube reactor: Towards a better control of the polymerization reaction. *Chemical Engineering Science* **62,** 5245–5250 (2007) (cit. on p. 21).

86. Enright, T. E., Cunningham, M. F. & Keoshkerian, B. Nitroxide-Mediated Bulk and Miniemulsion Polymerization in a Continuous Tubular Reactor: Synthesis of Homo-, Di- and Triblock Copolymers. *Macromolecular Reaction Engineering* **4,** 186–196 (2010) (cit. on pp. 21, 22).

87. Moad, G. RAFT (Reversible addition-fragmentation chain transfer) crosslinking (co)polymerization of multi-olefinic monomers to form polymer networks. *Polymer International* **64,** 15–24 (2015) (cit. on p. 23).

88. Diehl, C., Laurino, P., Azzouz, N. & Seeberger, P. H. Accelerated Continuous Flow RAFT Polymerization. *Macromolecules* **43,** 10311–10314 (2010) (cit. on p. 23).

89. Hornung, C. H., Guerrero-Sanchez, C., Brasholz, M., Saubern, S., Chiefari, J., Moad, G., Rizzardo, E. & Thang, S. H. Controlled RAFT Polymerization in a Continuous Flow Microreactor. *Organic Process Research & Development* **15,** 593–601 (2011) (cit. on pp. 23, 26).

90. Hornung, C. H., Postma, A., Saubern, S. & Chiefari, J. A Continuous Flow Process for the Radical Induced End Group Removal of RAFT Polymers. *Macromolecular Reaction Engineering* **6,** 246–251 (2012) (cit. on p. 26).

91. Hornung, C. H., Nguyen, X., Dumsday, G. & Saubern, S. Integrated Continuous Processing and Flow Characterization of RAFT Polymerization in Tubular Flow Reactors. *Macromolecular Reaction Engineering* **6,** 458–466 (2012) (cit. on p. 26).

92. Hornung, C. H., Nguyen, X., Kyi, S., Chiefari, J. & Saubern, S. Synthesis of RAFT block copolymers in a multi-stage continuous flow process inside a tubular reactor. *Australian Journal of Chemistry* **66,** 192–198 (2013) (cit. on pp. 26, 103).

93. Micic, N., Young, A., Rosselgong, J. & Hornung, C. H. Scale-up of the Reversible Addition-Fragmentation Chain Transfer (RAFT) Polymerization Us-

ing Continuous Flow Processing. *Processes* **2,** 58–70 (2014) (cit. on pp. 26, 27).

94. Hornung, C. H., von Känel, K., Martinez-Botella, I., Espiritu, M., Nguyen, X., Postma, A., Saubern, S., Chiefari, J. & Thang, S. H. Continuous Flow Aminolysis of RAFT Polymers Using Multistep Processing and Inline Analysis. *Macromolecules* **47,** 8203–8213 (2014) (cit. on pp. 26, 36).

95. Hornung, C. H., Postma, A., Saubern, S. & Chiefari, J. Sequential flow process for the controlled polymerisation and thermolysis of RAFT-synthesised polymers. *Polymer* **55,** 1427–1435 (2014) (cit. on p. 26).

96. Vandenbergh, J., de Moraes Ogawa, T. & Junkers, T. Precision synthesis of acrylate multiblock copolymers from consecutive microreactor RAFT polymerizations. *Journal of Polymer Science Part A: Polymer Chemistry* **51,** 2366–2374 (2013) (cit. on p. 28).

97. Qiu, L., Wang, K., Zhu, S., Lu, Y. & Luo, G. Kinetics study of acrylic acid polymerization with a microreactor platform. *Chemical Engineering Journal* **284,** 233–239 (2016) (cit. on p. 29).

98. Cutié, S. S., Smith, P. B., Henton, D. E., Staples, T. L. & Powell, C. Acrylic acid polymerization kinetics. *Journal of Polymer Science Part B: Polymer Physics* **35,** 2029–2047 (1997) (cit. on p. 29).

99. Lorber, N., Pavageau, B. & Mignard, E. Droplet-Based Millifluidics as a New Miniaturized Tool to Investigate Polymerization Reactions. *Macromolecules* **43,** 5524–5529 (2010) (cit. on p. 29).

100. Iwasaki, T. & ichi Yoshida, J. Free Radical Polymerization in Microreactors. Significant Improvement in Molecular Weight Distribution Control. *Macromolecules* **38,** 1159–1163 (2005) (cit. on p. 29).

101. Nyrop, J. L., Soheili, A., Xiang, R., Meng, F., Waldman, J. H., Jia, X., Parmar, R. G., Thuronyi, B. W., Williams, J. M., Dimichele, L., Journet, M., Howell, B. J., Mao, B., Davies, I. W., Colletti, S. L., Sepp-Lorenzino, L. &

Guidry, E. N. Comparison of flow and batch polymerization processes for production of vinyl ether terpolymers for use in the delivery of siRNA. *Journal of Polymer Science, Part A: Polymer Chemistry* **52,** 1119–1129 (2014) (cit. on p. 30).

102. Szwarc, M. 'Living' Polymers. *Nature* **178,** 1168–1169 (1956) (cit. on p. 30).

103. Geacintov, C., Smid, J. & Szwarc, M. Kinetics of Anionic Polymerization of Styrene in Tetrahydrofuran. *Journal of the American Chemical Society* **84,** 2508–2514 (1962) (cit. on p. 30).

104. Bhattacharyya, D. N., Lee, C. L., Smid, J. & Szwarc, M. Reactivities and Conductivities of Ions and Ion Pairs in Polymerization Processes. *The Journal of Physical Chemistry* **69,** 612–623 (1965) (cit. on p. 30).

105. Hostalka, V. H., Figini, R. V. & Schulz, G. V. Zur anionischen polymerisation des styrols in tetrahydrofuran. *Die Makromolekulare Chemie* **71,** 198–203 (1964) (cit. on p. 30).

106. Von Löhr, G. & Schulz, G. V. Die geschwindigkeitskonstanten für die dissoziation und die assoziation des polystyrolnatriums in tetrahydrofuran (THF). *Die Makromolekulare Chemie* **77,** 240–243 (1964) (cit. on p. 30).

107. Löhr, G., Schmitt, B. J. & Schulz, G. V. Das Strömungsrohr als kontinuierlicher Reaktor zur kinetischen Untersuchung schneller Polymerisationsprozesse. *Zeitschrift für Physikalische Chemie* **78,** 177–198 (1972) (cit. on p. 30).

108. Baeten, E., Verbraeken, B., Hoogenboom, R. & Junkers, T. Continuous poly (2-oxazoline) triblock copolymer synthesis in a microfluidic reactor cascade. *Chemical Communications* **51,** 11701–11704 (2015) (cit. on p. 31).

109. Aoi, K. & Okada, M. Polymerization of oxazolines. *Progress in Polymer Science* **21,** 151–208 (1996) (cit. on p. 32).

110. Kagiya, T., Narisawa, S., Maeda, T. & Fukui, K. Ring-opening polymerization of 2-substituted 2-oxazolines. *Journal of Polymer Science Part B: Polymer Letters* **4,** 441–445 (1966) (cit. on p. 32).

111. Wiesbrock, F., Hoogenboom, R., Leenen, M. A. M., Meier, M. A. R. & Schubert, U. S. Investigation of the Living Cationic Ring-Opening Polymerization of 2-Methyl-, 2-Ethyl-, 2-Nonyl-, and 2-Phenyl-2-oxazoline in a Single-Mode Microwave Reactor. *Macromolecules* **38,** 5025–5034 (2005) (cit. on p. 32).

112. Wiesbrock, F., Hoogenboom, R., Abeln, C. H. & Schubert, U. S. Single-Mode Microwave Ovens as New Reaction Devices: Accelerating the Living Polymerization of 2-Ethyl-2-Oxazoline. *Macromolecular Rapid Communications* **25,** 1895–1899 (2004) (cit. on p. 32).

113. Wiesbrock, F., Hoogenboom, R., Leenen, M., van Nispen, S. F. G. M., van der Loop, M., Abeln, C. H., van den Berg, A. M. J. & Schubert, U. S. Microwave-Assisted Synthesis of a 42-Membered Library of Diblock Copoly(2-oxazoline)s and Chain-Extended Homo Poly(2-oxazoline)s and Their Thermal Characterization. *Macromolecules* **38,** 7957–7966 (2005) (cit. on p. 32).

114. Hoogenboom, R., Fijten, M. W., Paulus, R. M., Thijs, H. M., Hoeppener, S., Kickelbick, G. & Schubert, U. S. Accelerated pressure synthesis and characterization of 2-oxazoline block copolymers. *Polymer* **47,** 75–84 (2006) (cit. on p. 32).

115. Arvanitopoulos, L. D., Greuel, M. P., King, B. M., Shim, A. K. & Harwood, H. J. in *Controlled Radical Polymerization* 316–331 (). <http://pubs.acs.org/doi/abs/10.1021/bk-1998-0685.ch020> (cit. on p. 33).

116. Knowles, J. P., Elliott, L. D. & Booker-Milburn, K. I. Flow photochemistry: Old light through new windows. *Beilstein Journal of Organic Chemistry* **8,** 2025–2052 (2012) (cit. on p. 33).

117. Junkers, T. & Wenn, B. Continuous photoflow synthesis of precision polymers. *Reaction Chemistry & Engineering* **1,** 60–64 (2016) (cit. on p. 33).

118. Wenn, B., Conradi, M., Carreiras, A. D., Haddleton, D. M. & Junkers, T. Photo-induced copper-mediated polymerization of methyl acrylate in continuous flow reactors. *Polymer Chemistry* **5,** 3053–3060 (2014) (cit. on p. 33).

119. Anastasaki, A., Nikolaou, V., Zhang, Q., Burns, J., Samanta, S. R., Waldron, C., Haddleton, A. J., McHale, R., Fox, D., Percec, V., Wilson, P. & Haddleton, D. M. Copper(II)/Tertiary Amine Synergy in Photoinduced Living Radical Polymerization: Accelerated Synthesis of ω-Functional and α,ω-Heterofunctional Poly(acrylates). *Journal of the American Chemical Society* **136,** 1141–1149 (2014) (cit. on p. 34).

120. Kundu, S., Bhangale, A. S., Wallace, W. E., Flynn, K. M., Guttman, C. M., Gross, R. A. & Beers, K. L. Continuous Flow Enzyme-Catalyzed Polymerization in a Microreactor. *Journal of the American Chemical Society* **133,** 6006–6011 (2011) (cit. on p. 36).

121. Yamada, M., Nakashima, M. & Seki, M. Pinched Flow Fractionation: Continuous Size Separation of Particles Utilizing a Laminar Flow Profile in a Pinched Microchannel. *Analytical Chemistry* **76,** 5465–5471 (2004) (cit. on p. 36).

122. Haven, J. J., Vandenbergh, J. & Junkers, T. Watching polymers grow: real time monitoring of polymerizations via an on-line ESI-MS/microreactor coupling. *Chemical Communications* **51,** 4611–4614 (2015) (cit. on p. 37).

123. Kumacheva, E. & Garstecki, P. *Microfluidic Reactors for Polymer Particles* 7–15, 22–145. <http://dx.doi.org/10.1002/9780470979228> (John Wiley & Sons, Ltd, 2011) (cit. on p. 38).

124. Kumari, A., Yadav, S. K. & Yadav, S. C. Biodegradable polymeric nanoparticles based drug delivery systems. *Colloids and Surfaces B: Biointerfaces* **75,** 1–18 (2010) (cit. on p. 38).

125. Reis, R. L. & Cohn, D. *Polymer Based Systems on Tissue Engineering, Replacement and Regeneration* 1–426. doi:10.1007/978-94-010-0305-6 (2002) (cit. on p. 38).

126. Silvestre, C., Duraccio, D. & Cimmino, S. Food packaging based on polymer nanomaterials. *Progress in Polymer Science* **36,** 1766–1782 (2011) (cit. on p. 38).

127. Srivastava, S., Schaefer, J. L., Yang, Z., Tu, Z. & Archer, L. A. 25th Anniversary Article: Polymer-Particle Composites: Phase Stability and Applications in Electrochemical Energy Storage. *Advanced Materials* **26,** 201–234 (2014) (cit. on p. 38).

128. Meier, W. Polymer nanocapsules. *Chemical Society Reviews* **29,** 295–303 (2000) (cit. on p. 38).

129. Yow, H. N. & Routh, A. F. Formation of liquid core-polymer shell microcapsules. *Soft Matter* **2,** 940–949 (2006) (cit. on p. 38).

130. Balazs, A. C., Emrick, T. & Russell, T. P. Nanoparticle Polymer Composites: Where Two Small Worlds Meet. *Science* **314,** 1107–1110 (2006) (cit. on p. 38).

131. Loxley, A. & Vincent, B. Preparation of Poly(methylmethacrylate) Microcapsules with Liquid Cores. *Journal of Colloid and Interface Science* **208,** 49–62 (1998) (cit. on p. 38).

132. Dowding, P. J., Atkin, R., Vincent, B., & Bouillot, P. Oil Core-Polymer Shell Microcapsules Prepared by Internal Phase Separation from Emulsion Droplets. I. Characterization and Release Rates for Microcapsules with Polystyrene Shells. *Langmuir* **20,** 11374–11379 (2004) (cit. on p. 38).

133. Peyratout, C. S. & Dähne, L. Tailor-Made Polyelectrolyte Microcapsules: From Multilayers to Smart Containers. *Angewandte Chemie International Edition* **43,** 3762–3783 (2004) (cit. on p. 38).

134. Chu, L.-Y., Xie, R., Zhu, J.-H., Chen, W.-M., Yamaguchi, T. & ichi Nakao, S. Study of SPG membrane emulsification processes for the preparation of monodisperse core-shell microcapsules. *Journal of Colloid and Interface Science* **265,** 187–196 (2003) (cit. on p. 38).

135. Ma, G. H., Su, Z. G., Omi, S., Sundberg, D. & Stubbs, J. Microencapsulation of oil with poly(styrene-N,N-dimethylaminoethyl methacrylate) by SPG emulsification technique: Effects of conversion and composition of oil phase. *Journal of Colloid and Interface Science* **266,** 282–294 (2003) (cit. on p. 38).

136. Liu, R., Ma, G., Meng, F.-T. & Su, Z.-G. Preparation of uniform-sized PLA microcapsules by combining Shirasu Porous Glass membrane emulsification technique and multiple emulsion-solvent evaporation method. *Journal of Controlled Release* **103,** 31 43 (2005) (cit. on p. 38).

137. Seo, M., Nie, Z., Xu, S., Mok, M., Lewis, P. C., Graham, R. & Kumacheva, E. Continuous microfluidic reactors for polymer particles. *Langmuir* **21,** 11614–11622 (2005) (cit. on p. 40).

138. Nie, Z., Xu, S., Seo, M., Lewis, P. C. & Kumacheva, E. Polymer Particles with Various Shapes and Morphologies Produced in Continuous Microfluidic Reactors. *Journal of the American Chemical Society* **127,** 8058–8063 (2005) (cit. on pp. 42, 43).

139. Garstecki, P., Weibel, D., Gitlin, I., Takeuchi, S., Xu, S., Nie, Z., Seo, M., Lewis, P., Kumacheva, E., Stone, H. & Whitesides, G. *Systems and methods of forming particles* US Patent App. 11/368,263. 2007. <`https://www.google.com/patents/US20070054119`> (cit. on p. 42).

140. Kumacheva, E. *Polymer-based nanocomposite materials and methods of production thereof* US Patent 7,033,524. 2006. <`http://www.google.ch/patents/US7033524`> (cit. on p. 42).

141. Kumacheva, E. *Multiple continuous microfluidic reactors for the scaled up synthesis of gel or polymer particles* US Patent App. 12/451,886. 2010. <`https://www.google.ch/patents/US20100184928`> (cit. on p. 42).

142. Braun, D. & Heeger, A. J. Visible light emission from semiconducting polymer diodes. *Applied Physics Letters* **58,** 1982–1984 (1991) (cit. on p. 43).

143. Liang, Y. & Yu, L. A New Class of Semiconducting Polymers for Bulk Heterojunction Solar Cells with Exceptionally High Performance. *Accounts of Chemical Research* **43,** 1227–1236 (2010) (cit. on p. 43).

144. Chouvardas, V., Miliou, A. & Hatalis, M. Tactile displays: Overview and recent advances. *Displays* **29,** 185–194 (2008) (cit. on p. 43).

145. Xu, S., Nie, Z., Seo, M., Lewis, P., Kumacheva, E., Stone, H. A., Garstecki, P., Weibel, D. B., Gitlin, I. & Whitesides, G. M. Generation of Monodisperse Particles by Using Microfluidics: Control over Size, Shape, and Composition. *Angewandte Chemie* **117,** 734–738 (2005) (cit. on p. 43).

146. Bannock, J. H., Krishnadasan, S. H., Nightingale, A. M., Yau, C. P., Khaw, K., Burkitt, D., Halls, J. J. M., Heeney, M. & de Mello, J. C. Continuous Synthesis of Device-Grade Semiconducting Polymers in Droplet-Based Microreactors. *Advanced Functional Materials* **23,** 2123–2129 (2013) (cit. on pp. 43, 44).

147. Iovu, M. C., Sheina, E. E., Gil, R. R. & McCullough, R. D. Experimental Evidence for the Quasi-"Living" Nature of the Grignard Metathesis Method for the Synthesis of Regioregular Poly(3-alkylthiophenes). *Macromolecules* **38,** 8649–8656 (2005) (cit. on p. 44).

148. Achord, B. C. & Rawlins, J. W. Evidence of Ni(0) Complex Diffusion during Grignard Metathesis Polymerization of 2,5-Dibromo-3-hexylthiophene. *Macromolecules* **42,** 8634–8639 (2009) (cit. on p. 44).

149. Köhler, J. M., Kraus, I., Faerber, J. & Serra, C. Continuous-flow preparation of nanoporous metal/polymer composite particles by in situ synthesis of silver nanoparticles in photopolymerized acrylate/diethylene glycol droplets. *Journal of Materials Science* **48,** 2158–2166 (2012) (cit. on p. 45).

150. Visaveliya, N. & Köhler, J. M. Simultaneous size and color tuning of polymer microparticles in a single-step microfluidic synthesis: particles for fluorescence labeling. *Journal of Materials Chemistry C* **3,** 844–853 (2015) (cit. on p. 45).

151. Walton, D. J. & Lorimer, J. P. *Polymers* 1–153. ISBN: 9780198503897 (Oxford university Press, 2000) (cit. on p. 49).

152. Solomon, G. & Moad, D. H. Second Edition, 1–585. <http://www.sciencedirect.com/science/article/pii/B9780080442884500200> (Elsevier Science Ltd, 2005) (cit. on pp. 49, 56).

153. Matyjaszewski, K. in *Controlled Radical Polymerization: Mechanisms* 1–17 (2015). <http://pubs.acs.org/doi/abs/10.1021/bk-2015-1187.ch001> (cit. on p. 49).

154. Yokozawa, T., Ajioka, N. & Yokoyama, A. in, 1–77 (Springer Berlin Heidelberg, 2008). ISBN: 978-3-540-69808-1. <http://dx.doi.org/10.1007/12_2007_125> (cit. on p. 49).

155. Friedrich, J. Mechanisms of Plasma Polymerization - Reviewed from a Chemical Point of View. *Plasma Processes and Polymers* **8,** 783–802 (2011) (cit. on p. 49).

156. Haddleton, D. M. Polymer Chemistry: Rooftop reactions. *Nature Chemistry* **5,** 366–368 (2013) (cit. on p. 49).

157. Staudinger, H. Über Polymerisation. *Berichte der deutschen chemischen Gesellschaft (A and B Series)* **53,** 1073–1085 (1920) (cit. on p. 49).

158. Gross, R. A. & Kalra, B. Biodegradable Polymers for the Environment. *Science* **297,** 803–807 (2002) (cit. on p. 50).

159. Norrish, R. G. W. & Smith, R. R. Catalyzed polymerization of methyl methacrylate in the liquid phase. *Nature* **150,** 336–337 (1942) (cit. on p. 51).

160. Von Trommsdorff, E., Köhle, H. & Lagally, P. Zur polymerisation des methacrylsäuremethylesters1. *Die Makromolekulare Chemie* **1,** 169–198 (1948) (cit. on p. 51).

161. Boutevin, B. in, 69–105 (Springer Berlin Heidelberg, 1990). <http://dx.doi.org/10.1007/BFb0043061> (cit. on p. 51).

162. Corner, T. in, 95–142 (Springer Berlin Heidelberg, 1984). <http://dx.doi.org/10.1007/BFb0024036> (cit. on p. 51).

163. Ashcroft, C. P., Dunn, P. J., Hayler, J. D. & Wells, A. S. Survey of Solvent Usage in Papers Published in Organic Process Research & Development 1997-2012. *Organic Process Research & Development* **19,** 740–747 (2015) (cit. on p. 53).

164. Prat, D., Hayler, J. & Wells, A. A survey of solvent selection guides. *Green Chemistry* **16,** 4546–4551 (2014) (cit. on p. 53).

165. Hanlon, M. C. & Seybert, D. W. The pH Dependence of Lipid Peroxidation Using Water-Soluble Azo Initiators. *Free Radical Biology and Medicine* **23,** 712–719 (1997) (cit. on pp. 53, 64).

166. Grubisic, Z., Rempp, P. & Benoit, H. A universal calibration for gel permeation chromatography. *Journal of Polymer Science Part B: Polymer Letters* **5,** 753–759 (1967) (cit. on p. 58).

167. Balke, S. T., Hamielec, A. E., LeClair, B. P. & Pearce, S. L. Gel Permeation Chromatography. *Industrial & Engineering Chemistry Product Research and Development* **8,** 54–57 (1969) (cit. on p. 58).

168. Striegel, A., Yau, W. W., Kirkland, J. J. & Bly, D. D. *Modern size-exclusion liquid chromatography: practice of gel permeation and gel filtration chromatography* (John Wiley & Sons, 2009) (cit. on p. 58).

169. 18-09-2015. <www.waters.com> (cit. on p. 58).

170. 18-11-2015. <www.malvern.com> (cit. on p. 58).

171. Purcell, E. M., Torrey, H. C. & Pound, R. V. Resonance Absorption by Nuclear Magnetic Moments in a Solid. *Physical Review* **69,** 37–38 (1946) (cit. on p. 60).

172. Bloch, F. Nuclear Induction. *Physical Review* **70,** 460–474 (1946) (cit. on p. 60).

173. Bloch, F., Hansen, W. W. & Packard, M. Nuclear Induction. *Physical Review* **70,** 474–485 (1946) (cit. on p. 60).

174. Spevácek, J., Suchopárek, M. & Al-Alawi, S. Characterization of the stereochemical structure of poly(acrylic acid) by one- and two-dimensional 13C-1H nuclear magnetic resonance spectra. *Polymer* **36,** 4125–4130 (1995) (cit. on p. 63).

175. Hu, Y., Jiang, X., Ding, Y., Ge, H., Yuan, Y. & Yang, C. Synthesis and characterization of chitosan-poly(acrylic acid) nanoparticles. *Biomaterials* **23,** 3193–3201 (2002) (cit. on p. 63).

176. Loiseau, J., Doërr, N., Suau, J. M., Egraz, J. B., Llauro, M. F., Ladavière, C. & Claverie, J. Synthesis and Characterization of Poly(acrylic acid) Produced by RAFT Polymerization. Application as a Very Efficient Dispersant of CaCO3, Kaolin, and TiO2. *Macromolecules* **36,** 3066–3077 (2003) (cit. on pp. 63, 65, 67).

177. Chan, H. W.-. S., Levett, G. & Matthew, J. A. Thermal isomerisation of methyl linoleate hydroperoxides. Evidence of molecular oxygen as a leaving group in a radical rearrangement. *Journal of the Chemical Society, Chemical Communications,* 756–757 (1978) (cit. on p. 63).

178. Porter, N. A., Lehman, L. S., Weber, B. A. & Smith, K. J. Unified mechanism for polyunsaturated fatty acid autoxidation. Competition of peroxy radical hydrogen atom abstraction, β-scission, and cyclization. *Journal of the American Chemical Society* **103,** 6447–6455 (1981) (cit. on p. 63).

179. Maillard, B., Ingold, K. U. & Scaiano, J. C. Rate constants for the reactions of free radicals with oxygen in solution. *Journal of the American Chemical Society* **105,** 5095–5099 (1983) (cit. on p. 63).

180. Ladavière, C., Dörr, N. & Claverie, J. P. Controlled Radical Polymerization of Acrylic Acid in Protic Media. *Macromolecules* **34,** 5370–5372 (2001) (cit. on p. 65).

181. Katchalsky, A. & Eisenberg, H. Molecular weight of polyacrylic and polymethacrylic acid. *Journal of Polymer Science* **6,** 145–154 (1951) (cit. on p. 67).

182. Moulay, S., Boukherissa, M., Abdoune, F. & Benabdelmoumene, F. Z. Low molecular weight poly(acrylic acid) as a salt scaling inhibitor in oilfield operations. *Journal of the Iranian Chemical Society* **2,** 212–219 (2005) (cit. on p. 67).

183. Minari, R. J., Caceres, G., Mandelli, P., Yossen, M. M., Gonzalez-Sierra, M., Vega, J. R. & Gugliotta, L. M. Semibatch Aqueous-Solution Polymerization of Acrylic Acid: Simultaneous Control of Molar Masses and Reaction Temperature. *Macromolecular Reaction Engineering* **5,** 223–231 (2011) (cit. on p. 67).

184. Protocol batch polymerisation Unilever (2012) (cit. on pp. 67, 70–72).

185. Liu, M., an Mao, X., Ye, C., Huang, H., Nicholson, J. K. & Lindon, J. C. Improved WATERGATE Pulse Sequences for Solvent Suppression in NMR Spectroscopy. *Journal of Magnetic Resonance* **132,** 125–129 (1998) (cit. on p. 69).

186. Adams, R. W., Holroyd, C. M., Aguilar, J. A., Nilsson, M. & Morris, G. A. 'Perfecting' WATERGATE: clean proton NMR spectra from aqueous solution. *Chemical Communications* **49,** 358–360 (2013) (cit. on pp. 69, 73).

187. Aguilar, J. A. & Kenwright, S. J. Robust NMR water signal suppression for demanding analytical applications. *Analyst* **141,** 236–242 (2016) (cit. on pp. 69, 73).

188. Brandrup, J. *Polymer handbook* (Wiley New York, 1999) (cit. on p. 70).

189. Cameron, G. G., Davie, F. & Kane, D. R. The thermal degradation of poly(methyl acrylate). IV. Gel formation. *Die Makromolekulare Chemie* **135,** 137–144 (1970) (cit. on p. 73).

190. Castro-Guerrero, C. F., Morales-Cepeda, A., Rivera-Armenta, J., Mendoza-Martínez, A. & Álvarez-Castillo, A. Gels from acrylic acid and hydroxypropyl cellulose via free radical polymerization. *e-Polymers* **8,** 1697–1704 (2013) (cit. on p. 73).

191. Modjarrad, K. & Ebnesajjad, S. *Handbook of polymer applications in medicine and medical devices* 1–353 (Elsevier, 2013) (cit. on p. 102).

192. Ashraf, R. S., Schroeder, B. C., Bronstein, H. A., Huang, Z., Thomas, S., Kline, R. J., Brabec, C. J., Rannou, P., Anthopoulos, T. D., Durrant, J. R. & McCulloch, I. The Influence of Polymer Purification on Photovoltaic Device Performance of a Series of Indacenodithiophene Donor Polymers. *Advanced Materials* **25,** 2029–2034 (2013) (cit. on p. 102).

193. Chen, J. J., Ahmad, A. L. & Ooi, B. S. Thermo-responsive properties of poly(N-isopropylacrylamide-co-acrylic acid) hydrogel and its effect on copper ion removal and fouling of polymer-enhanced ultrafiltration. *Journal of Membrane Science* **469,** 73–79 (2014) (cit. on p. 102).

194. Hassell, D. C. & Bow, E. M. Process Analytical Chemistry for Spectroscopists. *Applied Spectroscopy* **52,** 18A–29A (1998) (cit. on p. 102).

195. Stephan, M., Grosse, S., Stintz, M. & Blankschein, U. Microphotometric inline determination of polymer blend morphologies during extrusion processing. *Journal of Applied Polymer Science* **103,** 258–262 (2007) (cit. on p. 103).

196. Bally, F., Serra, C. A., Brochon, C., Anton, N., Vandamme, T. & Hadzioannou, G. A continuous-flow polymerization microprocess with online GPC and inline polymer recovery by micromixer-assisted nanoprecipitation. *Macromolecular Reaction Engineering* **5,** 542–547 (2011) (cit. on p. 103).

197. Barnes, S. E., Cygan, Z. T., Yates, J. K., Beers, K. L. & Amis, E. J. Raman spectroscopic monitoring of droplet polymerization in a microfluidic device. *Analyst* **131,** 1027–1033 (2006) (cit. on p. 103).

198. Alb, A. M., Drenski, M. F. & Reed, W. F. Automatic continuous online monitoring of polymerization reactions (ACOMP). *Polymer International* **57,** 390–396 (2008) (cit. on p. 103).

199. Neufeld, C. H. H. & Marvel, C. S. The use of dialysis in polymer purification. *Journal of Polymer Science Part A-1: Polymer Chemistry* **4,** 2907–2908 (1966) (cit. on p. 104).

200. Nightingale, M. S., Tsai, S.-C. & Gaylor, J. L. Testicular Sterols VI. Incorporation of mevalonate into squalene and sterols by cell-free preparations of testicular tissue. *Journal of Biological Chemistry* **242,** 341–349 (1967) (cit. on p. 104).

201. Mulder, M. in (eds Howell, J. A., Sanchez, V. & Field, R. W.) 13–54 (Springer Netherlands, 1993). <http://dx.doi.org/10.1007/978-94-011-2156-9_2> (cit. on p. 104).

202. Scopes, R. K. *Protein purification: principles and practice* (Springer Science & Business Media, 2013) (cit. on p. 104).

203. Cipriani, T. R., Mellinger, C. G., de Souza, L. M., Baggio, C. H., Freitas, C. S., Marques, M. C. A., Gorin, P. A. J., Sassaki, G. L. & Iacomini, M. A Polysaccharide from a Tea (Infusion) of Maytenus ilicifolia Leaves with Antiulcer Protective Effects. *Journal of Natural Products* **69,** 1018–1021 (2006) (cit. on p. 104).

204. Peniston, Q. P. & McCarthy, J. L. Lignin. I. Purification of Lignin Sulfonic Acids by Continuous Dialysis. *Journal of the American Chemical Society* **70,** 1324–1328 (1948) (cit. on p. 104).

205. Ghidoni, R., Sonnino, S. & Tettamanti, G. Behavior of gangliosides on dialysis. *Lipids* **13,** 820–822 (1978) (cit. on p. 104).

206. Pitombeira, N. A. O., Neto, J. G. V., Silva, D. A., Feitosa, J. P. A., Paula, H. C. B. & de Paula, R. C. M. Self-assembled nanoparticles of acetylated cashew

gum: Characterization and evaluation as potential drug carrier. *Carbohydrate Polymers* **117,** 610–615 (2015) (cit. on p. 104).

207. Bustamante, J., Navarro, P., Arana, G., de Diego, A. & Madariaga, J. M. Ultrasound assisted dialysis of semi-permeable membrane devices for the simultaneous analysis of a wide number of persistent organic pollutants. *Talanta* **114,** 32–37 (2013) (cit. on p. 104).

208. Fishman, M. L. & Eirich, F. R. Interactions of aqueous poly(N-vinylpyrrolidone) with sodium dodecyl sulfate. I. Equilibrium dialysis measurements. *The Journal of Physical Chemistry* **75,** 3135–3140 (1971) (cit. on p. 104).

209. Millner, S. N. Apparatus for preparation of bacterial extracellular enzymes. *Applied Microbiology* **17,** 639–640 (1969) (cit. on p. 104).

210. Kwon, B., Shon, H. K. & Cho, J. Characterizations of Colloidal Organic Matter Isolated from Surface Water. *Separation Science and Technology* **44,** 3224–3238 (2009) (cit. on p. 105).

211. Song, S., Singh, A. K., Shepodd, T. J. & Kirby, B. J. Microchip Dialysis of Proteins Using in Situ Photopatterned Nanoporous Polymer Membranes. *Analytical Chemistry* **76,** 2367–2373 (2004) (cit. on p. 105).

212. Brinkman, R. & Steinfoorn, J. V. Ultrafiltration and concentration by ultrafiltration by a centrifuge method. *Biochemical Journal* **30,** 1523–1525 (1936) (cit. on p. 106).

213. García-Otero, N., Alonso-Lorenzo, J., del Carmen Barciela-Alonso, M., Bermejo-Barrera, P. & Moreda-Piñeiro, A. Developments on matrix-assisted laser desorption/ionization time-of-flight mass spectrometry for identifying dissolved and particulate proteins in seawater after two-dimensional sodium dodecyl sulfate-polyacrylamide gel electrophoresis. *Microchemical Journal* **122,** 50–56 (2015) (cit. on p. 106).

214. Cho, C.-W., Lee, D.-Y. & Kim, C.-W. Concentration and purification of soluble pectin from mandarin peels using crossflow microfiltration system. *Carbohydrate Polymers* **54,** 21–26 (2003) (cit. on p. 106).

215. Staudinger, H., Ashdown, A. A., Brunner, M., Bruson, H. A. & Wehrli, S. Über hochpolymere Verbindungen. 22. Mitteilung. Über die Konstitution des Poly-indens. *Helvetica Chimica Acta* **12,** 934–957 (1929) (cit. on p. 123).

216. Schildknecht, C. E., Zoss, A. O. & McKinley, C. Vinyl Alkyl Ethers. *Industrial & Engineering Chemistry* **39,** 180–186 (1947) (cit. on p. 123).

217. Schildknecht, C. E., Gross, S. T., Davidson, H. R., Lambert, J. M. & Zoss, A. O. Polyvinyl Isobutyll Ethers. *Industrial & Engineering Chemistry* **40,** 2104–2115 (1948) (cit. on p. 123).

218. Coates, G. W. Precise Control of Polyolefin Stereochemistry Using Single-Site Metal Catalysts. *Chemical Reviews* **100,** 1223–1252 (2000) (cit. on p. 123).

219. Baggett, J. M. & Pruitt, M. E. *Catalysts for the polymerization of olefin oxides* US Patent 2,706,181. 1955. <http://www.google.ch/patents/US2706181> (cit. on p. 123).

220. Baggett, J. M., Bloomfield, R. J., Pruitt, M. E. & Templeton, J. H. *Polymerization of olefin oxides* US Patent 2,706,182. 1955. <https://www.google.ch/patents/US2706182> (cit. on p. 123).

221. Baggett, J. M. & Pruitt, M. E. *Solid polymers of propylene oxide* US Patent 2,706,189. 1955. <https://www.google.ch/patents/US2706189> (cit. on p. 123).

222. Natta, G., Pasquon, I. & Giachetti, E. Kinetik der stereospezifischen Polymerisation des Propylens zu isotaktischen Polymeren. *Angewandte Chemie* **69,** 213–219 (1957) (cit. on pp. 123, 126).

223. Price, C. C. & Osgan, M. The Polymerization of l-Propylene Oxide. *Journal of the American Chemical Society* **78,** 4787–4792 (1956) (cit. on p. 123).

224. Childers, M. I., Longo, J. M., Zee, N. J. V., LaPointe, A. M. & Coates, G. W. Stereoselective Epoxide Polymerization and Copolymerization. *Chemical Reviews* **114,** 8129–8152 (2014) (cit. on p. 123).

225. Zhong, Z., Dijkstra, P. J. & Feijen, J. [(salen)Al]-Mediated, Controlled and Stereoselective Ring-Opening Polymerization of Lactide in Solution and without Solvent: Synthesis of Highly Isotactic Polylactide Stereocopolymers from Racemic d,l-Lactide. *Angewandte Chemie International Edition* **41,** 4510–4513 (2002) (cit. on p. 124).

226. Ziegler, K., Holzkamp, E., Breil, H. & Martin, H. Das Mülheimer Normaldruck-Polyäthylen-Verfahren. *Angewandte Chemie* **67,** 541–547 (1955) (cit. on pp. 125, 126).

227. Crabtree, R. H. Some Structure-Activity Relationships in Homogeneous Transition Metal Catalysts. *Comments on Inorganic Chemistry* **4,** 229–240 (1985) (cit. on p. 125).

228. Rosa, C. D. & Auriemma, F. Structure and physical properties of syndiotactic polypropylene: A highly crystalline thermoplastic elastomer. *Progress in Polymer Science* **31,** 145–237 (2006) (cit. on p. 125).

229. Kaminsky, W. *Polyolefins: 50 years after Ziegler and Natta II* 1–366. doi:10.1007/978-3-642-40805-2 (Springer-Verlag Berlin Heidelberg, 2011) (cit. on p. 125).

230. Ohtaki, H., Deplace, F., Vo, G. D., LaPointe, A. M., Shimizu, F., Sugano, T., Kramer, E. J., Fredrickson, G. H. & Coates, G. W. Allyl-Terminated Polypropylene Macromonomers: A Route to Polyolefin Elastomers with Excellent Elastic Behavior. *Macromolecules* **48,** 7489–7494 (2015) (cit. on p. 125).

231. De Ballesteros, O. R., Rosa, C. D., Auriemma, F., Girolamo, R. D. & Scoti, M. Thermoplastic elastomers from binary blends of syndiotactic polypropylenes with different stereoregularity. *Polymer* **85,** 114–124 (2016) (cit. on p. 125).

232. Natta, G. & Pasquon, I. in, 1–68 (Academic Press, 1959). <http://www.sciencedirect.com/science/article/pii/S0360056408604162> (cit. on p. 126).

233. Cossee, P. Ziegler-Natta catalysis I. Mechanism of polymerization of α-olefins with Ziegler-Natta catalysts. *Journal of Catalysis* **3,** 80–88 (1964) (cit. on p. 127).

234. Ballard, D. G. H. Transition metal alkyl compounds as polymerization catalysts. *Journal of Polymer Science: Polymer Chemistry Edition* **13,** 2191–2212 (1975) (cit. on p. 127).

235. Ivin, K. J., Rooney, J. J. & Stewart, C. D. Ring-opening polymerization of norbornene catalysed by ethyl aluminium dichloride; olefin metathesis in the absence of a transition metal. *Journal of the Chemical Society, Chemical Communications,* 603–604 (14 1978) (cit. on p. 127).

236. Ivin, K. J., Rooney, J. J., Stewart, C. D., Green, M. L. H. & Mahtab, R. Mechanism for the stereospecific polymerization of olefins by Ziegler-Natta catalysts. *Journal of the Chemical Society, Chemical Communications,* 604–606 (14 1978) (cit. on p. 127).

237. Boor, J. in, 32–463 (Academic Press, 1979). <http://www.sciencedirect.com/science/article/pii/B978012115550650024X> (cit. on p. 128).

238. Ewen, J. A. Mechanisms of stereochemical control in propylene polymerizations with soluble Group 4B metallocene/methylalumoxane catalysts. *Journal of the American Chemical Society* **106,** 6355–6364 (1984) (cit. on p. 128).

239. Ewen, J. A., Haspeslach, L., Atwood, J. L. & Zhang, H. Crystal structures and stereospecific propylene polymerizations with chiral hafnium metallocene catalysts. *Journal of the American Chemical Society* **109,** 6544–6545 (1987) (cit. on p. 128).

240. Ewen, J. A., Jones, R. L., Razavi, A. & Ferrara, J. D. Syndiospecific propylene polymerizations with Group IVB metallocenes. *Journal of the American Chemical Society* **110,** 6255–6256 (1988) (cit. on p. 128).

241. Chung, T. C. Synthesis of polyalcohols via Ziegler-Natta polymerization. *Macromolecules* **21,** 865–869 (1988) (cit. on p. 128).

242. Ramakrishnan, S., Berluche, E. & Chung, T. C. Functional group-containing copolymers prepared by Ziegler-Natta process. *Macromolecules* **23,** 378–382 (1990) (cit. on p. 128).

243. Chung, T. C. Polyboranes, their synthesis and applications in functional polyolefins. *Journal of Inorganic and Organometallic Polymers* **1,** 37–51 (1991) (cit. on p. 128).

244. Kesti, M. R., Coates, G. W. & Waymouth, R. M. Homogeneous Ziegler-Natta polymerization of functionalized monomers catalyzed by cationic Group IV metallocenes. *Journal of the American Chemical Society* **114,** 9679–9680 (1992) (cit. on p. 128).

245. Collins, S. & Ward, D. G. Group-transfer polymerization using cationic zirconocene compounds. *Journal of the American Chemical Society* **114,** 5460–5462 (1992) (cit. on p. 128).

246. Yasuda, H., Yamamoto, H., Yokota, K., Miyake, S. & Nakamura, A. Synthesis of monodispersed high molecular weight polymers and isolation of an organolanthanide(III) intermediate coordinated by a penultimate poly(MMA) unit. *Journal of the American Chemical Society* **114,** 4908–4910 (1992) (cit. on p. 128).

247. Corradini, P., Guerra, G. & Cavallo, L. Do New Century Catalysts Unravel the Mechanism of Stereocontrol of Old Ziegler-Natta Catalysts? *Accounts of Chemical Research* **37,** 231–241 (2004) (cit. on p. 128).

248. Sun, Z., Duan, R., Yang, J., Zhang, H., Li, S., Pang, X., Chen, W. & Chen, X. Bimetallic Schiff base complexes for stereoselective polymerisation of racemic-lactide and copolymerisation of racemic-lactide with ε-caprolactone. *RSC Advances* **6,** 17531–17538 (21 2016) (cit. on p. 128).

249. Wegner, G. Topochemische Reaktionen von Monomeren mit konjugierten Dreifachbindungen/Tochemical Reactions of Monomers with conjugated triple Bonds. *Zeitschrift für Naturforschung B* **24,** 824–832 (1969) (cit. on p. 130).

250. Wegner, G. Topochemical reactions of monomers with conjugated triple-bonds. IV. Polymerization of bis-(p-toluene sulfonate) of 2.4-hexadiin-1.6-diol. *Die Makromolekulare Chemie* **145,** 85–94 (1971) (cit. on p. 130).

251. Kaiser, J., Wegner, G. & Fischer, E. W. Topochemical Reactions of Monomers with Conjugated Triple-Bonds VII Mechanism of Transition from Monomer to Polymer Phase During Solid-State Polymerisation. *Israel Journal of Chemistry* **10,** 157–171 (1972) (cit. on pp. 130, 131).

252. Baughman, R. H. Solid-state synthesis of large polymer single crystals. *Journal of Polymer Science: Polymer Physics Edition* **12,** 1511–1535 (1974) (cit. on pp. 130, 136, 137, 224–226).

253. Baughman, R. H. & Yee, K. C. Solid-state polymerization of linear and cyclic acetylenes. *Journal of Polymer Science: Macromolecular Reviews* **13,** 219–239 (1978) (cit. on pp. 130, 226).

254. Enkelmann, V. in, 91–136 (Springer Berlin Heidelberg, 1984). <`http://dx.doi.org/10.1007/BFb0017652`> (cit. on p. 130).

255. Enkelmann, V. & Wegner, G. Crystallographic Analysis of a Topochemical Polymerization. *Angewandte Chemie International Edition in English* **16,** 416–416 (1977) (cit. on p. 131).

256. Kobelt, D. & Paulus, E. F. Poly-[1,2-bis-(*p*-tolylsulfonyloxymethylen)-1-buten-3-inylen]. *Acta Crystallographica Section B* **30,** 232–234 (1974) (cit. on p. 131).

257. Rondeau-Gagné, S., Néabo, J. R., Desroches, M., Larouche, J., Brisson, J. & Morin, J.-F. Topochemical Polymerization of Phenylacetylene Macrocycles: A New Strategy for the Preparation of Organic Nanorods. *Journal of the American Chemical Society* **135,** 110–113 (2013) (cit. on p. 131).

258. Woodward, R. B. & Hoffmann, R. Stereochemistry of Electrocyclic Reactions. *Journal of the American Chemical Society* **87,** 395–397 (1965) (cit. on p. 132).

259. Hoffmann, R. & Woodward, R. B. Selection Rules for Concerted Cycloaddition Reactions. *Journal of the American Chemical Society* **87,** 2046–2048 (1965) (cit. on p. 132).

260. Deschamps, J., Balog, M., Boury, B., Yahia, M. B., Filhol, J.-S., van der Lee, A., Choueiry, A. A., Barisien, T., Legrand, L., Schott, M. & Dutremez, S. G. Tuning Topochemical Polymerization of Diacetylenes: A Joint Synthetic, Structural, Photophysical, and Theoretical Study of a Series of Analogues of a Known Reactive Monomer, 1,6-Bis(diphenylamino)-2,4-hexadiyne (THD). *Chemistry of Materials* **22,** 3961–3982 (2010) (cit. on p. 133).

261. Hoang, T., Lauher, J. W. & Fowler, F. W. The Topochemical 1,6-Polymerization of a Triene. *Journal of the American Chemical Society* **124,** 10656–10657 (2002) (cit. on p. 133).

262. Jover, J., Spuhler, P., Zhao, L., McArdle, C. & Maseras, F. Toward a mechanistic understanding of oxidative homocoupling: the Glaser-Hay reaction. *Catalysis Science & Technology* **4,** 4200–4209 (2014) (cit. on p. 134).

263. Wang, X., Hu, J., Li, Y., Jie, J., Xia, A., Zhu, S., Wang, Y. & Zhang, S. X.-A. Light-Induced Ring-Closing Dynamics of a Hydrogen-Bonded Adduct of Benzo[1,3]oxazine in Protic Solvents. *The Journal of Physical Chemistry C* **120,** 598–605 (2016) (cit. on p. 136).

264. D'alelio, G. F., Meyers, F. R., Strazik, W. F. & Germonprez, R. L. Polymeric Schiff Bases. XVI. Alternative Syntheses for the Iminobenzylidene Polymers.

Journal of Macromolecular Science: Part A - Chemistry **2,** 1333–1351 (1968) (cit. on pp. 136, 138).

265. Xu, R., Gramlich, V. & Frauenrath, H. Alternating Diacetylene Copolymer Utilizing Perfluorophenyl-Phenyl Interactions. *Journal of the American Chemical Society* **128,** 5541–5547 (2006) (cit. on pp. 137, 138, 226).

266. Xu, R., Schweizer, W. B. & Frauenrath, H. Soluble Poly(diacetylene)s Using the Perfluorophenyl-Phenyl Motif as a Supramolecular Synthon. *Journal of the American Chemical Society* **130.** PMID: 18652461, 11437–11445 (2008) (cit. on pp. 140, 229, 230).

267. Chernykh, A., Agag, T. & Ishida, H. Novel benzoxazine monomer containing diacetylene linkage: An approach to benzoxazine thermosets with low polymerization temperature without added initiators or catalysts. *Polymer* **50,** 3153–3157 (2009) (cit. on pp. 142, 232, 233).

268. Morosin, B. & Harrah, L. Two forms of 1,6-diphenoxy-2,4-hexadiyne and the hydrogenated analog, 1,6-diphenoxyhexane. *Acta Crystallographica Section B* **33,** 1760–1764 (1977) (cit. on p. 143).

269. Jones, G. E., Kendrick, D. A. & Holmes, A. B. in *Organic Syntheses* 52–59 (2003). <`http://dx.doi.org/10.1002/0471264180.os065.09`> (cit. on pp. 145, 227).

270. Wipf, P. & Coish, P. D. G. Total Synthesis of (±)-Nisamycin. *The Journal of Organic Chemistry* **64,** 5053–5061 (1999) (cit. on pp. 145, 237).

271. Manley, D. W. & Walton, J. C. A Clean and Selective Radical Homocoupling Employing Carboxylic Acids with Titania Photoredox Catalysis. *Organic Letters* **16,** 5394–5397 (2014) (cit. on pp. 145, 237).

272. Xiao, R., Yao, R. & Cai, M. Practical Oxidative Homo- and Heterocoupling of Terminal Alkynes Catalyzed by Immobilized Copper in MCM-41. *European Journal of Organic Chemistry* **2012,** 4178–4184 (2012) (cit. on p. 146).

273. Jones, S. & Selitsianos, D. A Simple and Effective Method for Phosphoryl Transfer Using TiCl4 Catalysis. *Organic Letters* **4,** 3671–3673 (2002) (cit. on pp. 146, 239, 240).

274. Jones, S., Selitsianos, D., Thompson, K. J. & Toms, S. M. An Improved Method for Lewis Acid Catalyzed Phosphoryl Transfer with Ti(t-BuO)4. *The Journal of Organic Chemistry* **68,** 5211–5216 (2003) (cit. on pp. 146, 239, 240).

275. Eisenblaetter, J., Bruns, M., Fehrenbacher, U., Barner, L. & Barner-Kowollik, C. Synthesis of polymers with phosphorus containing side chains via modular conjugation. *Polymer Chemistry* **4,** 2406–2413 (2013) (cit. on pp. 146, 239, 240).

276. Maezaki, N., Furusawa, A., Hirose, Y., Uchida, S. & Tanaka, T. 3-Phosphono-2-(N-cyanoimino)thiazolidine derivatives, new phosphorylating agents for alcohols. *Tetrahedron* **58,** 3493–3498 (2002) (cit. on pp. 146, 239, 240).

277. Werner, C., Hopf, H., Dix, I., Bubenitschek, P. & Jones, P. 1,x-Elimination Reactions: Extending the Limits of a Classical Organic Reaction. *Chemistry - A European Journal* **13,** 9462–9477 (2007) (cit. on pp. 148, 241).

278. Paegle, E., Belyakov, S., Petrova, M., Liepinsh, E. & Arsenyan, P. Cyclization of Diaryl(hetaryl)alkynes under Selenobromination Conditions: Regioselectivity and Mechanistic Studies. *European Journal of Organic Chemistry* **2015,** 4389–4399 (2015) (cit. on pp. 151, 155, 249, 251).

279. Fulmer, G. R., Miller, A. J. M., Sherden, N. H., Gottlieb, H. E., Nudelman, A., Stoltz, B. M., Bercaw, J. E. & Goldberg, K. I. NMR Chemical Shifts of Trace Impurities: Common Laboratory Solvents, Organics, and Gases in Deuterated Solvents Relevant to the Organometallic Chemist. *Organometallics* **29,** 2176–2179 (2010) (cit. on pp. 198, 211, 222).

280. Coulson, D. R., Satek, L. C. & Grim, S. O. Tetrakis(triphenylphosphine)palladium(0). *Inorganic Syntheses,* 121–124 (2007) (cit. on p. 223).

281. Wang, X., Whitten, J. E. & Sandman, D. J. Ultraviolet photoelectron spectroscopy study of the thermochromic phase transition in urethane-substituted polydiacetylenes. *The Journal of Chemical Physics* **126,** 184905 (2007) (cit. on p. 224).

282. Rougeau, L., Picq, D., Rastello, M. & Frantz, Y. New irreversible thermochromic polydiacetylenes. *Tetrahedron* **64,** 9430–9436 (2008) (cit. on p. 228).

283. Mo, J., Eom, D., Lee, E. & Lee, P. H. Hybrid System of Metal/Brønsted Acid Relay Catalysis for the Intramolecular Double Hydroarylation and Cationic Cyclization of Diyne Diethers and Diamines. *Organic Letters* **14,** 3684–3687 (2012) (cit. on p. 234).

284. Fan, X., Li, N., Shen, T., Cui, X.-M., Lv, H., Zhu, H.-B. & Guan, Y.-H. A mild CuI-catalyzed Glaser-type homo-coupling reaction using α,α-dibromo-β-dicarbonyl compounds as oxidants. *Tetrahedron* **70,** 256–261 (2014) (cit. on p. 235).

285. Lei, A., Srivastava, M. & Zhang, X. Transmetalation of Palladium Enolate and Its Application in Palladium-Catalyzed Homocoupling of Alkynes: A Room-Temperature, Highly Efficient Route To Make Diynes. *The Journal of Organic Chemistry* **67,** 1969–1971 (2002) (cit. on p. 236).

286. Barak, A. H., de Ruiter, G., Lahav, M., Sharma, S., Gidron, O., Evmenenko, G., Dutta, P., Bendikov, M. & van der Boom, M. E. Coordination-Based Molecular Assemblies of Oligofurans and Oligothiophenes. *Chemistry - A European Journal* **19,** 8821–8831 (2013) (cit. on p. 250).

Experimental information 1

Experimental Information Chapter 2

Equipment and solvents

Analysis equipment

Unless otherwise stated, ^{1}H NMR spectra were recorded at 296.5 K and were calibrated to the residual solvent according to the literature. [279] The spectra were recorded on either a Bruker-Avance 400, Varian VNMRS-600 or Varian VNMRS 9.4 Tesla magnet (400 MHz) spectrometer.

Unless otherwise stated, GPC spectra were recorded at 323.15 K. The spectra were recorded at a Viscotek GPC max 2001 triple-detection purchased from Malvern using an aqueous solution (0.05 M $NaNO_3$, 2.81 mM NaOH and MeOH (ratio 4:1)) as solvent.

Solvents

Deionised water was obtained *via* a PURELAB 3000 Series system from ELGA LabWater.

Deuterated solvents for NMR analysis were purchased from Apollo Scientific.

Flow system

The flow system used was a FlowSyn system containing PEEK T-pieces, a 52 mL FEP tubular coil (1.64 m x 1/8" OD Tubing) and an upchurch 100 psi back pressure

regulator all purchased from Uniqsis Ltd (http://www.uniqsis.com/paProducts.aspx).

Materials

Acrylic acid (**7**) (Alfa Aesar, 99%), 2,2'-azobis(2-methylpropionamidine) dihydrochloride (**4**) (Sigma Aldrich, 97%), sodium selenite (Alfa Aesar, 98%), 4,4'-azobis(4-cyanovaleric acid) (**3**) (Sigma Aldrich, 75 %), 1,2-dimethoxyethane (DME, Alfa Aesar, 99% stabilized with BHT) and deionised water were used without further purification.

Batch procedure

A 100 mL flask was loaded with acrylic acid (**7**) (2.5 g, 34.7 mmol, 2.38 mL) and 40 mL deionised water was added. The solution was degassed by sonification, bubbling nitrogen through and sonification for a second time, each step was performed for twenty minutes. The solution was kept at room temperature and 2,2'-azobis(2-methylpropionamidine) dihydrochloride (**4**) (96.8 mg, 0.36 mmol) was added. The mixture was sonificated for ten minutes and then heated at 70 °C for up to four hours.

Results

Table containing data used in Chapter 2, Figure 2.16 and described the output for the parameters, given in Table 2.3, and the output (conversion, molecular weight and dispersity) for the polymerisation in flow of acrylic acid (**7**) is shown in column 6 to 8. In these graphs only the data obtained using 60 °C is plotted.

Entry	[acrylic acid] (mM)	[Initiator] (mol%)	Temperature (°C)	Residence time (min)	Conversion (%)$^{1H\ NMR}$	Molecular weight (g mol^{-1})	Dispersity
1	0.4	1.25	60	20	58		
2	0.4	1.25	60	10	31	263,000	1.51
3	0.4	2.5	60	20	89	435,000	1.50
4	0.4	2.5	60	10	51	377,000	1.18
5	0.4	3.75	60	20	92	353,000	1.29
6	0.4	3.75	60	10	73	292,000	1.20
7	0.7	1.25	60	20	6	855,000	1.35
8	0.7	1.25	60	10	32		
9	0.7	2.5	60	20	60		
10	0.7	2.5	60	10	48	670,000	1.11
11	0.7	3.75	60	20	82	423,000	1.27

Continued on next page

Continued from previous page

Entry	[acrylic acid] (mM)	[Initiator] (mol%)	Temperature (°C)	Residence time (min)	Conversion (%)^{1}H NMR	Molecular weight (g mol^{-1})	Dispersity
12	0.7	3.75	60	10	84	401,000	1.19
13	1.0	1.25	60	20	16	65,000	5.32
14	1.0	1.25	60	10	17		
15	1.0	2.5	60	20	58	220,000	1.63
16	1.0	2.5	60	10	63	850,000	1.11
17	1.0	3.75	60	20	85	720,000	1.22
18	1.0	3.75	60	10	66	594,000	1.11

Table containing data used in Chapter 2, 70 °C, 80 °C and 90 °C. Table containing data used in Chapter 2, Figures 2.17, 2.18 to 2.21 and described the output for the parameters given in Table 2.3. The output (conversion, molecular weight and dispersity) for the polymerisation in flow of acrylic acid (**7**) is shown in column 6 to 8.

Entry	**[acrylic acid] (mM)**	**[Initiator] (mol%)**	**Temperature (°C)**	**Residence time (min)**	**Conversion (%)$^{1H\ NMR}$**	**Molecular weight (g mol^{-1})**	**Dispersity**
1	0.4	1.25	70	30	80	231,000	1.57
2	0.4	1.25	80	30	93	129,000	2.19
3	0.4	1.25	90	30	96	67,000	2.17
4	0.4	1.25	70	20	81	182,000	1.73
5	0.4	1.25	80	20	91	78,000	2.35
6	0.4	1.25	90	20	92	60,000	3.25
7	0.4	1.25	70	10	77	269,000	1.50
8	0.4	1.25	80	10	78	112,000	1.89
9	0.4	1.25	90	10	90	63,000	2.51
10	0.4	1.25	70	5	32	212,000	1.45
11	0.4	1.25	80	5	66	134,000	1.35

Continued on next page

Continued from previous page

Entry	[acrylic acid] (mM)	[Initiator] (mol%)	Temperature (°C)	Residence time (min)	Conversion (%)$^{1H\ NMR}$	Molecular weight (g mol^{-1})	Dispersity
12	0.4	1.25	90	5	82	48,000	1.58
13	0.4	2.5	70	30	95	157,000	2.08
14	0.4	2.5	80	30	97	69,000	2.60
15	0.4	2.5	90	30	99	33,000	2.11
16	0.4	2.5	70	20	94	193,000	2.54
17	0.4	2.5	80	20	97	73,000	2.93
18	0.4	2.5	90	20	98	56,000	3.10
19	0.4	2.5	70	10	87	214,000	1.79
20	0.4	2.5	80	10	92	75,000	1.97
21	0.4	2.5	90	10	95	44,000	2.74
22	0.4	2.5	70	5	59	248,000	1.14
23	0.4	2.5	80	5	78	55,000	1.43
24	0.4	2.5	90	5	89	29,000	1.58

Continued on next page

Continued from previous page

Entry	[acrylic acid] (mM)	[Initiator] (mol%)	Temperature (°C)	Residence time (min)	Conversion (%)$^{1H\ NMR}$	Molecular weight (g mol^{-1})	Dispersity
25	0.4	3.75	70	30	93	115,000	2.38
26	0.4	3.75	80	30	98	58,000	2.81
27	0.4	3.75	90	30	99	29,000	2.12
28	0.4	3.75	70	20	93	146,000	2.17
29	0.4	3.75	80	20	97	61,000	2.75
30	0.4	3.75	90	20	98	38,000	3.29
31	0.4	3.75	70	10	97	105,000	1.80
32	0.4	3.75	80	10	99	139,000	1.82
33	0.4	3.75	90	10	97	35,000	2.98
34	0.4	3.75	70	5	89	231,000	1.25
35	0.4	3.75	80	5	94	61,000	1.44
36	0.4	3.75	90	5	95	31,000	1.49
37	0.7	1.25	70	30	89	490,000	1.69

Continued on next page

Continued from previous page

Entry	[acrylic acid] (mM)	[Initiator] (mol%)	Temperature (°C)	Residence time (min)	Conversion (%)^{1}H NMR	Molecular weight (g mol^{-1})	Dispersity
38	0.7	1.25	80	30	95	212,000	3.14
39	0.7	1.25	90	30	98	112,000	3.29
40	0.7	1.25	70	20	82	404,000	1.40
41	0.7	1.25	80	20	93	201,000	2.47
42	0.7	1.25	90	20	96	105,000	3.21
43	0.7	1.25	70	10	70	357,000	1.24
44	0.7	1.25	80	10	87	160,000	1.60
45	0.7	1.25	90	10	93	91,000	2.76
46	0.7	1.25	70	5	80	156,000	2.02
47	0.7	1.25	80	5	88	80,000	2.05
48	0.7	1.25	90	5	90	52,000	2.10
49	0.7	2.5	70	30	93	275,000	2.39
50	0.7	2.5	80	30	98	156,000	4.09

Continued on next page

Continued from previous page

Entry	[acrylic acid] (mM)	[Initiator] (mol%)	Temperature (°C)	Residence time (min)	Conversion (%)^{1}H NMR	Molecular weight (g mol^{-1})	Dispersity
51	0.7	2.5	90	30	99	88,000	4.00
52	0.7	2.5	70	20	91	113,000	1.64
53	0.7	2.5	80	20	96	143,000	3.35
54	0.7	2.5	90	20	98	67,000	3.67
55	0.7	2.5	70	10	85	291,000	1.51
56	0.7	2.5	80	10	91	151,000	2.46
57	0.7	2.5	90	10	96	71,000	2.81
58	0.7	2.5	70	5	65	366,000	1.29
59	0.7	2.5	80	5	85	169,000	2.00
60	0.7	2.5	90	5	92	79,000	2.34
61	0.7	3.75	70	30	95	267,000	2.79
62	0.7	3.75	80	30	99	130,000	3.41
63	0.7	3.75	90	30	100	87,000	3.33

Continued on next page

Continued from previous page

Entry	[acrylic acid] (mM)	[Initiator] (mol%)	Temperature (°C)	Residence time (min)	Conversion (%)^{1}H NMR	Molecular weight (g mol^{-1})	Dispersity
64	0.7	3.75	70	20	96	220,000	2.41
65	0.7	3.75	80	20	98	124,000	4.04
66	0.7	3.75	90	20	99	79,000	5.68
67	0.7	3.75	70	10	90	189,000	1.52
68	0.7	3.75	80	10	95	135,000	2.79
69	0.7	3.75	90	10	98	32,000	3.60
70	0.7	3.75	70	5	77	333,000	1.40
71	0.7	3.75	80	5	88	140,000	1.95
72	0.7	3.75	90	5	94	68,000	2.37
73	1.0	1.25	70	30	88	540,000	1.52
74	1.0	1.25	80	30	96	292,000	3.14
75	1.0	1.25	90	30	98	169,000	3.04
76	1.0	1.25	70	20	76	460,000	1.20

Continued on next page

Continued from previous page

Entry	[acrylic acid] (mM)	[Initiator] (mol%)	Temperature (°C)	Residence time (min)	Conversion (%)^{1}H NMR	Molecular weight (g mol^{-1})	Dispersity
77	1.0	1.25	80	20	93	260,000	1.88
78	1.0	1.25	90	20	97	142,000	2.31
79	1.0	1.25	70	10	71	428,000	1.25
80	1.0	1.25	80	10	82	455,000	1.23
81	1.0	1.25	90	10	90	276,000	1.89
82	1.0	1.25	70	5	52	329,000	1.42
83	1.0	1.25	80	5	77	256,000	1.77
84	1.0	1.25	90	5	86	134,000	2.91
85	1.0	2.5	70	30	93	411,000	2.11
86	1.0	2.5	80	30	98	302,000	3.72
87	1.0	2.5	90	30	99	149,000	3.82
88	1.0	2.5	70	20	91	367,000	1.48
89	1.0	2.5	80	20	97	246,000	3.52

Continued on next page

Continued from previous page

Entry	[acrylic acid] (mM)	[Initiator] (mol%)	Temperature (°C)	Residence time (min)	Conversion (%)^{1}H NMR	Molecular weight (g mol^{-1})	Dispersity
90	1.0	2.5	90	20	99	150,000	5.03
91	1.0	2.5	70	10	86	384,000	1.47
92	1.0	2.5	80	10	94	152,000	2.68
93	1.0	2.5	90	10	97	97,000	3.47
94	1.0	2.5	70	5	75	384,000	1.38
95	1.0	2.5	80	5	87	161,000	2.43
96	1.0	2.5	90	5	93	113,000	3.89
97	1.0	3.75	70	30	97	379,000	2.11
98	1.0	3.75	80	30	99	232,000	3.49
99	1.0	3.75	90	30	100	150,000	3.69
100	1.0	3.75	70	20	95	315,000	1.82
101	1.0	3.75	80	20	98	168,000	4.34
102	1.0	3.75	90	20	99	115,000	5.74

Continued on next page

Continued from previous page

Entry	[acrylic acid] (mM)	[Initiator] (mol%)	Temperature (°C)	Residence time (min)	Conversion (%)^{1}H NMR	Molecular weight (g mol^{-1})	Dispersity
103	1.0	3.75	70	10	90	244,000	1.64
104	1.0	3.75	80	10	96	115,000	2.60
105	1.0	3.75	90	10	98	67,000	3.58
106	1.0	3.75	70	5	80	227,000	1.97
107	1.0	3.75	80	5	90	126,000	2.98
108	1.0	3.75	90	5	95	95,000	4.08

Experimental information 2

Experimental Information Chapter 3

Equipment and solvents

Analysis equipment

Unless otherwise stated, ^{1}H NMR spectra were recorded at 296.5 K and were calibrated to the residual solvent according to the literature. [279] The spectra were recorded on either a Bruker-Avance 400 or Varian VNMRS-600 spectrometer.

Solvents

Deionised water was obtained *via* a PURELAB 3000 Series system from ELGA LabWater.

Deuterated solvents for NMR analysis were purchased from Apollo Scientific.

Flow system

he flow system used was a FlowSyn system containing PEEK T-pieces, a 52 mL FEP tubular coil (1.64 m x 1/8" OD Tubing) and an upchurch 100 psi back pressure regulator all purchased from Uniqsis Ltd (http://www.uniqsis.com/paProducts.aspx).

Purification was performed using one, two or three Vivaflow 200 membranes with a MWCO of 2000 Da and a masterflex economy drive variable speed peristaltic pump purchased from Sartorius Stedim Biotech (https://www.sartorius.com/en/product-family/product-family-detail/m-vivaflow-200/).

Analysis

The residual acrylic acid (**7**) concentration was determined by ^{1}H NMR using dimethoxyethane as internal standard which was used to calculate the initial residual acrylic acid (**7**). The assumption was made the amount of polymer stayed the same in the sample. Therefore, the integral of the peaks corresponding to poly(acrylic acid) (**8**) can be used in combination with the integral of acrylic acid (**7**) peaks to calculate the corresponding residual acrylic acid (**7**) percentage.

For example, the initial (t = 0 min, entry 1) residual acrylic acid (**7**) percentage in the first table is 28.86%. This follows from dividing the integral of acrylic acid (**7**) (3.16) by the total integral of the peaks (3.16 + 7.79 = 10.95). Multiply this by 100% and the result is the residual acrylic acid (**7**) percentage (28.86%).

Influence of flow design

The following data is used in Figure 3.4

Table: Influence of flow design membranes in series.

Time (min)	**∫ acrylic acid**	**∫ polymer**	**∫ total**	**res. acrylic acid (%)**
0	3.16	7.79	10.95	28.86
10	3.15	18.95	22.10	14.25
20	3.13	54.43	57.56	5.44
40	3.05	537.23	540.28	0.56
60	0.00	2.66	2.66	0.00

Table: Influence of flow design membranes in parallel/ series separate outlet.

Time (min)	∫ acrylic acid	∫ polymer	∫ total	res. acrylic acid (%)
0	3.14	7.43	10.57	29.71
10	3.12	15.08	18.20	17.14
20	3.13	36.82	39.95	7.83
40	3.13	160.71	163.84	1.91
60	3.09	783.69	786.78	0.39

Table: Influence of flow design membranes in parallel/ series combined outlet.

Time (min)	∫ acrylic acid	∫ polymer	∫ total	res. acrylic acid (%)
0	3.14	7.44	10.58	29.68
10	3.14	16.7	19.84	15.83
20	3.13	46.88	50.01	6.26
40	3.07	418.16	421.23	0.73
60	0.00	2.67	2.67	0.00

Table: Influence of flow design 2 membranes in parallel.

Time (min)	∫ acrylic acid	∫ polymer	∫ total	res. acrylic acid (%)
0	3.14	6.50	9.64	32.57
10	3.16	11.49	14.65	21.57
20	3.15	21.45	24.60	12.80
40	3.07	66.71	69.78	4.40
60	3.20	325.57	328.77	0.97

Table: Influence of flow design 3 membranes in parallel.

Time (min)	∫ acrylic acid	∫ polymer	∫ total	res. acrylic acid (%)
0	3.16	7.40	10.56	29.92
10	3.16	16.71	19.87	15.90
20	3.17	35.13	38.30	8.28
40	3.13	202.79	205.92	1.52
60	3.10	937.13	940.23	0.33

2 membranes in parallel

The following data is used in Figure 3.5

Table: 2 membranes in parallel, concentration residual acrylic acid (**7**) is 0.2 mM.

Time (min)	∫ acrylic acid	∫ polymer	∫ total	res. acrylic acid (%)
0	3.14	6.50	9.64	32.57
10	3.16	11.49	14.65	21.57
20	3.15	21.45	24.60	12.80
40	3.07	66.71	69.78	4.40
60	3.20	325.57	328.77	0.97

Table: 2 membranes in parallel, concentration residual acrylic acid (**7**) is 0.1 mM.

Time (min)	∫ acrylic acid	∫ polymer	∫ total	res. acrylic acid (%)
0	3.14	6.44	9.58	32.78
10	3.17	9.40	12.57	25.22
20	3.14	13.02	16.16	19.43
40	3.16	26.17	29.33	10.77
60	3.14	51.71	54.85	5.72

Table: 2 membranes in parallel, concentration residual acrylic acid (**7**) is 0.05 mM.

Time (min)	**∫ acrylic acid**	**∫ polymer**	**∫ total**	**res. acrylic acid (%)**
0	3.17	6.96	10.13	31.29
10	3.14	9.19	12.33	25.47
20	3.13	11.79	14.92	20.98
40	3.16	19.34	22.50	14.04
60	3.12	32.12	35.24	8.85

Table: 2 membranes in parallel, concentration residual acrylic acid (**7**) is 0.03 mM.

Time (min)	**∫ acrylic acid**	**∫ polymer**	**∫ total**	**res. acrylic acid (%)**
0	3.15	6.25	9.40	33.51
10	3.15	8.77	11.92	26.43
20	3.13	10.80	13.93	22.47
40	3.15	15.41	18.56	16.97
60	3.11	21.37	24.48	12.70

Table: 2 membranes in parallel, concentration residual acrylic acid (**7**) is 0.025 mM.

Time (min)	**∫ acrylic acid**	**∫ polymer**	**∫ total**	**res. acrylic acid (%)**
0	3.14	6.20	9.34	33.62
10	3.38	7.64	11.02	30.67
20	3.16	8.86	12.02	26.29
40	3.20	11.77	14.97	21.38
60	3.14	16.54	19.68	15.96

3 membranes in parallel

The following data is used in Figure 3.6

Table: 3 membranes in parallel, concentration residual acrylic acid (**7**) is 0.2 mM.

Time (min)	∫ acrylic acid	∫ polymer	∫ total	res. acrylic acid (%)
0	3.16	7.40	10.56	29.92
10	3.16	16.71	19.87	15.90
20	3.17	35.13	38.30	8.28
40	3.13	202.79	205.92	1.52
60	3.10	937.13	940.23	0.33

Table: 3 membranes in parallel, concentration residual acrylic acid (**7**) is 0.1 mM.

Time (min)	∫ acrylic acid	∫ polymer	∫ total	res. acrylic acid (%)
0	3.13	6.96	10.09	31.02
10	3.21	10.94	14.15	22.69
20	3.16	19.04	22.20	14.23
40	3.10	52.83	55.93	5.54
60	3.14	158.03	161.17	1.95

Table: 3 membranes in parallel, concentration residual acrylic acid (**7**) is 0.05 mM.

Time (min)	∫ acrylic acid	∫ polymer	∫ total	res. acrylic acid (%)
0	3.17	6.81	9.98	31.76
10	3.15	9.56	12.71	24.78
20	3.14	14.27	17.41	18.04
40	3.15	29.62	32.77	9.61
60	3.19	69.63	72.82	4.38

Table: 3 membranes in parallel, concentration residual acrylic acid (**7**) is 0.03 mM.

Time (min)	**∫ acrylic acid**	**∫ polymer**	**∫ total**	**res. acrylic acid (%)**
0	3.15	7.01	10.16	31.00
10	3.15	11.87	15.02	20.97
20	3.13	16.75	19.88	15.74
40	3.12	26.07	29.19	10.69
60	3.13	43.77	46.90	6.67

Table: 3 membranes in parallel, concentration residual acrylic acid (**7**) is 0.025 mM.

Time (min)	**∫ acrylic acid**	**∫ polymer**	**∫ total**	**res. acrylic acid (%)**
0	3.15	6.87	10.02	31.44
10	3.15	8.90	12.05	26.14
20	3.13	11.14	14.27	21.93
40	3.14	17.73	20.87	15.05
60	3.13	28.68	31.81	9.84

3 membranes in series

The following data is used in Figure 3.7

Table: 3 membranes in series, concentration residual acrylic acid (**7**) is 0.2 mM.

Time (min)	∫ acrylic acid	∫ polymer	∫ total	res. acrylic acid (%)
0	3.16	7.79	10.95	28.86
10	3.15	18.95	22.10	14.25
20	3.13	54.43	57.56	5.44
40	3.05	537.23	540.28	0.56
60	0.00	2.66	2.66	0.00

Table: 3 membranes in series, concentration residual acrylic acid (**7**) is 0.1 mM.

Time (min)	∫ acrylic acid	∫ polymer	∫ total	res. acrylic acid (%)
0	3.16	7.95	11.11	28.44
10	3.16	15.66	18.82	16.79
20	3.16	31.69	34.85	9.07
40	3.15	140.40	143.55	2.19
60	3.04	713.26	716.30	0.42

Table: 3 membranes in series, concentration residual acrylic acid (**7**) is 0.05 mM.

Time (min)	∫ acrylic acid	∫ polymer	∫ total	res. acrylic acid (%)
0	3.19	7.34	10.53	30.29
10	3.10	9.84	12.94	23.96
20	3.09	14.53	17.62	17.54
40	3.16	46.81	49.97	6.32
60	3.47	313.64	317.11	1.09

Table: 3 membranes in series, concentration residual acrylic acid (**7**) is 0.03 mM.

Time (min)	**∫ acrylic acid**	**∫ polymer**	**∫ total**	**res. acrylic acid (%)**
0	3.14	6.94	10.08	31.15
10	3.14	9.73	12.87	24.40
20	3.14	14.07	17.21	18.25
40	3.15	29.95	33.10	9.52
60	3.11	65.40	68.51	4.54

Table: 3 membranes in series, concentration residual acrylic acid (**7**) is 0.025 mM.

Time (min)	**∫ acrylic acid**	**∫ polymer**	**∫ total**	**res. acrylic acid (%)**
0	3.13	6.94	10.07	31.08
10	3.13	9.13	12.26	25.53
20	3.13	11.48	14.61	21.42
40	3.12	20.32	23.44	13.31
60	3.10	35.63	38.73	8.00

Influence conversion

The following data is used in Figure 3.8

Table: Influence of residual monomer at purification time, [I] = 1.25 mol%, 5 min residence time.

Time (min)	∫ acrylic acid	∫ polymer	∫ total	res. acrylic acid (%)
0	3.08	1.37	4.45	69.21
10	3.13	5.36	8.49	36.87
20	3.13	19.55	22.68	13.80
40	3.15	408.51	411.66	0.77
60	3.28	1022.39	1025.67	0.32

Table: Influence of residual monomer at purification time, [I] = 1.25 mol%, 10 min residence time.

Time (min)	∫ acrylic acid	∫ polymer	∫ total	res. acrylic acid (%)
0	3.16	7.79	10.95	28.86
10	3.15	18.95	22.10	14.25
20	3.13	54.43	57.56	5.44
40	3.05	537.23	540.28	0.56
60	0.00	2.66	2.66	0.00

Table: Influence of residual monomer at purification time, [I] = 2.50 mol%, 10 min residence time.

Time (min)	∫ acrylic acid	∫ polymer	∫ total	res. acrylic acid (%)
0	3.14	10.60	13.74	22.85
10	3.14	33.02	36.16	8.68
20	3.13	98.82	101.95	3.07
40	3.09	1003.88	1006.97	0.31
60	0.00	2.67	2.67	0.00

Sample decrease

The following data is used in Figure 3.10

Table: Purification of 5 mL sample diluted to 25 mL total volume.

Time (min)	∫ acrylic acid	∫ polymer	∫ total	res. acrylic acid (%)
0	3.20	6.46	9.66	33.13
10	3.18	51.46	54.64	5.82
20	3.13	330.89	334.02	0.94
30	0.00	1.00	1.00	0.00
40	0.00	1.00	1.00	0.00

Experimental information 3

Experimental Information Chapter 4

Equipment and solvents

Analysis equipment

Unless otherwise stated, ^{1}H, ^{13}C, ^{19}F and ^{31}P NMR spectra were recorded at 296.5 K and were calibrated to the residual solvent according to the literature. [279] The spectra were recorded on a Bruker-Avance 400 spectrometer.

High resolution mass spectra (HR-MS) were recorded on a Waters Micromass LCT Premier spectrometer using time of flight with positive electrospray ionisation (ESI+), an ABI/MDS Sciex Q-STAR Pulsar with ESI+ and an atmospheric pressure solids analysis probe ionisation (ASAP), or a Bruker BioApex II 4.7e FTICR equipped with a direct insertion probe.

Liquid chromatography-mass spectroscopy (LC-MS) spectra were recorded on an Agilent HP 1100 series chromatograph containing a Mercury Luna 3μ C18 (2) column attached to a Waters ZQ2000 mass spectrometer with ESCi ionisation source in ESI mode.

Gas chromatography-mass spectroscopy (GC-MS) spectra were recorded on a Shimadzu QP2010-Ultra chromatograph. For EI GC non polar compounds a Rxi-5Sil MS (0.15 μm x 10 m x 0.15 mm) column was used, and for EI GC polar compounds a Rxi-17Sil MS (0.15 μm x 10 m x 0.15 mm) or Stabilwax (0.15 μm x 10 m x 0.15 mm) column was used. For CI GC non polar compounds a Rxi-5Sil MS

(0.15 μm x 10 m x 0.15 mm) column was used, and for CI GC polar compounds a Stabilwax (0.15 μm x 10 m x 0.15 mm) column was used.

X-ray was performed using a Bruker D8 Venture and the structure was solved using ShelXS 2013/1 (Sheldrick, 2008) software.

Raman spectra were recorded on a Horiba LabRAM HR using red light (633 nm) for excitation.

IR spectra were recorded neat on a Perkin-Elmer Spectrum Two FT-IR spectrometer. The absorbency of the peaks was defined as: weak (w, < 40% of most the intense peak), medium (m, 40 - 75% of the most intense peak), strong (s, > 75% of the most intense peak) and broad (br).

Melting points were recorded on an Optimelt automated melting point system. The heating gradient was 1 °C min^{-1}.

Solvents

Solvents were purchased from Fisher Scientific and used without further purification.

Dry solvents were obtained from the departmental dry solvent facilities and had the specifications mentioned below.

Solvent	**Water content (ppm)**
acetonitrile	2.7
chloroform	3.4
DCM	5.9
diethyl ether	14.2
DMF	61.8
n-hexane	5.6
THF	10.8
toluene	7.9

$Pd(PPh_3)_4$ was prepared following a procedure reported by Coulson *et al.* [280].

Deuterated solvents for NMR analysis were purchased from Apollo Scientific.

Synthetic procedures

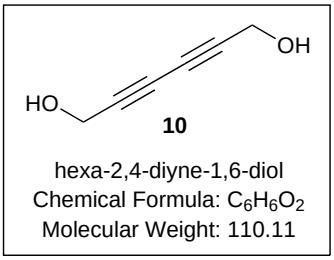

10

hexa-2,4-diyne-1,6-diol
Chemical Formula: $C_6H_6O_2$
Molecular Weight: 110.11

Hexa-2,4-diyne-1,6-diol (**10**) [252]: DME (30 mL) was sonicated (30 min) before it was used as solvent for the Glaser coupling. Propargylic alcohol (**9**) (1.121 g, 1.154 mL, 20 mmol) was added to the solvent and the mixture was stirred for 5 min. Next TMEDA (232.5 mg, 0.299 mL, 2 mmol) and CuI (190.5 mg, 1 mmol) were added to the reaction mixture. The mixture was heated to 55 °C for 2 hours with constant oxygen bubbling through from a balloon. The system was then sealed and kept at 55 °C under an atmosphere of oxygen overnight. The reaction mixture was cooled down, filtered over Celite, washed with brine (3 x 30 mL), dried over anhydrous magnesium sulfate and concentrated under vacuum. The product was obtained as an off white powder in a yield of 86% (947 mg).

^{1}H NMR (400 MHz, DMSO-d^6): δ (ppm) 5.40 (t, J = 6.0 Hz, 2H), 4.17 (d, J = 5.8 Hz, 4H).

^{13}C NMR (100 MHz, DMSO-d^6): δ (ppm) 80.0 (2 x C), 68.4 (2 x C), 49.8 (2 x CH_2).

IR (neat) ν 3276 (sb), 2930 (m), 1480 (m), 1444 (m), 1352 (m), 1219 (w), 1033 (s), 913 (s), 665 (m), 555 (m) cm^{-1}.

GC-MS (EI GC nonpolar compounds(Ultra)) calculated for $C_6H_6O_2$ is 110.04, Retention Time 3.610 min, (M+) 110.090 (37.66%), (M + 1 - CHO) 81.050 (100.00%) Da. [281]

Melting point: 104.4 - 109.3 °C.

Table: Elemental analysis.

	% C	% H	% N
Expected	65.45	5.49	0
Measured	62.24	5.29	0

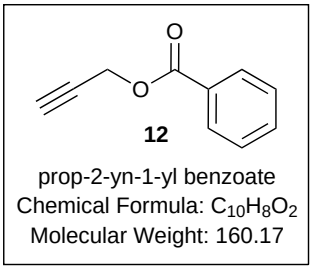

prop-2-yn-1-yl benzoate
Chemical Formula: $C_{10}H_8O_2$
Molecular Weight: 160.17

Prop-2-yn-1-yl benzoate (**12**) [252]: A flask was charged with dry CH_2Cl_2 (15 mL) and commercially available benzoyl chloride (**11**) (3.51 g, 2.90 mL, 25 mmol). To the solution was added propargyl alcohol (**9**) (1.40 g, 1.46 mL, 25 mmol) and Et_3N (2.53 g, 3.49 mL, 25 mmol) at room temperature. The reaction mixture was stirred at room temperature for 6 hours and H_2O (50 mL) was added. An aqueous work up was performed with CH_2Cl_2 (3 x 30 mL) and the organic phases were combined, dried over anhydrous magnesium sulfate, filtered and concentrated under vacuum. Purification of the crude product was performed by silica gel chromatography using n-hexane and EtOAC (80:20) as eluent. Compound **12** was obtained as an slight yellow oil in a yield of 78% (3.12 g).

^{1}H NMR (400 MHz, $CDCl_3$): δ (ppm) 8.09 (m, 2H) 7.59 (m, 1H), 7.46 (m, 2H), 4.94 (d, J = 2.4 Hz, 2H), 2.55 (t, J = 2.5Hz, 1H).

^{13}C NMR (100 MHz, $CDCl_3$): δ (ppm) 165.8 (CO2), 133.3 (CH), 129.8 (2 x CH), 129.4 (C), 128.5 (2 x CH), 77.8 (C) 75.1 (C), 52.5 (CH_2).

IR (neat) ν 3296 (w), 1720 (s), 1601 (w), 1452 (m), 1315 (w), 1262 (s), 1095 (s), 1070 (s), 1026 (m), 980 (m), 707 (s), 568 (m) cm^{-1}.

GC-MS (EI GC nonpolar compounds(Ultra)) calculated for $C_{10}H_8O_2$ is 160.05, Retention Time 3.527, (M+) 160.070 (8.62%), (M - C_3H_2O) 105.040 (100.00%) Da.

ASAP calculated for calculated for $C_{10}H_8O_2$ is 160.05, Retention Time 0.764

min, (M + H) 161.080 (40.54%) Da.

HR-MS calculated for calculated for $C_{10}H_8O_2$ is 160.05, found 161.0603 (Δ = -3.1 ppm) Da.

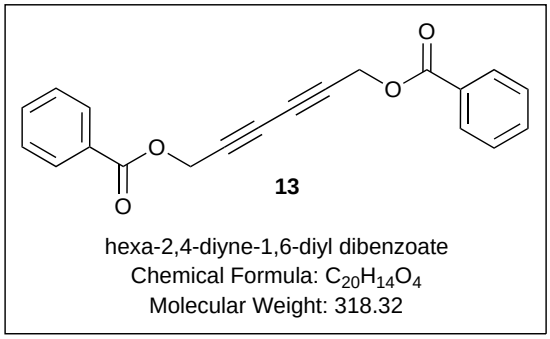

Hexa-2,4-diyne-1,6-diyl dibenzoate (**13**) [252, 253, 265]: A flask was charged with dry degassed DMF (25 mL) and compound **12** (3.46 g, 21 mmol). In a second flask was prepared the Hay catalyst, by mixing CuCl (107 mg, 1.08 mmol), TMEDA (101 mg, 130 μL, 0.87 mmol) and pyridine (1.18 g, 1.20 mL, 14.80 mmol). The catalyst mixture was stirred for 40 min before it was transferred *via* a pipette to the reaction mixture of compound **12** and oxygen was bubbled through using a balloon for 30 min at room temperature. The reaction mixture was then heated for two hours at 55 °C with constant oxygen bubbling through using a balloon. The system was sealed and kept at 55 °C under an atmosphere of oxygen overnight. The reaction mixture was cooled to room temperature before an aqueous work up with EtOAc (3 x 50 mL) was performed and the organic phases were combined, dried over anhydrous magnesium sulfate, filtered and concentrated under vacuum. Purification of the crude product was performed by silica gel chromatography using n-hexane and EtOAC (80 : 20) as eluent. Compound **13** was obtained as an off white solid in a yield of 81% (2.707 g).

^{1}H NMR (400 MHz, $CDCl_3$): δ (ppm) 8.08 (m, 4H), 7.60 (ddt, J = 8.0, 6.9, 1.4 Hz, 2H), 7.47 (m, 4H), 5.01 (s, 4H).

^{13}C NMR (100 MHz, $CDCl_3$): δ (ppm) 165.6 (2 x CO2), 133.5 (2 x CH), 129.9 (4 x CH), 129.2 (2 x C), 128.5 (4 x CH), 73.8 (2 x C), 70.6 (2 x C), 52.8 (2 x C).

IR (neat) ν 1721 (s), 1600 (w), 1451 (m), 1245 (s), 1087 (s), 1067 (s), 1026 (s),

980 (m), 705 (s), 684 (s), 568 (w) cm^{-1}.

GC-MS (EI GC nonpolar compounds(Ultra)) calculated for $C_{20}H_{14}O_4$ is 318.09, Retention Time 6.797, (M+) 318.119 (1.52%), (M - $C_{13}H_9O_3$) 105.051 (100.00%) Da.

ASAP calculated for calculated for $C_{20}H_{14}O_4$ is 318.09, Retention Time 0.639 min, (M+) 318.107 (11.17%), (M + 1) 319.099 (24.19%), (M+ - $C_7H_5O_2$) 197.069 (100.00%) Da.

HR-MS calculated for calculated for $C_{20}H_{14}O_4$ is 318.09, found 318.0891 (Δ = 1.6 ppm) Da.

Melting point: 69.9 - 73.3 °C.

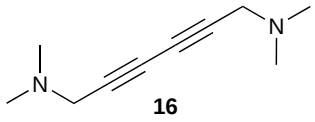

16

N^1,N^1,N^6,N^6-tetramethylhexa-2,4-diyne-1,6-diamine
Chemical Formula: $C_{10}H_{16}N_2$
Molecular Weight: 164.25

N^1,N^1,N^6,N^6-tetramethylhexa-2,4-diyne-1,6-diamine (**16**) [269]: To 14 mL of acetone 3-dimethylamino-1-propyne (**29**) (2.00 g, 24.08 mmol) and the mixture stirred for 5 min. In a second flask was prepared the Hay catalyst, by mixing CuI (240 mg, 2.4 mmol), TMEDA (0.120 mL, 0.08 mmol) and pyridine (1.18 g, 1.20 mL, 14.80 mmol). The catalyst mixture was stirred for 40 min before it was transferred *via* a pipette to the reaction mixture of compound **16**. Oxygen was bubbled through the reaction mixture using a balloon whilst stirring at room temperature for 2 hours. The reaction mixture was filtered over Celite and concentrated under vacuum. The crude material was dissolved in diethyl ether (30 mL) and washed with brine (3 *x* 30 mL), dried over anhydrous magnesium sulfate and concentrated under vacuum. The product was obtained as a dark yellow oil in a yield of 59% (1.17 g).

^{1}H NMR (400 MHz, $CDCl_3$): δ (ppm) 3.30 (s, 4H), 2.25 (s, 12H).

^{13}C NMR (100 MHz, $CDCl_3$): δ (ppm) 73.5 (2 *x* C), 69.6 (2 *x* C), 48.3 (2 *x*

CH_2), 44.0 (4 *x* CH_3).

IR (neat) ν 2941 (m), 2824 (m), 2773 (m), 1452 (m), 1357 (m), 1319 (s), 1260 (m), 1156 (m), 1033 (s), 900 (m), 836 (s), 814 (m), 585 (m) cm^{-1}.

GC-MS (EI GC nonpolar compounds(Ultra)) calculated for $C_{10}H_{16}N_2$ is 164.13, Retention Time 3.940, (M+) 164.141 (96.93%), (M - C_2H_6N) 120.100 (100.00%) Da.

ASAP calculated for calculated for $C_{10}H_{16}N_2$ is 164.13, Retention Time 0.660 min, (M + 1) 165.160 (100.00%), (M - C_2H_6N) 120.105 (70.97%) Da.

HR-MS calculated for calculated for $C_{10}H_{16}N_2$ is 164.13, found 165.1373 (Δ = -1.9 ppm) Da.

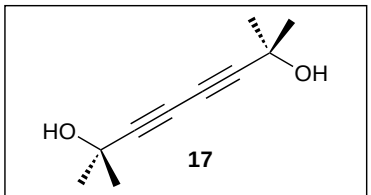

17

2,7-dimethylocta-3,5-diyne-2,7-diol
Chemical Formula: $C_{10}H_{14}O_2$
Molecular Weight: 166.22

2,7-dimethylocta-3,5-diyne-2,7-diol (**17**) [282]: DME (20 mL) was sonicated (30 min) prior to use in the Glaser coupling. 2-Methyl-3-butyn-2-ol (**28**) (1.68 g, 1.95 mL, 20 mmol) was dissolved in the sonicated DME and the mixture was stirred for 5 min. TMEDA (233 mg, 2 mmol, 0.30 mL) and CuI (191 mg, 1 mmol) were added to the reaction mixture and the mixture heated at 55 °C for two hours bubbling oxygen through using a balloon. The system was sealed and kept at 55 °C under an atmosphere of oxygen overnight. The reaction mixture was cooled to room temperature, filtered over Celite, washed with brine (3 *x* 30 mL), dried over anhydrous magnesium sulfate and concentrated under vacuum. The product was obtained as a slightly yellow powder in a yield of 88% (1.46 g).

^{1}H NMR (400 MHz, DMSO-d_6): δ (ppm) 1.37 (s, 12H).

^{13}C NMR (100 MHz, DMSO-d_6): δ (ppm) 86.1 (2 *x* C), 65.5 (2 *x* C), 64.1 (2 *x* C), 31.5 (4 *x* CH_3).

IR (neat) ν 3569 (w), 3206 (mb), 2983 (m), 1363 (m), 1209 (m), 1165 (s), 952

(s) cm^{-1}.

GC-MS (EI GC nonpolar compounds(Ultra)) calculated for $C_{10}H_{14}O_2$ is 166.10, Retention Time 3.5933, (M+) 166.100 (4.24%), (M+1 - OH) 151.100 (49.01%), (M+1 - 2 *x* OH - 2 *x* CH_3) 133.100 (42.19%), (M+1 - OH - 2 *x* CH_3) 123.100 (21.14%), Retention Time 2.143 min, (M + 1 - C_5H_7O) 84.057 (100.00%) Da.

LC-MS (ESI LC nonpolar coumpounds) calculated for $C_{10}H_{14}O_2$ is 166.10, Retention Time 1.689, (M+23) 190.059 (25.47%), (M+1) 167.045 (0.59%), (M - C_5H_8O) 82.962 (100.00%).

HR-MS calculated for $C_{10}H_{14}O_2$ is 166.10, found 166.1488 (Δ = -2.1 ppm) Da.

Melting point: 130.9 - 132.5 °C.

Table: Elemental analysis.

	% C	**% H**	**% N**
Expected	72.26	8.49	0
Measured	71.75	8.43	0

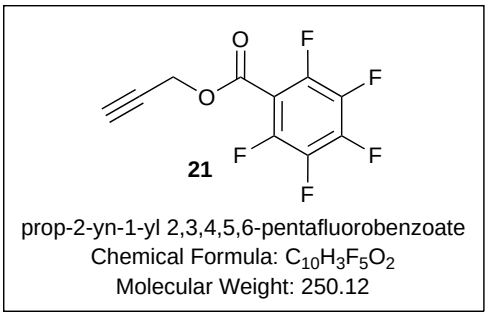

prop-2-yn-1-yl 2,3,4,5,6-pentafluorobenzoate
Chemical Formula: $C_{10}H_3F_5O_2$
Molecular Weight: 250.12

Prop-2-yn-1-yl 2,3,4,5,6-pentafluorobenzoate (**21**) [266]: A flask was charged with dry CH_2Cl_2 (15 mL) and pentafluorobenzoyl chloride (**20**) (2.00 g, 1.25 mL, 8.68 mmol). To the reaction solution was added propargyl alcohol (**9**) (486 mg, 0.5 mL, 8.68 mmol) and Et_3N (878 mg, 1.21 mL, 8.68 mmol). The reaction mixture was stirred at room temperature for 4 h. The reaction mixture was washed with H_2O (2 *x* 20 mL) and the combined aqueous layers were extracted with CH_2Cl_2 (2 *x* 15 mL) the organic phases were combined, dried over anhydrous magnesium sulfate, filtered and concentrated under vacuum. Purification of the crude product

was performed by silica gel chromatography using *n*-hexane and EtOAC (80:20) as eluent. Compound **21** was obtained as an slightly yellow oil in a yield of 79% (1.72 g).

^{1}H NMR (400 MHz, $CDCl_3$): δ (ppm) 4.97 (d, J = 2.5 Hz, 2H), 2.59 (t, J = 2.4 Hz, 1H).

^{13}C NMR (100 MHz, $CDCl_3$): δ (ppm) 158.2 (CO_2), 145.5 (m, J = 257 Hz, 2 x CF), 143.5 (m, J = 258 Hz, CF), 137.7 (m, J = 254 Hz, 2 x CF), 107.3 (dt, J = 4.1 and 15.4 Hz, C), 75.1 (C), 76.0 (CH), 53.8 (CH_2).

^{19}F NMR (376 MHz, $CDCl_3$): δ (ppm) -137.7 - -138.1 (m, 2F), -147.9 - -148.3 (m, 1F), -160.5 - -160.9 (m, 2F).

IR (neat) ν 3309 (w), 1741 (s), 1652 (m), 1495 (s), 1423 (w), 1372 (m), 1325 (s), 1211 (s), 1102 (w), 998 (s), 937 (s), 752 (m), 641.44 (m) cm^{-1}.

GC-MS (EI GC nonpolar compounds(Ultra)) calculated for $C_{10}H_3F_5O_2$ is 250.01, Retention Time 3.127 min, (M+) 250.000 (11.94%), (M+ - C_3H_3O) 194.950 (100.00%) Da.

ASAP calculated for $C_{10}H_3F_5O_2$ is 250.01, Retention Time 0.247 min, (M + 1) 251.011 (58.09%), (M+) 250.000 (15.63%), (M + 3 - CH) 240.043 (100.00%) Da.

HR-MS calculated for $C_{10}H_3F_5O_2$ is 250.01, found 251.0114 (Δ = -1.6 ppm) Da.

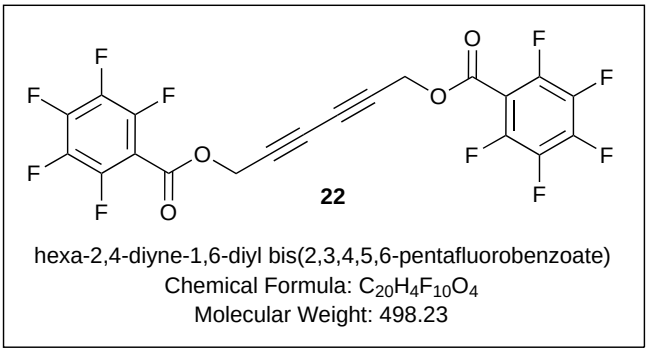

22

hexa-2,4-diyne-1,6-diyl bis(2,3,4,5,6-pentafluorobenzoate)
Chemical Formula: $C_{20}H_4F_{10}O_4$
Molecular Weight: 498.23

Hexa-2,4-diyne-1,6-diyl bis(2,3,4,5,6-pentafluorobenzoate) (**22**) [266]: DMF (15 mL) was sonicated (30 min) prior to use in the Glaser coupling. Compound **21** (2.14 g, 8.54 mmol) was dissolved and the mixture was stirred for 5 min. In a second flask was prepared the Hay catalyst, by mixing CuCl (43 mg, 0.43 mmol),

TMEDA (50 mg, 65 μL, 0.43 mmol) and pyridine (0.59 g, 0.6 mL, 7.45 mmol). The catalyst mixture was stirred for 40 min before it was transferred *via* a pipette to the reaction mixture of compound **21**. Oxygen was bubbled through the reaction mixture using a balloon whilst stirring at room temperature for 30 min. The reaction mixture was heated for 2 hours at 55 °C with constant oxygen bubbling through. The system was sealed and kept at 55 °C under an atmosphere of oxygen overnight. The reaction mixture was cooled to room temperature before an aqueous work up with EtOAc (3 *x* 20 mL) was performed and the organic phases were combined, dried over anhydrous magnesium sulfate, filtered and concentrated under vacuum. Purification of the crude product was performed by silica gel chromatography using *n*-hexane and EtOAC (70:30) as eluent. Compound **22** was obtained as light red flakes in a yield of 61% (1.30 g).

^{1}H NMR (400 MHz, $CDCl_3$): δ (ppm) 5.06 (s, 4H).

^{13}C NMR (100 MHz, $CDCl_3$): δ (ppm) 158.2 (2 *x* CO_2), 147.0 (2 *x* CF), 144.4 (4 *x* CF), 139.0 (4 *x* CF), 136.5 (2 *x* C), 76.1 (2 *x* C), 72.7 (2 *x* C), 54.0 (2 *x* CH_2).

^{19}F NMR (376 MHz, $CDCl_3$): δ (ppm) -137.3 (m, 4F), -147.3 (m, 2F), -160.2 (m, 4F).

IR (neat) ν 1742 (s), 1652 (m), 1524 (m), 1495 (s), 1423 (w), 1368 (w), 1324 (s), 1206 (s), 1101 (w), 997 (s), 755 (w) cm^{-1}.

GC-MS (EI GC nonpolar compounds(Ultra)) calculated for $C_{20}H_4F_{10}O_4$ is 497.99, Retention Time 5.983 min, (M+) 498.001 (2.46%), (M - $C_{13}H_4F_5O_3$) 194.966 (100.00%) Da.

ASAP calculated for $C_{20}H_4F_{10}O_4$ is 497.99, Retention Time 0.717 min, (M+) 498.005 (7.93%), (M - $C_7F_5O_2$) 287.022 (100.00%) Da.

HR-MS calculated for $C_{20}H_4F_{10}O_4$ is 497.99, found 497.9949 (Δ = 1.1 ppm) Da.

Melting point: 50.8 - 53.1 °C.

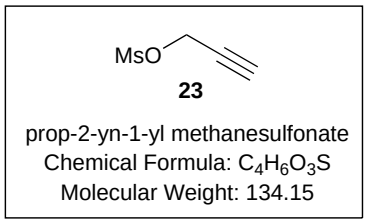

Prop-2-yn-1-yl methanesulfonate (**23**) [267]: A flask charged with dry CH_2Cl_2 (50 mL) and propargyl alcohol (**9**) (5.61 g, 5.8 mL, 0.1 mol) and the mixture cooled to 0 °C. To the reaction mixture was added mesyl chloride (12.03 g, 8.11 mL 0.1 mol) and Et_3N (10.63 g, 14.65 mL, 0.1 mol) and the reaction stirred for 1 h at 0 °C. The reaction mixture was allowed to warm to room temperature over 2 h with stirring and then further stirred at room temperature for 2 h. The reaction mixture was extracted with CH_2Cl_2 (3 x 30 mL) and the combined organic phases were dried over anhydrous magnesium sulfate, filtered and concentrated under vacuum. The (**23**) was obtained as a brown oil in 98% (13.15 g) yield and used without any further purification.

^{1}H NMR (400 MHz, $CDCl_3$): δ (ppm) 4.80 (d, J = 2.5 Hz, 2H), 3.08 (s, 3H), 2.75 (t, J = 2.5 Hz, 1H).

^{13}C NMR (100 MHz, $CDCl_3$): δ (ppm) 78.2 (C), 75.8 (C), 57.4 (CH_2), 38.9 (CH_3).

IR (neat) ν 3284 (m), 1348 (s), 1169 (s), 963 (s), 924 (s), 803 (s), 667 (m), 525 (s) cm^{-1}.

GC-MS (EI GC nonpolar compounds(Ultra)) calculated for $C_4H_6O_3S$ is 134.00, Retention Time 2.743 min, (M+ - SO_2CH_3) 55.037 (43.99%), (M+H - OC_3H_3) 80.000 (88.48%), (M+ - CH_3) 118.996 (5.01%), (M+H) 135.050 (4.81%) Da.

ASAP calculated for $C_4H_6O_3S$ is 134.00, Retention Time 0.369 min, (M+1) 135.011 (17.37%) Da.

HR-MS calculated for $C_4H_6O_3S$ is 134.00, found 135.0116 (Δ = -5.2 ppm) Da.

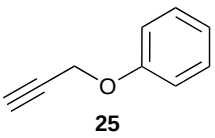

25

(prop-2-yn-1-yloxy)benzene
Chemical Formula: C_9H_8O
Molecular Weight: 132.16

(Prop-2-yn-1-yloxy)benzene (**25**) [267]: A flask was charged with MeCN (70 mL) and 2-prop-1-yl-metane sulfonate (**23**) (11.32 g, 84.0 mmol). The mixture was stirred for ten min in order to solubilise the starting material before phenol (**24**) (9.88 g, 105 mmol), NaI (929 mg, 6.2 mmol) and Cs_2CO_3 (35.84 g, 110 mmol) were added. The reaction mixture was heated at 70 °C overnight and then cooled to room temperature. Deionised water (50 mL) was added and extracted extensively with Et_2O (6 *x* 15 mL). The combined organic phases were dried over anhydrous magnesium sulfate, filtered and concentrated under vacuum. Purification of the crude product was performed by silica gel chromatography using *n*-hexane and EtOAC (99:1) as eluent. Compound **25** was obtained as a slightly yellow oil in a yield of 75% (8.33 g).

^{1}H NMR (400 MHz, $CDCl_3$): δ (ppm) 7.42 - 7.38 (m, 2H), 7.11 - 7.06 (m, 3H), 4.75 (d, J = 2.4 Hz, 2H), 2.60 (t, J = 2.4 Hz, 1H).

^{13}C NMR (100 MHz, $CDCl_3$): δ (ppm) 157.6 (CO), 129.6 (2 *x* CH), 121.7 (CH), 115.0 (2 *x* CH), 78.8 (C), 75.6 (CH), 55.8 (CH_2).

IR (neat) ν 3290 (m), 1598 (m), 1494 (s), 1212 (s), 1174 (m), 1034 (s), 751 (s), 689 (s) 637 (s), 505 (m) cm^{-1}.

GC-MS (EI GC nonpolar compounds(Ultra)) calculated for C_9H_8O is 132.06, Retention Time 2.96 min, (M + 1) 133.101 (3.96%), (M+) 132.100 (43.04%), (M - 1) 131.100 (100.00%) Da.

ASAP calculated for C_9H_8O is 132.06, Retention Time 0.408 min, (M + 1) 133.065 (100.00%) Da.

HR-MS calculated for C_9H_8O is 132.06, found 133.0648 (Δ = -3.8 ppm) Da.

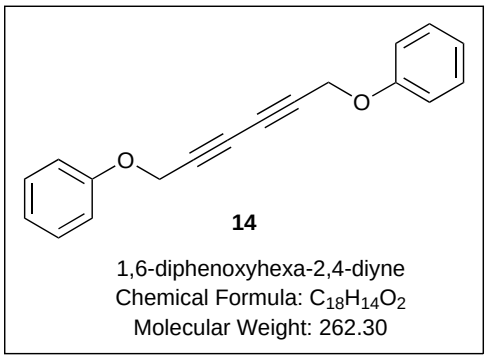

14

1,6-diphenoxyhexa-2,4-diyne
Chemical Formula: $C_{18}H_{14}O_2$
Molecular Weight: 262.30

Hexa-2,4-diyne-1,6-diyl dibenzoate (**14**) [283]: A flask was charged with dry sonicated (30 min) DMF (30 mL) and compound **25** (6.17 g, 46.69 mmol). In a second flask was prepared the Hay catalyst, by mixing CuCl (232 mg, 2.34 mmol), TMEDA (200 mg, 258 μL, 1.72 mmol) and pyridine (2.54 g, 2.59 mL, 32.2 mmol). The catalyst mixture was stirred for 40 min before it was transferred *via* a pipette to the reaction mixture of compound **25**. Oxygen was bubbled through the reaction mixture using a balloon whilst stirring at room temperature for 30 min. The reaction mixture was heated for two hours at 55 °C with constant oxygen bubbling through. The system was sealed and kept at 55 °C under an atmosphere of oxygen overnight. The reaction mixture was cooled to room temperature before the reaction mixture was diluted with DMF (70 mL) filtered over silica gel and the product precipitated from deionised water (200 mL). Compound **14** was obtained as an off-white clay. This was turned into a powder by extracting with deionised water (70 mL) and EtOAc (4 *x* 50 mL), combining the organic phases, drying over anhydrous magnesium sulfate and concentrating under vacuum to obtain this dialkyne in a yield of 53% (3.25 g).

^{1}H NMR (400 MHz, $CDCl_3$): δ (ppm) 7.36 - 7.32 (m, 4H), 7.04 (m, 2H), 6.99 - 6.97 (m, 4H), 4.78 (s, 4H).

^{13}C NMR (100 MHz, $CDCl_3$): δ (ppm) 157.4 (2 *x* C), 129.6 (4 *x* C), 121.8 (2 *x* C), 114.9 (4 *x* C), 74.7 (2 *x* C), 71.0 (2 *x* C), 56.2 (2 *x* CH_2).

IR (neat) ν 3073 (w), 2161 (w), 1587 (m), 1493 (m), 1366 (m), 1234 (s), 1032 (s), 746 (s), 685 (s) cm^{-1}.

GC-MS (EI GC nonpolar compounds(Ultra)) calculated for $C_{18}H_{14}O_2$ is 262.10, Retention Time 6.003 min, (M+) 262.100 (12.75%), (M+ - OC_6H_5) 168.050 (100.00%) Da.

ASAP calculated for $C_{18}H_{14}O_2$ is 262.10, Retention Time 0.746 min, (M+1) 263.102 (100.00%) Da.

HR-MS calculated for $C_{18}H_{14}O_2$ is 262.10, found 263.1062 (Δ = -3.8 ppm) Da.

Melting point: 80.7 - 82.1 °C.

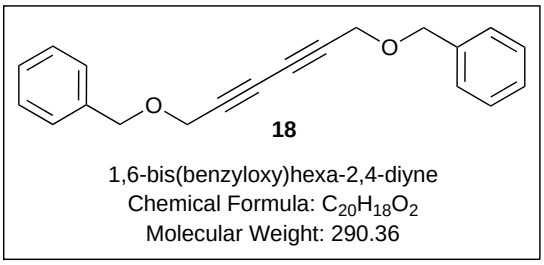

18

1,6-bis(benzyloxy)hexa-2,4-diyne
Chemical Formula: $C_{20}H_{18}O_2$
Molecular Weight: 290.36

1,6-bis(benzyloxy)hexa-2,4-diyne (**18**) [284]: A flask was charged with dry sonicated (30 min) DMF (15 mL) and benzyl propargyl ether (**26**) (3.00 g, 20.52 mmol). In a second flask was prepared the Hay catalyst, by mixing CuCl (102 mg, 1.03 mmol), TMEDA (93 mg, 127 μL, 0.80 mmol) and pyridine (1.24 g, 1.18 mL, 14.9 mmol). The catalyst mixture was stirred for 40 min before it was transferred *via* a pipette to the reaction mixture of compound **26**. Oxygen was bubbled through the reaction mixture using a balloon whilst stirring at room temperature for 30 min. The reaction mixture was heated for 2 hours at 55 °C with constant oxygen bubbling through. The system was sealed and kept at 55 °C under an atmosphere of oxygen overnight. The reaction mixture was cooled to room temperature before the reaction mixture was filtered over Celite, concentrated under vacuum, dissolved in EtOAc (50 mL) and washed with brine (3 x 25 mL). The organic phase was dried over anhydrous magnesium sulfate, filtered and concentrated under vacuum. Purification of the crude product was performed by silica gel chromatography using *n*-hexane and EtOAC (95:5) as eluent. Compound **19** was obtained as a slightly yellow oil in a yield of 53% (1.58 g).

^{1}H NMR (400 MHz, $CDCl_3$): δ (ppm) 7.45 (m, 10H), 4.69 (s, 4H), 4.33 (s, 4H).

^{13}C NMR (100 MHz, $CDCl_3$): δ (ppm) 137.1 (2 *x* C), 128.6 (4 *x* CH), 128.2 (4 *x* CH), 128.1 (2 *x* CH), 75.5 (2 *x* C), 71.9 (2 *x* CH_2), 70.7 (2 *x* C), 57.6 (2 *x* CH_2).

IR (neat) ν 3031 (w), 2858 (w), 1496 (w), 1454 (m), 1345 (m), 1070 (s), 1028 (m), 938 (w), 735 (s), 695 (s), 603 (m) cm^{-1}.

LC-MS calculated for calculated for $C_{20}H_{18}O_2$ is 290.13, Retention Time 0.496 min, (M + H) 291.149 (3.65%), (M - C_6H_5) 213.103 (98.85%) Da.

HR-MS calculated for calculated for $C_{20}H_{18}O_2$ is 290.13, found 291.1206 (Δ = -3.8 ppm) Da.

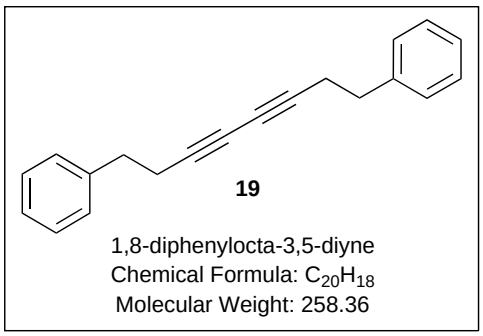

1,8-Diphenylocta-3,5-diyne (**19**) [285]: A flask was charged with dry sonicated (30 min) DMF (15 mL) and 4-phenyl-1-butyn (**27**) (3.00 g, 23.05 mmol). In a second flask was prepared the Hay catalyst, by mixing CuCl (114 mg, 1.15 mmol), TMEDA (99 mg, 127 μL, 0.85 mmol) and pyridine (1.24 g, 1.29 mL, 15.6 mmol). The catalyst mixture was stirred for 40 min before it was transferred *via* a pipette to the reaction mixture of compound **27**. Oxygen was bubbled through the reaction mixture using a balloon whilst stirring at room temperature for 30 min. The reaction mixture was heated for 2 hours at 55 °C with constant oxygen bubbling through. The system was sealed and kept at 55 °C under an atmosphere of oxygen overnight. The reaction mixture was cooled to room temperature before it was filtered over Celite, concentrated under vacuum, dissolved in EtOAc (50 mL) and washed with brine (3 *x* 25 mL). The organic phase was dried over anhydrous magnesium sulfate, filtered and concentrated under vacuum. Purification of the crude product was performed by silica gel chromatography using *n*-hexane and EtOAC (95:5) as eluent. Compound **19** was obtained as off white crystals in a yield of 89% (2.65 g).

^{1}H NMR (400 MHz, $CDCl_3$): δ (ppm) 7.39 - 7.32 (m, 4H), 7.27 (m, 6H), 2.89 (t, J = 7.5 Hz, 4H), 2.59 (t, J = 7.6 Hz, 4H).

^{13}C NMR (100 MHz, $CDCl_3$): δ (ppm) 140.2 (2 x C), 128.5 (4 x CH), 128.4 (4 x CH), 126.5 (2 x CH), 76.9 (2 x C), 66.0 (2 x C), 34.7 (2 x CH_2), 21.5 (2 x CH_2).

IR (neat) ν 3062 (w), 2861 (w), 2147 (w), 1452 (m), 699 (s) cm^{-1}.

GC-MS (EI GC nonpolar compounds(Ultra)) calculated for $C_{20}H_{18}$ is 258.36, Retention Time 6.010 min, (M+) 258.150 (25.64%), (M+ - $C_{13}H_{13}$) 91.050 (100.00%) Da.

ASAP calculated for $C_{20}H_{18}$ is 258.36, Retention Time 0.377 min, (M + 1) 259.151 (100.00%), (M+) 258.150 (45.08%) Da.

HR-MS calculated for $C_{20}H_{18}$ is 258.36, found 258.14 (Δ = -3.5 ppm) Da.

Melting point: 60.2 - 61.2 °C.

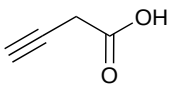

31

but-3-ynoic acid
Chemical Formula: $C_4H_4O_2$
Molecular Weight: 84.07

But-3-ynoic acid (**31**) [270, 271]: Two round bottom flasks (250 mL) were charged with deionised water (45 mL) and cooled to 0 °C using an ice bath. To one flask was added 65% HNO_3 (2.5 mmol, 0.17 mL, 5 mol%), $Na_2Cr_2O_7$ (0.15 g, 0.5 mmol, 1 mol%) and $NaIO_4$ (23.53 g, 110 mmol) and the mixture stirred for 15 min at 0 °C. To the second flask was added 3-butyn-1-ol (**30**) (3.78 mL, 50 mmol). The mixture of compound **30** was pipetted slowly to the first reaction mixture. The combined reaction mixture was stirred for 32 h whilst the ice slowly melted. The mixture was extracted with diethyl ether (5 x 30 mL). The organic layer was dried over anhydrous magnesium sulfate, filtered and concentrated under vacuum. The crude material was then triturated with DCM (10 mL), obtaining but-3ynoic acid (**31**) as colourless liquid in 88% yield (3.70 g).

^{1}H NMR (400 MHz, $CDCl_3$): δ (ppm) 3.39 (d, J = 2.7 Hz, 2H), 2.25 (t, J = 2.7

Hz, 1H).

^{13}C NMR (100 MHz, $CDCl_3$): δ (ppm) 174.5 (C_2H), 74.8 (C), 72.4 (CH), 25.6 (CH_2).

IR (neat) ν 3294 (m), 2926 (mb), 1969 (m), 1695 (s), 1399 (m), 1185 (m), 860 (m), 668 (m) cm^{-1}.

LC-MS calculated for $C_4H_4O_2$ is 84.02, Retention Time 3.559 min, (M) 84.335 (5.67%), (M - H) 83.171 (100.00%) Da.

HR-MS calculated for $C_4H_4O_2$ is 84.02 was performed but no peak was found.

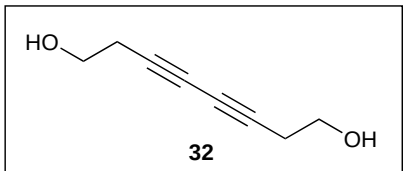

32

octa-3,5-diyne-1,8-diol
Chemical Formula: $C_8H_{10}O_2$
Molecular Weight: 138.16

Octa-3,5-diyne-1,8-diol (**32**): A flask was charged with sonicated (30 min) dimethoxyethane (30 mL) and 3-butyn-1-ol (**27**) (1.40 g, 20 mmol). To the solution was added TMEDA (232 mg, 300 μL, 2.0 mmol) and CuI (190 mg, 1.0 mmol). Oxygen was bubbled through the reaction mixture using a balloon whilst stirring at room temperature for 30 min. The reaction mixture was heated for two hours at 55 °C with constant oxygen bubbling through. The system was sealed and kept at 55 °C under an atmosphere of oxygen overnight. The reaction mixture was cooled to room temperature before it was filtered over Celite, concentrated under vacuum, dissolved in EtOAc (50 mL) and washed with brine (3 x 25 mL). The organic phase was dried over anhydrous magnesium sulfate, filtered and concentrated under vacuum. Purification of the crude product was performed by silica gel chromatography using n-hexane and EtOAC (9:1 to 7:3) as eluent. Compound **32** was obtained as a pale yellow oil in a yield of 89% (1.23 g).

^{1}H NMR (400 MHz, DMSO-d_6): δ (ppm) 4.85 (s, 2H), 3.49 (s, 4H), 2.37 (t, J = 6.7 Hz, 4H).

^{13}C NMR (100 MHz, DMSO-d_6): δ (ppm) 76.3 (2 x C), 66.3 (2 x C), 59.8 (2 x CH_2), 23.3 (2 x CH_2).

IR (neat) ν 3307 (m, OH), 2888 (m), 2159 (w), 1635 (w), 1416 (w), 1375 (w), 1325 (w), 1035 (s), 844 (m) cm^{-1}.

GC-MS (EI GC nonpolar compounds(Ultra)) calculated for $C_8H_{10}O_2$ is 138.07, Retention Time 4.163 min, (M+) 138.100 (23.19%), (M+ - CH_3O) 107.056 (78.91%) Da.

ASAP calculated for $C_8H_{10}O_2$ is 138.07, Retention Time 0.503 min, (M + 1) 139.076 (32.81%) Da.

HR-MS calculated for $C_8H_{12}O_2$ is 138.16, found 139.0759 (Δ = 2.9 ppm) Da.

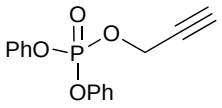

34

diphenyl prop-2-yn-1-yl phosphate
Chemical Formula: $C_{15}H_{13}O_4P$
Molecular Weight: 288.24

Diphenyl prop-2-yn-1-yl phosphate (**34**) [273–276]: Titanium tetrachloride (0.04 mL, 0.34 mmol) was dissolved in dry THF (40 mL), followed by the addition of propargylic alcohol (**9**) (952 mg, 0.98 mL, 17 mmol), Et_3N (3.6 mL, 25.5 mmol) and a solution of diphenyl chlorophosphate (**33**) (6.85 g, 5.3 mL, 25.5 mmol) dissolved in dry THF (10 mL). The reaction mixture was stirred for 2 h at room temperature before deionised water (30 mL) was added. The mixture was then extensively extracted with CH_2Cl_2 (5 x 30 mL). The combined organic phases were dried over anhydrous magnesium sulfate, filtered and concentrated under vacuum. Purification of the crude product was performed by silica gel chromatography using n-hexane and EtOAC (9:1) as eluent. Diphenyl phosphate **34** was obtained as a colourless oil in a yield of 84% (4.12 g).

^{1}H NMR (400 MHz, $CDCl_3$): δ (ppm) 7.37 - 7.32 (m, 4H), 7.28 - 7.25 (m, 4H), 7.22 - 7.18 (m, 2H), 4.85 (dd , J = 10.8, 2.5 Hz, 2H), 2.63 (t, J = 2.5 Hz).

^{13}C NMR (100 MHz, $CDCl_3$): δ (ppm) 150.4 (C), 150.3 (C), 129.9 (4 x CH), 125.6 (2 x CH), 120.2 (4 x CH), 77.0 (C), 76.8 (CH), 56.4 (CH_2).

^{31}P NMR (162 MHz, $CDCl_3$): δ (ppm) -11.8 (t, J = 7 Hz).

IR (neat) ν 3296 (w), 1589 (m), 1487 (s), 1285 (m), 1184 (s), 1024 (s), 942 (s), 753 (s), 686 (s) cm^{-1}.

GC-MS (EI GC nonpolar compounds(Ultra)) calculated for $C_{15}H_{13}O_4P$ is 288.06, Retention Time 5.360 min, (M+) 288.075 (98.49%), (M - OC_6H_5) 195.000 (91.10%) Da.

ASAP calculated for $C_{15}H_{13}O_4P$ is 288.06, Retention Time 0.697 min, (M + 1) 289.086 (100.00%) Da.

HR-MS calculated for $C_{15}H_{13}O_4P$ is 288.06, found 289.0630 (Δ = -0.7 ppm) Da.

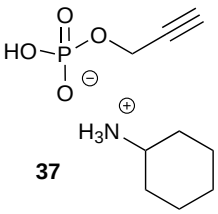

37

prop-2-yn-1-yl hydrogen phosphate cyclohexylamine salt
Chemical Formula: $C_9H_{18}NO_4P$
Molecular Weight: 235.22

Prop-2-yn-1-yl hydrogen phosphate cyclohexylamine salt (**37**) [273–276]: Propargylic alcohol (**9**) (38.80 g, 692 mmol) and Et_3N (10 mL) were mixed in a round bottom flask for 10 min at room temperature. To this solutions was added H_3PO_3 (1.65 g, 20 mmol) and the mixture stirred until all the H_3PO_3 dissolved. Iodine (7.60 g, 30 mmol) was added to the reaction mixture over 5 min and then stirred for an additional 10 min. The reaction mixture was added slowly to a mixture of acetone (400 mL) and Et_3N (15 mL) and stirred for 2 h at room temperature. Cyclohexylamine (30 mL) was added, the precipitate was filtered and recrystallised from ethanol and a few drops of cyclohexylamine. This gave salt **37** in a yield of 79% (3.74 g).

^{1}H NMR (400 MHz, D_2O): δ (ppm) 4.27 (dd, J = 7.1, 2.5 Hz, 1H), 3.02 (m,

1H), 1.86 (m, 2H), 1.68 (m, 2H), 1.52 (m, 1H), 1.22 (m, 4H), 1.06 (m, 1H).

^{13}C NMR (100 MHz, D_2O): δ (ppm) 81.0 (C), 74.4 (CH), 52.0 (CH_2), 50.3 (CH), 30.3 (2 x CH_2), 24.3 (CH_2), 23.8 (2 x CH_2).

^{31}P NMR (161 MHz, D_2O): δ (ppm) 3.5 (t, J = 7.0 Hz).

IR (neat) ν 2935 (m), 3305 (w, CH), 2223 (m, CC), 1061 (s, CO), 975 (s), 800 (s) cm^{-1}.

HR-MS calculated for $C_9H_{18}NO_4P$ 235.22 and negative ion 134.98, found 134.9847 (Δ = 4.4 ppm) for negative ion.

Melting point: 187.3 - 196.6 °C.

Table: Elemental analysis.

	% C	**% H**	**% N**
Expected	45.96	7.71	5.95
Measured	45.34	7.64	5.76

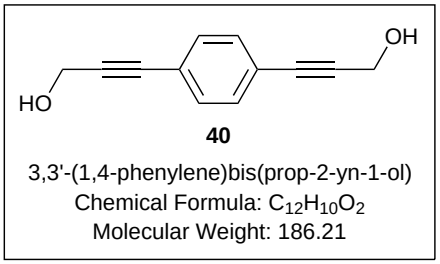

40

3,3'-(1,4-phenylene)bis(prop-2-yn-1-ol)
Chemical Formula: $C_{12}H_{10}O_2$
Molecular Weight: 186.21

3,3'-(1,4-phenylene)bis(prop-2-yn-1-ol) (**40**) [277]: A solution of 1,4-dibromobenzene (**39**) (5.00 g, 21 mmol), propargyl alcohol (**9**) (3.80 mL, 65 mmol) and $Pd(PPh_3)_4$ (0.64 g, 0.55 mmol) in anhydrous propylamine (60 mL) was refluxed under nitrogen for 24 h. To the reaction mixture was added saturated aqueous $NaHCO_3$ (80 mL) and extensively extracted with Et_2O (5 x 30 mL). The combined organic phases were dried over anhydrous magnesium sulfate, filtered and concentrated under vacuum. The solid residue was recrystallised from n-hexane and EtOAC (1:1) obtaining colourless crystals. The obtained yield was 81% (3.19 g).

^{1}H NMR (400 MHz, DMSO-d_6): δ (ppm) 7.42 (s, 1H), 4.32 (d, J = 5.8 Hz, 1H).

^{13}C NMR (100 MHz, DMSO-d_6): δ (ppm) 132.0 (4 x C), 122.9 (2 x C), 92.3 (2 x C), 83.5 (2 x C), 49.9 (2 x C).

IR (neat) ν 3296 (m, broad, OH), 2238 (w, C≡C), 1016 (s), 953 (s), 831 (s) cm^{-1}.

GC-MS (EI GC nonpolar compounds(Ultra)) calculated for $C_{12}H_{10}O_2$ is 186.07, Retention Time 5.203 min, (M+) 186.100 (100.00%), (M+1 - OH - CH_2) 157.050 (22.41%), (M+ - 2 x OH - $CCCH_2$) 128.100 (54.54%) Da.

ASAP calculated for $C_{12}H_{10}O_2$ is 186.07, Retention Time 0.332 min, (M+1) 187.076 (2.62%) Da.

HR-MS calculated for $C_{12}H_{10}O_2$ 186.21, found 187.08 (Δ = 3.2 ppm) Da.

Melting point: 122.0 - 125.8 °C.

Table: X-ray: structure information compound **40**. CIF file name: 16srv091.

Parameter	**Output**
Space group	P 2_1/c
a (Å)	11.1043(4)
b (Å)	4.9103(2)
c (Å)	18.1060(7)
α (°)	90.0000
β (°)	107.7377(12)
γ (°)	90.0000
Cell volume	940.306
Z,Z'	Z: 4 Z': 0
R-Factor (%)	4.22

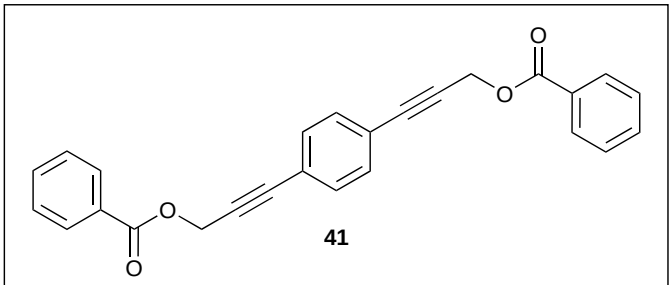

41

1,4-phenylenebis(prop-2-yne-3,1-diyl) dibenzoate
Chemical Formula: $C_{26}H_{18}O_4$
Molecular Weight: 394.42

1,4-phenylenebis(prop-2-yne-3,1-diyl) dibenzoate (**41**): Compound **40** (93 mg, 0.50 mmol) was dissolved in MeCN (5 mL) and cooled to 0 °C. To the mixture was added in order Et_3N (126 mg, 174 μL, 1.25 mmol), 4-dimethylaminopyridine (153 mg, 1.25 mmol) and benzoyl chloride (**11**) (176 mg, 145 μL, 1.25 mmol). The reaction mixture was stirred for 1 h at 0 °C and then allowed to warm to room temperature over 30 min. Water (30 mL) was added to the reaction mixture and the precipitated product was filtered and washed with water (50 mL), yielding compound **41** as an off white powder in 73% (144 mg).

^{1}H NMR (400 MHz, $CDCl_3$): δ (ppm) 8.13 (m, 4H), 7.63 - 7.59 (m, 2H), 7.50 - 7.48 (m, 4H), 7.44 (s, 4H), 5.18 (s, 4H).

^{13}C NMR (100 MHz, DMSO-d_6): δ (ppm) 165.9 (2 *x* CO_2), 133.3 (2 *x* CH), 131.8 (4 *x* CH), 129.8 (4 *x* CH), 129.5 (2 *x* C), 128.5 (4 *x* CH), 122.6 (2 *x* C), 86.0 (2 *x* C), 85.0 (2 *x* C), 53.2 (2 *x* CH_2).

IR (neat) ν 1723 (s), 1259 (s), 1094 (s), 706 (s) cm^{-1}.

ASAP calculated for $C_{26}H_{18}O_4$ is 394.12, Retention Time 1.014 min, (M+) 394.145 (8.00%), (M+1) 395.158 (16.82%) Da.

HR-MS calculated for $C_{26}H_{18}O_4$ is 394.12, found 394.1217 (Δ = -3.8 ppm) Da.

Melting point: 105.5 - 107.8 °C.

Table: X-ray: structure information compound **41**. CIF file name: 16srv147.

Parameter	Output
Space group	P 2_1/n
a (Å)	7.8099(3)
b (Å)	5.2705(2)
c (Å)	23.7463(10)
α (°)	90.0000
β (°)	96.6960(16)
γ (°)	90.0000
Cell volume	970.78
Z,Z'	Z: 2 Z': 0
R-Factor (%)	4.79

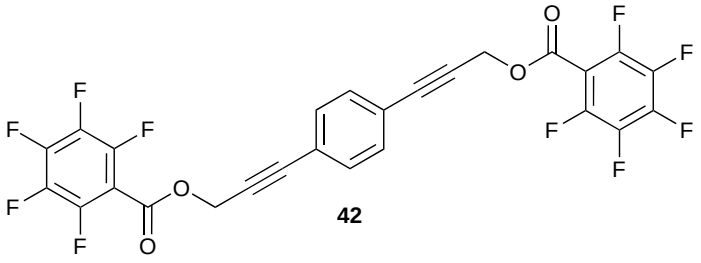

1,4-phenylenebis(prop-2-yne-3,1-diyl) bis(2,3,4,5,6-pentafluorobenzoate)
Chemical Formula: $C_{26}H_8F_{10}O_4$
Molecular Weight: 574.32

1,4-phenylenebis(prop-2-yne-3,1-diyl) bis(2,3,4,5,6-pentafluorobenzoate) (**42**): Compound **40** (93 mg, 0.50 mmol) was dissolved in MeCN (5 mL) and cooled to 0 °C. Et_3N (126 mg, 174 μL, 1.25 mmol), 4-dimethylaminopyridine (153 mg, 1.25 mmol) and pentafluorobenzoyl chloride (**20**) (288 mg, 180 μL, 1.25 mmol) were added to the reaction mixture in this order. The reaction mixture was stirred for 1 h at 0 °C and then allowed to warm to room temperature over 30 min. Water (30 mL) was added to the reaction mixture and the precipitated product was filtered and washed with water (50 mL). The crude product was purified by silica gel chromatography

(100% DCM) yielding compound **42** as an off white powder in 86% (247 mg).

^{1}H NMR (400 MHz, $CDCl_3$): δ (ppm) 7.44 (s, 4H), 5.22 (s, 4H).

^{19}F NMR (376 MHz, $CDCl_3$): δ (ppm) -137.5 - -137.5 (m, 4F), -147.5 - 147.7 (m, 2F), -160.0 - 160.2 (m, 4F).

^{13}C NMR (100 MHz, $CDCl_3$): δ (ppm) 158.5 (2 *x* CO_2), 146.8 (2 *x* CF), 144.8 (CF), 144.3 (2 *x* CF), 142.2 (CF), 138.9 (2 *x* CF), 136.5 (2 *x* CF), 131.8 (4 *x* CH), 122.4 (2 *x* C), 86.9 (2 *x* C), 83.6 (2 *x* C), 54.7 (2 *x* CH_2).

IR (neat) ν 1743 (w), 1652 (w), 1498 (m), 1326 (m), 1212(m), 1007 (m), 949 (m), 904 (s), 726 (s) cm^{-1}.

ASAP calculated for $C_{26}H_8F_{10}O_4$ is 574.03, Retention Time 0.744 min, (M+ - $C_7F_5O_2$) 363.054 (100%), (M+) 574.033 (44.88%), (M+1) 575.033 (19.43%) Da.

HR-MS calculated for $C_{26}H_8F_{10}O_4$ is 574.03, found 574.0244 (Δ = -1.2 ppm) Da.

Melting point: 106.2 - 107.9 °C.

Table: X-ray: structure information compound **42**. CIF file names: 16srv119 and 16srv220.

Parameter	**Output 120 K**	**Output 230 K**
Space group	C -1	P 2_1/n
a (Å)	0.7107(14)	21.6124(11)
b (Å)	3.7932(12)	4.8034(2)
c (Å)	7.8962(17)	11.0273(5)
α (°)	16.794(8)	90.0000
β (°)	81.539(6)	101.132(2)
γ (°)	89.477(7)	90.0000
Cell volume	4383.39	1123.24(9)
Z,Z'	Z: 8 Z': 0	Z: 2 Z': 0
R-Factor (%)	7.64	5.06

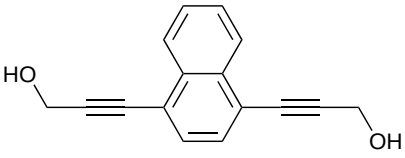

44

3,3'-(naphthalene-1,4-diyl)bis(prop-2-yn-1-ol)
Chemical Formula: $C_{16}H_{12}O_2$
Molecular Weight: 236.27

3,3'-(naphthalene-1,4-diyl)bis(prop-2-yn-1-ol) (**44**): 1,4-dibromonaphthalene (**43**) (429 mg, 1.5 mmol) was dissolved in a mixture of THF (10 mL) and $^{i}Pr_2NH$ (10 mL). $Pd(PPh_3)_4$ (104 mg, 0.09 mmol), CuI (17 mg, 0.09 mmol) and propargylic alcohol (**9**) (336 mg, 350 μL 6.00 mmol) were added to the reaction mixture. The mixture was stirred at 70 °C for 48 h under nitrogen atmosphere. After the reaction mixture was cooled to room temperature, the solvent was concentrated under vacuum. The resulting oil was dissolved in DCM (60 mL), washed with 10% HCl (2 x 50 mL) and water (4 x 50 mL), dried over sodium sulfate and concentrated under vacuum. The crude product was purified by reprecipitation from DCM / MeCN (9:1) to obtain compound **44** as a red powder in a yield of 43% (152 mg).

NMR spectra were recorded on a Varian VNMRS-700 at 298.1 K.

^{1}H NMR (700 MHz, DMSO-d_6): δ (ppm) 8.31 (m, 2H), 7.68 (m. 2H), 7.63 (s, 2H), 5.49 (t, J = 6.0 Hz, 2H) 4.46 (d, J = 5.9 Hz, 4H).

^{13}C NMR (100 MHz, DMSO-d_6): δ (ppm) 132.8 (2 x CCCH), 130.0 (2 x CCHCHC), 128.1 (2 x CCHCH), 126.6 (2 x CHCHCH), 121.1 (2 x CHCCCH), 97.2 (2 x CH_2C), 81.6 (2 x CH_2CC), 50.2 (2 x CH_2).

IR (neat) ν 3328 (b), 1438 (m), 1388 (m), 1120 (m), 1025 (s), 767 (m), 724 (s), 694 (m) 541 (s) cm^{-1}.

ASAP calculated for $C_{16}H_{12}O_2$ is 236.08, Retention Time 0.951 min, (M - OH) 219.083 (100.00%), (M) 236.091 (50.06%), (M+1) 237.083 (33.63%) Da.

HR-MS calculated for $C_{16}H_{12}O_2$ is 236.08, found 236.0837 (Δ = 1.3 ppm) Da.

Melting point: 148.2 - 150.8 °C.

Table: X-ray: structure information compound **44**. CIF file names: 16srv334.

Parameter	**Output**
Space group	P 2_1 2_1 2_1
a (Å)	4.9666(3)
b (Å)	10.5824(7)
c (Å)	22.2494(14)
α (°)	90.0000
β (°)	90.0000
γ (°)	90.0000
Cell volume	1169.4
Z,Z'	Z: 4 Z': 0

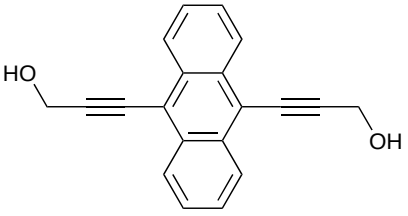

46

3,3'-(anthracene-9,10-diyl)bis(prop-2-yn-1-ol)
Chemical Formula: $C_{20}H_{14}O_2$
Molecular Weight: 286.32

3,3'-(anthracene-9,10-diyl)bis(prop-2-yn-1-ol) (**46**): 9,10-dibromoanthracene (**45**) (489 mg, 1.5 mmol) was dissolved in a mixture of THF (10 mL), $^{i}Pr_2NH$ (10 mL) and Et_3N (5 mL). $Pd(PPh_3)_4$ (104 mg, 0.09 mmol), CuI (17 mg, 0.09 mmol) and propargylic alcohol (**9**) (336 mg, 350 μL 6.00 mmol) were added to the reaction mixture. The mixture was stirred at 70 °C for 48 h under nitrogen atmosphere. After the reaction mixture was cooled to room temperature, the solvent was concentrated under vacuum. The resulting oil was dissolved in DCM (60 mL), washed with 10% HCl (2 x 50 mL) and water (4 x 50 mL), dried over sodium sulfate and concentrated under vacuum. The crude product was purified by reprecipitation from

DCM / MeCN (9:1) to obtain compound **46** as a red powder in a yield of 51% (219 mg).

NMR spectra were recorded on a Varian VNMRS-700 at 298.1 K.

^{1}H NMR (700 MHz, DMSO-d^6): δ (ppm) 8.52 (m, 4H), 7.68 (m, 4H), 5.65 (t, J = 6.0 Hz, 2H), 4.65 (d, J = 5.6 Hz, 4H).

^{13}C NMR (176 MHz, DMSO-d^6): δ (ppm) 131.7 (4 x CCCH), 127.8 (4 x CHCHCH), 127.1 (CHCHC), 117.9 (2 x CCCCH), 103.8 (2 x CH$_2C$C), 80.2 (2 x CH$_2$CC), 50.5 (2 x CH$_2$).

IR (neat) ν 3274 (b), 1438 (w), 1391 (w), 1152 (w), 1101 (w), 1015 (m), 765 (s), 641 (m) cm^{-1}.

ASAP calculated for $C_{20}H_{14}O_2$ is 286.10, Retention Time 1.048 min, (M - OH) 269.111 (100.00%), (M) 286.121 (24.96%) Da.

HR-MS calculated for $C_{20}H_{14}O_2$ is 286.10, found 286.0994 (Δ = -2.1 ppm) Da.

Table: Elemental analysis.

	% C	**% H**	**% N**
Expected	83.90	4.93	0.00
Measured	79.69	5.10	0.08

Table: X-ray: structure information compound **46**. CIF file names: 16srv311.

Parameter	Output
Space group	P -1
a (Å)	4.2685(3)
b (Å)	16.7277(11)
c (Å)	16.9386(11)
α (°)	117.220(2)
β (°)	93.930(3)
γ (°)	93.019(3)
Cell volume	1068.16
Z,Z'	Z: 3 Z': 0

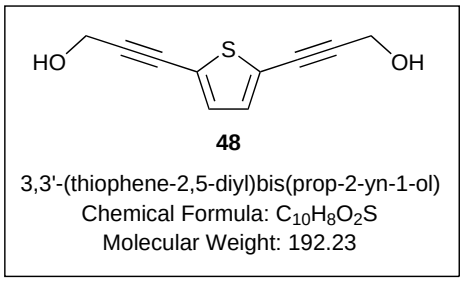

48

3,3'-(thiophene-2,5-diyl)bis(prop-2-yn-1-ol)
Chemical Formula: $C_{10}H_8O_2S$
Molecular Weight: 192.23

3,3'-(thiophene-2,5-diyl)bis(prop-2-yn-1-ol) (**48**) [278]: A mixture of 2,5-dibromothiophene (**47**) (1.50 g, 0.70 mL, 6.20 mmol), propargylic alcohol (**9**) (1.04 g, 1.08 mL, 18.60 mmol), $Pd(PPh_3)_4$ (143 mg, 0.127 mmol) and CuI (47 mg, 0.248 mmol) in water (60 mL) was prepared. To the vigorously stirred mixture was added pyrrolidine (1.55 mL, 18.60 mmol) and the mixture stirred for 10 min. The reaction mixture was then stirred for 16 h at 70 °C. After cooling the reaction mixture to room temperature, the reaction was extracted with ethyl acetate (6 x 100 mL). The combined organic phases were washed with saturated brine (2 x 150 mL), dried over anhydrous sodium sulfate, filtered, and concentrated under vacuum. The crude product was purified by silica gel chromatography (10% ethyl acetate : 90% n-hexane to 50% ethyl acetate : 50% n-hexane) yielding compound **50** as a slight yellow powder in a

yield of 80% (953 mg).

^{1}H NMR (400 MHz, DMSO-d_6): δ (ppm) 7.23 (s, 2H), 5.43 (t, J = 6.0 Hz, 2H), 4.32 (d, J = 6.0 Hz, 4H).

^{13}C NMR (100 MHz, DMSO-d_6): δ (ppm) 132.9 (2 x CH), 123.7 (2 x CS), 95.5 (2 x C), 76.7 (2 x C), 50.0 (2 x CH_2).

IR (neat) ν 3248 (sb), 2219 (w), 1520 (w), 1448 (w), 1301 (m), 1187 (m), 1057 (m), 994 (s), 918 (s), 801 (s), 538 (s) cm^{-1}.

ASAP calculated for $C_{10}H_8O_2S$ is 192.02, Retention Time 1.042, (M + H) 193.044 (1.85%) Da.

HR-MS calculated for $C_{10}H_8O_2S$ is 192.02, found 193.0323 (Δ = 0.0 ppm) Da.

Table: Elemental analysis.

	% C	**% H**	**% N**
Expected	62.48	4.19	0.00
Measured	62.05	4.28	-0.14

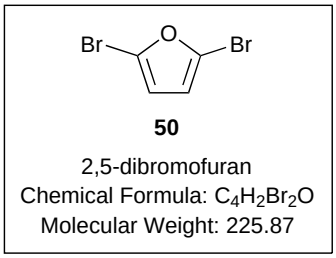

50

2,5-dibromofuran
Chemical Formula: $C_4H_2Br_2O$
Molecular Weight: 225.87

2,5-dibromofuran (**50**) [286]: A solution of furan (**49**) (22.39 g, 7.3 mL, 100 mmol) in DMF (100 mL) was prepared and cooled to 0 °C followed by the drop wise addition of bromine (31.96 g, 10.3 mL, 200 mmol). The reaction mixture was stirred overnight whilst not exceeding 25 °C. The mixture was poured in water (500 mL) and stirred vigorously for ten min. This mixture was then extracted with diethyl ether (5 x 70 mL). The combined organic layers were washed extensively with saturated aqueous $NaHCO_3$ (3 x 80 mL) and water (3 x 80 mL). The organic layer was then dried over sodium sulfate and concentrated under vacuum. The dark brown oil was

purified by vacuum distillation (53 °C and 10 mbar) obtaining a yellow oil in 56% yield (12.65 g).

^{1}H NMR (400 MHz, $CDCl_3$): δ (ppm) 6.32 (s, 2H).

^{13}C NMR (100 MHz, $CDCl_3$): δ (ppm) 121.9 (2 *x* C), 124.2 (2 *x* CH).

IR (neat) ν 1810 (m), 1560 (m), 1470 (m), 1324 (w), 1190 (m), 1086 (s), 1007 (m), 926 (s), 777 (m) cm^{-1}.

GC-MS (EI GC nonpolar compounds(Ultra)) calculated for $C_4H_2Br_2O$ is 223.85, Retention Time 2.523, (M+) 225.850 (100%) Da.

ASAP calculated for $C_4H_2Br_2O$ is 223.85, Retention Time 0.698, (M + H) 226.862 (53.35%) Da.

HR-MS calculated for $C_4H_2Br_2O$ is 223.85, found 223.8483 (Δ = 4.9 ppm) Da.

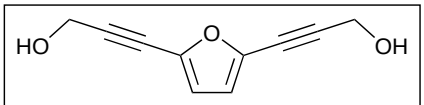

51

3,3'-(furan-2,5-diyl)bis(prop-2-yn-1-ol)
Chemical Formula: $C_{10}H_8O_3$
Molecular Weight: 176.17

3,3'-(furan-2,5-diyl)bis(prop-2-yn-1-ol) (**51**) [278]: A mixture of 2,5-dibromofuran (**50**) (2.0 g, 8.8 mmol), propargylic alcohol (**9**) (1.49 g, 1.54 mL, 26.6 mmol), $Pd(PPh_3)_4$ (286 mg, 0.248 mmol) and CuI (94 mg, 0.496 mmol) in water (60 mL) was prepared. To the vigorously stirred mixture was added pyrrolidine (2.22 mL, 26.6 mmol) and the mixture stirred for 10 min. The reaction mixture was then stirred for 16 h at 70 °C. After cooling the reaction mixture to room temperature, the reaction was extracted with ethyl acetate (6 *x* 100 mL). The combined organic phases were washed with saturated brine (2 *x* 150 mL), dried over anhydrous sodium sulfate, filtered, and concentrated under vacuum. The crude product was purified by silica gel chromatography (10% ethyl acetate : 90% *n*-hexane to 50% ethyl acetate : 50% *n*-hexane) yielding compound **50** as a slight yellow oil in a yield of 46% (713 mg).

^{1}H NMR (400 MHz, DMSO-d_6): δ (ppm) 6.82 (s, 2H), 5.39 (t, J = 5.8 Hz, 2H),

4.32 (d, J = 5.8 Hz, 4H).

^{13}C NMR (100 MHz, DMSO-d_6): δ (ppm) 131.8 (2 x CH), 121.2 (2 x CO), 94.6 (2 x C), 74.9 (2 x C), 48.8 (2 x CH_2).

IR (neat) ν 3195 (sb), 2241 (w), 1516 (w), 1310 (w), 1324 (m), 1101 (m), 971 (s), 908 (s), 559 (s) cm^{-1}.

LC-MS calculated for $C_{10}H_8O_3$ is 176.05, Retention Time 2.05 min, (M + H) 177.213 (32.61%) Da.

HR-MS calculated for $C_{10}H_8O_3$ is 176.05, found 177.0561 (Δ = 5.1 ppm) Da.